

**The Koga Feldspathoidal Syenite, Northwestern Pakistan: Mineralogy and
Industrial Applications**

**Thesis submitted for the degree of
Doctor of Philosophy
at the University of Leicester**

by

**Iftikhar Hussain Baloch
Department of Geology
University of Leicester**

July 1994

UMI Number: U070360

All rights reserved

INFORMATION TO ALL USERS

The quality of this reproduction is dependent upon the quality of the copy submitted.

In the unlikely event that the author did not send a complete manuscript and there are missing pages, these will be noted. Also, if material had to be removed, a note will indicate the deletion.



UMI U070360

Published by ProQuest LLC 2015. Copyright in the Dissertation held by the Author.
Microform Edition © ProQuest LLC.

All rights reserved. This work is protected against
unauthorized copying under Title 17, United States Code.



ProQuest LLC
789 East Eisenhower Parkway
P.O. Box 1346
Ann Arbor, MI 48106-1346



This thesis is dedicated
to

Honourable Muhammad Hafeez Ullah Qadri,
Barela Shareef, District Gujrat, Punjab, Pakistan,
with esteem and adoration.

The Koga Feldspathoidal Syenite, Northwestern Pakistan: Mineralogy and
Industrial Applications

Iftikhar Hussain Baioch

Abstract

The Koga feldspathoidal syenite complex is a part of the alkaline igneous province of Northwest Pakistan lying between Loe Shilman and Tarbela. It consists of sodalite - cancrinite rich pegmatites, foyaites, feldspathoidal syenites, pulaskitic and garnet bearing feldspathoidal syenites, alkali syenite, lamprophyres, carbonatites and fenites.

The Koga complex rocks have SiO_2 concentrations from 55 - 62 % with Agpaitic Index $(\text{Na}_2\text{O} + \text{K}_2\text{O})/(\text{Al}_2\text{O}_3 \text{ mol. prop})$ for feldspathoidal syenites range from 0.98 to 1.12 indicating both miaskitic and agpaitic character, showing considerable variation in the concentration and distribution of major oxides. $\text{Na}_2\text{O} > \text{K}_2\text{O}$ except in one rock (alkali syenite). The mafics occur as aggregates, almost without amphibole except in one sample. There are two distinct trends of silica undersaturation. The foyaites and foyaitic feldspathoidal syenites display both a phonolitic trend (eventual decrease in silica with differentiation) and a trachytic trend towards oversaturation of silica.

The Koga feldspathoidal syenite rocks are depleted in TiO_2 , MgO , CaO , Sr , Ba and heavy rare earth elements. Ba and Sr show a strong geochemical coherence. K/Rb ratios are different in different groups ranging from 274 to 758 and are higher than the main trend of igneous suites. Rocks are rich in light rare earths and depleted in heavy rare earths with Ce negative anomaly.

The composition of the nepheline is mostly restricted to the Morozewicz - Buerger convergence field in the system $\text{Ne} - \text{Ks} - \text{Qz}$, which is a characteristic of subsolvus nepheline syenites. The recrystallization process at lower temperatures might have given rise to subsolvus types from a single high temperature feldspar hypersolvus assemblage. The composition of all the groups of the Koga feldspathoidal syenites suggest a pressure > 1 and < 5 Kb, except sodalite rich foyaites.

The geochemical and mineralogical evidence suggests a magmatic progression from Babaji soda granite \rightarrow Babaji nordmarkite \rightarrow alkali syenite \rightarrow garnet bearing feldspathoidal syenite \rightarrow foyaitic feldspathoidal syenite \rightarrow feldspathoidal syenite \rightarrow foyaitic feldspathoidal syenite \rightarrow feldspathoidal foyaites, miaskitic \rightarrow feldspathoidal foyaites, agpaitic \rightarrow sodalite - cancrinite rich foyaites and finally sodalite rich foyaites.

The processing of the raw material is more effective on $-250 +125 \mu$ size fraction and total alkalis increase relative to the starting material and Fe_2O_3 contents decrease to 0.13%. Following chemical analyses of sieved and magnetically separated fractions of a number of representative rocks, it is clear that the Koga feldspathoidal syenite could be beneficiated to make commercially accepted material.

Acknowledgements

I find myself unable, rather it can not be possible for any one to thank Al-Mighty Allah, the Most Beneficent, the Most Merciful in its true spirit, who enabled me to complete this work in spite of many hindrances created by my so-called friends and colleagues.

I am specially indebted to Professor A. C. Dunham who was my teacher in M. Sc., a very tolerant, giving and an accommodative person, for his supervision, encouragement, guidance, valuable comments, discussions, accessibility and support throughout this study otherwise, it could not have been possible for me to complete this work.

Professor M. Nawaz Ch., who is an excellent geologist, teacher, scientist and above all a trust worthy friend, the Punjab University, is thanked for his help, guidelines and advice, available throughout this study in every field.

This study was sponsored by the ODA (UK) under the Punjab - Leicester University Link in the field of Industrial Mineralogy, administered by the British Council. All concerned are thanked especially Mrs Nathaniel, the British Council Office, Lahore, Ms Marion Murphy, and Ms Hazei Thompson, the British Council Office, Nottingham, for their co-operation and efforts to make this Link successful.

My sincere gratitudes are due to Mr Abdul Mateen, Centre for Nuclear Studies, Islamabad, for his valuable comments, suggestions and discussions which enabled me to understand the geochemistry of the alkaline complex. My gratitudes are for Dr. Munir Ghazanfar, the Punjab University, a very competent person in all respects if one can get hold of him. Nevertheless, I was very lucky to persuade him in spite of his detestation to the field and gained a lot from him.

Professor P. W. Scott enlightened me in the beginning of this project on various problems. I learned a lot from him and he is cherished for his help and teachings. The author appreciate the facilities extended by Professor Shafique Ahmed, Director, Institute of Geology, the Punjab University, during this study.

My special thanks are due to different friends and relatives in UK for their encouragement, help, support and at the time of trouble throughout this study, viz. Mr Jamil Ahmed (Doncaster), Dr. M. Aslam (Nottingham University), Professor John Fletcher (City Hospital Nottingham), Mohammed Aiam (Leicester) Mr Khadim Hussain, Mr Johar Zahri (London), and their families.

Special gratitudes to Dr. C. H. Emeleus for his suggestions and advice on mineralogy. My gratitudes are for C. Wang, M. Arif and A. Amin for their help from time to time during this project.

All the members of the clerical and technical staff, Department of Geology, Leicester University, particularly Bill Teasdale - the King, Ann Montgomery, Pat, Donna, Rob Wilson, Nick Marsh, Rob Kelly, Brian Dickey, Andrew Smith, Chris Beckett, who worked hard to fix one or the other problem of my computer and Paul Ayto are wished gratitudes for their help and friendly behaviour.

All the academic staff members of Geology Department, Leicester University, especially Andy Saunders and M. J. Le Bas are thanked for their valuable opinions and suggestions.

My sincere gratitudes are for honourable Sufi Abdul Majeed Sahib of Sheikhu Pura, Pakistan, for his invaluable guidance in all the walks of life. Syed Yusuf Raza Gilani who gave the last push in finalising the Link, is specially thanked for his help and favour. The author is also thankful to the Director, Atomic Energy Mineral Centre, Lahore for providing facilities to process the material, especially Mr Shahid who helped a lot during processing.

I am also indebted to Dr. A. A. Jethwa, University Health Centre, for his help and proper treatment during my ailment. I would like to thank Mr P. Z. Doshi for his help. I wish to thank Mr Faqir Mohammed and Mr Minhas Geology Department, Punjab University, Lahore, who helped me during this study.-

It would be improper if I do not thank Syed Qamar Abbas, President, Punjab University Academic Staff Association, for his help and support in every difficulty arisen during this study. I am also indebted to my father - in - law, Col. (Rtd) Fazle Akbar and mother - in - law, for taking care of my family and their encouragement and support. I also appreciate the help and support of my uncle Major (Rtd) Kh. M. Hafeez which was available throughout the period of my study.

My mother, brothers, Munawwar Hussain Khan and Akbar Ali Khan, sister and other members of the family are greatly acknowledged for their sincere wishes and prays for my success which enabled me to finish this work.

At last but not least I pay homage to my wife Dr Ruhina, son Sohaib and daughter Minahii who suffered the most during my studies for their tolerance and emotional deprivations.

The Koga Feldspathoidal Syenite, Northwestern Pakistan: Mineralogy and Industrial Applications

Contents

	Page Number
Abstract	
Acknowledgements	
List of Figures	i
List of Tables	iii
List of Appendices.....	v
Chapter One	Introduction
1.1 Aims of the Project	1
1.2 Fieldwork and Sampling	3
1.3 Sample Preparation and Analysis	3
1.4 Data Processing.....	3
1.5 Layout of the Thesis.....	4
1.6 Previous Work.....	4
Chapter Two	General Uses of Nepheline Syenite
2.1 Glass Manufacture	8
2.2 Ceramics.....	12
2.3 Paints and Filler Applications.....	17
2.4 Resistance to Frosting.....	18
2.5 Use in Plastics	19
2.6 Use In Rubber, Sealants and Adhesives.....	20
2.7 Alumina, Cement and Alkali Products.....	20
2.8 Roofing Granules	23
2.9 Radioactive Waste Disposal	24
2.10 Mineral Wool and Glass Fibre	25
2.11 Ornamental and Constructional Uses	26
2.12 Miscellaneous Applications.....	26
Chapter Three	General Geology of the Alkaline Province
3.1 The Loe Shilman Carbonatite Complex	27
3.1.1 Amphibole Sovite	29
3.1.2 Biotite Sovite.....	30
3.1.3 Ankeritic Dolomite Carbonatite	30
3.2 Shewa Shahbaz Garhi Alkaline Rocks.....	30
3.3 Silai Patti Carbonatite Complex	32
3.4 Warsak Porphyritic Micro Granites and Alkaline Granites	33
3.4.1 Porphyritic Micro Granite.....	33
3.4.2 Alkaline Granite.....	33
3.5 Malakand Granite	34
3.6 Tarbela Alkaline Complex.....	35

Chapter Four Geology of the Nepheline Syenite

4.1	Nepheline Syenite	38
4.2	Sodalite Nepheline Syenite	43
4.3	Foyaite	44
4.3.1	Sodalite Foyaite	44
4.4	Pulaskite	44
4.5	Litchfieldite	45
4.6	Pegmatites	45
4.6.1	Type 4 Microcline-Albite-Nepheline-Pyroxene Pegmatite	46
4.6.2	Type 5 Microcline-Albite-Nepheline Pegmatite	47
4.6.3	Type 6 Nepheline-Microcline Pegmatite	47
4.6.4	Type 7 Microcline-Nepheline-Cancrinite-Fluorite Pegmatite	47
4.6.5	Type 8 Nepheline-Cancrinite-Albite-Pyroxene-Calcite Pegmatite	48
4.6.6	Type 9 Sodalite-Nepheline-Cancrinite-Microcline Pegmatite	48
4.6.7	Type 10 Nepheline-Cancrinite Pegmatite	49
4.7	Carbonatite	49
4.8	Fenite	51
4.9	Lamprophyres	51
4.10	Acid Dykes	52
4.11	Ambela Granite - Syenite Complex	52
4.12	The Ambela Uta Granite	52
4.13	Babaji Syenite	53
4.14	Changalai Granodiorite	54

Chapter Five Petrography

5.1	Feldspathoid Syenite, Foyaites and Foids	57
5.1.1	Nepheline	58
5.1.2	Microcline	58
5.1.3	Albite	58
5.1.4	Cancrinite	58
5.1.5	Sodalite	63
5.1.6	Mafic Minerals	63

Chapter Six Mineralogy

6.1	Feldspars	64
6.1.1	Albite	64
6.1.2	K-feldspars	70
6.2	Nepheline	70
6.3	Pyroxenes	72
6.4	Biotites	77
6.5	Cancrinite	84
6.6	Sodalite	84
6.7	Sphene	84
6.8	Garnet	84
6.9	Magnetite	89
6.10	Amphibole	90

Chapter Seven Geochemistry

7.1	Samples.....	92
7.2	Major Element Geochemistry	93
7.2.1	Total Alkali - Silica Diagram	104
7.2.2	Alkalinity.....	105
7.2.3	Geochemical Variations in Major Oxides.....	111
7.2.3.1	SiO ₂	111
7.2.3.2	TiO ₂	113
7.2.3.3	(Fe ₂ O ₃ + MnO + MgO) and CaO	113
7.2.3.4	Na ₂ O + K ₂ O.....	114
7.2.4	Average Chemical Composition of the Koga Feldspathoidal Rocks.....	114
7.3	Trace Element Geochemistry	115
7.3.1	Large Ion Lithophile Elements (K, Rb, Sr and Ba).....	115
7.3.1.1	Rb	119
7.3.1.2	Sr and Ba	120
7.3.1.3	K/Rb and K/Ba Ratios.....	121
7.3.2	Compatible Transition Elements (V, Cr and Sr).....	122
7.3.3	High Field Strength Elements (Ti, Nb, Zr, Th, Y and LREE).....	126
7.3.3.1	Ti.....	129
7.3.3.2	Nb	129
7.3.3.3	Zr	131
7.3.4	Rare Earth Elements (REE).....	135

Chapter Eight Weathering

8.1	Mineralogy	143
8.2	Field Observations	143
8.3	Comparison of Chemical Compositions	150

Chapter Nine Petrogenesis

9.1	The Alkaline Igneous Province Of Northwest Pakistan.....	152
9.2	Regional Setting.....	153
9.3	Origin of the Alkaline Rocks and Carbonatite Complexes: Tectonic Constraints.....	154
9.4	Major Elements	156
9.5	Trace Elements.....	160
9.6	Rare Earth Elements	161

Chapter Ten Mineral Processing

10.1	Procedure Adopted in Leicester.....	164
10.1.1	Crushing.....	164
10.2	Procedure Adopted in Pakistan	164
10.2.1	Sieving and Washing.....	165
10.3	Sizing Analysis.....	166
10.4	Magnetic Separators	167
10.5	Liberation Behaviour and Magnetic Separation Results	170
10.5.1	General	170
10.5.2	Grain Size and Mode of Locking	172

10.5.2.1 Coarse Crystal Locking	172
10.5.2.2 Finer Crystal Locking	172
10.6 Inclusions and Disseminations.....	174
10.7 Results.....	174
10.8 Comparison with Industrially Processed Material	181

Chapter Eleven Conclusions and Recommendations

11.1 Geology	183
11.2 Petrographic Compositions.....	183
11.3 Chemical Compositions.....	184
11.4 Petrogenetic Indications	185
11.5 Magnetic Separation	185
11.6 Mineral Processing.....	186
11.7 Resources.....	187
11.8 Mining Proposal and Location for the Quarry	187
11.9 Recommendations	188

Appendices	189
-------------------------	------------

References	200
-------------------------	------------

List of Figures

	Page Number
Chapter One Introduction	
Figure 1.1 Locality map of the study area	2
Chapter Two General uses of the Nepheline Syenite	
Figure 2.1 Ternary diagram showing mineral composition of the traditional ceramics	14
Chapter Three General Geology of the Alkaline Province	
Figure 3.1 Geological map of the alkaline province of Northwest Pakistan	28
Chapter Four Geology of the Nepheline Syenite	
Figure 4.1 Geological map of the study area	39
Chapter Five Petrography	
Figure 5.1 Photomicrographs of (a) fresh grains of nepheline (b) braided microperthite	59
Figure 5.2 Photomicrographs of (a) nepheline megacryst (b) inclusions of mafics.....	60
Figure 5.3 Photomicrographs of (a) grains of feldspathoids (b) inclusions in sodalite	61
Figure 5.4 Photomicrographs of (a) grains of mafics (b) aegirine phenocryst	62
Chapter Six Mineralogy	
Figure 6.1 Observed 2 θ values of 060 against 2 θ values of 204 for feldspars	64
Figure 6.2 Nepheline and feldspars compositions in NaAlSi ₃ O ₈ -KAlSi ₃ O ₈ -SiO ₂ system.....	67
Figure 6.3 Ca-Mg-Fe and Na pyroxenes with accepted names.....	74
Figure 6.4 Pyroxenes in the system Ae+Jd - Di - Ac.....	76
Figure 6.5 Pyroxenes compositions (published data).....	76
Figure 6.6 Biotite composition	81
Figure 6.7 Biotite composition in MgO - FeO - Al ₂ O ₃ system	81
Figure 6.8 Biotite analyses in Mg - Al - Fe ²⁺ system	83
Figure 6.9 Fe/Mg variation of biotites with Mn	83
Figure 6.10 CaO.SiO ₂ - FeO - CaO.TiO ₂ triangle plot of sphene	85
Figure 6.11 Garnets plot on CaO.SiO ₂ - Fe ₂ O ₃ .Al ₂ O ₃ - CaO.TiO ₂ system	86
Figure 6.12 Variation of Si with Ti in garnets	87
Figure 6.13 Variation of Si with Al in garnets	87
Figure 6.14 Variation of Si with Fe in garnets	87
Figure 6.15 Variation of Al with Ti in garnets	88
Figure 6.16 Fe ₂ O ₃ +MnO - TiO ₂ - Fe ₂ O ₃ +Al ₂ O ₃ triangle plot of magnetite.....	88
Chapter Seven Geochemistry	
Figure 7.1 Total alkali - silica diagram	105
Figure 7.2 Total alkali against alumina mol. proportions.....	106
Figure 7.3 Na ₂ O against K ₂ O	108
Figure 7.4 Alsatric index against Na ₂ O %	109

Figure 7.5	Harker diagram for major oxides against SiO ₂	110
Figure 7.6	CaO and (Fe ₂ O ₃ +MnO+MgO) against TiO ₂	112
Figure 7.7	Ba and Sr against SiO ₂	117
Figure 7.7	Rb and K/Rb against SiO ₂	118
Figure 7.8	Variations of (a)Rb with Sr (b) linear correlation of Ba and Sr.....	119
Figure 7.9	Relationship of Rb in Koga and Ba in Babaji syenite in Rb - Sr - Ba triangle.....	120
Figure 7.10	Rb against K/Rb, Ba against K/Ba and Sr against Rb/Sr.....	123
Figure 7.11	Variation diagrams of (Fe ₂ O ₃ +MnO+MgO), CaO, TiO ₂ and Sc against V.....	124
Figure 7.12	Cr/Sc - Cr relationship.....	126
Figure 7.13	Variation plot of La, Ce, Y, Nb, Zr and Th with SiO ₂	128
Figure 7.14	Sr, Y, Zr and La against TiO ₂	130
Figure 7.15	Rb, Sr and Ba against Nb.....	132
Figure 7.16	Variation trends of TiO ₂ , Y, La, Zr and Th against Nb.....	133
Figure 7.17	La and Y against Zr.....	134
Figure 7.18	REE patterns of (a) sodalite - cancrinite rich (b) feldspathoidal foyaite.....	138
Figure 7.19	REE patterns of (a) foyaitic (b) feldspathoidal syenites.....	139
Figure 7.20	REE patterns of (a) pulaskitic feldspathoidal syenite (b) alkali syenite.....	140

Chapter Eight Weathering

Figure 8.1	XRD trace of weathered rock.....	145
Figure 8.2	Photographs of (a) fresh rock boulders (b) progressing weathering.....	146
Figure 8.3	Photographs of (a) transition of rock to powder (b) deep weathering.....	147
Figure 8.4	Comparison of chemical composition of fresh rocks with weathered rocks.....	148
Figure 8.5	Comparison of chemical composition of fresh rocks with weathered rocks.....	149

Chapter Nine Petrogenesis

Figure 9.1	Normative nepheline in Ne - Qz - Ks system.....	157
Figure 9.2	Average normative nepheline in Ne - Qz - Ks.....	157

Chapter Ten Mineral Processing

Figure 10.1	Comparison of >63 μ original material with processed material.....	175
Figure 10.2	Comparison of >125 μ original material with processed material.....	176
Figure 10.3	Comparison of -170+200 mesh original material with processed material.....	177
Figure 10.4	Comparison of >63 μ of material at different runs.....	178
Figure 10.5	Comparison of >125 μ of material at different runs.....	179
Figure 10.6	Comparison of -170+200 mesh at different runs.....	180

List of Tables

		Page Number
Chapter Six Mineralogy		
Table 6.1	Microprobe analyses of albites	65
Table 6.2	Microprobe analyses of K-feldspars.....	68
Table 6.3	Microprobe analyses of nephelline.....	73
Table 6.4	Microprobe analyses of aegirine	75
Table 6.5	Microprobe analyses of biotites	79
Table 6.6	Microprobe analyses of cancrinite.....	82
Table 6.7	Microprobe analyses of sodalite.....	85
Table 6.8	Microprobe analyses of sphene	86
Table 6.9	Microprobe analyses of garnets.....	89
Table 6.10	Microprobe analyses of magnetite	90
Table 6.11	Microprobe analyses of amphibole.....	91
Chapter Seven Geochemistry		
Table 7.1	Rock types analysed from the Koga complex with symbols used in figures	94
Table 7.2	Major and trace elements analyses of sodalite/ cancrinite rich foyaites	95
Table 7.3	Major and trace elements analyses of feldspathoidal foyaites	96
Table 7.4	Major and trace elements analyses of foyaitic felds. syenites (phonolitic).....	97
Table 7.5	Major and trace elements analyses of feldspathoidal syenites (trachytic)	98
Table 7.6	Major and trace elements analyses of pulaskitic felds. syenites	99
Table 7.7	Major and trace elements analyses of garnet bearing felds. and alkali syenite	100
Table 7.8	Average composition of feldspathoidal syenites of the Koga complex	101
Table 7.9	Representative major and trace elements of alkaline complexes of world	102
Table 7.10	Selected compatible and incompatible trace elements ratios of the Koga rocks ...	103
Table 7.11	REE contents and their fractionation ratios of the Koga complex	136
Chapter Eight Weathering		
Table 8.1	Chemical composition of fresh and weathered rocks of study area	150
Chapter Ten Mineral Processing		
Table 10.1	Weight recoveries of different fractions of samples after sieving and washing	164
Table 10.2	Chemical analyses of different samples before processing	165
Table 10.3	Chemical analyses of different samples before processing	165
Table 10.4	Percent recovery of different samples after sieving and washing	166
Table 10.5	Weight of different samples before processing.....	166
Table 10.6	Percent recovery of non-magnetics and magnetics of different size fractions	170
Table 10.7	Chemical analyses of non-magnetic fractions	171
Table 10.8	Chemical analyses of magnetic fractions	172
Table 10.9	Chemical analyses of non-magnetics fractions from belt magnetic separator	173
Table 10.10	Chemical analyses of repeated fractions on belt magnetic separators.....	173
Table 10.11	Product specification of nepheline syenite of glass grades.....	182
Table 10.12	Product specification of nepheline syenite of ceramic grades.....	182

Chapter Eleven Conclusions and Recommendations

Table 11.1 Average and range of Fe₂O₃, total alkalis and CaO 185

List of Appendices

Appendix 5.1 List of samples studied 189
Appendix 6.1 Method for microprobe analyses 190
Appendix 7.1 Geochemical data acquisition 192

*Chapter One***INTRODUCTION**

The Koga feldspathoidal syenite complex lies in the middle part of the Ambela igneous complex. It is located at the latitude $34^{\circ} 23' N$ and longitude $70^{\circ} 32' E$ (Topo Sheet 43B/11) Fig. 1.1.

It is a horse shoe shaped, with the convex part of the horse shoe (Siddiqui et al. 1968) surrounded by Babaji syenite on the Northwest, west and Southwest. The outer part of the southern limb is in contact with Changalai granodiorite gneiss. The concave side is represented by an alluvial fill on the Northeast.

The Koga nepheline syenite is not an isolated and independent local derivative, but is a part of the alkaline province running from Loe Shilman, on the border with Afghanistan to Tarbela (Ashraf and Chaudhry, 1977), a distance of 150 Km.

1.1 Aims of the Project

The present study aims at the following :

- To develop mineral deposits in Pakistan in accordance with the link between Pakistan and UK.
- To examine field relationships, mineralogy and chemistry of the Koga feldspathoidal complex with the view to its development as a supplier of commercial grade of nepheline syenite. The Koga feldspathoidal syenite is the only deposit in Pakistan and is near to the main rail head (70 Km), which can be a quick means of transportation of the processed material to different industries. The climate of the area is suitable for working through out the year.
- As a result of this work, it was hoped to provide some insight into the nature and origin of the Koga complex rocks, in addition to the assessment of its economic potential.

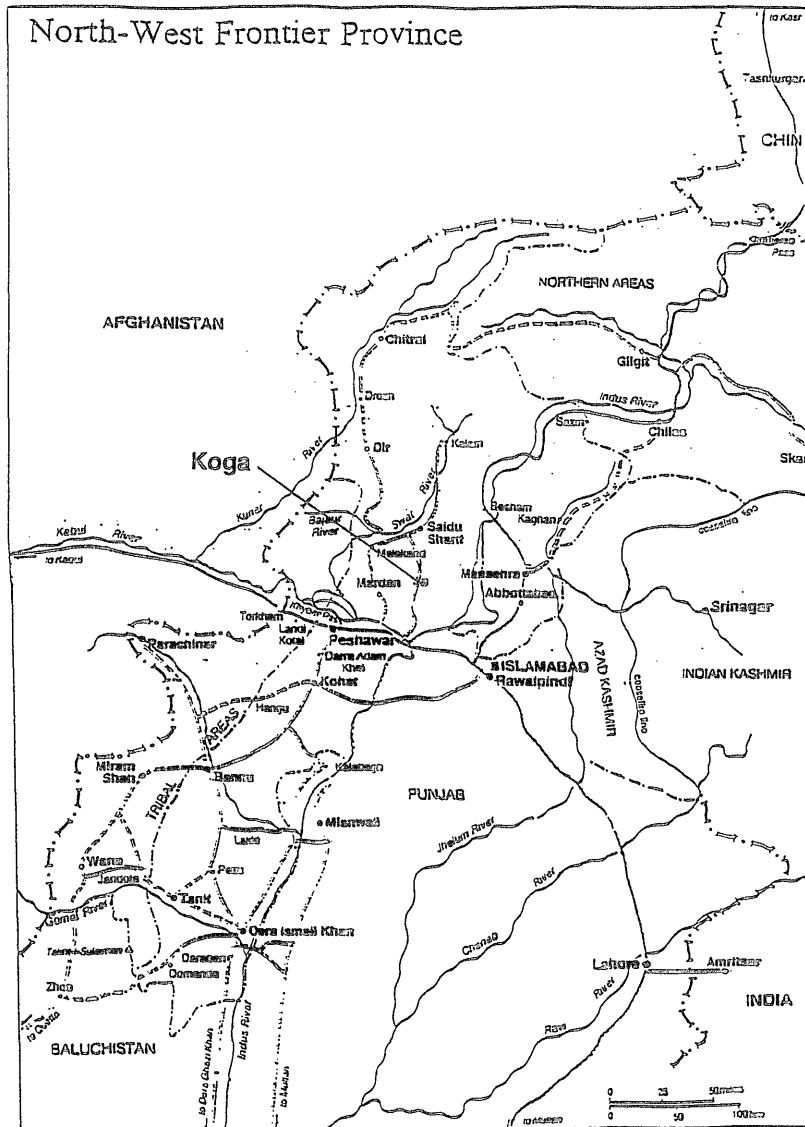


Fig. 1.1 Locality map of the study area

1.2 Fieldwork and Sampling

Fieldwork on the project area was carried out during second visit. The first extended field visit was carried out to understand the field relationships and to collect samples from the different lithological units. During the second field visit, the previous map by Shahid et al., (1979) was improved with the help of Professor Nawaz Ch. and Mr Munir Ghazanfar (Punjab University, Lahore, Pakistan) and some new pegmatites were mapped. Seven bulk samples (15 Kg) were collected from different lithological units for mineral processing at Leicester University, to add to the fifty five samples collected for mineralogical and chemical analysis. Eight weathered samples were also collected.

Finally bulk samples, weighing 30 Kg were collected to process in Pakistan for industrial utilisation. Some lamprophyres were also delineated.

1.3 Sample Preparation and Analyses

Thin sections of all the samples were prepared and petrographic study was done by light microscopy. Thirty five polished thin sections were made and their minerals were analysed by electron microprobe.

All the samples were halved, one half was powdered in agate tema for major and trace analyses by the XRF and REE by Inductively Coupled Plasma Emission Spectrometry (ICP). The other half was divided into two portions, one portion was kept for reference and the other powdered by the micronizing mill for XRD studies.

1.4 Data Processing

The analytical data was processed using a number of computer programmes available on the main frame of the University as well as on the P.C.

The main computer packages involved were MICA, used mostly for microprobe data processing, (excellent for triangle drawings, cations proportions and statistical calculations), Excel for scatter, histograms and REE data plotting,

Igpet3 for the CIPW Norms calculations and finally Aldus Free Hand was used for labelling and drawing field boundaries.

1.5 Layout of the Thesis

The general uses of nepheline syenite is given in chapter 2.

Chapter 3 - 4 provide the geology of the Alkaline Province and geology of nepheline syenite. These include the map of Alkaline province and the geological map of the area.

The petrography of the area is given in chapter 5 with the new classification of the Koga complex. The mineralogy is described in chapter 6, the XRD analyses and the electron microprobe analyses of different minerals with their comparison to other world deposits of alkaline rocks are also given.

Chapter 7 contains the detailed discussion of major, trace and rare earth elements present in the Koga feldspathoidal complex.

Chapter 8 gives a brief description of weathering, minerals present in rock samples it also compares the change in the bulk chemistry of the original rock samples with the weathered ones adjoining to them.

Chapter 9 gives the possible genesis of feldspathoidal rocks of Koga on the basis of major, trace and rare earth elements. It also contains the regional setting of the complex and its position in the Alkaline Province of Pakistan.

Mineral processing and the results obtained are discussed in chapter 10.

Finally chapter 11 contains conclusions, recommendations and the site for first quarry.

1.6 Previous Work

Coulson, (1936) was the first to report rocks of alkaline affinity in north Pakistan. He identified minerals like arfvedsonite and aegirine in rocks which were collected from Shewa Shahbaz Garhi area as well as the Khyber agency by Lewis Fermor. The genetic affinities between the alkaline rocks of Khyber and Shewa Shahbaz Garhi area of Mardan district were suggested on the basis of

their petrochemistry by Coulson, (1936). Ahmed et al. (1951) described what they considered to be acidic granitic schists from Warsak area. These rocks are in fact alkaline granites and gneisses exposed in the Warsak dam area. The geology of Warsak area was further described by Ahmed et al. (1969). Martin et al. (1962) were the first to investigate geologically the area on a reconnaissance basis where feldspathoidal syenites were subsequently discovered. Martin et al. (1962) however, did record the occurrence of zircon in the pegmatites present in a massive and porphyritic portion of the Ambela complex near Koga ($34^{\circ} 23' 72^{\circ} 30'$). Siddiqui, (1965) recognised the feldspathoidal syenites from the Koga area. This was followed by the identification of carbonatite near Naranji Kandao (Siddiqui, 1967).

The Koga nepheline syenite is not an isolated intrusion. It is a part of the now well recognised alkaline province which extends from Loe Shilman near the Afghan border in the west to Tarbela in the east. The rocks of this province have been discussed and described variously by Coulson, (1936) Siddiqui, (1965, 1967), Siddiqui et al. (1968). Jan and Kempe, (1970), Ashraf et al. (1977), and Chaudhry et al. (1981). Martin et al. (1962) briefly discussed the geology of Shewa Shabaz Garhi area. They included these rocks in their Shewa formation and characterised them as albite porphyries. Siddiqui et al. (1965) described a huge granitic body 3 km north of Shewa Shahbaz Garhi outcrop. This intrusion was named by him as the Ambela complex. He grouped different types of granites within what he called the Ambela complex. He also proposed a genetic link between the alkaline rocks of Shewa Shahbaz Garhi and the rocks of Ambela complex. Siddiqui, (1967) reported the occurrence of carbonatite in association with Koga feldspathoidal syenite at Naranji Kandao. Siddiqui et al. (1968) gave a petrographic and petrochemical account of the feldspathoidal syenite of the Koga area. The feldspathoidal syenite lies in the west central part of what he called the Ambela granitic complex. Their Ambela granitic complex

occupied a large area of Buner, Chamla and Khudu Khel areas of southern Swat. They defined three main petrologic types in the Ambela granitic complex of the Koga area as follows:

- 1) A calc-alkaline body named Changalai granodiorite gneiss.
- 2) Peralkaline syenites and granites called Babaji syenites and characterised by granitoid texture and abundance of xenoliths.
- 3) Feldspathoidal syenites or Koga syenites.

Kempe and Jan, (1970) reported aegirine and riebeckite bearing granite from Tarbela area. Siddiqui, (1973), discovered hornblende-melteigites, albitites and microgranite porphyries from the same area. He also described a mafic-ultramafic differentiated body composed of kaersutite-bearing gabbroic rocks as well as olivine-clinopyroxenites. Jan et al. (1981) suggested that rocks of the Tarbela alkaline complex developed as a result of differentiation and immiscibility of an alkali-olivine- basalt magma under high but variable CO₂ pressure. Kempe, (1973) tried to redefine the limits of the alkaline province of North Pakistan. Ahmed et al. (1974), gave an account of petrochemistry of Ambela granite. Ashraf and Chaudhry, (1977), discovered sills, dikes and ring dikes of carbonatite near Silai Patti, Malakand agency. They reported calcite, siderite, ilmenite, titanomagnetite, arfvedsonite, vermiculite, potash feldspar, apatite and chlorite from these bodies. They also reported the values of Nb, Sr and La contents confirming the carbonatite affinities of these bodies. Jan and Kempe, (1979), reported their close association with granitic rocks similar to the Malakand granite gneiss. Chaudhry et al. (1981), studied in some detail the major element chemistry and petrography of Koga nepheline syenite and tried to work out a generalised evolutionary sequence of the Koga complex, which is as follows;

Pulaskite, nepheline syenite, foyaite, sodalite syenite, fenite, carbonatite.

Chaudhry and Shams, (1983), gave an account of the petrology of the Shewa porphyries. They suggested that these rocks developed from "an anatectic melt generated at deep crustal level and emplaced roughly along en-echelon planes of weakness along a zone which suffered intermittent and alternate periods of variable tension and compression. The alkaline rocks developed during the period of tension whereas acidic rocks had developed during the period of non- tension to compression". Alkaline affinities and genetic connections amongst some of the alkaline rocks of North Pakistan were also considered by Coulson, (1936), Siddiqui, (1965, 1967) and Siddiqui et al. (1970). The idea of an alkaline province was further developed by Kempe and Jan, (1970), Kempe, (1973), Kempe and Jan, (1980), Butt et al. (1981), Jan et al. (1981), Chaudhry et al. (1981) and Kempe, (1983). Butt et al. (1980), suggested an extensional environment for the generation of magmas of alkaline affinities as a result of bending due to subduction of the Indo-Pak plate crustal segments under the Eurasian plate. Chaudhry and Shams, (1983), proposed intermittent and alternate periods of variable tension and compression for the development of alkaline and non alkaline granite respectively within the limits of the alkaline province.

*Chapter Two***GENERAL USES OF NEPHELINE SYENITE**

The main uses of nepheline syenite are as follows :

- 1) Glass Manufacture
- 2) Ceramics
- 3) Paint and Filler Applications
- 4) Resistance to Frost
- 5) Use in Plastics
- 6) Use in Rubber, Sealants and Adhesives
- 7) Alumina, Cement and Alkali Products
- 8) Roofing Granules
- 9) Radioactive Waste Disposal
- 10) Mineral Wool and glass Fibre
- 11) Ornamental and Constructional uses
- 12) Miscellaneous

2.1 Glass Manufacture

Nepheline syenite finds its main application in glass making due to the fact that it provides alumina (in addition to alkalis) which lower the tendency of glass to devitrify and improves chemical durability. High contents of alkalis in nepheline syenite also adds to the total fluxing activity of the melt. The reactivity of nepheline syenite in the presence of free silica makes it a desirable material in the glass making tank. The nepheline syenite lowers the melting temperature of the glass batch causing faster melting, high production unit and fuel savings due to its lower fusion point.

Nepheline syenite is used in the manufacture of glass products like container glass, fibre glass, opal glass, plate glass, sheet glass, table ware glass,

television tubes, lamp bulbs, glass blocks and glass wool. It is also used in the manufacture of the heat resistant and chemically resistant borosilicate glasses where it is an essential constituent of the batch when all-electrical methods of melting are employed.

More than 70% of the nepheline syenite produced in Canada, is consumed in glass manufacture, mainly in container ware (Minnes et al. 1983). According to Annon, (1968) glass industry consumed nepheline syenite more than 60 % of the Western world consumption.

Glass technology has undergone radical changes since the turn of the century when glass was used only in windows, mirrors, bottles, vases and lenses. Appropriate processes have since been formulated which enable the glass manufacturers to overcome problems such as the inability of glass to resist mechanical and thermal shock. Large scale production methods based on automation were introduced which required uniformity both in the condition of glass making process and in the glass making materials for optimum economic operations. It enabled the glass manufacturer to produce glass for its intended use with the appropriate physical properties and chemical durability (McLellan, 1966).

Although silica glass is the simplest commercial glass possessing desirable qualities, free from devitrification and expansion, resistance to chemical attack and low coefficient of expansion, it is the most difficult glass to manufacture as it has a high fusion point. High viscosity of the melt hinders the removal of bubbles, and the rapid increase in viscosity on cooling makes the glass too stiff to be moulded into the desired shapes. Flux is used in order to reduce the melting temperature and to form the homogeneous melt. Soda is the most effective flux for silica and is usually added as sodium carbonates but the resulting glass lacks chemical durability and tends to dissolve in water. Lime must therefore be added to increase its chemical durability. With the increase in the quantity of lime, glass

develops a tendency to devitrify. This requires an oxide like alumina to stabilise the glass.

In Poland, calcined alumina is replaced by nepheline syenite for the melting purposes in the manufacture of borosilicate glass, where potash and alumina oxide are the imported materials. It lowers the fuel price consumption by about 2 % (Galewicz et al. 1992).

Nepheline syenite is used due to the effect of "double alkali" in the glass industry, it can substitute pure and expensive alkali as it has high contents of Na and K. It can also aid to the melting of material and flowing ability of the melting fluid, it can improve, clear the homogeneity level of glass. It reduces the bubbles and stripes, therefore, it improves the appearance of the glass surface. It improves the glass mechanical intensity, so reduce the rate of broken glass.

Nepheline syenite is high in Al_2O_3 and lower in SiO_2 improves the chemical stability, therefore reduce the tendency of crystallisation (Qian, 1991).

The maximum desirable iron contents in nepheline in the manufacture of colourless glass is 0.03% expressed as Fe_2O_3 and the nepheline syenite has usually been beneficiated to contain not more than 0.08 % Fe_2O_3 . This value is still high as compared to the acceptable iron contents, specified for glass sands in British Standards 2975: 1988 are given below;

	Maximum content per cent Fe_2O_3
Sand for fine grade optical glassware	0.013
Sand for tableware and lead crystal glasses	0.013
Sand for general colourless glassware, including containers	0.030
Sand for clear flat glass	0.030
Sand for coloured container glasses	0.250
Sand for insulating fibres	0.300

It must be noted that even if the iron content of the sand is reduced to 0.025 %, the resultant glassware will still have a greenish tint which is undesirable in the food container market. Small amounts of selenium are added as a decolouriser in the glass batch generally. Nepheline syenite with iron content greater than 0.1 per cent Fe_2O_3 can be used in other kinds of glass. Nepheline syenite with an iron content of 0.5 per cent Fe_2O_3 can be used for amber glass. In USSR dark green bottle glass has long been manufactured from nepheline concentrates with 3 to 4 % Fe_2O_3 . Due to the successful use of nepheline concentrates valuable savings have been made in soda ash and sodium sulphate consumption (Kaplan, 1961, Taylor, 1990). The increased strength of such glass has made it possible to reduce the weight of the manufactured products. Most of the nepheline syenite used by the glass industry is ground to pass a sieve equivalent to the British Standard 25-mesh screen. Finer grinding may lead in the normal furnace to an excessive amount of material being carried into the regenerator chambers of the heat exchange system. However, this dust problem does not arise in pot melting, and so advantage may be taken of the increased fluxing power of the more finely ground grades of nepheline syenite.

As a source of alumina, nepheline syenite competes with various forms of calcined or hydrous alumina, alkali feldspar and aplite. Feldspar is widely used for this purpose and high soda to potash ratio (2:1) is preferred because of the lower melting and higher alumina content of soda feldspar. The modern glass making plants are automatic where the raw materials are unloaded into silos, automatically weighed, mixed and conveyed mechanically to the furnace. A container glass furnace can hold about hundred tons of molten glass. The automatic plants require constant conditions for their efficient operation. The use of uniform raw material both in composition and grain size is therefore needed in the process.

It was observed that nepheline syenite mixes up with quartz in the furnace and aids in melting, reduces the melting temperature and shorten the melting time. The test indicated melting of the material by 40°C at lower temperature by using nepheline instead of feldspar and the melting took place one hour earlier and the furnace lasts longer (Qian, 1991).

In 1987 Qin-huan-Dao glass institute introduced nepheline syenite in the glass manufacture instead of feldspar which gave the following results;

- 1) There was not big difference in the upper limit of crystallisation.
- 2) It substituted more alkali than using feldspar.
- 3) It decreased the viscosity of the fluid melt and the melting temperature was also shorten, so saving the energy.

It was estimated that in the production of 25000 tons of glass, 435 tons of nepheline syenite is required which saves 124 tons of alkali. In other words 100 Kg glass material requires 7% nepheline syenite and saves 2 Kg of alkali according to the data from the production. In the consumption of 1 ton of nepheline syenite, it can save 287 Kg of pure alkali (Qian, 1991).

2.2 Ceramics

The term "ceramic" is used differently in different countries. In USA, it has a very broad meanings, whereas in Continental Europe the term ceramic is more restricted. Dietzel, (1964) defined the term, which covers inorganic, non metallic materials mainly of crystalline nature, insoluble in water and formed by heating to high temperatures during production or use. A variety of raw materials is used in the manufacture of these products which have a wide range of physical properties. The traditional ceramic bodies produced by the pottery or whiteware industries are based mainly on three components;

- 1) An appropriate amount of plastic clay for desired shaping of the body and the retention of shape during the course of drying.

2) Non-plastic material, such as quartz or flint, to prevent the body from cracking during drying and firing.

3) Enough fluxing materials to generate a sufficient amount of glass for the moulded body to hold during firing but not in excess to prevent warpage.

The traditional flux has been feldspar or certain materials containing feldspar.

The traditional ceramic bodies are a mixture of clay, quartz or flint and feldspar. The relative proportions of these components are expressed on a ternary diagram in Fig (2.1). which shows the mineralogical composition of most of the commercial wares. Nepheline syenite is an alternative flux to feldspar. Nepheline syenite is a widely used raw material in the ceramic industry of North America and Europe. Nepheline syenite finds its main application in ceramics in the manufacture of a wide variety of vitreous whitewares where it substitutes for feldspar. A recent study in Canada showed that nepheline syenite is 20 % cheaper than soda spar (Barham et al. 1989). It is also utilized in glazes, enamels and certain structural clay products (tiles). In whitewares, the maximum acceptable iron content in nepheline syenite is 0.1% expressed as Fe_2O_3 . To achieve this nepheline syenite is beneficiated to contain not more than 0.08 % Fe_2O_3 . Nepheline syenite which contains 2 or 3% Fe_2O_3 can also be used, where whiteness of the fired products is not necessary, as in structural clay products. The nepheline syenite used in ceramics is generally ground to pass a B.S 200 mesh sieve. Finer grinding increases the fluxing activity of nepheline syenite. The products of the whiteware industry cover a wide range, however they can be classified into three basic types.

1. White Earthenware: white, opaque and porous with a modulus of rupture around 8,000 lb./in² having water absorption varying from 6 to 12 percent.
2. Bone China: white and translucent with a modulus of rupture around 12,000 lb./in², with little or no water absorption.

3. Vitreous China: white and usually opaque with a modulus of rupture around 10,000 lb./in², and little or no water absorption.

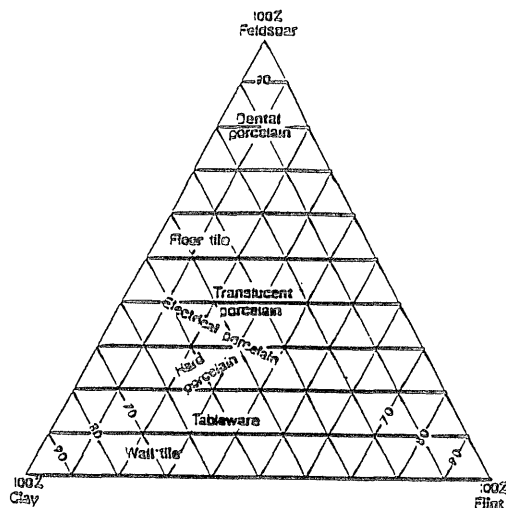


Fig. 2.1 Ternary diagram showing mineral compositions of the main types of traditional ceramic wares. After Singer and Singer.

In UK white earthenware is used mostly for the manufacture of table and kitchenware. It is also used for some tiles, some sanitary ware and some artware. It is necessary for the production of earthenware to check the sintering of the body to give a product with a water absorption between fairly close limits.

Vitreous china is used for hotel and institution tableware. An increasing proportion of sanitary ware, some tiles and some fine tableware and electro-ceramics are also fashioned out of vitreous china. These whiteware include the whole range of porcelain bodies, e.g. hard porcelain, which is used in high quality tableware. It is also used in electrical porcelain in which whiteness, translucency and refractoriness are not too strict in order to use fluxes that give better electrical properties. In the production of vitreous china, a more vigorous flux is used than earthenware production. Nepheline syenite is a satisfactory substitute to the traditional feldspar flux for this purpose and is much better than feldspar in a number of applications. Notwithstanding the fact that potash feldspar melts at a

higher temperature than soda feldspar, the feldspar generally used in ceramic industry is characterized by a high potash to soda ratio. It is preferred because potash feldspar imparts to ceramic bodies an extended vitrification range. Nepheline syenite has a higher alkali content than feldspar and is therefore a better flux. The melted feldspar and feldspathoids do not appear to act directly as the fluxing agents. The mechanism appears to be a diffusion of potash or soda into the body to react with the clay minerals, thereby lowering the temperature at which liquid appears and thereby commencing the process of vitrification. Melting temperatures increase greatly with increasing alumina (clay) contents. The isotherms in the field indicate a relatively steep temperature gradient, so broader firing ranges are obtained by using nepheline syenite as a flux in ceramic bodies of high clay content than of high flint content. The grain size influences the reaction of nepheline syenite with free silica during firing. It is thus more important that nepheline syenite should be more finely ground than feldspar in whiteware bodies. The removal of free crystalline silica from the system in whiteware bodies would be helped by the use of nepheline syenite as a number of disadvantages have been observed by its presence. More over nepheline syenite not only has less combined silica than feldspar but also has no free silica. The commercially available feldspars contain a percentage of silica. It was found that ceramics made with nepheline syenite fused three cones below those made with potassium feldspar and exhibited better wetting characteristics. In sanitary porcelain it was possible to lower the firing temperature by two or three cones by direct substitution. A longer vitrification range and less warpage were achieved, by substituting nepheline syenite for feldspar and firing normally, particularly when the flux was finely ground (Anon, 1968). Similar results were obtained with floor tile bodies, whereas in hotel dinnerware the greater fluxing activity of nepheline syenite made it possible, either to lower the temperature or reduce the amount of flux material.

The British Ceramic Research Association has investigated bodies made of nepheline syenite, flint and clay, and has successfully compounded vitreous and sanitary ware bodies; work trials have confirmed these results. A substantial amount of nepheline syenite is being used in British whiteware manufacture. The entry of nepheline syenite into the field of whiteware production was facilitated by the desire of American manufacturers to employ the more refractory American clays instead of imported English clays. Experiments proved that nepheline syenite could be included in the flux without disturbing the ratio of non-plastics to plastics in the body. An increasing proportion of nepheline syenite were utilised as improved results were obtained.

In electrical porcelain bodies early vitrification is achieved by the use of nepheline syenite which lowers the firing temperature as compared to bodies which use feldspar as a flux. Transverse strength is increased, and the bodies are dense and well vitrified at the maturing temperature whereas the thermal expansions are comparable with feldspar-fluxed bodies and so with few glazing problems. Large quantities of expensive calcined alumina is added in electrical insulators to increase its mechanical strength in the ceramic mix. The use of nepheline syenite as a flux also overcomes the presence of even a small amount of free quartz which results in a substantial lowering of the mechanical and electrical strength of the fired product. Fused nepheline syenite will react with quartz and remove it from the system depending upon the degree of the melting in the body (U S Pat No 2,898,217, 1959).

Nepheline syenite is used in dental porcelains and in the production of porcelain balls and mill liners. In addition to the whiteware applications, nepheline syenite is used as a frit ingredient in glazes, enamels and structural clay products. Nepheline syenite with minimum iron content is used where the colour of the glaze is important, but higher contents of iron are acceptable in such applications as sewer pipe glazes. The high fluxing capacity as well as ready fusibility of

nepheline syenite benefits manufacturers by allowing reduced body flux content, lower firing temperatures, or faster firing schedules than could be obtained with other raw material combinations.

In 1986, Construction Material Institute of Chinese Academy of Science, an experiment was carried out to use nepheline syenite in the manufacture of glazed tiles. It was found that in nepheline syenite glazed tiles the temperature was 980°C, whereas in the case of wollastonite glazed tiles the temperature difference was 110°C. While in other case it was 960 - 1049°C, so 30 - 119°C difference and firing took place one hour earlier and saved 20% energy. It satisfied the International Standard GB 400-83 (Qian, 1991).

2.3 Paints and Filler Applications

Nepheline syenite is used as a filler in plastics rubber, and in paints as an extender in a micronised form. It has an advantage as it is naturally occurring substance, and is exempted from Toxic Substance Control Act Inventory in the USA. Nepheline syenite is micronised to pass 325 mesh, United States Bureau of Standards and is marketed in various products ranging from 2-30 micron in average size. The perfect paint protects the substrate from water and chemical attack. It would not burnish, crack, chip or peel and will retain its original colour. These problems are associated with the solids in the paints. Nepheline syenite products find use in interior and exterior formulations in both solvent and water-based coatings. The products are used in highly pigmented as well as translucent stains and clear films. Applications range from relatively crude and inexpensive traffic paints to fine furniture finishes to tannin stabilisers due to its low viscosity, pigment, actual vehicle demand being much lower than the oil absorption data. Low vehicle means high pigment volume concentrations so important to high solid coatings and the traffic segment. The integrity of dry film, which is in part a function of particle packing, is appreciably improved by the use of nepheline syenite. It was observed in the electron micrograph, the serrated edges of the

nepheline syenite particles appear to snag on each other resulting tighter and more rigid packing than a more rounded particle might allow. Weather ability which includes resistance to chalking and better tint retention during prolonged exposure, is a function of better film integrity. Nepheline syenite does not possess the subtle colour undertones of grey, pink, cream or buff usually associated with other mineral fillers and extenders. Due to low tint strength pigment, maximum colour development is achieved using smaller amounts of expensive colouring pigments. In the course of prolonged exterior exposure, paints do lose some of their colour and brightness and consequently their aesthetic appeal. This is mainly result of "chalking" or "frosting". Nepheline syenite products were rated as offering the best resistance to chalking over 18 other extenders (Mommsen, 1984).

The chemistry of nepheline syenite fosters easy wetting of the particle's surface, promoting rapid dispersion in latex systems. Research on the surface chemistry of nepheline syenite indicates regions of hydrophobicity, which helps in explaining its easy dispersion in oleoresinous systems too. Nepheline syenite exhibits a tendency, due to hydrophobicity, to settle oleoresinous systems which can however be countered by employing small quantities of anti-settling agents (Mommsen, 1984).

In the manufacture of foam carpet backing, nepheline syenite is used as an inert filler (Minnes et al. 1983).

A certain amount of long term in-can paint stability is inherent in the nepheline syenite products due to its buffering capacity (around pH 9.9).

2.4 Resistance to Frosting

Most of the constituent minerals in nepheline syenite are relatively inert. However, nepheline has an exchangeable sodium ion capable of ion exchanging with H^+ (acid). It leaves the sodium ion free to combine with anions, like CO_3^{2-} and form salts on the surface of the film. This frosting problem effects films

exposed in the acid environments and in general, only with highly porous films such as acrylic latexes. The problem does not occur in alkyl formulations, and in any case in white exterior formulations the "frosting" is not easily observed (Mommsen, 1984).

2.5 Use in Plastics

Nepheline syenite is a constituent of products used in polyester microwave ware and large animal feeders, high traffic vinyl flooring, PVC cove base moulding, polyacrylate corrugated roofing, and polyester signs and building facades (Mommsen, 1984).

Following is a list of some physical properties that make the finely ground nepheline syenite plastic products attractive;

- Low vehicle demand and low viscosity at high pigment loading,
- High dry brightness and low tint strength,
- Resistance to stains, abrasion, and chemical attack,
- Easy dispersibility.

Nepheline syenite has an average index of refraction (1.526-1.546) very close to that of the most commonly used vinyl resin (1.53) as well as a low optical dispersion (Minnes et al. 1983). Nepheline syenite therefore virtually vanishes into the relatively clear resin. These most desirable properties make colour development with smaller quantities of expensive colouring agents possible. Recent research has indicated that nepheline syenite is not only transparent to ultra violet radiation, but also to microwave radiation. The use of nepheline syenite in microwave ware is an excellent example and gives all the advantages in one application. Firstly it keeps the finished product from heating up when exposed to microwave radiation. This not only eliminate burns, but it also helps to minimise the deterioration of the resin matrix. Ware formulated with nepheline syenite has an excellent stain resistance, whereas ware formulated with carbonates and kaolins stain badly, especially when exposed to formulated ware

too. This is because of the refractive index of nepheline syenite which allows a reduction in the amount of colouring agents required and usually results in a very white, china-like finished piece. The most important, are the flow property of a newly mixed batch of fibre reinforced polyester resin. High advantage flow characteristics are achieved when batches are formulated with nepheline syenite, even at loading of up to 60% by weight. Good batch flow properties result in more thorough filling of surface moulds, resulting in very attractive finishes and fewer finished rejects.

2.6 Use in Rubber, Sealants and Adhesives

Due to refractive index of 1.53, high dry brightness, ease of dispersion and resistance to abrasion, chemical attack and staining nepheline syenite is finding increasing application in silicone rubber automobile parts, neoprene rubber gaskets, styrene butadiene rubber building products, and polyvinyl acetate adhesives.

The adhesive like plastics, take the advantage of low optical dispersion and refractive index. Adhesive can be manufactured that dries clear on wood products and relatively translucent when used on glass products. Nepheline syenite is relatively new in the silicone rubber industry which has been dominated by ground and pyrogenic silica for some time. The properties of cured silicone rubber formulated with nepheline syenite are identical to those of silica filled silicone rubber, but the silicone rubber products made with nepheline syenite are much whiter which is definitely an advantage.

The reinforcing properties combined with resistance to abrasion make nepheline syenite ideal for static rubber applications.

2.7 Alumina, Cement and Alkali Products

In the USSR, nepheline syenite and nepheline have been used since 1951 to manufacture alumina, aluminium, sodium and potassium carbonate and Portland cement, because of an almost total lack of good quality bauxite deposits.

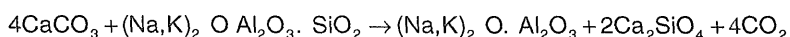
The production comes from the Kola apatite mines and Kiya Shaltyrsk. The USBM (Anon; 1961-71) estimates that the present level of consumption of nepheline syenite in the USSR is one million long tonnes per year, recent data on nepheline syenite production in 1990, is 1,650,000 tonnes (World Mineral Statistics, 1986-90). In addition, Volkhov, Piakalevo, and Achinsk alumina plants require at least three million long tons of nepheline syenite annually. So far Russia is the only country where nepheline or nepheline syenite is being used for the production of alumina, aluminium metal, Portland cement and alkali carbonates (Anon, 1971). Valuable by-products of this treatment, in addition to the cement are alkali products, notably caustic soda, potassium sulphate and soda ash which is an important constituent for this process.

The nepheline syenite concentrate is mixed with ground limestone. The mixture is pulped and reground in the wet state. The limestone should have less than 1 % MgO and low in SiO₂ (Minnes et al. 1983) . To achieve the optimum efficiency and operability in the process, it is essential to maintain the relative ratios of constituents in the initial feed to fixed values. In general the following proportion is adjusted to comply with (Anon, 1971).

$$\frac{\text{Na}_2\text{O} + \text{K}_2\text{O}}{\text{Al}_2\text{O}_3 + \text{Fe}_2\text{O}_3} = 1 \quad \text{and} \quad \frac{\text{CaO}}{\text{SiO}_2} = 2$$

The thoroughly mixed slurry is passed through a coal-fired sintered kiln, the temperature ranges from 1500 - 1600°C.

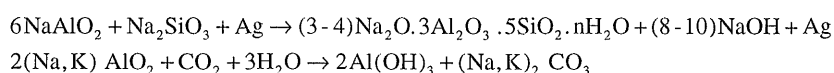
The CO₂ is driven off from the limestone and the resulting calcium oxide reacts chemically with the nepheline at 1300°C in the kiln. The final product is essentially beta dicalcium silicate and sodium and potassium aluminate (Anon, 1971 and Minnes et al. 1983). The chemical reaction is follows,



The sintered material is cooled to around 100°C and is crushed in a cone crusher and digested in two stages. The digestion takes place in a tubular vessel where it is leached with caustic soda and secondly in a rod mill, in the presence of recycled process liquor. During this process most of the alkali aluminates are taken in the solution, whereas the dicalcium silicate remains as residue and is filtered off. The residue contains 70 % dicalcium silicate, 10 % alkali and 10 % aluminium oxide. The dicalcium silicate slurry is washed and thickened to make Portland cement (Anon, 1971 and Minnes et al. 1983).

Contaminated silica is removed from the aluminate in the pressurised autoclaves and then carbonated to precipitate aluminium hydroxide. The CO₂ requirement is met from the gases given off in the sintering operation. The aluminium hydroxide is filtered off, whereas soda and potash remain in the solution as carbonates and are passed on for further processing (Anon, 1971).

The reactions are given by Minnes et al. (1983)



To manufacture Portland cement, dicalcium silicate (bellite) from the digestion section is milled with limestone. Alumina and iron oxide is added if required and fired in a cement kiln approximately at 1600°C. The clinker thus obtained is cooled and ground together with gypsum and other additives to achieve the final product (Anon, 1971).

Aluminium hydroxide is calcined to obtain high grade alumina, whereas the soda and potash are separated by selective crystallisation (Anon, 1971 and Minnes et al. 1983).

The operation costs for the production of alumina, soda, potash and cement are 10-15 % lower than those products obtained separately by conventional methods, but the capital cost is very high (Anon, 1971).

2.8 Roofing Granules

Nepheline syenite is one of the most important materials used for the production of roofing granules in USA. The main function of roofing granule is to protect the underlying asphalt coat from external deteriorating agents such as weathering which naturally includes sun light. A number of other materials, both natural and manufactured are used as roofing granules. These include a variety of rock types with suitable colour and texture encompassing rock types from acid to basic. Manufactured materials include various types of slags and a variety of clay products.

One of the basic requirements of roofing granules is that they should not need any maintenance for a period of at least twenty years. Granules have been used for a long time in their natural colour and form. At present the roofing granules are generally coloured for aesthetic reasons. This puts strict demand on the surface characteristics of materials to be used for granules. The main difficulty in the case of quartz bearing medium to coarse grained rocks is smooth and concoidal surface of quartz.

Nepheline syenite being free of quartz and composed almost entirely of feldspar and feldspathoids with their characteristic cleavage and surface properties is most suitable for coloured granules. In addition nepheline syenite possess properties, listed below, required for the intended use in manufacturing coloured roofing granules.

- a) It must be weather proof.
- b) It must possess surface characteristics amenable to colouring processes.
- c) Porosity must be low.
- d) The deposit must be uniform.
- e) Opacity to ultra violet light.
- f) It should be hard and tough.
- g) Crush must provide more or less equidimensional fragments.

In USA, which is the main user of nepheline syenite roofing granules, standard grades of granules from 2.5 to 5 cm are most popular (Mammsen, 1984).

2.9 Radioactive Waste Disposal

The increasing problem of disposing radioactive wastes is mainly due to ever increasing civil applications of atomic industry. The weakly radioactive wastes generally do not present any serious problem. The real problems are faced when it becomes to disposing the high radioactive wastes. The later may well be composed of a large number of radioactive constituents some of which are immobilised fission products undergoing rather slow decay. It is estimated that about 1.5 lb. of fission products which are a by product of 200,000 kW of electricity generated each day, composed of 36 or more radioactive elements including long lived strontium and caesium isotopes.

A number of methods have been suggested and employed for the safe storage of radioactive wastes which include the following:

- 1) Mixing of the radioactive wastes with sodium silicate to produce a pasty gel and then disposed/stored.
- 2) Absorption of radioactive wastes in clays which are then fired and disposed.
- 3) Incorporating the wastes in suitable glass and storing it.

It is the last method which is not only being used but has a potential for wider application through improving the characteristics of the retaining medium.

The effectiveness of the retaining medium depends to a large extent on its ability to withstanding corrosive characteristic of fluids, it is expected to encounter at the site of disposal.

Practice of the Atomic Energy of Canada Limited has shown nepheline syenite to be a suitable raw material for producing the glasses used for radioactive waste disposal. A suitable glass has been made for radioactive waste disposal from the nepheline syenite deposits of Ontario by fluxing it with lime (Allen and Charsley, 1968).

By adding suitable quantities of lime to nepheline syenite, which is already high in alumina, a reasonably high alumina glass is produced. This glass has a very low solubility in water. It has been found through extensive experimentation that a glass composed of 85 % nepheline syenite and 15 % of lime offers the best compromise in respect of high resistance to attack by water and flux concentration requirement and viscosity.

Although the glass of above composition is relatively viscous at 1350°C, yet it can incorporate 5% of requisite metal ions.

The requisite waste disposal glass is prepared by concentrating hot liquid wastes in nitric acid and then adding it to a mixture of 15% lime and 85% nepheline syenite. This produces a gelled slurry through acid attack, which fuses at 1350°C. Under conditions of maximum aqueous leaching an annual loss has been estimated at about one millionth of the actual mass. It has been estimated by the Atomic Energy of Canada Limited that the cost of radioactive waste disposal in this manner constitutes only one to two percent of the cost of production of electricity.

2.10 Mineral Wool and Glass Fibre

Mineral wool is a term applied to manufacture of silicate glass with useful properties of thermal and acoustic insulation resulting from their fibrous nature. Generally this term can be applied to rock, slag or glass wool. The manufacturing process consists of drawing glass filaments from the molten material which are then solidified by rapid cooling. It can also be produced by pouring rock melt on a fast spinning wheel (Mohsin, 1989). It is a low-priced commodity produced from a mixture of such raw materials as blast-furnace slag and these should be locally available for the process to be economical, but the purity standards are normally low. As the crude nepheline syenite in lump form has been found to impart useful properties to the fibres as well as promoting the melting process, it is used on a small scale in Canadian mineral wool production. Nepheline syenite imparts

desirable qualities of durability and resistance to vitrification to the glass fibres in addition to acting as a flux in the glass batch and is used on an appreciable scale in north America for glass wool and glass fibre.

2.11 Ornamental and Constructional Uses

The coarse grained feldspathoidal rocks have an attractive appearance due to the presence of deep coloured minerals in a light mass of nepheline and alkali feldspar. These coloured minerals are sodalite - deep blue, cancrinite - yellow or pink, or black ferromagnesian constituents. These rocks are polished and used for the internal decoration, because feldspathoidal rocks have poor resistance to weathering processes, so can not be used for external decoration, particularly in polluted urban atmospheres.

Nepheline syenites also provide a useful source of constructional materials in application such as road stone, concrete aggregate and ballast etc.

2.12 Miscellaneous Applications

Nepheline syenite has been used in abrasive industry as a material in manufacture of grinding wheels. Nepheline syenite have desirable properties due to the translucency and thermal shock resistance in the artificial corundum grains when heated to manufacture grinding wheels. Nepheline syenite has the possible application for the precision casting of metals and alloys by the lost wax method. It has been suggested that a solution of nepheline in sulphuric acid could be used as a substitute for aluminium sulphate in the paper industry, while such products as ultramarine, lac substitutes and laundry blue could be obtained from nepheline by the action of sulphuric dioxide gas in the presence of water (Volkov, 1932).

The possible utilisation of nepheline as a fertiliser have been given consideration but due to the slow rate of decomposition of nepheline under normal atmospheric conditions inhibits its use (Allen and Charsley, 1968).

*Chapter Three***GENERAL GEOLOGY OF THE ALKALINE PROVINCE.**

The known extent of the alkaline province of Northwest Pakistan is about 210 Km. from Loe Shilman on the Afghan border in the west to the Tarbela Dam area in the east. Although Kempe and Jan, (1970) and Kempe, (1973), predicted that more bodies will be found beyond the presently known longitudinal extent of this province, none has so far been discovered east of Tarbela, despite a thorough search. This alkaline igneous province has been named by Kempe, (1983), as "The Peshawar Plain Alkaline Igneous Province, Northwest Pakistan." This province is however, not restricted to the Peshawar Plain (Fig. 2.1). Its members occur in the mountains of Tarbela, Buner, Ambela, as well as mountainous areas of Silai Patti; Khyber Agency. This province also extends to the west in Afghanistan.

It is therefore suggested that this province be called as "The Alkaline Igneous Province of Northwest Pakistan".

The geology of the individual members of this province is described below;

3.1 The Loe Shilman Carbonatite Complex

This complex is located in the Khyber Agency about 50 Km Northwest of Peshawar and about 20 Km north of the Khyber Pass. It extends on both sides of Pakistan-Afghanistan border. Only those parts of the complex will be described which are located in Pakistan. This complex is not very well exposed as a whole. The exact extent of this complex can, therefore, only be revealed either by geophysical methods or drilling. A summary description of this complex given below is entirely based on the surface exposures in the area.

Substantial areas remain covered by alluvium east of the Pakistan-Afghanistan border. The complex is emplaced between metasediments of probable Paleozoic

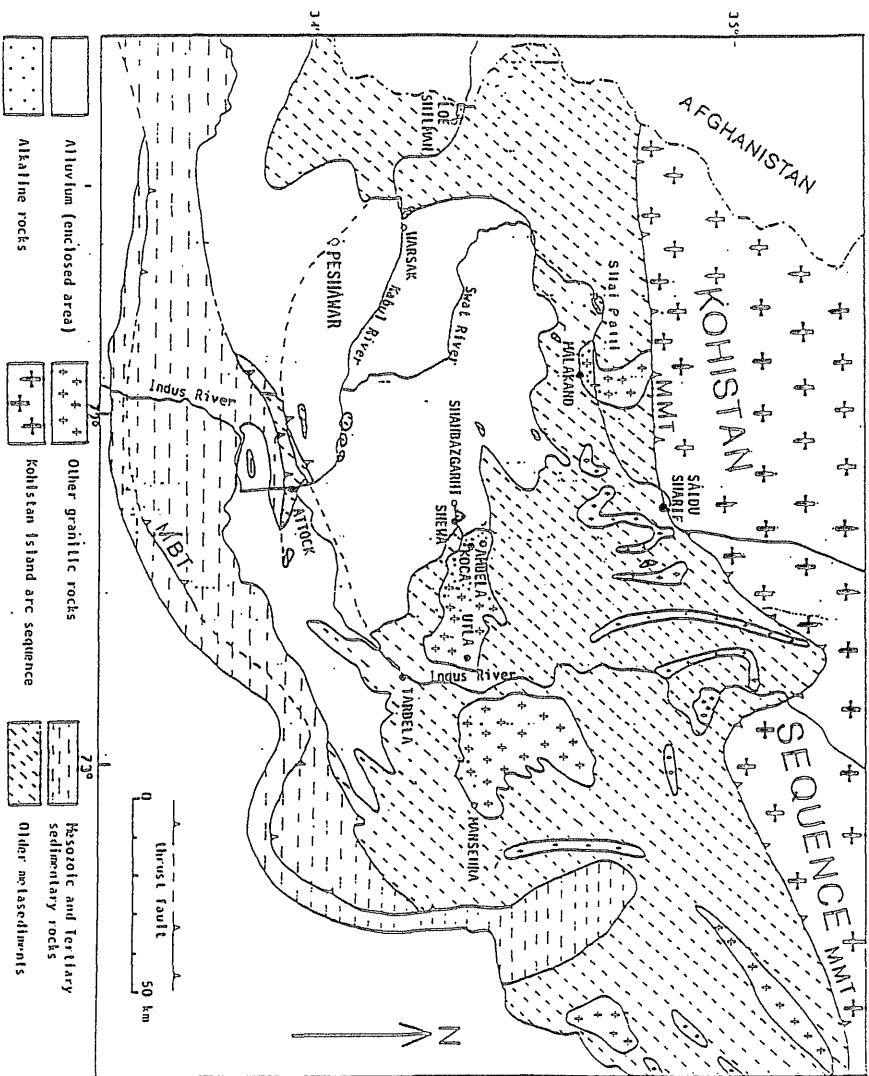


Fig. 3.1 Geological map of the alkaline igneous province of Northwest Pakistan (after Jan et al. 1970)

age? to the north and Precambrian phyllite and slates to the south, (Ahmed and Ali, 1977, Jan et al. 1981, Mian and Le Bas, 1987). The complex is believed to have been emplaced along a west to east trending and northward dipping thrust plane (Mian and Le Bas, 1987). The rift zone along which the Loe-Shilman complex was emplaced, subsequently was incorporated into the collisional domain of Himalaya. The complex is composed of nepheline syenite, syenite, carbonatite, fenite, gabbrodolerite sills and lamprophyres. Although Mian and Le Bas, (1986, 1987) and Le Bas et al. (1987) have called it the Loe-Shilman Carbonatite complex, an examination of the area on either side of the Durand line - the border between Pakistan and Afghanistan, as a whole reveals that all the lithologies mentioned above are represented. The geology of a part of this complex within Pakistan has been described by Ahmed et al. (1977), Jan et al. (1981), Kempe, (1983), Mian and Le Bas, (1986, 1987) and Le Bas et al. (1987). There are a large number of carbonatite bodies in the area. Many bodies are covered under alluvium and are only partially exposed. The main carbonatite intrusions according to Mian and Le Bas, (1987) are 170 metres wide and at least 3 Km long. These bodies strike in an east west direction and continue into Afghanistan. The carbonatites have been divided into the following four types;

- i) Amphibole sovite.
- ii) Biotite sovite.
- iii) Ankeritic dolomite carbonatite .
- iv) Late stage carbonatite veins.

3.1.1 Amphibole Sovite

The amphibole sovite is generally well foliated to banded and layered. These are composed of calcite, dolomite or both accompanied at places by siderite. Other important minerals are magnesio-arfvedsonite, magnesio-riebeckite and apatite. Titanium phlogopite and at places biotite, aegirine and aegirine-augite may also occur.

3.1.2 Biotite Sovite

This type may be closely associated with the syenite rock. It is composed essentially of carbonate and phlogopitic biotite. Subordinate to accessory amounts of alkali pyroxenes and amphiboles, alkali feldspar and apatite are also present.

3.1.3 Ankeritic Dolomite Carbonatite

This type occurs as sheet and tabular bodies intersecting the amphibole and biotite sovite. It is composed predominantly of dolomite ankerite, amphibole and apatite. The bodies of this type of carbonatite are from 0.75 to 20 m thick. The exact shapes of the syenite bodies with which the carbonatites are associated are not known. Kempe, (1983), has described an elongated intrusion in the eastern part of the area. These rocks consist of alkali feldspar which is mainly micro-perthite, alkali pyroxenes, apatite, iron oxide, sphene, rutile, zircon, biotite and some carbonates. He also describes quartz bearing pegmatite patches associated with the syenitic rocks. He further described an occurrence of feldspathoid bearing syenite with high colour index. Feldspathoid bearing syenite has also been encountered at other places (Butt, personal communication, 1993).

3.2 Shewa Shahbaz Garhi Alkaline Rocks

The triangular outcrops of rocks bounded by Shahbaz Garhi, Shewa and Machai at three corners has for quite some times been considered to be composed mainly of peralkaline porphyries (Martin et al. 1962, Siddiqui et al. 1968). However, this 85 square Km outcrop should be described as a metasediment-porphyry complex. The porphyries are subordinate to metasediments (Chaudhry and Shams, 1983). Lewis, (1935) collected porphyries from Shahbaz Garhi near Mardan. Coulson, (1936) carried out some sampling from this area and from the nearby areas of Turlandi and Gohati hills. He studied these rocks petrographically and published three analyses of these rocks, one from Mula Ghorri and two from Shahbaz Garhi areas. Coulson, (1936) compared the two occurrences petrographically as well as chemically and was the first

person to suggest consanguinity. The Shewa-Shahbaz Garhi-Machai triangular outcrops of rocks containing the alkali porphyries were mapped for the first time by Martin et al. (1962) when they produced the first ever geological map of the vast area lying between lower Swat and River Indus. This excellent map by Martin et al. (1962), and the accompanying paper throw further light on the occurrence and nature of these alkaline porphyries. The inherent alkaline nature of these rocks was pointed out by naming these rocks as " albite porphyries ". Siddiqui, (1965, 1967) and Siddiqui et al. (1968) discovered and described the alkaline complex and re-emphasised the petrogenetic affinities of the Ambela-Koga complex with the Shewa porphyries 16 Km to the Southeast. Kempe, (1973) on the basis of chemistry and mineral composition of Shewa porphyries equated these to the Warsak granites which lie about 100 Km to the west and described these as part of the Peshawar Plain alkaline igneous province. Kempe, (1983), proposed a quartz trachyte magma as parental to the whole of the Peshawar plain alkaline igneous province of Northwest Pakistan. Further work was carried out by Chaudhry and Shams, (1983), on the Shewa Shahbaz Garhi porphyries. They pointed out that the triangular outcrop of the area is composed of mica schist, phyllite and metaconglomerate intruded by four types of porphyries. The porphyries are acid black porphyries, riebeckite porphyries, acid grey porphyries and riebeckite gneisses. On the basis of petrographic, chemical and tectonic studies they pointed out that alkaline as well as normal acid porphyries both occur in the area. They proposed that these rocks were formed from an anatactic melt generated at deep crustal level, this melt was emplaced along roughly parallel but overlapping weak planes within a tectonic zone that suffered intermittent and alternate periods of variable tension and compression. It was further pointed out that the alkaline rocks were developed during the periods of tension whereas non-alkaline rocks were developed during periods of compression. This zone, therefore, was complementary to the regional belt of strong but variable

compression along the margin of Indo Pak Plate to the north. They proposed a melt of granitic composition from which both acidic and alkaline rocks originated.

3.3 Silai Patti Carbonatite Complex

The Silai Patti Carbonatite of Malakand Agency is located at a distance of about 31 Km from Dargai-Bajaur Road and 70 Km north of Peshawar. The carbonatite bodies in the area occur as sills, dikes and ring type bodies in the pelitic psammitic schists of Proterozoic age (Ashraf and Chaudhry, 1977). The biggest carbonatite sheet zone is from 2.5 to 22 m wide. Its exposed extent is about 10 Km. The carbonatite bodies are emplaced along a fault zone which dips to the south at high to moderate angle. To the north of the carbonatite zone occurs quartzite with amphibolite sheets and to the south occur pelite psammite schists and sheet granite gneisses. The metasedimentary sequence also contains quartzite and limestone. Le Bas et al. (1987) have suggested a southward dipping thrust along which carbonatite have been emplaced. The carbonatite bodies at Silai Patti are composed of variable amounts of calcite, siderite, vermiculite, apatite, soda pyroxene, ilmenite, magnetite, chlorite, biotite and feldspar (Ashraf and Chaudhry, 1977).

According to Le Bas et al. (1987), "The carbonatite at Silai Patti comprises a sheet of white biotite-apatite sovite, within a more extensive sheet of brown amphibole apatite sovite. At the top of the sheet, the carbonatites are in contact mostly with the granite gneiss, fenitization occurs in the granite gneiss above and in the pelitic schist below the carbonatite sheet." There are two main types of carbonatites in the area. The biotite sovite is coarse grained and composed predominantly of calcite with accessory to minor amount of biotite, vermiculite, apatite, illite and titanomagnetite. The amphibole sovite is medium to coarse grained and again composed predominantly of carbonates with calcite, ankerite and dolomite with subordinate to accessory amphibole, apatite, illite and titanomagnetite. It also contains accessories like pyrochlore and biotite. Fenitization in

this area is widespread; granite gneiss, amphibolite as well as dolerites and quartzites are fenitized. Both K-fenitization as well as Na-fenitization affect the area. Butt, et al. (1989) described the detailed geology, petrography and chemistry of Silai Patti Sheet Carbonatite. They interpreted the carbonatite to be a product of multiple intrusion. The early phase of the intrusive activity is represented by peralkaline ultrabasic rocks followed by carbonatite intrusion and attendant fenitization.

3.4 Warsak Porphyritic Micro Granites and Alkaline Granites

3.4.1 Porphyritic Micro Granite

This is a dark grey to almost black micro granite. These bodies according to Kempe, (1983) have been emplaced as composite injections of at least two magma types. The older sills are porphyritic in nature and are composed of albite microperthites, quartz and biotite. Sphene, magnetite and garnet are the common accessories. However, Kempe, (1983) has also listed other accessories like zircon, aegirine, epidote, apatite, muscovite and chlorite.

The second group of sills is peralkaline in nature and can be easily distinguished from the first group on the basis of sodic pyroxene. These rocks are composed of microperthite, quartz, albite, riebeckite and aegirine. The accessory minerals are iron ore, sphene, mica, apatite, epidote, calcite, aegirine and zircon. Occasionally some fluorite may also occur. Zircon in this group is more abundant than in the first group. According to Kempe, (1983), the peralkaline granite is medium grained, pale cream coloured and flow lined. Microcline is the predominant feldspar. The rock is composed of microcline, quartz, aegirine, riebeckite and astrophyllite. Accessories are illite, biotite, fluorite and zircon. On the basis of chemistry of these rocks Kempe, (1983), considered all of them alkaline in nature.

3.4.2 Alkaline Granite

The country rocks in which the Warsak granites have been emplaced, are low grade metasediments of probable Paleozoic age. According to Kempe, (1983)

the rocks may range in age from Silurian to Carboniferous. The area in which these rocks occur forms a northward plunging syncline. The alkaline granites (Coulson, 1936, Ahmed et al. 1969, Kempe and Jan, 1970 and Kempe, 1973) have a 9 Km north-south extent. There are a number of sill like bodies of porphyritic alkali micro granite. These bodies, which may be locally garnetiferous are tectonised. There are also exposures of small bodies of gneissic micro-granite between Warsak and Loe Shilman. The main Warsak alkali granite is a massive sill which is younger than the foliated to gneissic alkali granite. Hybrid gabbros and hybrid granites are found at places as a result of intrusion of granite into meta gabbros and meta dolerites.

3.5 Malakand Granite

The Malakand granite gneiss and Malakand granite has been studied in detail by Chaudhry et al. (1974, 1976) and Hamidullah et al. (1986). The Malakand granite and granite gneiss intrudes upper amphibolite facies metasediments of the Higher Himalaya block north of the Main Central Thrust (Chaudhry, personal communication, 1993)

The Malakand granite has been listed as a part of the alkaline province (Kempe, 1973, Kempe and Jan, 1979, Jan et al. 1981, and Kempe, 1983). However, the petrographic, geochemical and tectonic data and its interpretation (Chaudhry et al. 1974, 1976, and Chaudhry, personal communication, 1993), show that the Malakand granite complex is clearly calc-alkaline in nature.

Petrographic Evidence: i). The Malakand granite does not contain minerals like fayalite olivine, aegirine, aegirine augite, riebeckite or arfvedsonite etc. which are generally considered to be indicative of peralkaline granitoids.

ii). Malakand granite contains muscovite, biotite, tourmaline and at places garnet and ilmenite. These minerals may indicate peraluminous granitoids.

Chemical Evidence: Overall and as a whole, the Malakand granite analysis have

i). $Al_2O_3 < Na_2O + K_2O$ (Mol. Prop.).

ii). $Al_2O_3 > Na_2O + K_2O$ (Mol. Prop.).

The granite is therefore peraluminous rather than peralkaline.

Tectonic Evidence: The granite lies above MCT. No evidence of present or former rifting has documented. At present, it lies in a zone of compression and thrusting (Chaudhry, personal communication, 1993).

It is therefore concluded that the Malakand granite is not a part of the alkaline igneous province of the Peshawar Plain as suggested by Kempe, (1973), Kempe and Jan, (1979), Jan et al. (1981) and Kempe, (1983).

3.6 Tarbela Alkaline Complex

In Tarbela area prior to the construction of the dam a number of small bodies of alkali granites and porphyritic micro-granites of alkaline nature and bearing soda pyroxene were exposed, (Kempe and Jan, 1970), Kempe, (1973) and Jan et al. (1981)). These rocks have now been either removed or covered under the Tarbela Dam installations. However, there still remain outcrops of albitites and carbonate breccia. This set of rocks is intimately associated with dark gabbroic and dolerite intrusions.

According to Kempe, (1983), " The igneous rocks extend for 3.5 Km with a width up to 200 m intruded along a major fault separating the Precambrian Salkhala Series from the Younger Tanol quartzites of Tan[n] awal Formation. The fault is thought to be post-Early Eocene (< 45-50 Ma) " .

In addition to the rocks mentioned above Siddiqui, (1973), has described melteigites and ijolites from the north east of Tarbela. Some of the albitites according to Kempe, (1983), resemble adinoles - albitised metasediments. According to Kempe, (1983), "The Tarbela rocks perhaps present the most puzzling complex in the alkaline province. Preliminary trace element data show that the albite-carbonate rock is rich in Zr, Nb, Sn, Zn and REE (Ce and Y) whilst Sr and Ba, are low. Ti (in rutile) is high throughout the suite. These data do not

support a carbonatitic origin for the rocks, but strongly suggest association with, say alkaline granites."

*Chapter Four***GEOLOGY OF THE NEPHELINE SYENITE**

The nepheline syenite of the Koga area lies in the middle part of the Ambela igneous complex. The outcrop of the Koga nepheline syenite is horse shoe shaped (Fig 4.1). On the Northwest, west and Southwest, the convex part of the horse shoe (Siddiqui et al. 1968) is surrounded by Babaji syenite. The outer part of south-eastern limb is in contact with Changalai granodiorite. On the Northeast the concave side is represented by an alluvial fill. It is however quite probable that the nepheline syenite extends under the alluvial fill and the body itself may be elliptical with the longer axis aligned roughly Northeast Southwest. This is also shown by the small hillock of Bibi Dherai where the nepheline syenite makes a detached outcrop now showing from within the alluvial fill. The main mass of this nepheline syenite is composed of nepheline syenite *sensu-stricto*. However, it is intruded by a number of dikes and sills which vary both in texture as well as in composition (Siddiqui et al. 1968, Chaudhry et al. 1981). In addition, dikes and sills of nepheline syenite as well as foyaites cut both Babaji syenite as well as Changalai granodiorite gneiss. Areas east of Shapala and around Shapala as well as Naranji Kandao are fenitized. Two small carbonatite bodies occur west of Shapala, while the main body occurs close to Naranji Kandao (Siddiqui et al. 1968 and Chaudhry et al. 1981).

The colours of fresh nepheline syenite are generally light grey to medium grey with black specks and aggregates of mafics. The mafics are generally randomly distributed and often form small aggregates and clots. The weathering colours are generally grey to rusty grey and where effected by hydrothermal alteration, the colours are brick red. Nepheline syenite is generally well jointed and

spheroidal weathering is commonly seen. The nepheline syenite intrusion can be classified on a mineralogical basis into,

- a) nepheline syenite,
- b) sodalite nepheline syenite,
- c) foyaite,
- d) sodalite foyaite,
- e) pulaskite and
- f) litchfieldite.

4.1 Nepheline Syenite

In hand specimen, feldspar, nepheline, sodalite and mafics can be recognised. The nepheline syenite is generally medium to coarse grained, however sills, dikes and small irregular intrusions of later generation are fine to coarse grained and even pegmatitic. Very often the rocks show flow foliation. The contact between nepheline syenite (feldspathoidal syenite) and Changalal Granodiorite Gneiss is well exposed around Jalali Kandao on the road that connects Koga village with Miani Kandao. At this place the tectonic foliation in the older Changalal Granodiorite gneiss is ENE–WSW, whereas the foliation in nepheline syenite is roughly NS. The discordance therefore is obvious.

The Changalal Granodiorite Gneiss around and south of Jalali Kandao is intruded by a large number of nepheline syenite (actually feldspathoidal syenite and rarely foyaite) dikes and few sills.

The nepheline syenite contains a large number of xenoliths and screens of Changalal Granodiorite Gneiss in the zones adjacent to the contact. The xenoliths and screens which are intruded by veins of nepheline syenite and have locally been metasomatised to pulaskite and feldspathoidal syenite. These features can be observed north of Jalali Kandao on the road that connects Koga village with Miani Kandao.

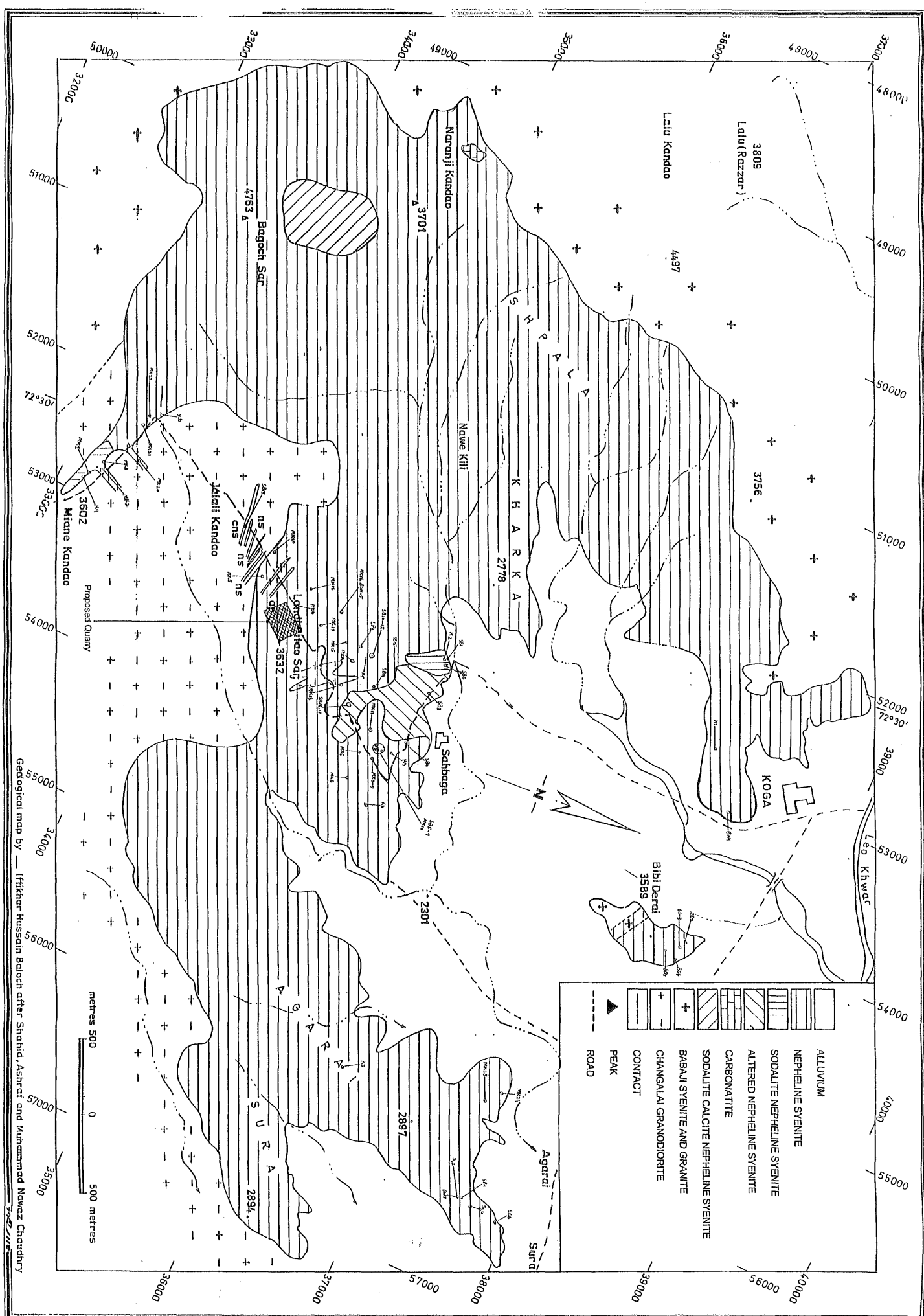


Fig. 4.1 Geological map of the study area.

Geological map by — Iftikhar Hussain Baloch after Shahid, Ashraf and Muhammad Nawaz Chaudhry

The contact between nepheline syenite and Babaji Syenite is variable. In the vicinity of carbonatite bodies, the actual contact, which is discordant in detail is over-printed by fenitization. Here fenitization, for instance in the transformation of Babaji syenite is as follows:

- 1 Quartz decreases rapidly and disappears near the contact.
- 2 Grey to black randomly oriented K-feldspar perthite increases.
- 3 Aegirine increases in amount close to the contact.
- 4 Very near the contact a very coarse grained rock composed essentially of grey K-feldspar perthite and aegirine develop.

The Koga feldspathoidal syenite has itself been fenitized and randomly oriented grey feldspar, bladed and sub radial aegirine and some carbonate along with some pale colour apatite develop.

The contact is quite discordant in the west of Koga and feldspathoidal syenite cuts Babaji Syenite. It dips under the Babaji Syenite at an angle of $40^{\circ} - 50^{\circ}$ whereas dip of foliation within feldspathoidal syenite is $70^{\circ} - 80^{\circ}$ NNE. At one place minor shearing within feldspathoidal syenite is seen, but it postdates intrusion.

A large number of screens and xenoliths of Babaji Syenite are present within the Koga feldspathoidal syenite. These are specially abundant around the village of Kharkai. This zone also contains a large number of syenite, quartz syenite and pulaskite pegmatites.

The nepheline syenite exposed around Bagoch Ser is leucocratic and varies from pulaskite to nepheline syenite. A large number of fine to medium grained sills, dikes and irregular bodies are exposed to the south, west and south west of Koga village. Another area where there are a fair number of fine to medium grained minor intrusions of later age are Agarai and Sura. The hydrothermally altered nepheline syenite invariably contains flakes and aggregates of tiny flakes of white mica, hematite, limonite, goethite, clay and relics of pyrite (Siddiqui et al. 1968 and

Chaudhry et al. 1981). Fine grained to aplitic as well as foyaitic pegmatites occur west of Koga in the central part of Bibi Dherai south of Agarai and Southeast of Sura near Miani Kandao (within Changalal granodiorite gneiss) and about 300 to 400 m north to north Northeast of Jalali Kandao. Lamprophyres dikes cut the nepheline syenite south of the village of Agarai and on the spur between Bagoch Ser and Naranji Kandao. These dikes range in width from 0.3 to 15 m and length from 4.5 to 60 m (Chaudhry et al. 1981). Abundant syenitic, nordmarkitic and pulaskitic pegmatites occur in Kharkai area.

The texture of nepheline syenite is variable (discussed in Ch 5). It is from fine to coarse grained. The medium grained foyaites are foliated and protoclastic (rare). Foyaitic texture (*sensu stricto*) is rare. Coarse grained foyaites are also rare. These are from coarse grained to pegmatitic. They are from subporphyritic to porphyritic and hypidiomorphic. The pegmatitic varieties show uneven segregation of constituent minerals. These are not flow lined, foyaitic texture is rare.

The fine grained feldspathoidal syenites are from saccharoidal to hypidiomorphic.

The medium to coarse grained feldspathoidal syenites are fluidal, hypidiomorphic, subporphyritic to porphyritic. They often contain segregations of pyroxene, biotite, sphene, magnetite and apatite.

Feldspathoidal syenite having nepheline > 50 % are rare and occur only near Miani Kandao and Sura / Agarai. These are invariably pegmatitic and lack flow foliation. They may or may not be porphyritic. They show very irregular segregation of the constituent minerals.

Comparatively fine grained nepheline syenites occur more abundantly near Koga, Bibi Dherai and Agarai. Another notable occurrence of fine grained nepheline syenite is 100 meter west of Sahbaga bridge. The fine grained nepheline syenite occurs as dikes with medium to coarse grained nepheline syenite. The thickness of these fine grained dikes varies from few centimetres to 30 m and length varies

from 4.5 to 270 m. The dikes dip from moderate to steep angles. The fine grained bodies are generally dark grey in colour. In hand specimen, feldspar, mica, nepheline, melanite, biotite and pyroxenes can be recognised. In the rest of the area medium to coarse grained nepheline syenite is predominant. It is not possible to separate the medium grained nepheline syenite from the coarse grained nepheline syenite. The two textural types are very intimately associated. They therefore can not be mapped as separate bodies. In medium to coarse grained nepheline syenite, mica, nepheline, pyroxene and biotite are persistent minerals which can be identified in hand specimen. Sodalite and cancrinite may also occur at places in medium to coarse grained nepheline syenite. The colour of nepheline ranges from light grey to light green. The coarse varieties contain even medium grained nepheline. At places the colour of nepheline may be olive green, microcline is light to dark grey, sodalite is inky blue while cancrinite is white to pale white and pink in colour. The pyroxenes are green to black in colour.

Xenoliths and screens in medium to coarse grained nepheline syenite are common and are generally of Changanai granodiorite gneiss or Babaji syenite. At places altered xenoliths of dolerites and lamprophyres are also seen. The mafic minerals generally may form clots or aggregates which are composed of pyroxene, biotite, sphene, zircon and ilmenite. The mafics in the nepheline syenite vary from place to place. The most light coloured and mafic poor nepheline syenites occur in the areas of Bagoch Ser and Naranji Kandao. These rocks contain very low amount of mafics and they are characterised by the presence of calcite. The darker colour nepheline syenites are generally fine grained to aplitic and as already mentioned occur at Agarai, Bibi Dherai and Koga. The dark colour of the rock is due to aplitic texture and higher quantities of mafics especially biotite. The rest of the area is occupied by nepheline syenite which is light grey to grey in colour and contains randomly distributed ferromagnesian minerals. This variety which is generally medium grained, coarsens randomly giving rise to pegmatitic

patches and areas. Nepheline, microcline, albite, amphibolite, pyroxene, biotite and ilmenite can be recognised in hand specimen, rarely fresh brown zircon and violet fluorite may be seen at places. An important variety of nepheline syenite is the sodalite nepheline syenite. The sodalite is either absent from medium grained nepheline syenite or occurs as very small grains which are difficult to identify in hand specimen.

4.2 Sodalite Nepheline Syenite

It occurs near Sahbaga bridge and the dike like body is about 200 m. long and about 80 m. wide. It shows irregular distribution of constituent minerals. The fresh colour of the rock is grey, dark grey and bluish grey, while the weathered colour is dirty grey to rusty grey. Although sodalite is present throughout this body yet it is usually only visible under the microscope. However, the northern part of the dike contains medium to coarse grained sodalite which can be easily identified. The amount of sodalite in this body is from traces to 15%. Nepheline, microcline, albite, cancrinite, pyroxene and biotite also can be recognised in the hand specimens. The amount of sodalite and nepheline are inversely related. The colour index of this body is from 1.5 to 10%. A medium grained dike of sodalite nepheline syenite trending Northeast-southwest, occurs at coordinates 5305360 of topo sheet 43 B/11. This dike is 50 m long and about 20 m thick. It contains 10 to 20% sodalite and very little cancrinite. It also has small crystals of zircon. Sodalite is also distributed widely in the nepheline syenite between Naranji Kandao and Bagoch Ser. This exposure of sodalite nepheline syenite is composed of sodalite, nepheline, albite, microcline, carbonates, pyroxene, biotite and rare zircon. Apatite and sphene are also present in this exposure. The area bearing sodalite is about 500 x 300 m. Where ever sodalite nepheline syenite occurs, hydrothermal alteration is also present in the country rock. This can be seen near Sahbaga bridge, Miani Kandao as well as between Bagoch Ser and Naranji Kandao. The

altered nepheline syenite assumes a brick red colour and contains aggregates of muscovite, grains of pyrite and variable amount of illitic clays.

4.3 Foyaites

Foyaites occur either as a facies variant of nepheline syenite or as dikes cutting both nepheline syenite as well as Changalai granodiorite gneiss. As a facies variant it occurs in the areas of Landi Patao. Here nepheline syenite grades into foyaites by the increase of nepheline. It is fine to medium grained rock and light grey in colour. Nepheline is either grey or greenish grey. In addition to nepheline, feldspar, aegirine, biotite and cancrinite are present.

Dikes of foyaites occur Northeast of Jalali Kandao within Changalai granodiorite gneiss as well as in Sura and Agarai area where they cut nepheline syenite.

These dikes range from 3 m. to 20 m. in thickness and from 15 m. to about 200 m in length. These dikes are medium to coarse grained and at places pegmatitic. They are generally greyish in colour and are composed of alkali feldspar, nepheline, aegirine, biotite, sphene and cancrinite.

4.3.1 Sodalite Foyaites

Some foyaitic dikes contain sodalite as an essential constituent and are therefore sodalite foyaites. These are coarse grained, subporphyritic to non porphyritic. They are hypidiomorphic and show uneven segregation of constituent minerals.

4.4 Pulaskites

Pulaskites are medium grained and light coloured rocks which occur to the west, west north of Sahbaga. Pulaskites are characterised by extensive weathering. These rocks are composed mainly of alkali feldspar, biotite and soda amphibole and generally lack foliation.

4.5 Litchfieldite

The litchfieldites occur as dikes within the Koga nepheline syenite. The litchfieldites are confined mainly to the south-eastern part of the intrusion. They are composed predominantly of albite with subordinate amounts of nepheline, mica, pyroxene and biotite. The accessory minerals are sodalite, cancrinite, iron oxides, zeolite and fluorite. These bodies are generally fine grained and may show a fluidal structure (Siddiqui et al. 1968 and Chaudhry et al. 1983).

These are distinctly flow lined. The flow crystals are mainly of off-white albite. They are subequigranular to often eumorphic.

4.6 Pegmatites

Nepheline syenite contains a large number of pegmatitic and aplitic veins. These veins vary in composition and texture. The pegmatites are both zoned and unzoned. They may be either intrusive or replacement bodies. While some of them have sharp contacts while others have extremely defused outlines. Quite a few pegmatites in Kharkai are not feldspathoidal. They are either syenitic (no quartz and no feldspathoid) or nordmarkitic (quartz syenite). All these are alkaline since they contain soda pyroxenes.

On the basis of mineralogy and the absence or presence of zones and zoned types, the pegmatites are divided into the following. Six of these types were briefly considered by Chaudhry et al. (1981). Four more types are described here for the first time (Nos. 1 to 3 and No 10).

- 1 Microcline pegmatites (Unzoned) G.R. (511353)
- 2 Microcline-Pyroxene-Albite-Biotite Pegmatite (Unzoned), G.R. (518354).
- 3 Microcline-Albite-Pyroxene-Biotite-Quartz Pegmatite (Unzoned). G.R. (520360).
- 4 Microcline-Albite-Nepheline-Pyroxene Pegmatite (Zoned & Unzoned).
- 5 Microcline-Albite-Nepheline-Pyroxene-Biotite-Ilmenite (Zoned and Unzoned).
- 6 Nepheline-Microcline Pegmatites (Zoned mostly & Unzoned)
- 7 Microcline-Nepheline-Cancrinite-Fluorite Pegmatite (Zoned).

- 8 Nepheline-Cancrinite-Albite-Pyroxene-Calcite Pegmatite (Zoned).
- 9 Sodalite-Nepheline-Cancrinite-Microcline Pegmatite (Zoned).
- 10 Nepheline-Cancrinite Pegmatite (Unzoned).

The first three types of pegmatite are generally restricted to Kharkai area and occur within a mix zone of Babaji Syenite and feldspathoidal syenite. Rarely these pegmatites may also occur in areas of Shapala and Lalu. These pegmatites are invariably unzoned. The pegmatites composed essentially of microcline with some mafics are most abundant. However, pegmatites composed of microcline, albite, amphibole and biotite and those composed of mica, albite, amphibole, biotite and quartz are subordinate. These pegmatites are being described for the first time. These vary from a few tens of cm to about 4 m in thickness and from 2 to 40 m in length. The first pegmatite is hosted in fenitized zone near Shapala and Narnji whereas the second and third types are in the screens of Babaji syenite and Pulaskites of Kharkai.

The 4th, 5th, 6th and 9th are present in the feldspathoidal syenite. The seventh type in foyaite, while the 8th in the cancrinite - calcite bearing feldspathoidal syenite to pulaskite. The last one in the contact zone between feldspathoidal syenite and Changalai Granodiorite Gneiss.

4.6.1 Type 4 Microcline-Albite-Nepheline-Pyroxene Pegmatites

Zoned pegmatites of this type are rare. One such zoned pegmatite occurs at coordinates 51553863 of topo sheet 43 B/7. This pegmatite is 4 m thick and about 8 m long. In this the outer intermediate zone is composed almost exclusively of light to off white albite with only accessory amounts of soda amphibole and a little biotite. The core is composed essentially of microcline, with small amounts of nepheline, pyroxene, a little ilmenite and biotite. Zircon crystals are randomly distributed in this zone. The border zone is extremely thin or missing altogether. It is composed of a thin layer of albite and mafics.

4.6.2 Type 5 Microcline-Albite-Nepheline-Pyroxene-Biotite-Ilmenite (Zoned)

One zoned pegmatite of this type is present at coordinates 513371 topo sheet 43 B/7. This pegmatite is well zoned and the following zones can be recognised in the field:-

- 1 Wall Zone: This zone is composed predominantly of microcline and albite with accessory amounts of soda amphibole and biotite. Traces of nepheline may be present.
- 2 Outer Intermediate Zone: This thin zone is composed of albite, microcline and aegirine.
- 3 Inner Intermediate Zone: This zone is composed of albite, microcline and muscovite.
- 4 Core: The core is composed of nepheline, albite and microcline.

Unzoned pegmatites of types of 4 and 5 are also present as thin veins and patches.

4.6.3 Type 6 Nepheline-Microcline Pegmatites

This pegmatite occurs at coordinates 543382 of topo sheet 43 B/11. These are composed mainly of nepheline and microcline; mafics occur only in accessory to trace amounts. These pegmatites may either be zoned or unzoned. These occur in the Agarai and Bibi Dherai outcrops. These pegmatites occur as irregular veins which vary in thickness from 0.3 to 0.6 m and their length is about 2.5 to 3 m. Nepheline in these pegmatites is green in colour whereas the microcline is light grey. Microcline and nepheline crystals grow generally from walls inwards. They may form alternate layers. At some places the outer zone is coarse grained whereas the core is comparatively fine grained.

4.6.4 Type 7 Microcline-Nepheline-Cancrinite-Fluorite Pegmatite

This pegmatite occurs at coordinates 556374 of topo sheet 43 B/11. It is about 1.3 m thick and about 7 m long. This pegmatite is composed of nepheline, microcline, cancrinite, fluorite, biotite, a little pyroxene and zircon. It has only two

zones, an outer zone and core. The outer zone is coarse, thin and composed of microcline, mafics and a little albite. The core is coarse grained, massive and consists of abundant microcline, nepheline, cancrinite and fluorite. Cancrinite and fluorite are very irregularly distributed.

4.6.5 Type 8 Nepheline-Cancrinite-Albite-Pyroxene-Calcite Pegmatite

This zoned pegmatite occurs at coordinates 505336 topo sheet 43 B/7. It is about 2 m thick and about 5 m long. The following is the description of various zones,

- a). Wall zone; This zone is very thin, (approximately 2 cm) and is composed mainly of amphibole with some albite and calcite. This zone is dull green in colour.
- b). Intermediate zone; This zone is essentially composed of albite and nepheline, accessory amounts of pyroxenes, microcline and chalcopyrite are present.
- c). Core; It is composed essentially of nepheline and cancrinite. Albite constitutes only a small portion of core.

4.6.6 Type 9 Sodalite-Nepheline-Cancrinite-Microcline Pegmatite

This pegmatite occurs at coordinates 529379 of topo sheet 43 B/11. This pegmatite is very rich in sodalite as well as nepheline. This occurs close to Koga village. It is 17 m long and 8 m thick. However, a few unzoned pegmatitic veins consisting of nepheline and microcline branch off from the main body of pegmatite. This is composed of three zones,

- a). Outer zone; This zone may also be termed as the microcline zone. This zone varies from 1 to 4 m in thickness and is asymmetric as the relative thickness of zones on either side of the core is different. Microcline is strongly perthitic and is light grey to white in colour. This zone also contains secondary patches of biotite, accessory amount of albite and soda amphibole may be present in it.
- b). Intermediate zone; This zone is composed essentially of nepheline but subordinate to accessory amount of microcline and cancrinite may also be present. Nepheline crystals range in size from 2 cm to about 30 cm. It has a

clearly greasy to resinous luster and is from black to dark grey in colour. Cancrinite occurs randomly distributed in this zone. It is from white to light pink. This zone also contains a few aggregates of ilmenite crystals. Euhedral zircon crystals may also be present in it. As contrast to the brown colour of zircon in the nepheline syenite body as a whole, the zircon in this zone is yellow in colour and varies in size from 3 mm to 12 mm.

C). Core; Light to deep blue sodalite is the predominant mineral of the core. Here it is associated with a replaced nepheline. This zone also contains albite, biotite and microcline.

In the area north Jalali Kandao the pegmatites strike NW – SE (300° N to 320° N) and dip from 40° to 70° due NE. However south of Jalali Kandao and within Changalai Granodiorite Gneiss these bodies trend from EW to NE – SW (45° to 260° N). In Sura and Agarai these bodies strike NE–SW.

4.6.7 Type 10 Nepheline-Cancrinite Pegmatite

This pegmatite occurs at coordinates 52803460 topo sheet B/11. This pegmatite is also being described for the first time. It is about 10 m thick and occurs near Jalali Kandao at coordinates (5270343). This pegmatite is composed almost entirely of nepheline and cancrinite with accessory amounts of magnetite and ilmenite. The cancrinite is from off white pale white and pinkish in colour, whereas nepheline is grey to greenish grey. The two minerals are irregularly segregated. However, due to strong shearing mineral segregation layering has developed in this body.

4.7 Carbonatite

The carbonatite bodies of Koga occur towards the western part of the area. They are concentrated mainly near Naranji Kandao. These bodies occur as veins, pockets and lenses (Siddiqui et al. 1968 and Chaudhry et al. 1981). Their width varies from a few m to about 130 m. They generally occur as discordant bodies within nepheline syenite. These bodies are generally massive and coarse grained.

In some veins however, the crystals may grow at high angles to the walls of the veins. Carbonatites are generally massive looking and lack layering. They are composed of calcite, pyroxenes, microcline and magnetite. Apatite, zircon and ilmenite may occur as accessories. Fenites are generally closely associated with carbonatites. The main occurrences of carbonatites in the area are as follows:

I). The biggest carbonatite body occurs at coordinates 497347 topo sheet no 43 B/7. This occurs at the contact of Koga nepheline syenite with the Babaji syenite, however the body is confined to nepheline syenite itself. This body is about 50 meters wide and 130 meters long. This occurs as a dike which cuts across the foliation of nepheline syenite. This carbonatite is fairly coarse grained and is composed of calcite, pyroxenes and microcline. Apatite, zircon, ilmenite and biotite occur as accessories. The pyroxenes generally occur as sub radial aggregates which are intimately intergrown with the carbonates. At places such parallel bundles of mainly pyroxene also occur. Microcline is very irregularly distributed. Apatite occurs as yellowish brown crystals. This carbonatite is surrounded by an envelope of fenite (Siddiqui et al. 1968 and Chaudhry et al. 1981). The host nepheline syenite has also been infused with carbonates. The outcrop of this carbonatite is fairly fresh.

II) This 18 m long and 0.3 to 1.5 m thick body occurs to the north of Naranji Kandao. It is again a discordant body with an eastwest trend. It is also composed of calcite as the predominant mineral with minor accessory amounts of pyroxenes, microcline and magnetite.

III) An other body of carbonatite occurs between Naranji Kandao and Shapala. A few small pockets and veins of carbonatite also occur associated with the main body. This body which occurs at coordinates 503350 topo sheet no 43 B/7 is about 32 m long and 3 to 8 m wide. It is coarse grained and has a mineralogy similar to the mineralogy of Naranji Kandao carbonatite.

IV) Another patch like body which is 3x3 m, is present in the vicinity of the second body. It is badly weathered and has the same mineralogy as body I and II.

V). At coordinates 515357 topo sheet 43 B/7, a rather fresh carbonatite body is exposed. This is about 11 m long and 5.5 m thick. This body is porphyritic in texture and is composed mainly of calcite with subordinate to accessory amount of microcline, titanomagnetite, pyroxene and apatite. The constituent minerals are fairly irregularly distributed.

4.8 Fenite

In the vicinity of carbonatite the nepheline syenite has often been strongly modified texturally as well as mineralogically. Carbonates have been introduced in the nepheline syenite. However, the most prominent feature of metasomatism is the development of fenite. Fenites are composed dominantly of light to dark grey and often well twinned microcline. Magnetite and calcite grains occur interstitially. Some pyroxenes also occur associated. However, pyroxene and calcite in the forms of veins are more common. Yellowish apatite may also occur in the fenite zone. The fenites as a whole are not very mafic in the Koga area.

4.9 Lamprophyres

Lamprophyres occur as dikes within medium to coarse grained nepheline syenite (Siddiqui et al. 1962 and Chaudhry et al. 1981). The rocks are dark green to dark greyish in colour. Fresh exposures are rare because white feldspar and cancrinite are prone to weathering. Due to weathering exact dimensions of these dikes is difficult to determine. At outcrop they have been seen to range from 0.5 to 3 m wide and length from 1.5 to about 8 m. These lamprophyre dikes are confined mainly to the areas, south of Agarai village. They are composed of amphibole, feldspar, abundant sphene, apatite and vermiculite. Coarse crystals of zircon with a yellowish brown colour are also present. Thin feldspar veins may cut the lamprophyre bodies.

Due to deep weathering and poor exposures it is difficult to assess the trend but, they appear to trend NE – SW.

4.10 Acid Dikes

Nepheline syenite is also cut by a few veins of acidic dikes. These dikes are mainly aplitic and trend NW – SE. However, a few fine to medium grained dikes are also seen. These dikes are generally from 2 to 30 m thick and from 20 to 80 m long. However, these dikes are not very frequent, they occur near coordinates 515343 topo sheet 43 B/7 and coordinates 532376 topo sheet 43 B/11. These dikes have a very sharp and often chilled contact with the host nepheline syenite.

4.11 Ambela Granite-Syenite Complex

This complex can be divided into an Ambela Utla granite complex and the Babaji syenite complex. The two together were described by Martin et al. (1962), as Ambela granite. This unit covers a large area in Swabi, Chamla and Buner. Siddiqui. (1965), named it as the Ambela granite complex. Siddiqui et al. (1968), regarded this unit as composed of granite and syenite. This unit separates the Swabi-Chamla sedimentary group of lower Paleozoic age in the south from the lower Swat-Buner schistose group (Martin et al. 1962), of rocks in the north.

4.12 The Ambela Utla Granite

These granitic rocks constitute the northern part of the complex. It extends from Utla in the east to Ambela in the west. Ahmed and Ahmed, (1974), published an account of these granites. They regard them as alkaline in character. The granites and granodiorite are coarse grained and often porphyritic. They are composed of alkali feldspar, oligoclase, quartz and biotite. Muscovite, chlorite, magnetite and zircon are the accessories. Dark yellowish green tourmaline may also occur at places. Although this unit does not contain soda pyroxene, and it has been regarded as alkaline in character by Ahmed and Ahmed, (1974), and Kempe, (1983). Khan and Hammad, (1978), have described the Utla granite which they regard as very similar to the Ambela granite. Sodic pyroxenes are absent from the

Utla granite while tourmaline and sphene may be present. The Ambela-Utla granites contain a large number of aplitic pegmatite and microgranite bodies. This complex is cut by a large number of dolerite bodies which are generally altered. Khan and Hammad, (1978), and Shafeeq et al. (1974), have studied parts of the Ambela-Utla granites. They have also described the petrochemistry of these rocks in some detail. One of the characteristic feature is that their mineralogical as well as chemical compositions vary within wide limits. Their modal composition varies as follows, plagioclase, (An 0-13) 14.5 to 24.9%, quartz, 5.1 to 37%, biotite, 1.2 to 10.4%, muscovite, 1.5 to 10.5%, chlorite, traces to 1% sericite and clays, 0.4 to 13.4%, magnetite, 0.4 to 2.5% and tourmaline, traces to 2.7%. According to Shafeequ et al. (1974), the chemistry of these rocks shows that they have an inherent alkaline affinity, but they lack a soda pyroxene.

4.13 Babaji Syenite

These rocks envelope the Koga nepheline syenite on the Northwest, west and Southwest, the convex part of the horse shoe (Siddiqui et al. 1968). These rocks have a granular texture. At places they show the effect of shearing due to local faulting. These rocks have sharp contact with the Ambela granite in the north. The Babaji syenites are lighter coloured as compared with Changalai granodiorite gneiss. Siddiqui et al. (1968), regard these syenites as comagmatic with the Koga feldspathoidal syenite. However, they regard these rocks as older than the feldspathoidal syenites. The Koga nepheline syenites are intrusive into Babaji syenite. The latter veins of nepheline syenite cut the Babaji syenite, while the Babaji syenite has suffered fenitization due to K-metasomatism. The Babaji syenite is not a uniform body but is composed of alkali granite and a nordmarkite. Nordmarkite contains arfvedsonite, sphene, apatite and ilmenite, whereas granitic member lacks arfvedsonite and contains very little sphene, apatite and ilmenite. It also contains considerable quartz. The nordmarkite member and at places the granite member contains porphyritic aplite dikes up to 30 cm thick, comprising

microcline phenocryst in a ground mass of quartz, microcline, albite, aegirine, augite and biotite, Kempe, (1983). The best exposures of Babaji syenite occur around the Ambela Babaji Kandao road. Here the rock is coarse grained and is composed of grey microcline, perthite, white albite, smoky quartz, grey green aegirine-augite, dull green arfvedsonite, greenish to reddish brown biotite and tabular ilmenite. The accessory minerals in the Babaji syenite are apatite, sphene, calcite, zircon and tourmaline.

4.14 Changalai Granodiorite

The Changalai granodiorite gneiss comes in contact with granite in the south, feldspathoidal syenite and pelitic schist in the north, Babaji syenite in the west and quartzite in the east. The contact of this granodiorite with the metasediments is sharp, while its contact with the syenitic and granitic rocks show interaction. This rock is medium to coarse grained, porphyritic and leucocratic. The weathering colours of the rock are grey and rusty grey. Changalai granodiorite gneiss according to Siddiqui et al. 1968, is a foliated and porphyritic rock of granodiorite to granitic composition. According to Siddiqui et al. (1968) "--- and is exposed all along the south eastern contact of the Koga syenite. Traced eastward it continues outside the mapped area as a belt 4x6.4 Km wide, through the entire length of the Ambela granitic complex. Moving westwards, this body comes to an abrupt end near Changalai against a northsouth trending brecciated zone which is presumably a fault zone " .

The outcrop has been thoroughly checked between Changalai to Naranji. No appreciable change in mineralogy is observed. This granodiorite gneiss does not appear to be alkaline in character. Its chemistry shows it to be peraluminous in character (Siddiqui et al. 1968). It contains abundant potash feldspar phenocrysts and biotite. It is very well foliated and is prone to weathering. This unit is composed of microcline, oligoclase, quartz and biotite. Minor to accessory minerals are amphibole, sphene, magnetite, tourmaline and chlorite. Phenocrysts

are mainly of well twinned microcline, perthite, which may range in size from 3 to 4 cm.

This unit is intruded by dolerite and aplite dikes. Some quartz veins also occur near the aplitic bodies. Many dikes and sills of foyaites, nepheline syenite, sodalite bearing foyaite and syenite occur in the contact-aureole near Koga nepheline syenite. Some of these bodies are very rich in feldspathoid and are therefore of economic value.

The aplitic sills and dikes vary from 20 cm to about 10 m in thickness. They may vary from a few metres to more than 100 m in length. The mineral composition of these aplitic bodies are fairly similar to the host granodiorite gneiss. However, their colour index is much lower and they have a pale white to off white colour. Xenoliths and clusters of xenoliths as well as screens of pelite and psammite composition are quite common in the granodiorite gneiss.

*Chapter Five***PETROGRAPHY**

In the following, definitions of some feldspathoidal syenites after Sorensen, (1974) are given. However the classification followed by the author differs from Sorensen. The rock types occurring in the area are herein defined in a different manner, keeping in view the natural grouping into which the rock types fall in the field.

According to Sorensen, (1974) nepheline syenite *senso stricto* is generally defined as having more K-feldspar than albite, and nepheline between 5% and 25%

Foyaites are defined as alkaline rocks having nepheline between 25 and 50%, a colour index of more than 10% and a foyaitic texture (Sorensen, 1974).

The above definitions given by Sorensen are general and can not be applied in the case of Koga area on the whole because the main mass of nepheline syenite varies randomly in modal composition from nepheline syenite to foyaite as defined by Sorensen.

Instead of using the term " Nepheline syenite " the author prefers to use the term " Feldspathoidal syenite " since in Koga area nepheline is not the only feldspathoid present and in certain parts of the complex significant amount of other feldspathoids like sodalite and cancrinite are present.

Thus feldspathoidal syenite is defined here as composed of alkali feldspar, with K-feldspar more than Na-feldspar, and feldspathoids more than 5% of the rock but less than total amount of alkali feldspar.

If Na-feldspar is more than K-feldspar then the rock may be called litchfieldite. However, the author proposes that in case of Koga area the feldspathoidal syenites and litchfieldites containing feldspathoids more than 20%

and less than total alkali feldspars be called foyaitic feldspathoidal syenites and foyaitic feldspathoidal litchfieldite.

Foyaites are defined as feldspathoidal syenites in which feldspathoids are more than total alkali feldspar. The author suggests that foyaites may not have more than 10 % colour index or a foyaitic texture. Thus the term foyaitic feldspathoidal syenite in this definition has no textural or colour constraint.

Foids are defined as rocks having more than 50 % feldspathoids irrespective of texture and colour index.

In the field feldspathoidal syenite and foyaitic feldspathoidal syenite as defined earlier, form distinct bodies. However, if the amount of sodalite and cancrinite is more than 5 % in the rock, it may be called as sodalite and cancrinite rich feldspathoidal syenite respectively.

Although the minerals present in all the sections are the same the name is given on the percentage of each mineral present in the particular section.

The following sizes were adopted as a general description of the mean grain size in a particular rock:

Coarse grained	=	> 5	mm.
Medium grained	=	1-5	mm.
Fine grained	=	< 1	mm.
Very fine grained	=	<0.5	mm.

5.1 Feldspathoidal Syenite, Foyaites and Foids

In order to avoid unnecessary repetition the petrographic description of various minerals is given as a whole.

The feldspathoidal syenites are of three grain sizes i.e. coarse grained, medium grained and fine grained. The coarse and medium grained varieties are more common, whereas the fine grained variety is rare.

Texturally coarse and medium grained are hypidiomorphic, porphyritic while the fine grained varieties are from saccharoidal to hypidiomorphic.

The important minerals are described below:

5.1.1 Nepheline

It occurs as subhedral to anhedral grains. There are two generations of nepheline, the fresh grains are subhedral, unaltered and at places forming clusters. Sometimes it is also present in the cracks and fractures of microcline. The anhedral nepheline is of first generation (Fig. 5.1a) and shows replacement by cancrinite and it is enclosed by it in some sections. The modal variation is from 5 to 30%.

5.1.2 Microcline

It is mostly present as subhedral to anhedral phenocrysts. Both the perthitic and non perthitic varieties are present and show flowage, banding and fracturing in some sections which could be due to latter movement. It shows perthitic growth and intergrowth with albite. It also shows the braided microperthite (Fig. 5.1b). Mostly microcline is replaced by cancrinite along fractures and cracks. Nepheline is also present in the cracks and fractures of microcline. There are also some fresh grains of microcline which suggest that microcline is also of two phases, early and late phase. Microcline contains inclusions of nepheline, cancrinite, biotite and magnetite.

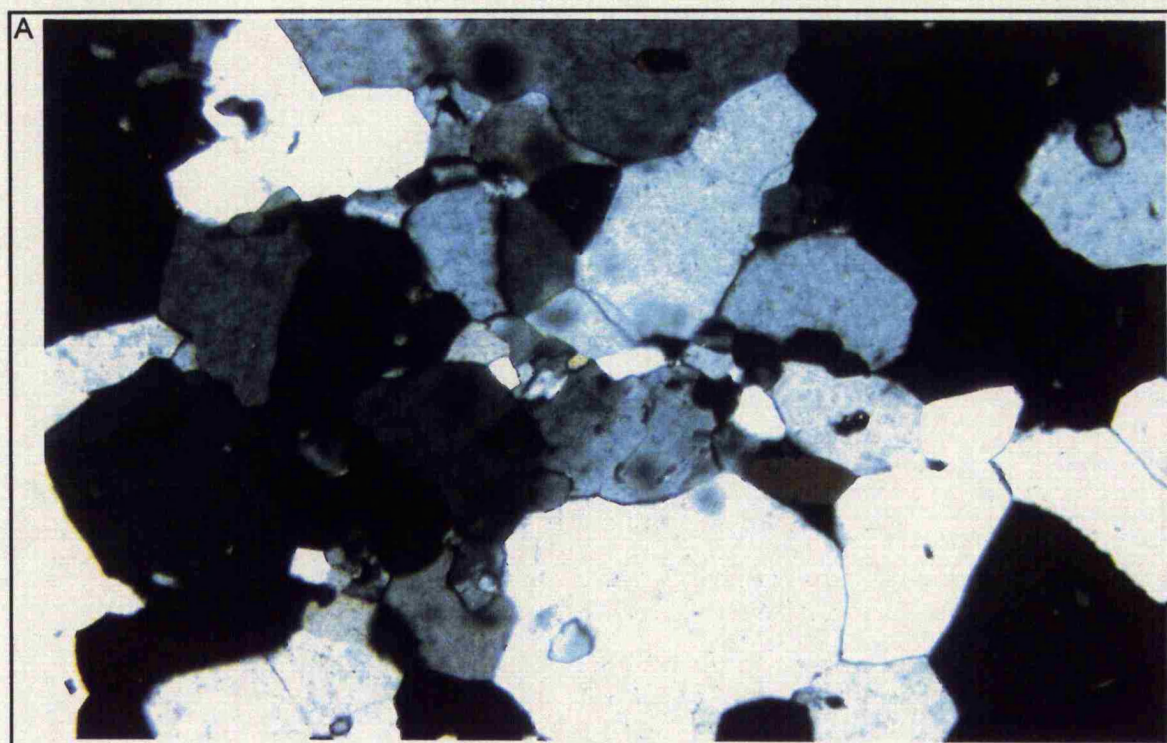
It is the most abundant mineral and its percentage is between 20 to 70%.

5.1.3 Albite

Albite occurs mostly as subhedral well twinned laths. It also shows replacement by cancrinite and at places by nepheline and also enclose by nepheline (Fig. 5.2a). It has inclusions of apatite? and biotite (Fig. 5.2b).

5.1.4 Cancrinite

Subhedral grains of cancrinite are present, mostly as a replacive mineral along the joints and fractures of microcline and albite. It also replaces nepheline of the first phase and make clusters in some sections (Fig. 5.3a). They make up to 15% in some sections.



0.5 mm

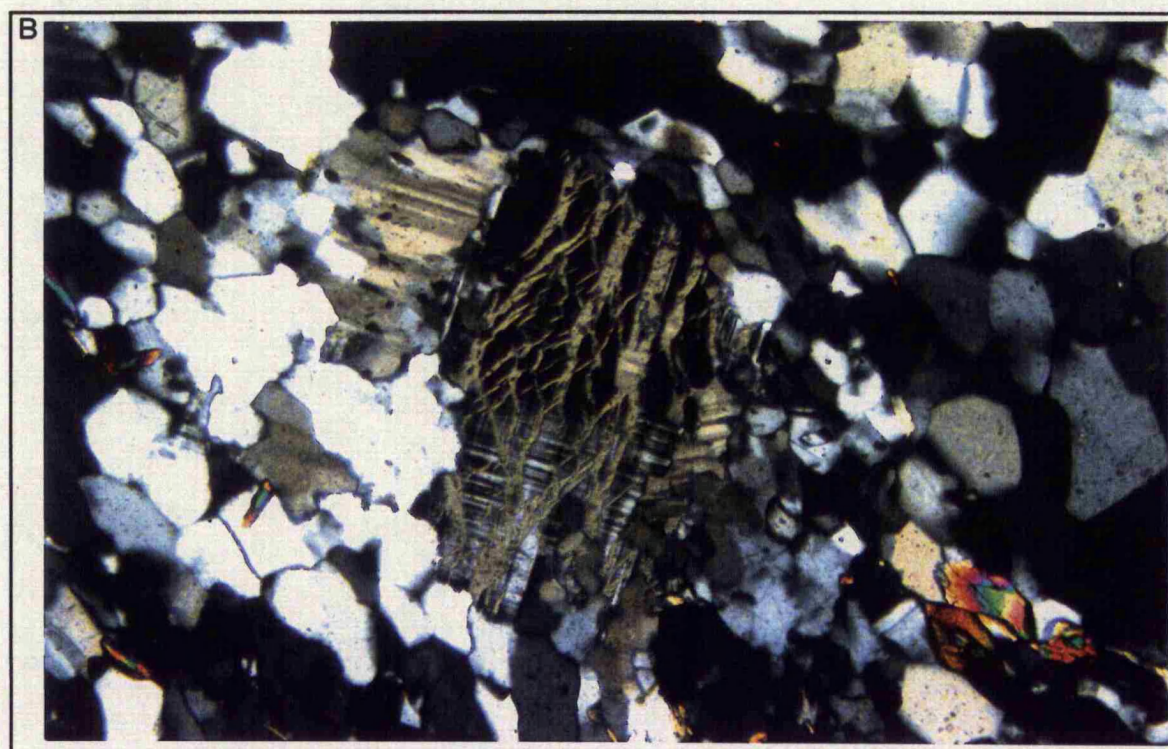
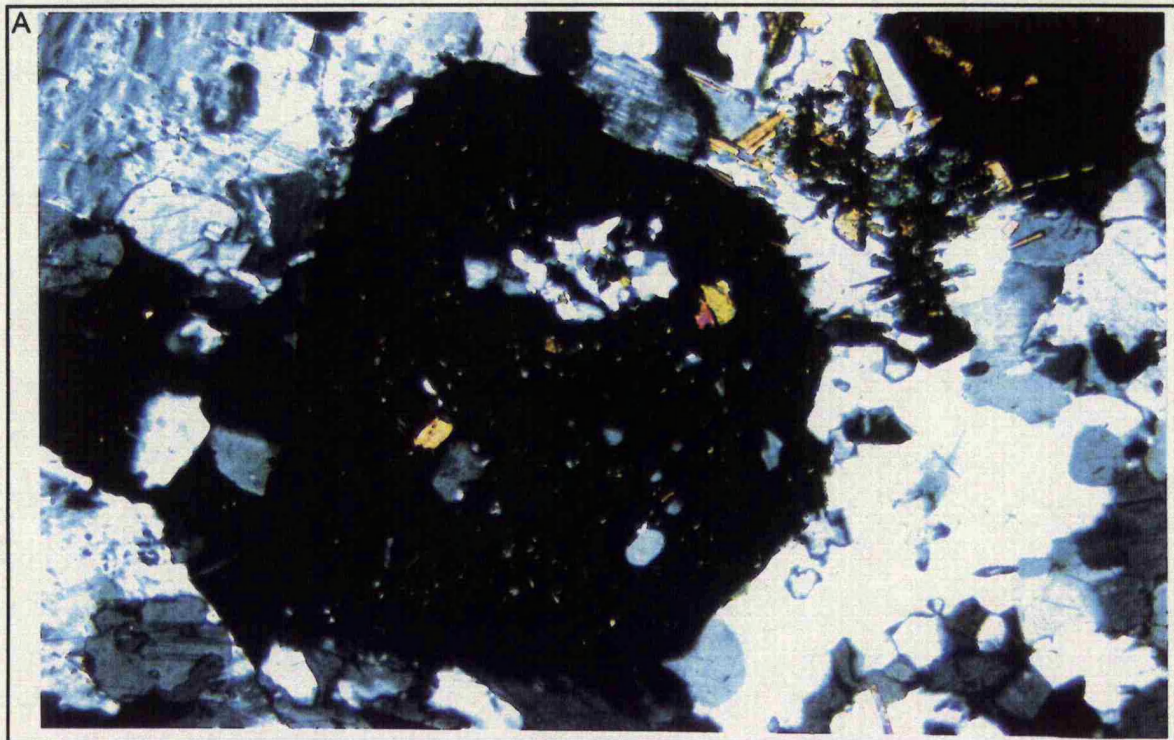


Fig. 5.1: Photomicrographs (crossed nicols): (A) fresh grains of nepheline (sample MK-3); (B) braided microperthite in microcline megacryst (sample SB-8).



0.5 mm

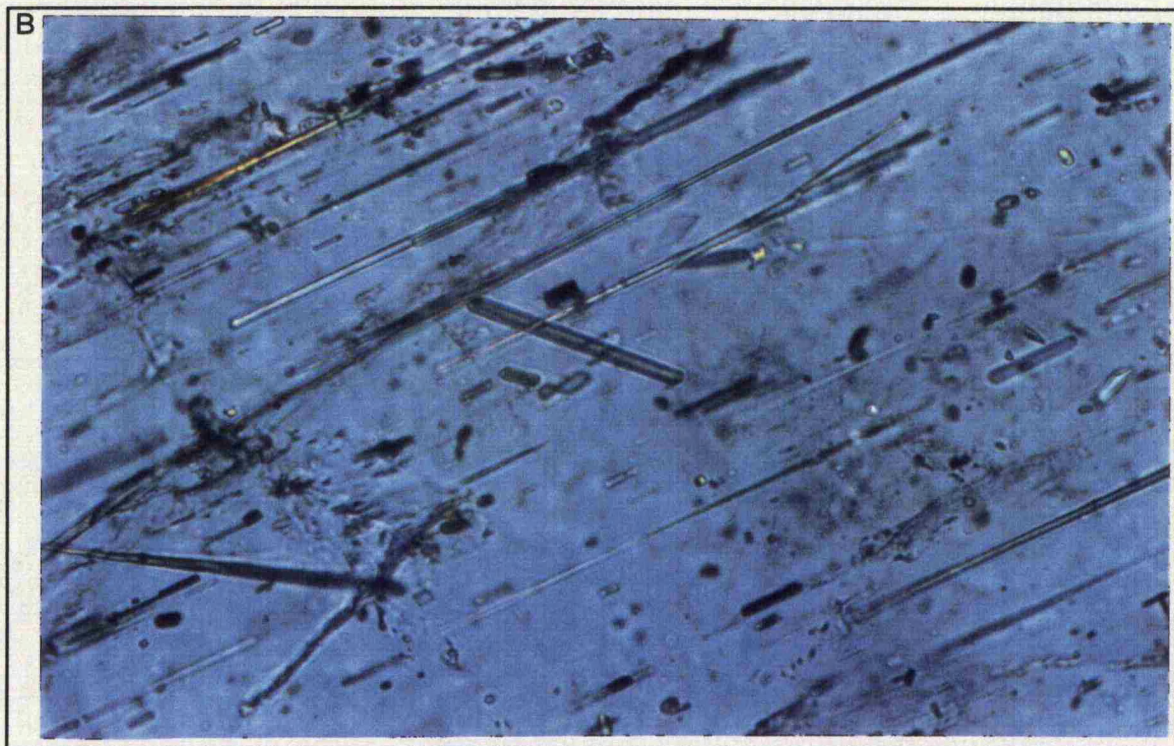


Fig. 5.2: Photomicrographs (crossed nicols): (A) nepheline megacryst enclosing albite crystal in ground mass of fine grained nepheline (sample BD-3); (B) (plane polarized light) needles like inclusions of apatite? and biotite (sample S-1).

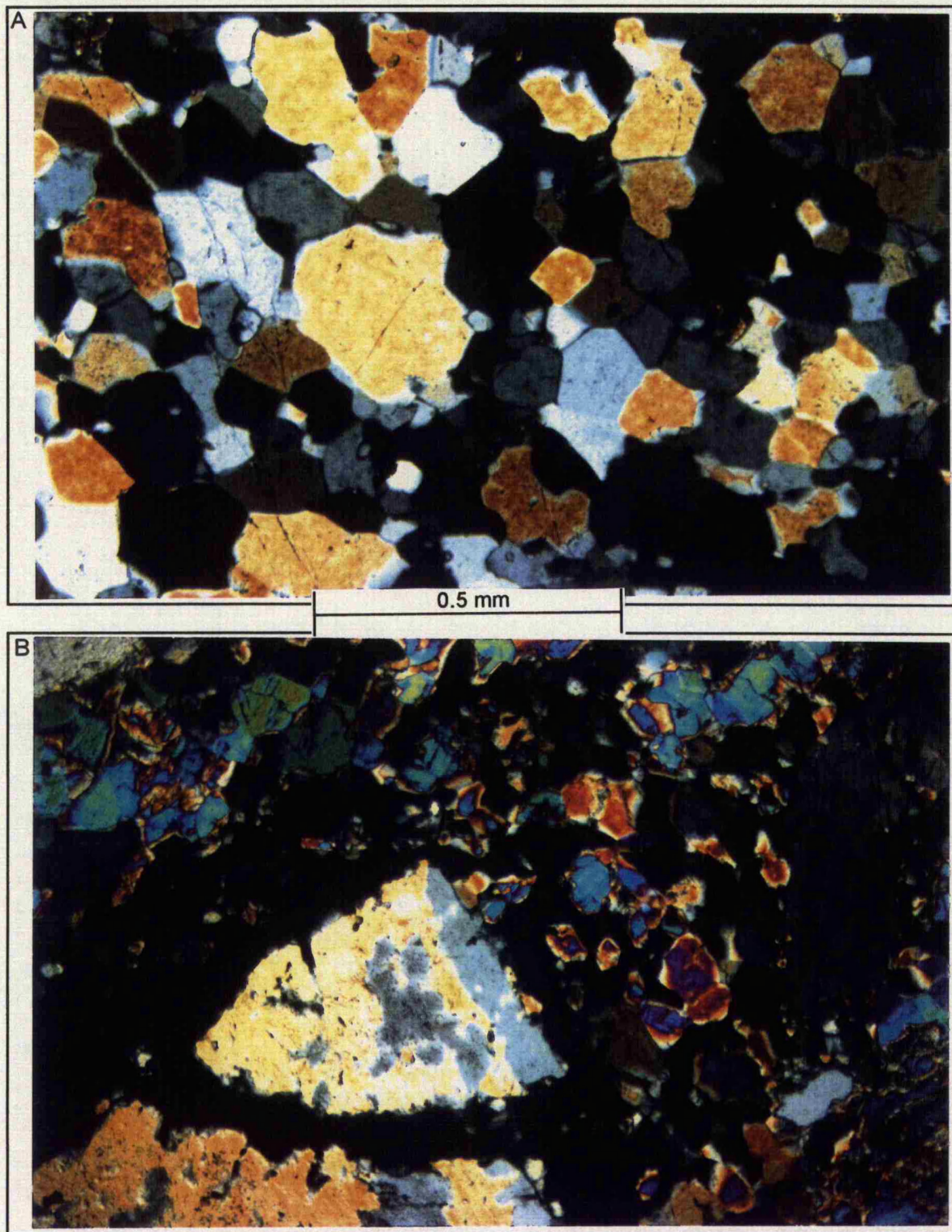


Fig. 5.3: Photomicrographs (crossed nicols): (A) grains of cancrinite (yellow), nepheline (grey) and sodalite (mainly very dark), crystals showing characteristic straight edges and 120° triple junctions (sample K-3); (B) fragments of feldspar and grains of cancrinite enclosed by sodalite (clusters of cancrinite and sodalite), (sample SB-1).

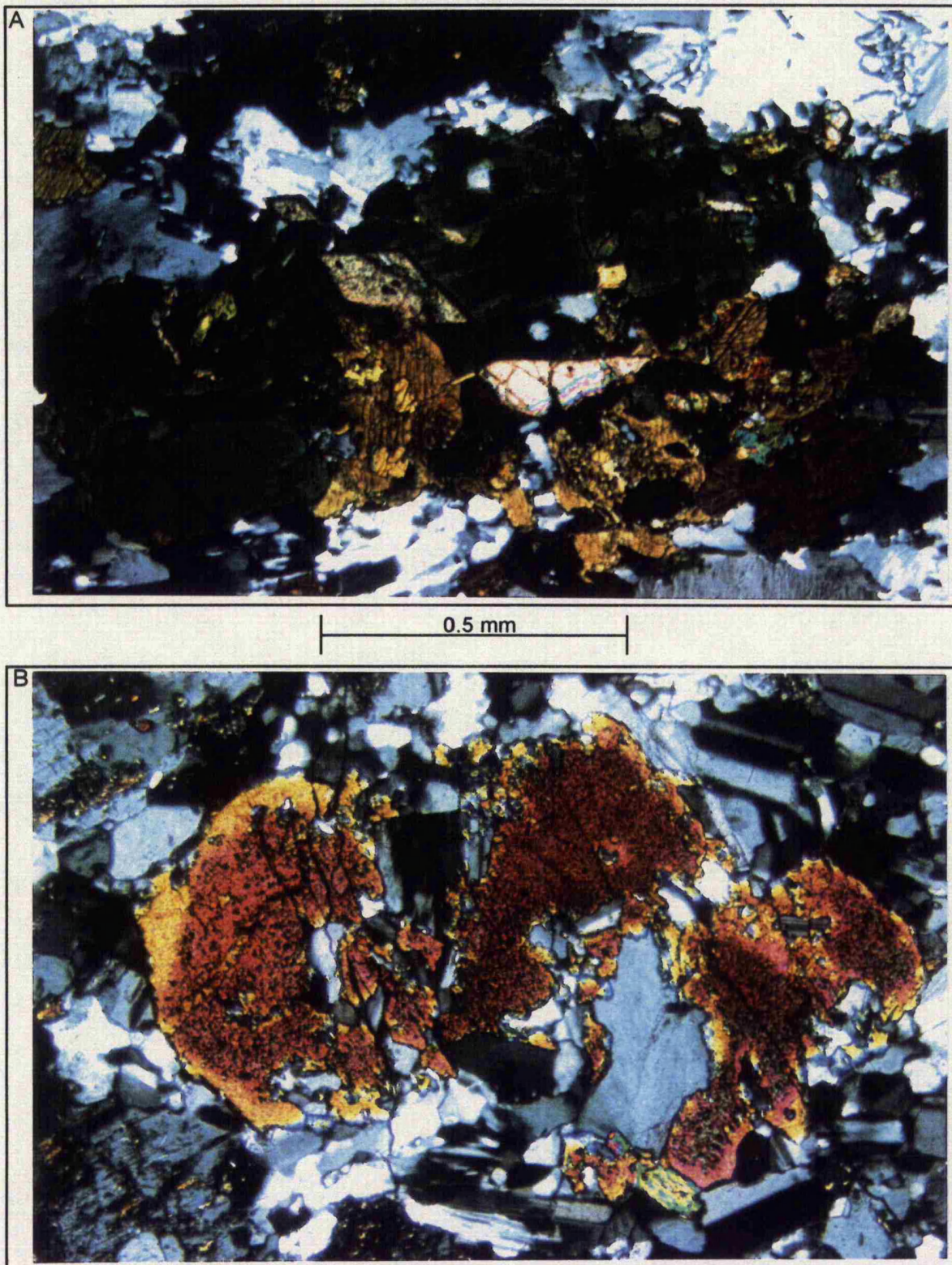


Fig. 5.4: Photomicrographs (crossed nicols): (A) mafic aggregates of biotite, pyroxene and sphene (sample BD-4); (B) aegirine phenocryst being replaced by later feldspar crystal (sample SB-15).

It is present in much more amount as mentioned by earlier workers (Siddiqui et al. 1967).

5.1.5 Sodalite

Subhedral grains of sodalite are present as replacive mineral along joints and enclose feldspars and cancrinite in some sections (Fig. 5.3b). It is also present as inclusions in the pegmatites and make up to 13 % in some sections.

5.1.6 Mafic Minerals

The mafic minerals occur as aggregates and clots (Fig. 5.4a). They are subhedral to euhedral and are of following types:

a) Pyroxene: Earlier workers described it as aegirine- augite (Siddiqui et al. 1968 and Khan et al. 1989) but it is aegirine. It is euhedral to subhedral and shows pleochroism and has typical perfect pyroxene cleavage. In some sections it is replaced by the later feldspar (Fig. 5.4b) It is also present as individual crystals in some thin sections. It is in between 2 to 3%.

b) Biotite: It is present in association with pyroxene in almost all the thin sections of the feldspathoidal syenite. It is subhedral to anhedral and its percentage varies from 1 to 4.

c) Sphene: Euhedral crystals of sphene occur mostly in association with other mafic minerals and occasionally as discrete crystals. It make up to 1% of the rock in some sections.

d) Iron Ore: It is mainly magnetite. In some sections, it is completely absent while in others it is up to 3% of the rock. It was suggested by the earlier worker to be ilmenite (Siddiqui et al. 1968).

e) Amphibole: It is present only one sample S-1, it was not recognised in the thin section as it resemble biotite. It was analysed in the microprobe and classified as amphibole.

Some minerals which are present in weathered rocks, are not described in this chapter.

Chapter Six

MINERALOGY

In this chapter the detailed mineralogy of the Koga feldspathoidal complex is described. The mineralogy was determined firstly by light microscopy followed by X-ray diffraction. Finally, the electron microprobe was used to determine the composition of different phases found in these rocks.

6.1 FELDSPARS

The Koga feldspathoidal syenite has a single highly exsolved feldspar, with a K-feldspar host. In a few rocks there is also a separate Na-feldspar hosted perthite.

6.1.1 Albites

The albites are unzoned and almost pure end members. They show very little solid solution between albite and K-feldspar. They are represented in terms of oxides percent with their standard deviation and cations proportions in Table 6.1.

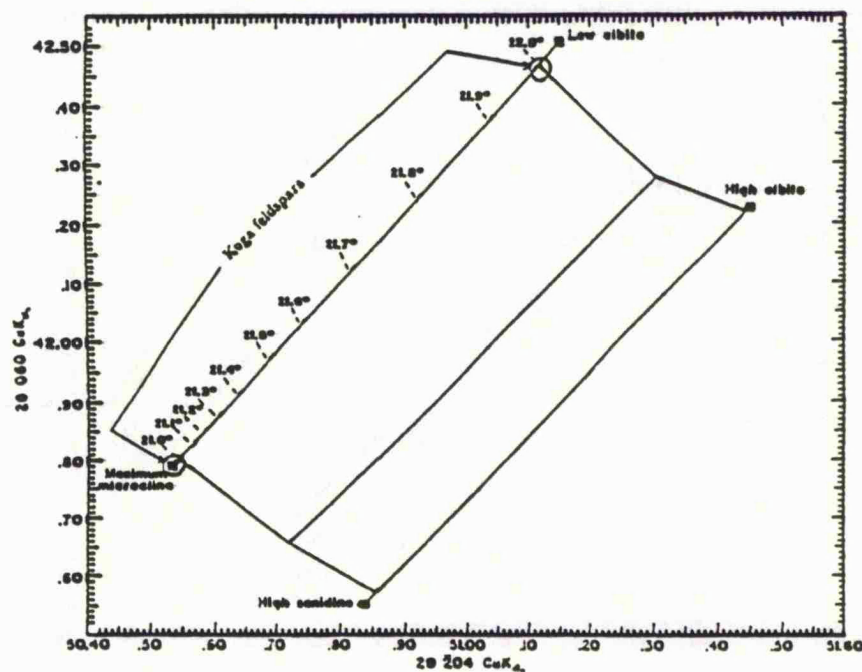


Fig. 6.1. Observed 2θ values of 060 plotted against observed 2θ values of 204 for feldspar after Wright, (1968).

Solid squares: Maximum microcline - low albite series Open circles: Koga feldspar.

Table 6.1

Microprobe analyses of albites from the Koga Complex

Rock Name	K1		K-2		K-3		K-4		K-5		K-6		K-8	
	mean	sd												
SiO ₂	68.89	0.34	68.64	0.33	68.61	0.36	68.69	0.38	68.84	0.19	68.64	0.32	68.51	0.25
Al ₂ O ₃	18.91	0.38	19.26	0.14	19.27	0.22	19.29	0.11	19.35	0.23	19.40	0.19	19.37	0.10
Na ₂ O	11.75	0.25	11.97	0.08	11.92	0.20	11.91	0.16	11.79	0.17	11.88	0.21	11.76	0.17
K ₂ O	0.12	0.03	0.11	0.04	0.11	0.05	0.13	0.04	0.12	0.12	0.10	0.06	0.19	0.20
Total No.	20		22		25		22		14		51		49	

No. of cations on the basis of 8 oxygens

Si	3.011	3.004	3.001	3.001	3.003	2.998	3.004
Al	0.974	0.989	0.993	0.994	0.995	0.999	0.993
Na	0.996	1.011	1.011	1.009	0.997	1.006	0.998
K	0.007	0.006	0.006	0.007	0.007	0.006	0.007

Rock Name	K-9		MK-1		MK-2		MK-3		MK-5		MK-6		MK-10	
	mean	sd												
SiO ₂	68.83	0.49	68.39	0.23	68.49	0.22	68.41	0.38	68.36	0.48	67.98	0.28	68.10	0.31
Al ₂ O ₃	19.30	0.19	19.19	0.10	18.86	0.09	19.19	0.10	19.22	0.24	19.27	0.09	19.35	0.11
Na ₂ O	11.80	0.10	11.84	0.08	11.79	0.08	11.80	0.10	11.82	0.12	11.76	0.10	11.72	0.10
K ₂ O	0.13	0.15	0.09	0.06	0.15	0.17	0.13	0.07	0.10	0.08	0.10	0.08	0.11	0.04
Total No.	23		19		31		22		21		58		22	

No. of cations on the basis of 8 oxygens

Si	2.998	3.001	3.013	3.001	3.001	2.996	2.996
Al	0.999	0.992	0.987	0.992	0.995	1.001	1.004
Na	0.998	1.008	1.006	1.003	1.006	1.005	1.000
K	0.011	0.005	0.008	0.007	0.007	0.006	0.006

Rock Name	MK-14		MK-16		MK-18		MK-20		MK-21		MK-24		MK-25	
	mean	sd												
SiO ₂	68.27	0.48	68.64	0.37	68.83	0.40	69.08	0.43	68.55	0.45	68.30	0.40	67.98	0.56
Al ₂ O ₃	19.39	0.30	19.41	0.15	19.31	0.19	19.28	0.14	19.29	0.16	19.21	0.09	19.25	0.14
Na ₂ O	11.65	0.10	11.96	0.14	11.59	0.49	11.81	0.11	11.71	0.12	11.66	0.08	11.63	0.10
K ₂ O	0.18	0.37	0.17	0.19	0.31	0.69	0.12	0.05	0.13	0.15	0.13	0.05	0.13	0.05
Total No.	36		49		88		33		21		29		15	

No. of cations on the basis of 8 oxygens

Si	2.997	2.996	3.005	3.007	3.003	3.003	2.999
Al	1.003	0.999	0.994	0.989	0.996	0.996	1.001
Na	0.992	1.012	0.981	0.997	0.994	0.994	0.995
K	0.010	0.009	0.017	0.007	0.007	0.007	0.007

(contd.) Table 6.1

Rock Name	SB-1		SB-5		SB-9		SB-11		SB-14		SB-15		S-1	
	mean	sd												
SiO ₂	69.09	0.24	69.19	0.40	68.53	0.21	68.79	0.41	68.78	0.34	68.68	0.25	68.84	0.25
Al ₂ O ₃	19.34	0.10	19.32	0.09	19.50	0.27	19.38	0.12	19.27	0.14	19.20	0.40	19.59	0.13
Na ₂ O	11.89	0.11	11.81	0.10	11.68	0.14	11.94	0.11	12.02	0.11	11.88	0.13	11.70	0.11
K ₂ O	0.10	0.10	0.08	0.08	0.28	0.16	0.11	0.09	0.14	0.07	0.11	0.04	0.13	0.04
Total No.	34		24		10		16		50		64		24	

No. of cations on the basis of 8 oxygens

Si	3.004	3.008	2.995	2.999	3.001	3.002	2.997
Al	0.991	0.990	1.005	0.996	0.991	0.989	1.006
Na	1.003	0.995	0.990	1.009	1.071	1.007	0.998
K	0.006	0.004	0.016	0.006	0.008	0.006	0.007

Rock Name	S-3		S-6		BD-1		BD-3		BD-4	
	mean	sd								
SiO ₂	68.50	0.25	69.02	0.34	69.13	0.25	68.82	0.36	68.48	0.35
Al ₂ O ₃	19.16	0.13	19.47	0.33	19.47	0.18	19.26	0.13	19.51	0.18
Na ₂ O	11.64	0.11	11.70	0.11	12.00	0.16	11.90	0.12	11.79	0.21
K ₂ O	0.18	0.10	0.16	0.08	0.10	0.04	0.09	0.04	0.18	0.15
Total No.	48		86		15		22		26	

No. of cations on the basis of 8 oxygens

Si	3.006	3.002	2.999	3.004	2.994
Al	0.991	0.998	0.996	0.991	1.005
Na	0.991	0.987	1.009	1.007	0.999
K	0.010	0.007	0.006	0.005	0.010

The composition and the structural state was determined by X-ray diffraction data using the 2θ values instead of cell parameters, method adopted by Wright, T. L. (1968). The composition of the feldspar is plotted in Fig. 6.1 which is maximum microcline and low albite.

The feldspars are plotted in the system $\text{AlSiO}_4\text{-KAlSiO}_4\text{-SiO}_2$ in Fig. 6.2 after Hamilton and MacKenzie (1965).

The feldspar cluster tightly around the end members with a little variation which reflects the high degree of exsolution and low temperature reorganization.

The Fe, Ba and Sr oxides were looked for in the feldspars but these were below detection limits.

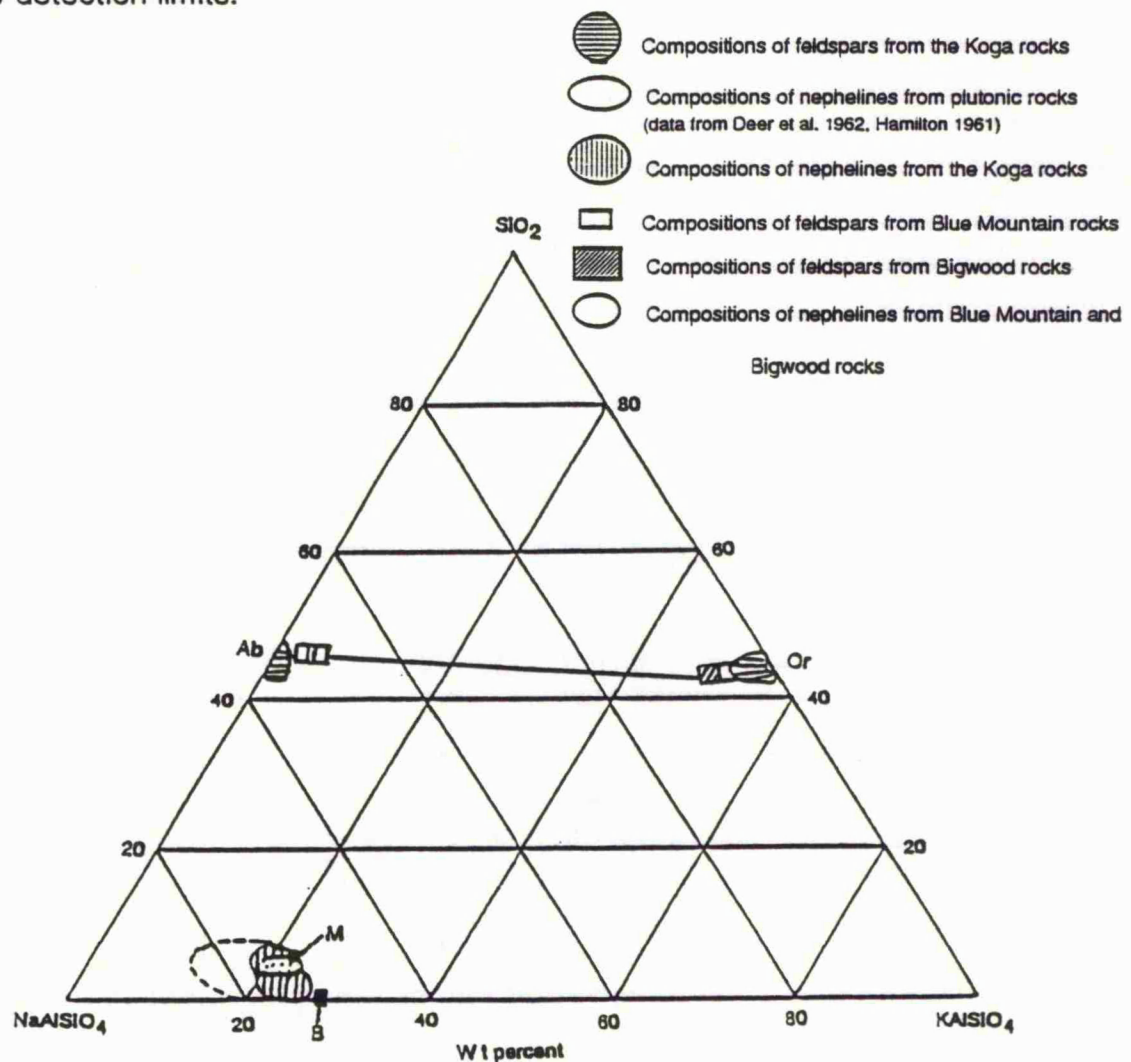


Fig. 6.2. Compositions of nephelines and feldspars from the Koga feldspathoidal syenites, Blue Mountain and Bigwood complexes plotted on the system $\text{NaAlSiO}_4\text{-KAlSiO}_4\text{-SiO}_2$ M and B are Morozewics and Buerger compositions.

Table 6.2

Microprobe analyses of K-feldspars from the Koga Complex

Rock Name	K-1		K-2		K-3		K-4		K-5		K-6		K-8	
	mean	sd												
SiO ₂	64.68	0.19	64.62	0.29	64.55	0.38	64.68	0.28	64.69	0.27	64.62	0.39	64.51	0.18
Al ₂ O ₃	18.51	0.11	18.17	0.11	18.14	0.32	18.17	0.07	18.14	0.19	18.47	0.47	18.26	0.17
Na ₂ O	0.68	0.13	0.42	0.13	0.40	0.14	0.47	0.17	0.48	0.32	0.33	0.10	0.58	0.13
K ₂ O	15.77	0.27	16.37	0.21	16.17	0.39	16.29	0.25	16.54	0.20	16.49	0.40	16.28	0.22
Total No.	24		19		13		16		12		11		28	

No. of cations on the basis of 8 oxygens

Si	2.993	3.002	3.004	3.002	3.001	2.993	2.996
Al	1.009	0.995	0.995	0.994	0.992	1.008	1.000
Na	0.061	0.038	0.036	0.042	0.043	0.030	0.052
K	0.931	0.970	0.960	0.965	0.979	0.974	0.965

Rock Name	K-9		MK-1		MK-2		MK-3		MK-5		MK-6		MK-10	
	mean	sd												
SiO ₂	65.01	0.27	64.42	0.16	64.38	0.14	64.37	0.25	64.54	0.34	64.00	0.50	62.80	0.31
Al ₂ O ₃	18.23	0.17	18.16	0.19	18.70	0.09	18.08	0.24	18.09	0.26	18.16	0.04	18.43	0.10
Na ₂ O	0.60	0.10	0.51	0.13	0.49	0.13	0.47	0.08	0.49	0.15	0.48	0.02	0.73	0.16
K ₂ O	16.30	0.40	16.19	0.09	15.66	0.15	16.22	0.19	16.10	0.32	15.66	0.37	15.13	0.31
Total No.	11		12		17		16		24		6		19	

No. of cations on the basis of 8 oxygens

Si	3.002	3.000	2.989	3.002	3.005	3.002	2.981
Al	0.992	0.997	1.024	0.993	0.993	1.004	1.031
Na	0.054	0.046	0.044	0.042	0.044	0.044	0.067
K	0.960	0.962	0.928	0.965	0.956	0.937	0.916

Rock Name	MK-14		MK-16		MK-18		MK-20		MK-21		MK-24		MK-25	
	mean	sd												
SiO ₂	64.47	0.33	64.25	0.35	64.79	0.24	64.46	0.35	64.32	0.13	64.06	0.31	64.08	0.25
Al ₂ O ₃	18.79	0.42	18.30	0.16	18.24	0.11	18.08	0.28	18.18	0.13	18.11	0.13	18.17	0.07
Na ₂ O	0.28	0.19	0.52	0.14	0.53	0.18	0.40	0.09	0.45	0.08	0.36	0.07	0.59	0.14
K ₂ O	15.75	0.31	15.91	0.25	16.21	0.47	15.92	0.19	16.10	0.14	16.21	0.29	15.85	0.30
Total No.	11		28		26		14		7		32		10	

No. of cations on the basis of 8 oxygens

Si	2.990	2.997	3.001	3.008	3.000	3.000	2.996
Al	1.027	1.006	0.996	0.995	1.000	1.000	1.001
Na	0.025	0.047	0.048	0.036	0.041	0.033	0.054
K	0.932	0.947	0.958	0.948	0.958	0.968	0.945

(contd.) Table 6.2

Rock Name	SB-1		SB-5		SB-11		SB-14		S-1		S-3		S-6	
	mean	sd												
SiO ₂	64.55	0.38	64.10	0.32	64.58	0.26	64.79	0.30	64.34	0.27	63.84	0.50	65.16	0.33
Al ₂ O ₃	18.21	0.16	18.19	0.14	18.18	0.12	18.17	0.18	18.46	0.12	18.17	0.36	18.44	0.14
Na ₂ O	0.51	0.13	0.47	0.07	0.51	0.13	0.57	0.10	0.71	0.09	0.54	0.12	0.63	0.15
K ₂ O	15.77	0.22	15.73	0.18	16.07	0.33	15.96	0.18	15.66	0.22	15.82	0.29	16.60	0.17
Total No.	21		9		15		23		16		49		14	

No. of cations on the basis of 8 oxygens

Si	3.005	3.001	3.003	3.006	2.997	2.997	2.994
Al	0.999	1.004	0.997	0.994	1.012	1.006	0.999
Na	0.046	0.043	0.046	0.051	0.064	0.049	0.056
K	0.937	0.940	0.953	0.954	0.929	0.947	0.973

Rock Name	BD-1		BD-3		BD-4	
	mean	sd	mean	sd	mean	sd
SiO ₂	65.08	0.19	64.73	0.20	64.53	0.32
Al ₂ O ₃	18.23	0.12	18.17	0.09	18.66	0.13
Na ₂ O	0.57	0.10	0.57	0.06	0.52	0.09
K ₂ O	16.09	0.20	15.85	0.14	15.46	0.22
Total No.	10		16		19	

No. of cations on the basis of 8 oxygens

Si	3.006	3.006	2.994
Al	0.993	0.995	1.021
Na	0.051	0.051	0.047
K	0.948	0.939	0.915

The Koga complex has a number of intrusions which are Na rich. The albite composition varies from Ab₁₀₀ to Ab₉₈.

6.1.2 K-feldspars

These are also almost pure end members with a composition Or₁₀₀ to Or₉₅. These microcline microperthites are very well developed and were developed by slow cooling of the magma.

The K-feldspars have low iron contents; the maximum percentage is 0.14 as FeO. However, in most of the K-feldspars, the iron is below detection limits. The composition of K-feldspars is shown in Fig 6.1, 6.2 and the oxide percent with their standard deviation in Table 6.2.

The alkali feldspars from the least evolved syenites of Pic Islands, Canada are homogeneous and vary in composition from Or₂₈Ab₆₈An₄ to Or₄₅Ab₅₃An₁. The feldspars from the more evolved rocks of Redsucker Cove, range in composition from Or₅₆Ab₄₂An₂ to Or₈₂Ab₁₈, whereas, the homogeneous feldspars vary from Or₅₀Ab₅₀ to Or₇₀Ab₃₀ (Mitchell et al. 1982).

The cumulus alkali feldspar from the Igdlertfigssalik nepheline syenite do not show a clear trend of compositional variation (Powell, 1978).

Feldspars from the nepheline syenite gneisses and pegmatites of Blue Mountain and Bigwood alkaline complexes of Ontario, Canada have less than 5 wt % An, whereas, those from amphibolite lenses have An_{6–12}. Or and Ab contents in the both the complexes of Blue Mountain and Bigwood are Or_{90–94}, Ab_{93–97} and Or_{88–91}, Ab_{93–97} respectively shown in the Fig. 6.2.

In Tenerife, Canary Islands, the non-exsolved feldspars in the nepheline syenites lie in the range Or_{36–Or49} (Wolf, 1987).

6.2 Nepheline

Analyses of the nephelines from the Koga feldspathoidal syenite complex are given in Table 6.3, calculated on the basis of 4 oxygens.

The nepheline analyses are plotted in the Ne – Ks – Qz system at P H₂O 1000 Kg/cm² after Hamilton and MacKenzie (1965) in Fig. 6.2, showing the composition of analysed nephelines and feldspars in the feldspathoidal syenite.

There is a little variation in nepheline composition from the Koga feldspathoidal syenite complex, although they show some variation in the Na:K ratio. This does not show ideal ratio of 3:1 due to the excess of ions such as SiO₂ and K₂O.

All nephelines under favourable conditions tend to approach the Morozewicz – Buerger convergence field (Tilley, 1954). This is a stable composition in which Na and Ca fill six out of eight alkali sites in the unit cell. In natural nephelines the remaining two larger sites reject Na and Ca and accommodate K so that a structural defect is induced. The degree of omission of solid solutions or vacancies in the nephelines structure increases with temperature and this chemical behaviour is reflected by the excess Si content in the composition of the phase (Bose, 1970). The amount of normative quartz (Hamilton, 1961) or albite in the solid solution may be possible indicator of the crystallisation temperature of the mineral.

The nephelines show an excess of Si and a deficiency of Al. The greater excesses of silica over that required by stoichiometry indicate temperatures in the general range of 750 to 950 °C (Hamilton, 1961): but the nephelines under study do not show much excess of Si, and these were not formed at such high temperatures but probably at temperature lower than 750 °C.

Morozewicz (1928) was strongly in the favour of the theory of constant chemical composition not related to the host rocks; whereas Bowen and Ellestad (1936) attributed the change in composition of nepheline to the host rocks. Miyashiro (1951) found a narrow range of chemical variation in nephelines from the plutonic rocks and pointed out that physical control plays an important role in

restricting the composition range. He also pointed out a great variation in the composition of nephelines from volcanic rocks (formed at high temperature).

Tilley (1954) has shown that composition of nepheline of subsolvus types is restricted to the Morozewicz – Buerger convergence field; whereas in the hypersolvus types, the composition of nephelines depend on the bulk composition of the rock.

The composition of nepheline from the Koga complex ($Ne_{80}Ks_{20}Qz_0$ to $Ne_{80}Ks_{15}Qz_5$) lie inside the Morozewicz – Buerger convergence field of plutonic nephelines (Tilley, 1954) and shows a limited range of solid solution as defined by Hamilton (1961), indicating that the Koga nephelines crystallized or recrystallized over a narrow range of temperature. The nephelines equilibration temperatures are consistent with the slow cooling or annealing at lower temperature. This must be followed by the relatively slow equilibration of nepheline to compositions within Morozewicz – Buerger field as found in other nepheline syenite complexes (Tilley, 1954).

The compositions of nephelines from different complexes of the world plot more or less in the same field as those from the Koga feldspathoidal syenite, only the nepheline from Blue Mountain and Bigwood complexes are plotted in Fig. 6.2.

6.3 Pyroxenes

Na – rich clinopyroxenes occur in most of the rocks. Analyses of pyroxenes are given in Table 6.4 calculated on the basis of 6 oxygens and 4 cations.

The nomenclature used in describing the pyroxenes follows that recommended by the International Mineralogical Association Subcommittee on Pyroxenes, Morimoto, (1988), see Fig. 6.3.

The Na – rich pyroxenes are aegirine (Ae) – jadeite (Jd) Fig. 6.3. The composition varies from $Ae_{75}Jd_{25}$ to $Ae_{80}Jd_{20}$. The aegirines are relatively unzoned and show variation in its Na_2O contents from 12.54 to 14.14 wt %, Al_2O_3

Table 6.3

Microprobe analyses of nephelines from the Koga Complex

Rock Name	K-2		K-6		K-8		K-9		MK-2		MK-5		MK-6	
	mean	sd												
SiO ₂	43.34	0.55	42.17	0.50	41.89	0.45	42.50	0.36	41.13	0.87	42.05	0.37	41.25	0.29
Al ₂ O ₃	33.79	0.43	32.73	0.35	34.33	0.34	34.10	0.72	33.21	0.82	34.39	0.67	34.19	0.17
Na ₂ O	16.70	0.59	16.53	0.27	16.18	0.21	16.56	0.38	15.99	0.37	16.36	0.10	16.17	0.15
K ₂ O	6.31	0.36	7.04	0.35	7.33	0.16	6.21	0.52	6.72	0.65	7.43	0.26	7.08	0.22
Total No.	10		29		11		18		7		5		18	

No. of cations on the basis of 4 oxygens

Si	1.040	1.017	1.016	1.028	1.023	1.016	1.011
Al	0.956	0.981	0.982	0.973	0.974	0.980	0.988
Na	0.777	0.773	0.761	0.777	0.771	0.767	0.769
K	0.193	0.217	0.227	0.192	0.213	0.229	0.221

Rock Name	MK-16		MK-18		MK-24		MK-25		SB-1		SB-11		SB-14	
	mean	sd												
SiO ₂	42.04	0.10	42.67	0.49	41.64	0.24	42.08	0.92	42.26	0.56	42.38	0.32	42.37	0.49
Al ₂ O ₃	34.47	0.14	33.87	0.73	34.17	0.12	34.02	0.48	33.99	0.67	34.04	0.53	34.13	0.45
Na ₂ O	16.54	0.06	16.38	0.61	16.10	0.11	16.16	0.16	16.43	0.25	16.54	0.21	16.51	0.24
K ₂ O	7.31	0.07	7.18	0.67	7.32	0.24	7.04	0.34	6.99	0.34	7.30	0.21	7.05	0.37
Total No.	7		7		18		15		12		13		14	

No. of cations on the basis of 4 oxygens

Si	1.015	1.030	1.016	1.023	1.024	1.023	1.023
Al	0.980	0.964	0.983	0.975	0.971	0.969	0.972
Na	0.774	0.767	0.761	0.762	0.772	0.774	0.773
K	0.225	0.221	0.228	0.218	0.216	0.225	0.217

Rock Name	S-1		S-3		S-6		BD-1		BD-3		BD-4	
	mean	sd										
SiO ₂	44.59	0.54	41.73	0.49	42.53	0.40	42.66	0.42	40.44	0.22	44.31	0.52
Al ₂ O ₃	33.74	0.21	33.81	0.38	34.47	0.32	33.96	0.53	34.59	0.29	33.34	0.34
Na ₂ O	16.38	0.14	15.89	0.11	16.10	0.15	16.61	0.13	16.66	0.24	16.92	0.20
K ₂ O	6.49	0.58	7.29	0.16	7.47	0.21	7.00	0.47	6.41	0.24	5.74	0.43
Total No.	6		4		19		11		7		19	

No. of cations on the basis of 4 oxygens

Si	1.055	1.022	1.023	1.028	0.997	1.057
Al	0.941	0.976	0.977	0.965	1.005	0.938
Na	0.760	0.755	0.751	0.776	0.796	0.783
K	0.198	0.228	0.228	0.215	0.202	0.175

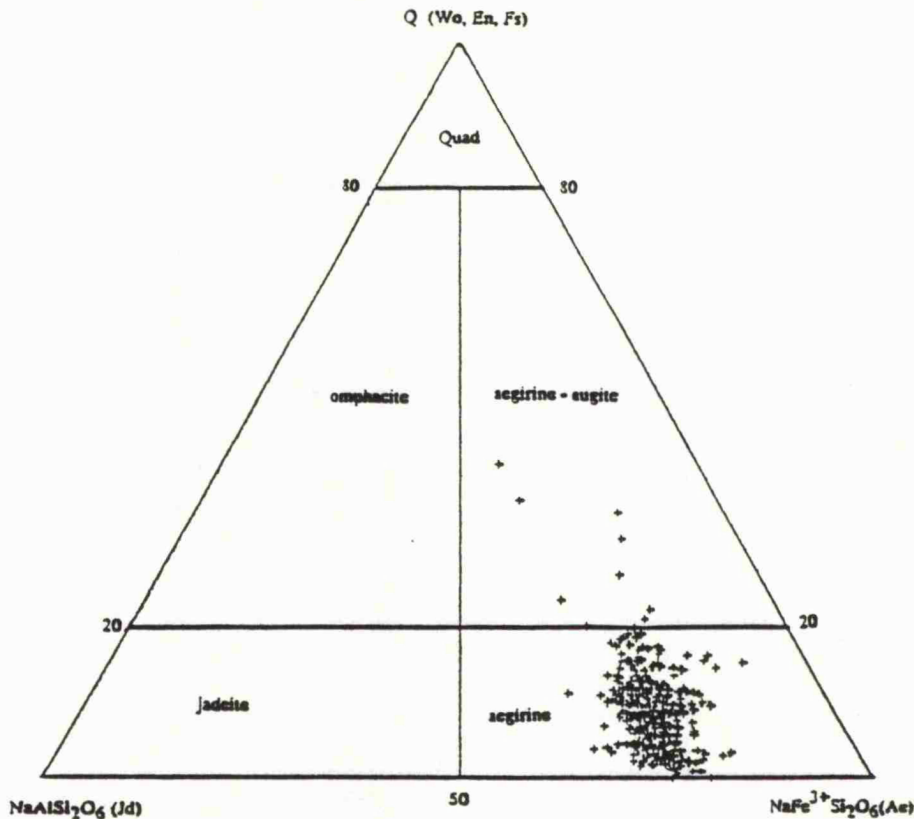


Fig 6.3 Ca – Mg – Fe and Na pyroxenes with accepted names. Quad represents the Ca–Mg-Fe pyroxenes area.

contents, 3.90 to 5.41 wt %, CaO 0.35 to 3.05 wt % and MgO from 0.00 to 0.93 wt %.

The Q [wollastonite (Wo), enstatite (En), ferrosilite (Fo)] contents are from Q_0 to Q_{42} , Fig. 6.3 which are aegirine – augite in composition but there are not more than 10 points in the field of aegirine – augite.

In Fig. 6.4 pyroxenes from the Koga feldspathoidal syenite are plotted on the Ae+Jd – Di – Hd instead of the usual plot of Ac – Di – Hd. These analyses mostly plot on the Ae – Jd – Di line and very few on the hedenbergite join. Pyroxenes show a typical peralkaline trend, (Yoder and Tilley, 1962). The data indicates that the compositional range mostly remain in the aegirine field.

Cumulus pyroxenes from the Igdlertfigssalik nepheline syenite intrusion, Greenland are essentially $\text{CaMgSi}_2\text{O}_6$ – $\text{CaFeSi}_2\text{O}_6$ solid solutions with varying

amounts of Ti, Zr, Mn and Al as minor amounts, whereas the acmite contents are low, Powell, (1978) Fig. 6.5.

Table 6.4

Microprobe analyses of aegirine from the Koga Complex

Rock Name	K-3		K-4		K-5		K-6		K-8		MK-2		MK-5	
	mean	sd												
SiO ₂	53.48	0.55	53.78	0.23	53.23	0.85	53.47	0.80	53.53	0.31	53.20	0.66	53.84	0.43
Al ₂ O ₃	3.90	1.30	4.69	0.58	4.84	0.78	5.13	0.71	5.46	0.75	4.88	0.66	5.40	0.47
FeO	25.16	1.32	23.71	0.85	23.84	0.72	24.48	1.05	22.61	1.03	22.54	0.69	23.26	0.62
MnO	0.20	0.08	0.22	0.11	0.18	0.07	0.22	0.19	0.29	0.25	0.11	0.08		0.00
MgO	0.52	0.26	0.73	0.42	0.43	0.16	0.13	0.11	0.59	0.25		0.00	0.12	0.07
CaO	1.44	0.57	2.15	0.85	1.56	0.36	0.55	0.18	2.08	0.81	0.35	0.33	0.52	0.12
Na ₂ O	13.63	0.41	13.03	0.35	13.37	0.41	13.99	0.44	12.86	0.34	13.94	0.42	14.14	0.16
Total No.	32		8		10		29		28		7		23	

No. of cations on the basis of 6 oxygens and total of 4 cations

Si	1.980	1.992	1.985	1.977	1.997	2.019	1.996
Al	0.170	0.205	0.212	0.223	0.240	0.218	0.236
Fe ₂	0.000	0.009	0.000	0.003	0.017	0.018	0.000
Fe ₃	0.779	0.725	0.743	0.754	0.689	0.698	0.721
Mn	0.006	0.007	0.006	0.007	0.009	0.004	0.000
Mg	0.029	0.040	0.024	0.007	0.033	0.002	0.007
Ca	0.057	0.085	0.063	0.022	0.083	0.014	0.020
Na	0.978	0.936	0.966	1.003	0.930	1.025	1.016

Rock Name	MK-6		MK-10		MK-21		SB-1		SB-5		SB-14		S-3	
	mean	sd												
SiO ₂	53.16	0.41	53.05	0.35	53.09	0.79	53.44	0.44	53.64	0.33	54.05	0.72	52.68	0.47
Al ₂ O ₃	5.41	0.85	4.93	0.60	4.88	0.87	4.07	0.42	4.25	0.39	4.75	1.59	5.32	0.61
FeO	22.38	1.03	23.09	0.74	22.01	0.87	23.83	0.63	24.06	0.66	22.98	4.83	20.38	0.57
MnO	0.19	0.07	0.27	0.09	0.42	0.12	0.35	0.08	0.30	0.06	0.73	0.24	0.37	0.08
MgO	0.32	0.18	0.51	0.29	0.93	0.24	0.72	0.41	0.40	0.12	0.32	0.10	0.89	0.20
CaO	1.38	0.39	2.11	0.68	2.77	0.72	2.54	0.48	1.79	0.42	1.37	0.58	3.05	0.44
Na ₂ O	13.53	0.28	13.10	0.52	12.73	0.45	12.99	0.59	13.48	0.29	13.68	0.43	12.54	0.31
Total No.	34		19		34		7		4		36		19	

No. of cations on the basis of 6 oxygens and total of 4 cations

Si	1.994	1.986	1.991	1.988	1.989	1.999	2.003
Al	0.239	0.217	0.220	0.178	0.186	0.206	0.238
Fe ₂	0.001	0.002	0.000	0.010	0.000	0.008	0.000
Fe ₃	0.701	0.721	0.689	0.731	0.746	0.703	0.648
Mn	0.006	0.008	0.013	0.011	0.009	0.023	0.012
Mg	0.018	0.029	0.051	0.040	0.022	0.018	0.050
Ca	0.055	0.085	0.107	0.101	0.071	0.055	0.124
Na	0.984	0.951	0.928	0.937	0.969	0.981	0.924

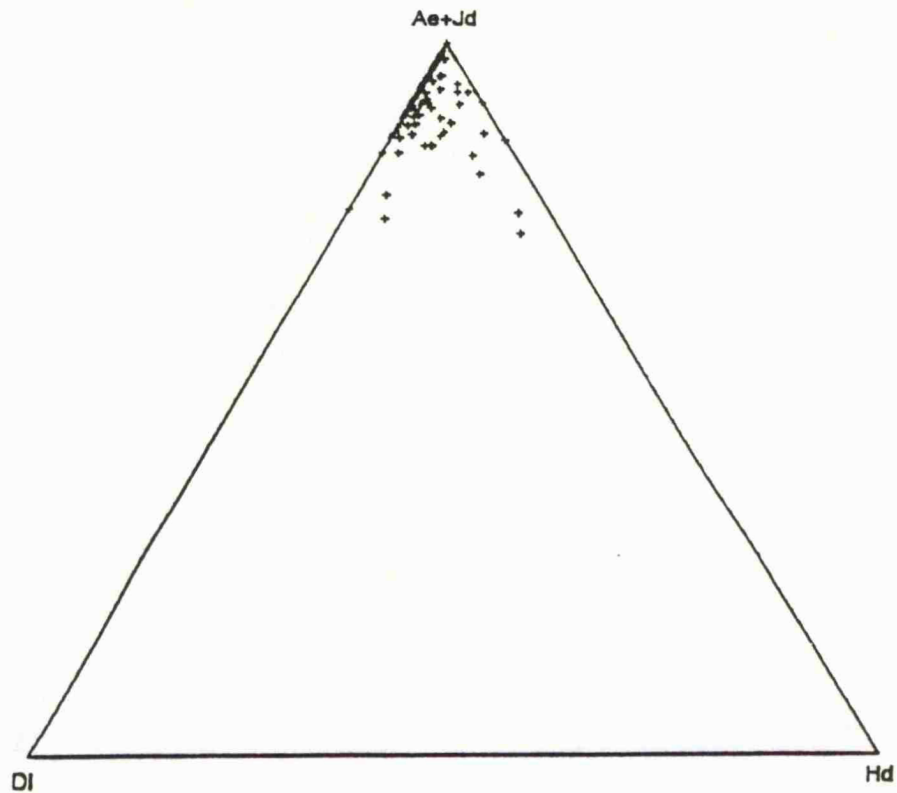


Fig. 6.4 Pyroxenes from the Koga feldspathoidal complex plotted on Ae + Jd - Di - Ac system.

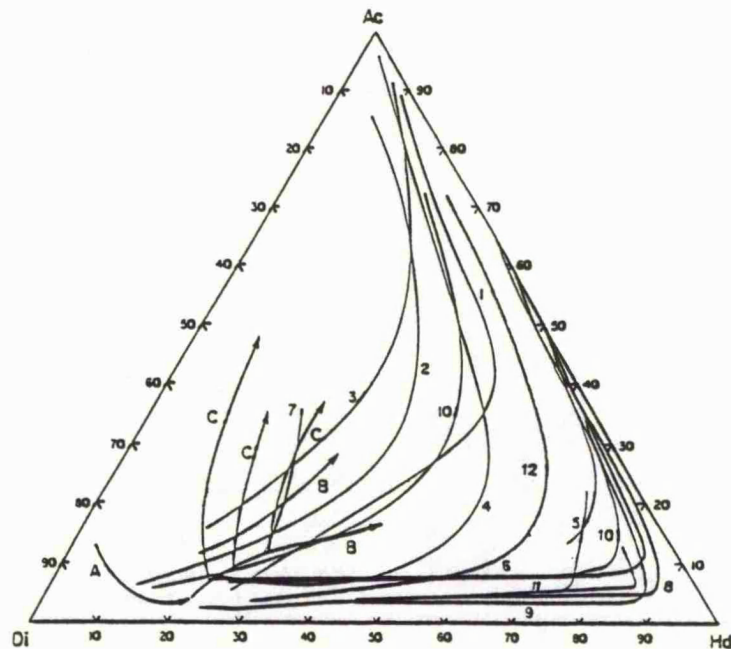


Fig. 6.5 Overall compositional trends of pyroxene compositions in the nepheline syenites compared with pyroxene compositional trends from other alkaline rocks (Published data). 1, Morotu (Yagi, 1953). 2, Uganda (Tyler & King, 1967). 3, Itapirapua (Gomes et al. 1970). 4, South Qoroq (Stephenson, 1972). 5, pantellerite (Nicholls & Carmichael, 1969. 6, Nandewar (Abbott, 1969). 7, Iron Hill (Nash, 1972). 8, Ilimaussaq (Larsen, 1976). 9, Coldwell ferroaugite syenite (Mitchell & Platt, 1978). 10, Igdlertfigssalik Centre (Powell, 1978). 11, Klokken complex (Parson, 1979). 12, Coldwell nepheline syenite (Mitchell & Platt, 1982). A, B, C, Fen (Mitchell, 1980).

Pyroxenes from the South Qoroq Centre, south Greenland are sodic and show existence of continuous solid solution series between compositions of $\text{Di}_{69}\text{Hd}_{25}\text{Ac}_6$ and $\text{Di}_6\text{Hd}_{17}\text{Ac}_{77}$. This trend further extends by aegirine and acmite from the pegmatites and by secondary acmites, which show range from $\text{Di}_4\text{Hd}_{10}\text{Ac}_{86}$ to Ac_{100} , Stephenson, (1972) Fig. 6.5.

The overall compositional trend of Tugtutoq Older Giant complex, south Greenland is comparable to those obtained from Si-undersaturated Igaliko Centre (Stephenson, 1972; Chambers, 1976; Powell, 1987; Jones, 1982) with a continuous variation from $\text{Di}_{69}\text{Hd}_{27}\text{Ac}_4$ to $\text{Di}_2\text{Hd}_2\text{Ac}_{96}$, (Upton et al. 1985).

Pyroxenes in the Coldwell Alkaline complex, Ontario, Canada show a wide range of composition. Most of the augite and ferroaugite having less than 15 mol. % acmite and plot close to the diopside hedenburgite join. Fig 6.5. Whereas majority of magnesian pyroxenes found in the layered syenite on Pic island plot along a trend of increasing Fe with out accompanying increase in Na_2O from $\text{Ac}_{10}\text{Hd}_{20}\text{Di}_{70}$ to $\text{Ac}_{10}\text{Hd}_{75}\text{Di}_{15}$, Mitchell et al. (1982).

Overall compositional trends of pyroxene compositions in the nepheline syenites are compared with pyroxene compositional trends from other alkaline rocks in Fig. 6.5.

6.4 Biotite

Biotite is present in all the rocks of the Koga feldspathoidal syenite complex. The analyses are given in Table 6.5, calculated on the basis of 22 oxygens, with total iron as FeO.

All the analyses gave Al + Si in Z total as suggested by Deer, Howie and Zussman, (1992), in the range of 7.87 – 9.117, mean 8.538. Only one analysis showed $\text{Al}+\text{Si} < 8$, i.e. 7.87, whereas all the others have $\text{Al}+\text{Si} > 8$. Deficiency of similar order in $\text{Al}+\text{Si}$ for alkaline rocks were reported by Nockolds, (1947), and Nash and Wilkinson, (1970).

The biotites from the Koga complex are relatively rich in alumina ($\text{Al}_2\text{O}_3 = 14.22 - 19.02$ wt. %), mostly the range is 14 – 15 wt. %.

In the majority of the biotites TiO_2 is between 1 and 2 wt %, but only in one sample it is up to 3.24 wt. %. It is interesting to note that TiO_2 has a significant negative correlation with MgO.

The biotites are plotted (Fig. 6.6) in the field outlined by Deer et al. (1992 p.298) to evaluate the composition, which gave four distinct groups as follows:

- a). $\text{An}_{70}\text{Sd}_{30}$ to $\text{An}_{60}\text{Sd}_{40}$ with 0 to 5 % phlogopite.
- b). $\text{An}_{80}\text{Sd}_{20}$ to $\text{An}_{65}\text{Sd}_{35}$ with 5 to 15 % phlogopite.
- c). $\text{An}_{95}\text{Sd}_5$ to $\text{An}_{73}\text{Sd}_{27}$ with 15 to 30 % phlogopite.
- d). $\text{An}_{90}\text{Sd}_{10}$ to $\text{An}_{73}\text{Sd}_{27}$ with 30 to 50 % phlogopite.

A major problem in the analyses of biotites by EMPA lies in the difficulty of assessing the relative amounts of FeO and Fe_2O_3 . However, examination of the cation proportion and charge balance shown in Table 6.5 suggests that most of the iron is present as Fe^{2+} . Thus these biotites differ from those given by Heinrich, (1946), quoted by Speer, (1984), (Fig. 30) where one group of biotites from the nepheline syenites has mostly equal proportion of FeO and Fe_2O_3 . When plotted on the triangle MgO – (total Fe as) FeO – Al_2O_3 after Nockolds, (1947) from the igneous rocks, Fig. 6.7 it gave more or less trend of biotites associated with other mafic minerals.

Al contents are constant in biotites from Mongolowe and Chaone, Chilwa Province, Malawi and are Mg - rich (Woolley et al. 1986). The Koga feldspathoidal syenite complex, biotites are neither Mg - rich nor Al contents constant. Al contents vary from 2.655 to 3.669 and Fe₂ : Mg ratios from ∞ to 2.02.

In Fig. 6.8, biotites from the Koga feldspathoidal syenite complex are plotted in Mg - Al - Fe₂ which shows a different trend from Shonkin Sag (Nash and Wilkinson, 1970), Kungnat Fjeld (Stephenson and Upton, 1982).

Table 6.5

Microprobe analyses of biotites from the Koga Complex

Rock Name	K-2		K-3		K-4		K-5		K-6		K-8		K-9	
	mean	sd												
SiO ₂	35.95	0.25	33.80	0.75	33.90	0.60	33.37	0.79	32.96	0.87	33.59	0.42	32.82	0.97
TiO ₂	2.21	0.19	2.19	0.13	1.48	0.12	1.53	0.05	1.64	0.24	1.39	0.07	1.64	0.68
Al ₂ O ₃	18.59	0.42	14.87	0.59	14.64	0.47	15.52	0.39	15.11	0.47	14.97	0.25	19.20	0.82
FeO	22.94	0.98	27.91	0.93	29.46	0.83	28.91	0.43	28.86	1.30	27.73	0.35	28.50	1.27
MnO	2.73	0.18	2.45	0.11	2.03	0.43	2.29	0.08	2.34	0.38	2.74	0.08	2.33	0.53
MgO	2.39	0.10	3.85	0.36	4.27	0.29	3.70	0.17	2.76	0.78	4.07	0.34	1.16	0.91
Na ₂ O	0.34	0.20	0.26	0.19	0.00	0.00	0.26	0.17	0.13	0.08	0.23	0.12	0.19	0.12
K ₂ O	9.63	0.15	9.44	0.27	9.43	0.32	9.30	0.24	9.16	0.17	9.55	0.13	9.57	0.15
Total No.	10		9		36		7		43		21		27	

No. of cations on the basis of 22 oxygens

Si	5.664	5.524	5.215	5.466	5.522	5.530	5.314
Ti	0.262	0.269	0.171	0.188	0.207	0.172	0.200
Al	3.453	2.865	2.655	2.997	2.985	2.905	3.665
Fe	3.023	3.815	5.077	3.961	4.044	3.818	3.859
Mn	0.364	0.339	0.265	0.318	0.332	0.382	0.320
Mg	0.561	0.938	0.979	0.903	0.689	0.999	0.280
Na	0.104	0.082	0.000	0.083	0.042	0.073	0.060
K	1.936	1.968	1.851	1.944	1.958	2.006	1.977

Rock Name	MK-1		MK-2		MK-5		MK-6		MK-10		MK-14		MK-16	
	mean	sd												
SiO ₂	32.78	1.12	32.61	0.54	33.79	0.28	32.96	0.87	32.94	0.35	33.16	0.25	32.73	0.74
TiO ₂	1.55	0.17	2.11	0.34	2.73	0.08	1.64	0.28	1.66	0.09	3.19	0.15	3.06	0.37
Al ₂ O ₃	19.02	0.45	16.06	0.32	15.05	0.18	15.11	0.47	15.31	0.26	14.74	0.51	15.42	0.33
FeO	27.71	1.05	24.07	0.52	27.47	0.51	28.86	1.30	29.88	0.63	28.42	0.54	33.52	0.85
MnO	1.91	0.28	5.30	0.30	1.86	0.06	2.34	0.38	1.91	0.14	1.02	0.10	1.65	0.11
MgO	1.27	0.79	1.60	0.07	3.80	0.05	2.76	0.78	2.86	0.61	2.99	0.11	0.20	0.10
Na ₂ O	0.51	0.13	0.13	0.02	0.16	0.09	0.13	0.08	0.09	0.03	0.14	0.14	0.15	0.23
K ₂ O	9.53	0.16	9.08	0.14	9.44	0.15	9.16	0.17	9.28	0.12	9.15	0.12	9.22	0.15
Total No.	41		19		18		43		11		16		48	

No. of cations on the basis of 22 oxygens

Si	5.364	5.531	5.519	5.522	5.480	5.516	5.410
Ti	0.191	0.269	0.335	0.207	0.208	0.399	0.380
Al	3.669	3.211	2.898	2.985	3.003	2.891	3.005
Fe	3.792	3.414	3.753	4.044	4.157	3.954	4.634
Mn	0.265	0.761	0.257	0.332	0.269	0.144	0.231
Mg	0.310	0.404	0.925	0.689	0.709	0.741	0.049
Na	0.048	0.043	0.051	0.042	0.000	0.045	0.048
K	1.990	1.965	1.967	1.958	1.970	1.942	1.944

(Contd.) Table 6.5

Rock Name	MK-18		MK-20		MK-21		MK-24		MK-25		SB-1		SB-5	
	mean	sd												
SiO ₂	33.58	0.85	33.44	0.58	34.69	0.28	33.01	0.33	33.50	0.37	33.67	1.29	34.66	1.09
TiO ₂	2.26	0.61	1.55	0.07	1.40	0.05	1.51	0.09	1.41	0.11	2.11	0.90	1.31	0.14
Al ₂ O ₃	14.96	0.63	14.90	0.46	15.37	0.29	14.76	0.20	14.22	0.23	15.54	1.12	14.61	0.82
FeO	30.31	2.39	29.71	0.49	24.81	0.19	28.78	0.54	26.96	0.70	29.59	2.73	27.14	1.93
MnO	1.91	0.23	1.58	0.09	3.14	0.09	3.14	0.10	2.80	0.13	1.60	0.47	1.86	0.53
MgO	2.76	1.84	3.62	0.25	5.29	0.14	3.14	0.17	4.44	0.27	3.39	2.78	6.03	1.59
Na ₂ O	0.23	0.56	0.16	0.11	0.12	0.04	0.10	0.06	0.11	0.11	0.17	0.20	0.21	0.27
K ₂ O	9.48	0.40	9.03	0.33	9.55	0.07	9.38	0.11	9.32	0.10	9.31	0.25	9.44	0.25
Total No.	58		28		5		34		45		35		18	

No. of cations on the basis of 22 oxygens

Si	5.500	5.529	5.605	5.507	5.749	5.477	5.582
Ti	0.278	0.193	0.170	0.189	0.172	0.258	0.159
Al	2.883	2.904	2.928	2.903	2.715	2.980	2.774
Fe	4.152	4.108	3.352	4.015	3.651	4.025	3.655
Mn	0.265	0.221	0.430	0.444	0.384	0.220	0.254
Mg	0.674	0.892	1.274	0.781	1.072	0.822	1.447
Na	0.073	0.051	0.038	0.032	0.035	0.054	0.066
K	1.981	1.905	1.968	1.996	1.925	1.932	1.939

Rock Name	SB-11		SB-15		S-1		S-3		S-6		BD-3	
	mean	sd										
SiO ₂	32.76	0.38	35.08	0.70	34.93	0.67	33.39	0.54	34.02	0.89	34.90	0.80
TiO ₂	3.24	0.53	1.43	0.09	1.20	0.28	1.40	0.11	1.43	0.13	1.13	0.26
Al ₂ O ₃	15.92	0.27	17.36	0.45	16.37	0.83	14.79	0.32	16.67	0.39	14.64	0.50
FeO	32.18	1.24	16.27	0.54	23.64	1.20	25.51	0.65	26.11	1.03	27.00	1.16
MnO	1.50	0.14	6.32	0.52	1.92	0.15	2.91	0.13	2.74	0.16	1.70	0.10
MgO	0.84	0.74	4.77	0.27	7.59	1.77	4.32	0.14	3.51	0.34	6.92	1.63
Na ₂ O	0.13	0.10	0.26	0.10	0.21	0.11	0.14	0.10	0.17	0.16	0.16	0.17
K ₂ O	9.36	0.12	9.25	0.17	9.82	0.16	9.25	0.17	9.94	0.15	9.42	0.13
Total No.	34		19		44		28		28		8	

No. of cations on the basis of 22 oxygens

Si	5.375	5.700	5.497	5.594	5.521	5.568
Ti	0.400	0.174	0.142	0.176	0.175	0.136
Al	3.080	3.323	3.037	2.921	3.189	2.754
Fe	4.416	2.211	3.111	3.574	3.544	3.603
Mn	0.208	0.870	0.256	0.413	0.377	0.230
Mg	0.205	1.156	1.780	1.079	0.849	1.645
Na	0.041	0.082	0.064	0.045	0.053	0.049
K	1.959	1.973	1.972	1.977	2.058	1.917

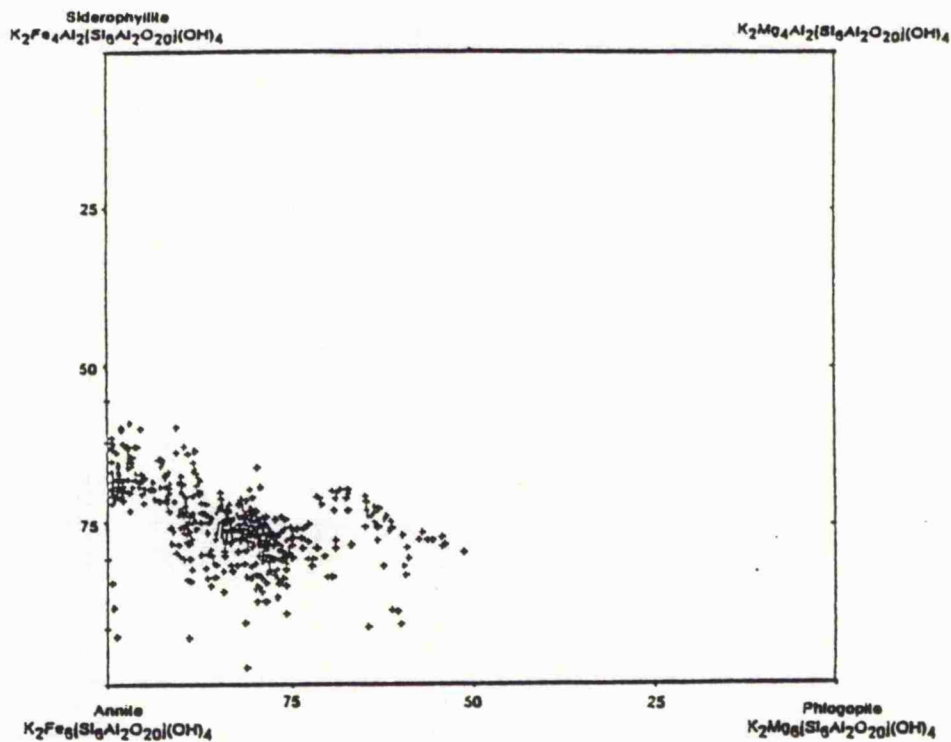


Fig. 6.6 Plot of biotites from the Koga feldspathoidal complex showing different compositions (after Deer et al. 1992).

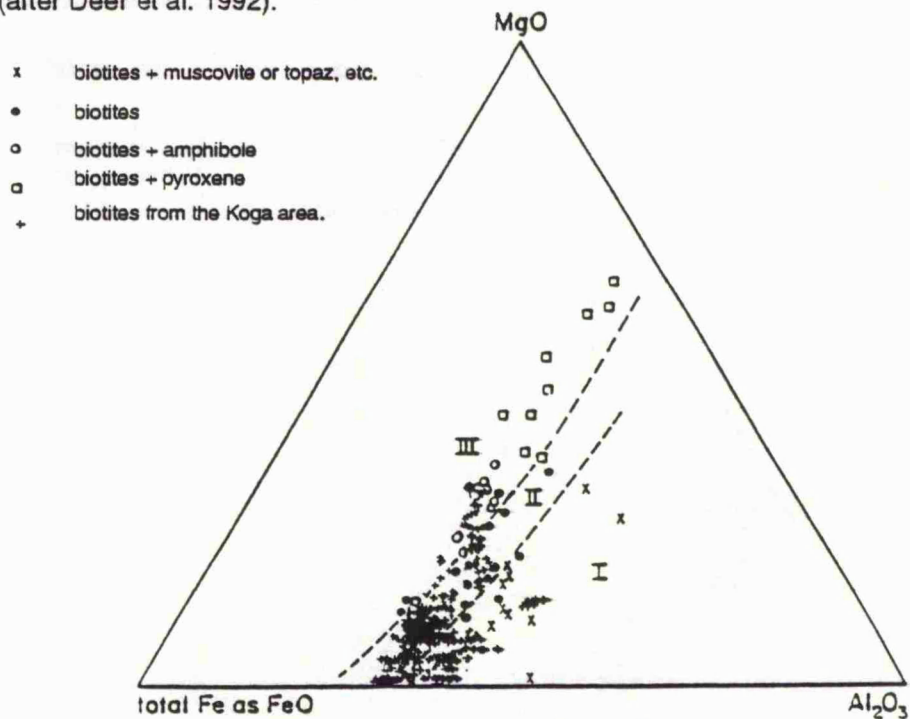


Fig. 6.7 Biotites from the Koga feldspathoidal syenite plotted on the triangle MgO – (total Fe as) FeO–Al₂O₃ with biotite compositions from igneous rocks after Nockolds (1947). Roman numerals refer to the fields of biotites associated with muscovite or topaz (I), unaccompanied by other mafic minerals (II) and biotites associated with hornblende, pyroxene, or olivine (III).

Table 6.6

Microprobe analyses of cancrinite from the Koga Complex

Rock Name	K-2		K-3		K-4		K-6		K-9		MK-1		MK-3	
	mean	sd												
SiO ₂	41.45	0.58	38.14	0.62	38.60	1.38	39.80	1.66	40.52	0.20	40.21	0.21	40.61	0.19
Al ₂ O ₃	33.81	0.44	31.10	0.38	31.36	1.46	32.73	1.78	33.45	0.27	33.32	0.21	33.18	0.37
CaO	4.99	0.27	4.82	0.09	4.65	0.61	7.21	0.45	6.58	0.82	7.10	0.15	6.77	0.08
Na ₂ O	17.72	1.24	19.72	0.19	18.17	1.21	17.78	0.78	17.74	0.78	16.19	0.31	16.63	0.25
Total No.	23		4		25		7		16		33		10	

No. of cations on the basis of 12 oxygens

Si	3.011	2.942	2.987	2.940	2.957	2.967	2.785
Al	2.895	2.828	2.855	2.850	2.878	2.898	2.874
Ca	0.338	0.398	0.385	0.571	0.515	0.561	0.533
Na	2.496	2.950	2.720	2.547	2.510	2.316	2.370

Rock Name	MK-5		MK-6		MK-10		MK-14		MK-16		MK-18		SB-1	
	mean	sd												
SiO ₂	39.85	1.62	40.26	0.37	40.01	0.49	40.71	0.37	40.82	1.07	39.43	0.77	41.15	1.13
Al ₂ O ₃	32.92	1.17	33.53	0.34	33.01	0.52	33.82	0.59	33.44	0.65	32.33	0.99	33.59	0.54
CaO	5.09	0.17	5.56	0.36	5.41	0.27	4.68	1.18	4.19	0.34	5.13	0.45	5.13	1.28
Na ₂ O	17.40	1.04	17.30	0.45	17.69	0.51	17.84	0.67	18.74	0.66	18.63	1.08	17.58	0.98
Total No.	5		21		5		18		27		19		9	

No. of cations on the basis of 12 oxygens

Si	2.984	2.972	2.976	2.987	2.997	2.965	3.007
Al	2.906	2.918	2.894	2.926	2.895	2.866	2.893
Ca	0.408	0.440	0.431	0.368	0.330	0.413	0.402
Na	2.527	2.476	2.551	2.538	2.668	2.716	2.490

Rock Name	SB-5		SB-11		S-1		S-3		BD-3	
	mean	sd								
SiO ₂	40.55	0.50	41.10	0.47	40.59	0.27	39.66	0.99	40.10	1.99
Al ₂ O ₃	33.45	0.34	33.77	0.43	33.74	0.21	32.31	1.40	32.44	1.69
CaO	5.86	0.57	4.63	0.36	9.17	0.23	4.42	0.51	3.36	0.39
Na ₂ O	16.66	0.24	18.04	0.76	14.43	0.28	18.88	0.65	19.68	0.92
Total No.	6		13		12		10		7	

No. of cations on the basis of 12 oxygens

Si	2.991	3.001	2.958	2.984	3.003
Al	2.909	2.907	2.899	2.866	2.864
Ca	0.463	0.362	0.716	0.356	0.270
Na	2.383	2.554	2.039	2.754	2.857

These biotites do not show an increase in Mn with an increase in Fe/Mg and no wider scatter, Fig. 6.9 as in case of the most evolved compositions, Upton et al. (1985).

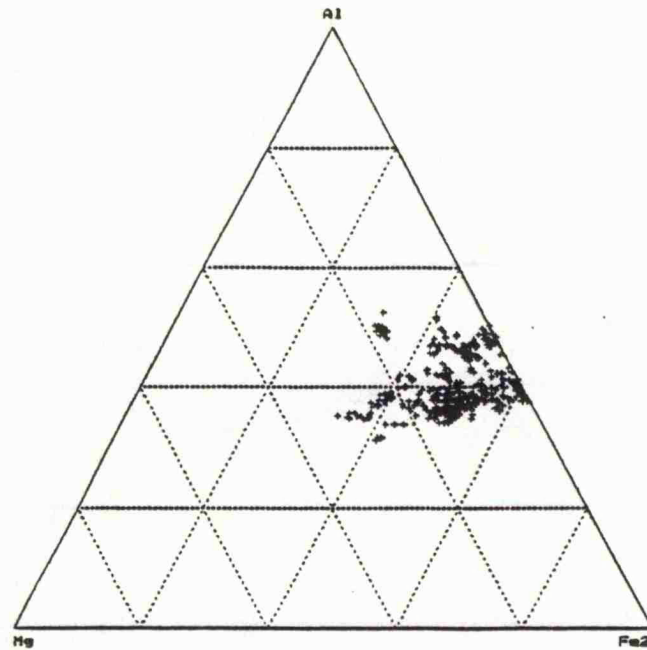


Fig. 6.8 Microprobe analyses of biotites from Koga plotted in terms of Mg - Al - Fe₂.

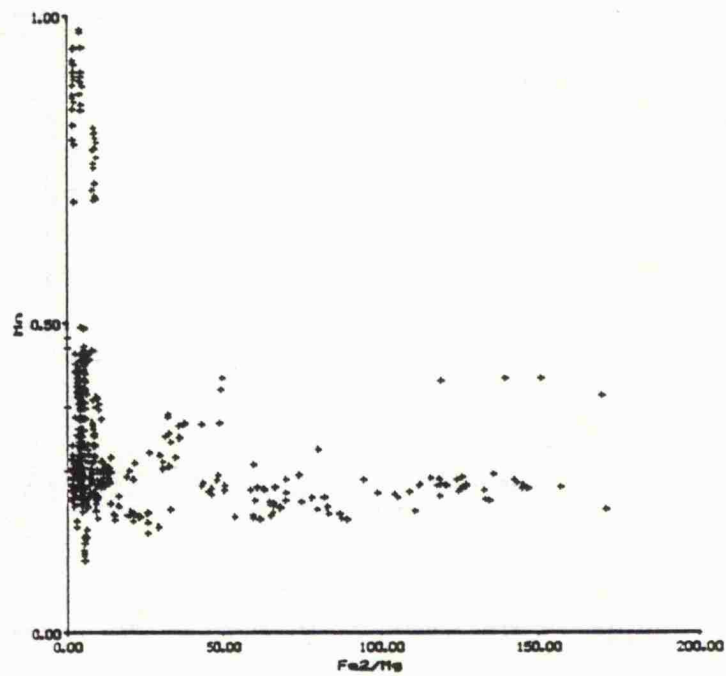


Fig. 6.9 Biotites from the Koga feldspathoidal syenite plotted on Fe / Mg versus Mn

6.5 Cancrinite

Cancrinite is present in the Koga feldspathoidal syenite complex principally in the pegmatites, which have larger quantities compared to the other units of the complex. The analyses are given in the Table 6.6, calculated on the basis of 12 oxygens. These cancrinites lack FeO and K₂O.

The SiO₂ and Al₂O₃ are present in excess as compared to the analyses shown by Phoenix et al. (1949), Takla et al. (1980) and Flohr et al. (1989). The CaO contents are less in the Koga complex from those of Takla et al. (1980) and Flohr et al. (1989).

6.6 Sodalite

Sodalite is present in the sodalite rich feldspathoidal syenite of the Koga complex. The analyses are presented in Table 6.7, calculated on the basis of 25 oxygens.

These sodalites are higher in SiO₂, Al₂O₃ and Na₂O as compared to those by Taylor, (1967), whereas they are similar to sodalite from the Coldwell alkaline complex N W Ontario by Roger et al. (1982).

Sodalite shows constant composition in different units of the Koga complex.

6.7 Sphene

Sphene is present in few samples of the Koga complex. The analyses are presented in Table 6.8, calculated on the basis of 5 oxygens.

The analyses are plotted in terms of CaO. SiO₂ – FeO – CaO.TiO₂ and are shown in Fig. 6.10. The Koga complex sphenes are non-stoichiometric, showing an excess of Ca over Ti.

6.8 Garnet

Garnet is present only in few samples from the Koga feldspathoidal syenite complex; in Bibi Dheri, Sura, and sodalite rich rocks in association with other mafics, mainly with the pyroxenes.

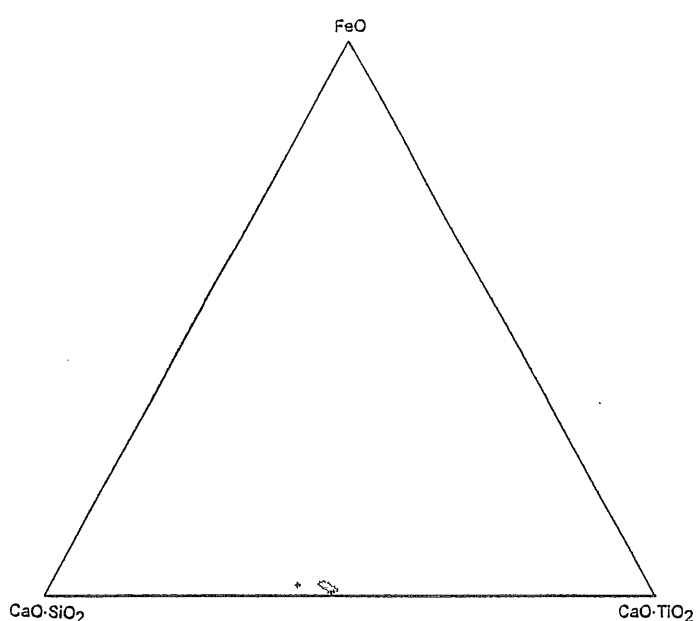
Fig. 6.10 Microprobe analyses of sphene plotted in terms of CaO, SiO₂ - FeO - CaO.TiO₂

Table 6.7

Microprobe analyses of sodalite from the Koga Complex

Rock Name	K-9		MK-1		MK-6		MK-10		SB-1		SB-5		SB-11	
	mean	sd	mean	sd	mean	sd	mean	sd	mean	sd	mean	sd	mean	sd
SiO ₂	39.93	0.47	39.45	0.31	39.32	0.37	39.51	0.60	39.91	0.32	39.81	0.22	39.75	0.28
Al ₂ O ₃	33.12	0.65	32.72	0.21	33.27	0.37	33.21	0.70	32.85	0.40	32.37	0.48	33.04	0.26
Na ₂ O	25.65	0.55	25.68	0.12	25.28	0.38	25.51	0.29	25.67	0.42	25.47	0.40	25.88	0.18
Total No.	6		13		9		3		7		3		3	
	No. of cations on the basis of 25 oxygens													
Si	6.113		6.101		6.069		5.782		6.129		6.160		6.096	
Al	5.978		5.965		6.054		6.304		5.947		5.905		5.974	
Na	7.614		7.700		7.565		7.963		7.643		7.642		7.695	

The analyses are given in Table 6.9, calculated on the basis of 12 oxygens and 8 cations. These are plotted in Fig. 6.11 in terms of CaO, SiO₂ - Fe₂O₃ Al₂O₃ - CaO.TiO₂. These analyses generally plot near to andradite, but some of them are richer in Ca, as shown by Huckenholz, (1969).

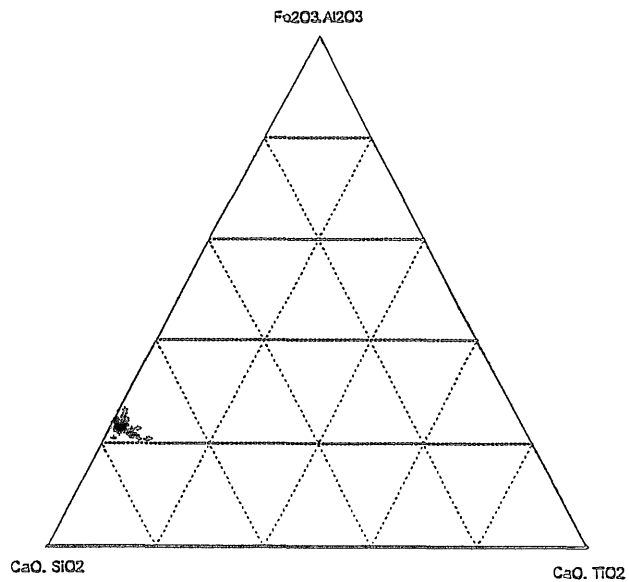
Table 6.8

Microprobe analyses of sphenes from the Koga Complex

Rock Name	K-3		K-5		MK-5		SB-1		SB-5		S-1	
	mean	sd										
SiO ₂	27.76	0.12	29.82	0.27	30.02	0.24	30.14	0.11	30.18	0.08	30.15	0.15
TiO ₂	33.80	0.65	33.76	0.75	34.98	0.96	33.78	0.61	33.96	0.71	34.76	0.89
Al ₂ O ₃	1.53	0.21	1.46	0.10	1.36	0.30	1.08	0.30	0.90	0.19	1.57	0.29
FeO	2.19	0.26	2.16	0.50	1.74	0.54	2.40	0.32	2.32	0.38	2.30	0.39
CaO	27.51	0.17	27.62	0.20	27.10	0.58	27.04	0.27	26.89	0.21	27.59	0.22
Na ₂ O	0.00		0.16	0.07	0.40	0.23	0.27	0.13	0.28	0.16	0.15	0.07
Total No.	9		14		12		8		5		21	

	No. of cations on the basis of 5 oxygens					
Si	0.989	1.031	1.029	1.045	1.048	1.026
Ti	0.905	0.878	0.901	0.881	0.886	0.889
Al	0.064	0.060	0.055	0.044	0.037	0.063
Fe	0.065	0.062	0.50	0.070	0.067	0.065
Ca	1.0250	1.024	0.995	1.004	1.000	1.006
Na	00	0.011	0.027	0.018	0.019	0.010

Andradite garnets having TiO₂ between 1 and 2 %, are classified as melanites, following the criterion of Deer et al. (1982). These melanites have high amounts of iron and manganese.

Fig. 6.11 Microprobe analyses of garnets plotted in terms of CaO. SiO₂ - Fe₂O₃ Al₂O₃ - CaO. TiO₂.

There is negative correlation between Si and Ti Fig. 6.12, whereas there is no correlation between Si and Al and Si and Fe⁺³, Fig. 6.13 and 6.14 respectively. There is a significant negative correlation between Al and Ti, Fig. 6.15.

The Koga melanites plot more or less in the same field in Si versus Ti Fig. 6.12 as garnets from the metasomatised ijolites of Diamond Jo quarry described by Flohr et al. (1989) and also show the same trend in Si versus Al plot, Fig. 6.13. They show a different trend on a Si versus Fe⁺³ plot Fig. 6.14.

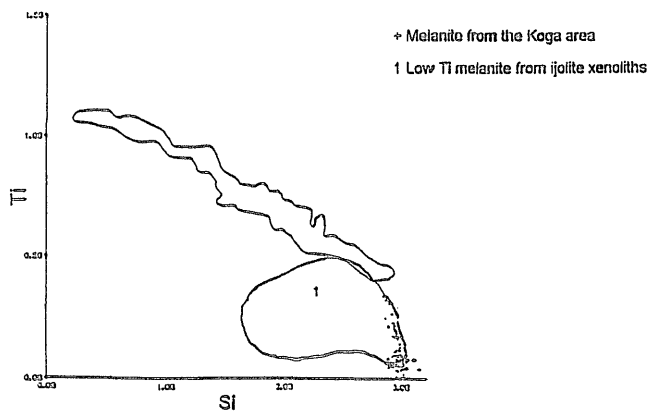


Fig. 6.12 Si versus Ti in Koga garnets in comparison with ijolite xenoliths of Diamond Jo quarry.

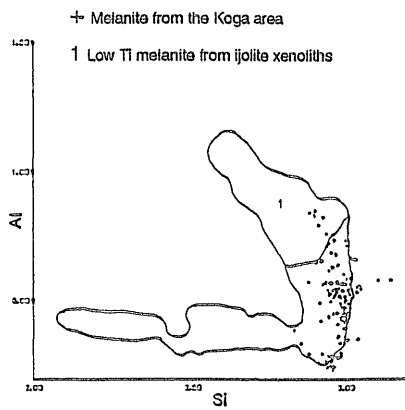


Fig. 6.13 Si versus Al

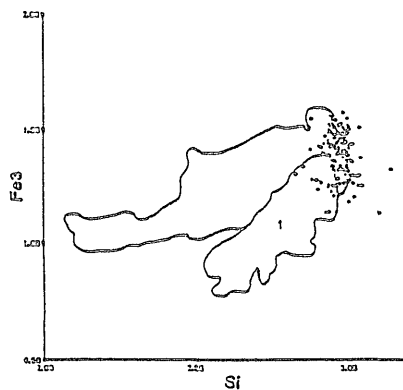


Fig. 6.14 Si versus Fe

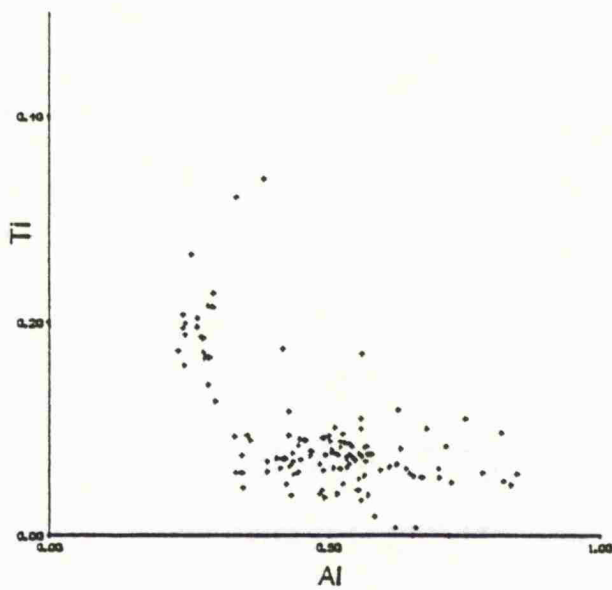


Fig. 6.15 Al versus Ti.

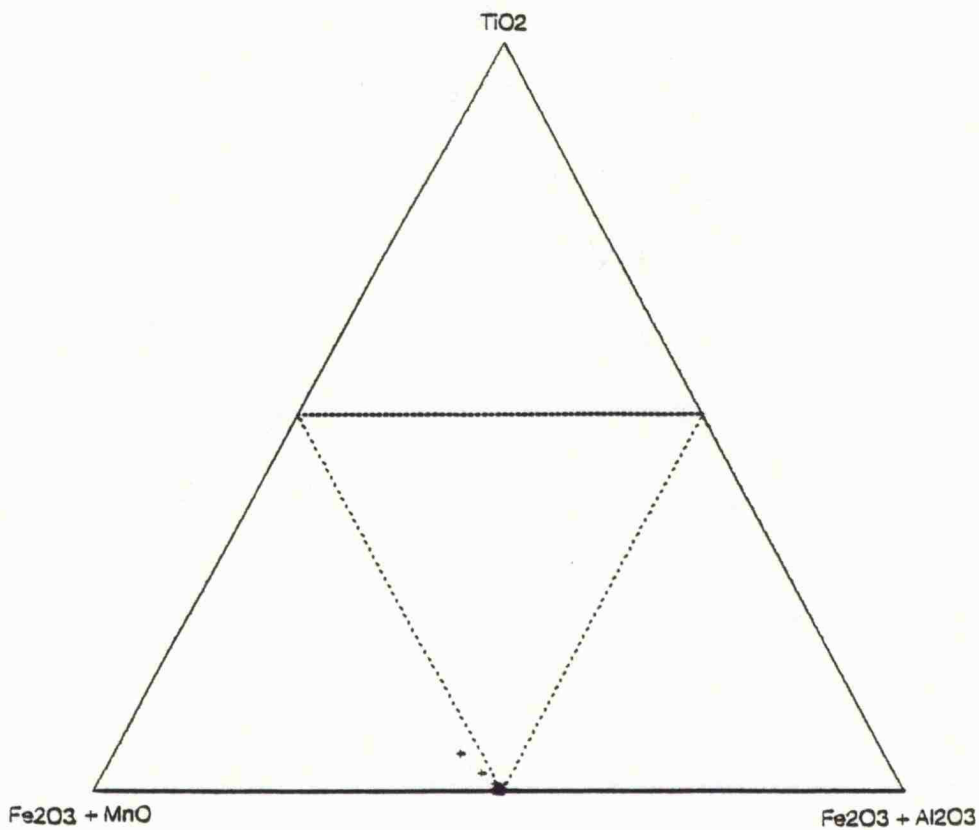


Fig. 6.16 Magnetites from the Koga complex plotted on $Fe_2O_3+MnO - TiO_2 - Fe_2O_3+Al_2O_3$.

Table 6.9

Microprobe analyses of garnets from the Koga Complex

Rock Name	K-4		K-8		MK-20		MK-21		SB-1		SB-5		SB-9	
	mean	sd												
SiO ₂	36.56	1.90	35.55	0.28	35.74	0.09	35.51	0.27	35.54	0.65	35.88	0.08	34.49	0.51
TiO ₂	1.06	0.31	1.12	0.26	1.30	0.28	1.66	0.55	1.47	0.83	1.08	0.18	3.12	0.78
Al ₂ O ₃	4.79	0.77	5.19	0.40	4.86	0.56	6.28	0.91	6.15	1.79	4.89	0.79	2.77	0.33
FeO	21.43	0.86	20.61	0.52	20.91	0.63	18.25	1.34	19.63	1.46	21.34	0.81	23.34	0.64
MnO	1.56	0.17	2.21	0.30	1.68	0.18	2.11	0.11	1.74	0.17	1.73	0.16	1.39	0.16
CaO	31.51	1.21	32.03	0.54	31.89	0.57	32.16	0.45	31.93	0.35	31.16	0.16	30.32	0.29
Na ₂ O	0.67	0.91	0.00		0.00		0.12	0.10	0.00		0.00		0.14	0.02
Total No.	5		11		15		7		5		4		23	

No. of cations on the basis of 12 oxygens and total of 8 cations

Si	3.002	2.964	2.975	2.963	2.962	2.989	2.941
Ti	0.066	0.070	0.081	0.104	0.092	0.067	0.200
Al	0.463	0.510	0.480	0.617	0.602	0.480	0.279
Fe ₂	0.010	0.022	0.057	0.013	0.079	0.081	0.201
Fe ₃	1.464	1.415	1.399	1.261	1.289	1.406	1.464
Mn	0.108	0.156	0.119	0.149	0.123	0.122	0.101
Ca	2.777	2.861	2.846	2.874	2.852	2.853	2.770
Na	0.105	0.001	0.043	0.019	0.000	0.000	0.023

Rock Name	S-1		S-3		S-6		BD-3	
	mean	sd	mean	sd	mean	sd	mean	sd
SiO ₂	36.08	0.11	35.19	0.38	36.06	0.38	36.60	0.58
TiO ₂	0.96	0.20	1.19	0.21	1.01	0.22	0.67	0.80
Al ₂ O ₃	6.94	1.06	5.20	0.67	4.90	1.15	5.71	1.56
FeO	19.98	1.28	18.78	0.92	20.83	1.22	20.44	1.27
MnO	2.35	0.31	2.07	0.92	2.43	0.35	2.13	0.34
CaO	32.32	0.34	31.36	0.61	32.13	0.47	21.71	0.53
Total No.	13		22		18		8	

No. of cations on the basis of 12 oxygens and total of 8 cations

Si	2.931	3.011	2.983	2.994
Ti	0.059	0.076	0.063	0.042
Al	0.679	0.524	0.477	0.529
Fe ₂	0.021	0.035	0.010	0.029
Fe ₃	1.337	1.309	1.432	1.370
Mn	0.162	0.150	0.170	0.147
Ca	2.813	2.875	2.849	2.867
Na	0.000	0.008	0.005	0.002

6.9. Magnetite

Analyses of magnetite from the Koga feldspathoidal syenite complex are given in Table 6.10, calculated on the basis of 32 oxygens and 24 cations.

These magnetites are almost pure as shown in Fig. 6.16. The magnetite from K-6, a feldspathoidal syenite has 3.40 % MnO, an order of magnitude higher than in the magnetite from other rocks.

Table 6.10

Microprobe analyses of magnetite from the Koga complex

Rock Name	K-1		K-2		K-6		K-9		MK-1		MK-16		MK-18	
	mean	sd												
SiO ₂	0.00		0.08	0.17	0.00		0.00		0.00		0.00		0.08	0.17
TiO ₂	0.00		0.27	0.48	0.00		0.00		0.00		0.07	0.06	0.36	0.96
Al ₂ O ₃	0.00		0.00		0.00		0.00		0.00		0.00		0.00	
FeO	92.05	0.71	91.09	1.57	88.42	0.52	91.78	1.78	90.99	0.25	88.37	6.63	91.76	1.91
MnO	0.48	0.17	0.40	0.28	3.40	0.31	0.33	0.08	0.34	0.06	0.16	0.11	0.35	0.42
Total No.	10		12		10		9		5		11		14	

No of cations on the basis of 32 oxygens and total of 24 cations

Si	000	0.024	000	000	000	000	0.026
Ti	000	0.064	000	000	000	0.017	0.081
Al	000	000	000	000	000	000	000
Fe ₂	7.874	7.893	7.113	7.912	7.909	7.977	8.017
Fe ₃	16.000	15.815	15.971	15.994	15.994	15.956	15.770
Mn	0.126	0.105	0.9000	0.088	0.091	0.042	0.091

6.10 Amphibole

Analyses of amphibole from the Koga feldspathoidal syenite complex are given in Table 6.11 calculated on the basis of 23 oxygens and 16 cations.

Amphibole is present only in one sample S-1. These are barkevikite similar to those reported from a nepheline syenite in Norway (Kunitz, 1930) and also reported from Girmar Phenai Mata, Gujrat, India (Sethna, 1989).

Table 6.11

Microprobe analyses of amphibole from the Koga Complex and cations proportions

	mean	sd		
SiO ₂	39.93	0.57	Si	6.352
TiO ₂	1.09	0.90	Ti	0.130
Al ₂ O ₃	11.05	0.70	Al	2.072
FeO	24.20	0.72	Fe	3.220
MnO	1.69	0.14	Mn	0.228
MgO	5.28	0.47	Mg	1.251
CaO	7.31	0.77	Ca	1.246
Na ₂ O	4.96	0.29	Na	1.529
K ₂ O	2.16	0.36	K	0.439
Total	41		Cations	16
			Oxygens	23

*Chapter Seven***GEOCHEMISTRY****Introduction**

Geochemical analysis of Koga nepheline syenite is aimed to determine the initial chemistry from which the success of mineral separation can be judged, to determine the origin of the rocks, to determine whether it is a single deposit or composed of different intrusions emplaced at different times; and finally any trends of differentiation.

7.1 Samples

All the samples were collected from Koga feldspathoidal syenite using the following criteria:

1. Samples were collected from all the different lithological units of Koga, Jalai Kandao, Landi Patao, Miani Kandao, Bibi Dheri, Agarai and Sura area.
2. All samples were homogeneous in terms of mineralogical composition.
3. All samples were regarded as representative.
4. Samples to determine the variation in composition within a unit were also collected.

The rock samples analysed from the Koga feldspathoidal syenite complex may be classified into the following types based on the mineralogical and chemical characteristics (Table 7.1). The rock types include:

Foyaites

- Sodalite rich foyaites
- Sodalite-Cancrinite rich foyaites
- Feldspathoidal foyaites

- Foyaitic feldspathoidal syenites

Feldspathoidal Syenites

- Garnet bearing feldspathoidal syenite
- Feldspathoidal syenites
- Pulaskitic feldspathoidal syenite

Syenites

- Alkali syenite

The majority of the foyaites and feldspathoidal syenites from the study area fall close to the agpaitic / miaskitic boundary. An alkaline rock is agpaitic if the molar ratio of $(\text{Na}_2\text{O} + \text{K}_2\text{O})$ to Al_2O_3 (Sorensen, 1974) is > 1 . The feldspathoidal foyaites, sodalite rich foyaites and foyaitic feldspathoidal syenites are the predominant rock suites occurring as plugs, intrusions and pegmatitic dikes. These units cover most of the area around Miani Kandao, Landi Patao, Sahbaga, Agarai and Sura. Unlike other agpaitic syenites, Koga foyaites, sodalite-rich foyaites and foyaitic feldspathoidal syenites are characterised by relatively low concentrations of TiO_2 , MgO , CaO , Sr , Ba and REE. Miaskitic feldspathoidal syenites of the area mainly occur as dikes and minor plugs intruded within the main mass of feldspathoidal syenite bodies. These are prominently exposed in Sahbaga, Sura, and Bibi Dheri. Garnet bearing feldspathoidal syenite and alkali syenite (Sample K-1) occur as dikes in Bibi Dheri and near Koga village respectively.

7.2 Major Element Geochemistry

Fifty five rock samples from the Koga alkaline complex area were analysed for major and trace elements. A complete set of analytical data and norms of the rocks is presented in Table 7.2 - 7.6. The differentiation indices (D.I) are calculated from the CIPW normative mineralogy according to the procedure of Thornton and Tuttle (1960). The chemical analyses indicate considerable variation in the concentration and distribution of major oxides in different rock units. The majority of the feldspathoidal syenites are agpaitic in character with a relatively high range

Table 7.1 Rock types analysed from the Koga Feldspathoidal Syenite Complex.

Rock type	Mode of occurrence	Alkaline character	Sample No.	K/Rb	K/Ba	Rb/Sr	Symbol
Sodalite – Cancrinite rich foyaïtes	Dikes & pegmatites	Agpaitic/Miaskitic	MK - 1	215	984	1.86	
			MK - 3	300	1349	1.27	
			SB-14	153	540	1.9	
			SB-15	155	3545	2.52	
			SB-16	165	711	2.19	+
			K - 5	126	169	0.77	
			K - 6	111	203	1.94	
			K - 9	242	1528	1.72	
Feldspathoidal foyaïtes	Dikes & pegmatites	Agpaitic	MK - 6	341	162	0.32	
			MK-16	383	86	0.16	
			SB - 5	410	32	0.08	Δ
			SB-11	502	73	0.11	
			S - 4	373	206	0.27	
			K - 2	274	171	0.31	
	Plugs & dikes		SB - 1	314	139	0.3	
SB - 6			558	62	0.08		
SB-10			287	171	0.21	Δ	
S - 1			398	34	0.06		
S - 2			413	118	0.13		
Foyaïtic feldspathoidal syenites (Phonoïitic trend)	Pegmatites & dikes	Agpaitic	MK - 2	249	636	1.3	
			MK-24	414	688	1.1	
			MK-25	372	1572	1.33	
			S - 5	329	814	0.85	■
			S - 6	322	715	0.88	
			K - 8	350	623	0.82	
Feldspathoidal syenites (Trachytic trend)	Plugs & dikes and intrusions	Agpaitic/Miaskitic	MK - 4	276	255	0.42	
			MK - 5	299	976	0.94	
			MK-11	336	226	0.29	
			MK-13	348	333	0.33	
			MK-14	348	187	0.24	
			MK-15	351	385	0.37	⊙
			MK-17	436	237	0.23	
			MK-20	316	227	0.37	
			MK-21	309	379	1.14	
			MK-22	319	400	1.00	
			S - 3	315	1347	1.14	
			BD - 1	545	655	0.41	
Pulaskitic feldspathoidal syenite	Dikes & intrusions	Agpaitic	MK - 8	324	104	0.28	
			MK - 9	338	177	0.27	
			MK-10	280	15	0.07	
			MK-12	323	226	0.30	
			MK-18	443	55	0.09	
			MK-19	353	56	0.14	
			SB - 2	370	47	0.14	
			SB - 7	299	27	0.09	○
			SB - 9	394	59	0.22	
			SB-12	370	250	0.40	
			K - 3	333	389	0.50	
			K - 4	328	159	0.32	
			BD - 2	510	73	0.14	
Garnet bearing feldspathoidal syenite	Dikes/plugs	Miaskitic	BD - 3	381	9	0.02	
			BD - 4	369	13	0.04	□
Alkali syenite			K - 1	758	83	0.08	○

Table 7.2: Major and trace element analyses of Feldspathoidal Sodalite/Cancrinite rich Foyaites.

MAJOR ELEMENTS	Sodalite rich foyaites						Sodalite - cancrinite rich foyaites				
	SB-14	SB-15	SB-16	K-5	K-6	Average	MK-1	MK-3	K-9	Average	
	SIO2	57.75	58.6	58.02	57.1	57.07	57.71	57.1	56.91	57.13	57.05
TIO2	0.24	0.14	0.14	0.13	0.15	0.16	0.17	0.13	0.14	0.15	
Al2O3	21.87	21.98	21.98	21.78	22.33	21.99	22.25	23.96	23.07	23.09	
Fe2O3	3.41	3.01	3	4.5	3.12	3.41	3.43	2.04	2.9	2.79	
MnO	0.22	0.16	0.16	0.14	0.15	0.17	0.15	0.11	0.16	0.14	
MgO	0	0	0.01	0.02	0.11	0.03	0.06	0.05	0.12	0.08	
CaO	0.69	0.58	0.57	0.79	1.93	0.91	1.04	0.52	1.03	0.86	
Na2O	10.3	11.39	12.7	12.09	11.26	11.55	10.22	10.98	10.12	10.44	
K2O	4.03	2.99	3.34	2.78	2.8	3.19	4.98	5.69	5.08	5.25	
P2O5	0	0.01	0.01	0.01	0.02	0.01	0.02	0.01	0.02	0.02	
Total	98.51	98.86	99.93	99.34	98.94	99.12	99.42	100.4	99.77	99.86	
CIPW NORM											
Or	23.82	17.67	16.43	16.55	16.55	18.20	29.43	33.63	30.02	31.03	
Ab	46.44	53.37	45.47	47.7	47.72	48.14	37.14	28.2	35.49	33.61	
An	1.54	0.02		2.12	2.12	1.16	0.13		2.52	0.88	
Ne	22.06	23.3	27.67	25.78	25.76	24.91	26.73	34.33	27.16	29.41	
Aeg(Ac)			5.06					1.18		0.39	
Di			0.11	0.59	0.59	0.26	0.32	0.27	0.64	0.41	
Wo	0.79	1.17	1.55	2.74	2.72	1.79	1.87	0.9	0.68	1.15	
Mt	0.02	0.12	0.08	0.05	0.05	0.06			0.12	0.04	
Il	0.46	0.27	0.25	0.28	0.28	0.31	0.32	0.24	0.27	0.28	
Hem	3.39	2.93	2.7	3.08	3.08	3.04	3.43	1.63	2.82	2.63	
Ap		0.02	0.02	0.05	0.05	0.03	0.05	0.02	0.05	0.04	
NORMATIVE MINERALOGY											
D.I.	92.32	94.34	89.57	90.03	90.03	91.26	93.3	96.16	92.67	94.04	
AN/AB+AN	0.03	0.00	0.00	0.04		0.02	0.00	0.00	0.07	0.02	
S.I.	0.00	0.00	0.05	0.10	0.64	0.16	0.32	0.27	0.66	0.42	
100Mg/Mg+Fe(Mol)											
Agpaltic Index	0.97	1	1.12	1.05	0.97	1.02	1	1.01	0.96	0.99	
TRACE ELEMENTS AND REE (ppm)											
Rb	220	161	169	183	209	188	193	158	20	123.53	
Li	83	70	58		96	61	77	49	13	44.35	
Sr	116	64	77	237	108	120	104	124	28	85.23	
Ba	62	7	39	137	19	53	42	35	28	34.87	
V	26	36	27	41	19	30	26	19	20	21.60	
Cr	u.d	8	n.d	n.d	n.d	2	2	n.d	n.d	0.63	
Zn	155	92	100	118	160	125	166	83	n.d	82.83	
Ga	49	49	47	n.d	n.d		38	40	39	38.83	
Sc	7	n.d	n.d	n.d	n.d		5	n.d	n.d	1.77	
Y	23	6	26	30	17	20	10	6	54	23.43	
Zr	2079	601	1398	813	369	1052	301	262	321	294.70	
Nb	219	33	184	156	31	124	35	38	n.d	24.27	
Th	15	18	4	29	10	15	9	8	0	5.65	
La	25	6	28	80	20	32	30	14	39	27.40	
Ce	48	9	43	128	30	52	37	20	54	37.07	
Pr	3.60			7.34	1.99		3.77		3.49		
Nd	10		7	34	9		8	4	13		
Sm	0.82			2.86	0.86		1.31		1.15		
Eu	0.37			0.93	0.32		0.43		0.47		
Gd	6.91			6.24	3.99		2.15		2.22		
Dy	1.91			3.09	1.47		1.19		1.01		
Er	2.01			2.17	1.08		1.05		0.93		
Yb	1.34			1.25	0.63		0.43		0.46		
Lu	0.26			0.09	0.10		0.07		0.29		

Table 7.3: Major and trace element analyses of Feldspathoidal Foyaites.

MAJOR ELEMENTS	Feldspathoidal Foyaites (agpaitic)							Feldspathoidal Foyaites (miaskitic)						
	MK-6	MK-16	SB-5	SB-11	S-4	K-2	Average	SB-1	SB-6	SB-10	S-1	S-2	Average	
SiO ₂	59.69	56.46	59.03	56.05	57.59	58.95	57.96	57.89	56.19	57.5	57.84	55.92	57.07	
TiO ₂	0.13	0.16	0.54	0.21	0.09	0.11	0.21	0.27	0.02	0.24	0.26	0.1	0.18	
Al ₂ O ₃	21.92	22.51	20.43	22.57	23.16	21.98	22.10	22.63	26.16	22.13	22.75	24.76	23.69	
Fe ₂ O ₃	1.78	2.78	3.94	3.36	1.88	2.41	2.69	2.87	0.53	3.29	2.74	2.38	2.36	
MnO	0.09	0.08	0.12	0.09	0.12	0.1	0.10	0.11	0.01	0.11	0.09	0.09	0.08	
MgO	0.02	0.01	0.17	0	0	0	0.03	0.06	0	0	0.16	0	0.04	
CaO	0.45	0.4	1.01	0.49	0.54	0.94	0.64	0.44	0.4	0.96	1.07	0.88	0.63	
Na ₂ O	9.36	10.85	9.83	11.29	12.54	11.5	10.90	8.95	12.05	10	9.04	10.48	10.10	
K ₂ O	5.91	6.28	5.63	5.97	3.8	4.19	5.30	5.48	5.24	5.06	5.37	5.24	5.28	
P ₂ O ₅	0.02	0.01	0.01	0.02	0	0.01	0.01	0.02	0.01	0.02	0.03	0.03	0.02	
Total	99.37	99.54	100.71	100.05	99.72	100.19	99.93	98.72	100.61	98.71	99.35	99.88	99.45	
CIPW NORM														
Or	34.93	37.11	33.27	35.28	22.46	24.76	31.30	32.99	30.97	29.9	31.74	30.97	31.19	
Ab	40.12	19.92	33.26	18.69	36.94	39.03	31.33	40.65	26.12	40.05	38.04	29.99	34.97	
An	0.34						0.06	2.05	1.82	0.55	5.11	4.17	2.74	
Ne	21.17	32.99	21.93	34.76	33.07	27.47	28.57	19	41.09	24.14	20.83	31.79	27.37	
Cor							0.00	1.22			0.19	0.32	0.35	
Aeg(Ac)		8.04	8.31	9.72	5.44	6.67	6.36							
Di	0.11	0.05	0.91		0.14		0.20							
Wo	0.63	0.67	0.99	0.8	1.05	1.92	1.01		0.03	0.29				
Mt						0.01								
Il	0.19	0.17	0.26	0.19	0.17	0.21	0.20	0.24	0.02	0.24	0.19	0.19	0.18	
Hem	1.78		1.07			0.1	0.49	2.87	0.53	3.29	2.74	2.38	2.36	
Ap	0.05	0.02	0.02	0.05		0.02	0.03	0.05	0.02	0.05	0.07	0.07	0.05	
NORMATIVE MINERALOGY														
D.I.	96.22	90.02	88.46	88.73	92.47	91.26	91.19	92.04	98.18	94.09	90.61		74.98	
AN/AB+AN	0.01						0.00	0.05	0.07	0.01	0.12	0.12	0.07	
S.I.	0.12	0.05	0.87	0.00	0.00	0.00	0.17	0.95	0.00	0.00	0.92	0.00	0.25	
100Mg/Mg+Fe(Mol)														
Agpaitic Index	1	1.1	1.09	1.11	1.07	1.07	1.07	0.91	0.98	0.99	0.91	0.93	0.94	
TRACE ELEMENTS AND REE (ppm)														
Rb	144	137	114	99	85	20	100	145	78	147	112	106	118	
Li	25	24	33	48	15	16	27	42	30	14	17	12	23	
Sr	451	834	1395	863	310	204	676	491	1019	691	1769	821	958	
Ba	303	606	1445	676	153	204	564	327	697	247	1296	370	587	
V	31	32	55	27	15	20	30	41	9	35	41	23	30	
Cr	6	5	41	2	n.d	n.d	9	3	24	n.d	3	7	7	
Zn	78	138	104	156	132	u.d	101	112	9	125	63	35	69	
Ga	32	29	32	32	63	35	37	36	36	36	30	32	34	
Sc	8	4	6	n.d	n.d	n.d		n.d	n.d	n.d	4	6	3	
Y	6	6	12	7	34	54	20	9	6	9	9	4	7	
Zr	172	663	738	70	3617	777	1006	177	303	224	156	34	179	
Nb	25	28	99	21	177	123	79	38	28	33	34	5	28	
Th	6	8	8	7	57	26	19	5	11	2	5	2	5	
La	14	19	29	14	60	43	30	21	11	20	27	15	19	
Ce	19	20	36	16	103	59	42	23	10	26	39	13	22	
Pr	2.8					5.3		3.2	4.2		8			
Nd	6	4	6.3		19.4	17		6.6	4.9	4	13			
Sm	0.40					2.12		0.38	0.49		1.26			
Eu	0.37					0.79		0.30	0.28		0.74			
Gd	6.20					3.66		5.55	1.80		4.14			
Dy	1.28					2.55		1.15	1.09		2.10			
Er	1.11					1.85		1.03	0.55		1.05			
Yb	0.45					1.08		0.33	0.20		0.63			
Lu	0.10					0.12		0.08	0.04		0.11			

Table 7.4: Major and trace element analyses of Foyaitic Feldspathoidal Syenites (phonolitic trend).								
		Foyaitic Feldspathoidal Syenites (Phonolitic trend)						
		MK-2	MK-24	MK-25	S-5	S-6	K-8	Average
MAJOR ELEMENTS								
SiO ₂		59.59	59.91	58.8	59.11	58.28	59.03	59.12
TiO ₂		0.13	0.05	0.3	0.2	0.15	0.17	0.17
Al ₂ O ₃		21.79	21.14	21.54	22.06	22.81	22.55	21.98
Fe ₂ O ₃		1.68	1.22	2.47	2.06	2.14	1.71	1.88
MnO		0.14	0.09	0.14	0.13	0.12	0.09	0.12
MgO		0.01	0.01	0.11	0.05	0.02	0.09	0.05
CaO		0.81	0.33	1.06	0.86	0.71	0.78	0.76
Na ₂ O		9.4	9.21	8.9	9.76	9.76	9.6	9.44
K ₂ O		6.67	7.87	6.06	5.49	5.34	5.79	6.20
P ₂ O ₅		0.05	0.01	0.03	0.02	0.02	0.03	0.03
Total		100.27	99.84	99.41	99.74	99.35	99.84	99.74
CIPW NORM								
Or		39.42	49.51	35.81	32.44	31.56	34.22	37.16
Ab		30.49	25.42	37.09	39.37	38.39	37.29	34.68
An				0.93	0.17	2.66	1.34	0.85
Ne		24.09	21.4	20.7	23.21	23.94	23.8	22.86
Aeg(Ac)		4.04	3.53					
Di		0.05	0.21	0.59	0.27	0.11	0.48	0.29
Wo		1.51	0.55	1.2	1.43	0.23	0.62	0.92
Mt		0.08						
Il		0.25	0.09	0.3	0.28	0.26	0.19	0.23
Hem		0.23		2.47	2.06	2.14	1.71	1.44
Ap		0.12	0.02	0.07	0.05	0.05	0.07	0.06
NORMATIVE MINERALOGY								
D.I.		94	96.33	93.6	95.02	93.89	95.31	94.69
AN/AB+AN				0.02	0.004	0.06	0.03	0.02
S.I.		0.06	0.05	0.63	0.29	0.12	0.52	0.28
100Mg/Mg+Fe(Mol)								
Alphatic Index		1.04	1.12	0.99	1	0.96	0.98	1.02
TRACE ELEMENTS AND REE (ppm)								
Rb		223	158	136	139	138	139	156
Li		59	13	18	51	46	14	33
Sr		172	144	102	164	156	168	151
Ba		87	95	32	56	62	77	68
V		16	12	26	20	20	16	18
Cr		4	13	2	1	12	2	5
Zn		140	38	47	57	62	34	63
Ga		50	31	28	32	36	33	35
Se		3	3	n.d	n.d	2	n.d	
Y		43	7	8	7	9	2	13
Zr		1513	334	176	265	564	182	506
Nb		164	10	67	55	55	39	65
Th		37	16	2	4	10	4	12
La		81	30	67	59	36	85	60
Ce		101	25	77	63	45	83	66
Nd		27	3	13	9	6	11	11
Pr			2.22		7.36		4.99	
Sm			0.66		1.40		0.95	
Eu			0.21		0.36		0.34	
Gd			1.99		1.83		2.90	
Dy			0.72		1.19		1.01	
Er			0.81		1.14		1.24	
Yb			0.32		0.67		0.53	
Lu			0.08		0.13		0.06	

Table 7.5: Major and trace element of Feldspathoidal Syenites (trachytic trend)													
Feldspathoidal Syenites (trachytic trend)													
	MK-4	MK-5	MK-11	MK-13	MK-14	MK-15	MK-17	MK-20	MK-21	MK-22	S-3	BD-1	Average
MAJOR ELEMENTS													
SiO ₂	60.8	60.67	60.9	60.63	59.23	59.76	61.12	60.7	60.08	60.71	59.43	59.47	60.29
TiO ₂	0.61	0.45	0.46	0.65	0.71	0.77	0.16	0.53	0.49	0.42	0.38	0.46	0.51
Al ₂ O ₃	19.38	19.46	20.05	19.3	19.99	20.02	21.03	19.5	19.29	19.48	21	20.95	19.95
Fe ₂ O ₃	2.84	2.91	2.93	2.79	2.97	3.44	2.12	3.31	3.46	3.21	2.93	2.72	2.97
MnO	0.16	0.13	0.13	0.13	0.13	0.17	0.11	0.12	0.15	0.17	0.17	0.12	0.14
MgO	0.23	0.22	0.04	0.22	0.16	0.17	0.01	0.14	0.23	0.21	0.14	0.2	0.16
CaO	1.19	1.07	0.93	1.27	1.23	1.3	0.46	1.05	1.14	1.08	1.21	1.19	1.09
Na ₂ O	8.06	7.29	9.49	7.91	8.23	7.94	8.66	7.79	8.15	8.19	8.28	7.75	8.15
K ₂ O	5.95	6.35	6.05	5.97	5.98	6.64	5.73	6.28	5.89	6.07	6.16	6.78	6.15
P ₂ O ₅	0.05	0.05	0.04	0.05	0.02	0.04	0.02	0.04	0.05	0.05	0.04	0.05	0.04
Total	99.27	98.6	101.02	98.92	98.65	100.25	99.42	99.46	98.93	99.59	99.74	99.69	99.46
CIPW NORM													
Or	35.16	37.53	35.75	35.28	35.34	39.24	33.86	37.11	34.81	35.87	36.4	40.07	36.37
Ab	45.39	45.18	36.04	45.82	42.02	38.31	47.14	44.62	43.43	43	39.43	36.5	42.24
An		1.62					1.59				1.94	2.35	0.63
Ne	11.47	8.94	18.1	10.95	14.91	15.01	14.16	11.23	12.46	12.68	16.59	15.75	13.52
Aeg(Ac)	1.44		8.48	0.79	0.09	1.03		0.51	2.23	2.55			1.43
Di	1.24	1.18	0.21	1.18	0.86	0.91	0.05	0.75	1.24	1.13	0.75	1.07	0.88
Wo	1.04	0.33	1.25	1.13	1.21	1.25	0.15	1.09	1.1	1.16	0.91	0.3	0.91
Il	0.34	0.28	0.28	0.28	0.28	0.36	0.24	0.26	0.32	0.36	0.36	0.26	0.30
Hem	2.34	2.91		2.52	2.94	3.08	2.12	3.13	2.69	2.33	2.93	2.72	2.48
Ap	0.12	0.12	0.09	0.12	0.05	0.09	0.05	0.09	0.12	0.12	0.09	0.12	0.10
NORMATIVE MINERALOGY													
D.I.	92.02	91.65	89.89	92.05	92.27	92.56	95.16	92.96	90.7	91.55	92.42	92.32	92.1292
AN/AB+AN		0.03	0.00	0.00	0.00	0.00	0.03	0.00	0.00	0.00	0.05	0.06	0.01
S.I.	1.35	1.31	0.22	1.30	0.92	0.93	0.06	0.80	1.30	1.19	0.80	1.15	0.94
100Mg/Mg+Fe(Mol)													
Agpaitic Index	1.02	0.97	1.11	1.01	1	1.01	0.97	1.01	1.03	1.03	0.97	0.96	
TRACE ELEMENTS AND REE (ppm)													
Rb	180	177	150	143	143	157	109	166	159	158	163	104	151
Li	68	73		30	40	40	26	29	58	61	22	16	39
Sr	428	188	518	428	601	430	473	452	140	158	143	253	351
Ba	194	54	222	149	266	143	201	230	129	126	38	86	153
V	32	48	42	43	53	51	36	37	44	49	35	37	42
Cr	n.d	n.d	2	n.d	n.d	2	n.d	n.d	2	n.d	5	40	4
Zn	139	111	123	113	110	80	70	76	111	178	67	43	102
Ga	32	28	30	30	30	37	24	27	33	30	28	23	29
Sc	5	6	6	3	3	n.d	4	4	6	4	4	4	4
Y	36	19	22	22	21	27	12	18	24	16	9	12	20
Zr	741	436	575	566	404	564	238	326	715	421	313	186	457
Nb	153	88	107	142	142	170	65	111	118	84	85	91	113
Th	28	15	14	16	13	20	5	10	18	7	6	12	14
La	105	49	47	61	62	68	31	49	58	38	63	41	56
Ce	165	71	71	87	98	107	48	80	83	55	89	64	85
Nd	42	18	19	21	24	22	11	21	17	14	17	14	20
Pr		9.49							12.25		9.11	7.55	
Sm		2.33							1.99		2.43	2.14	
Eu		0.89							1.16		0.59	0.64	
Gd		11.99							22.02		2.68	4.41	
Dy		2.96							4.05		1.83	2.05	
Er		2.41							3.53		1.45	1.64	
Yb		1.04							1.65		0.90	0.79	
Lu		0.16							0.30		0.16	0.13	

Table 7.6: Major and trace element analyses of Pulaskitic Feldspathoidal Syenites														
Pulaskitic Feldspathoidal Syenite														
	MK-8	MK-9	MK-10	MK-12	MK-18	MK-19	SB-2	SB-7	SB-9	SB-12	BD-2	K-3	K-4	Average
MAJOR ELEMENTS														
SiO ₂	61.72	61.05	61.31	61.39	60.44	61.49	61.96	59.29	60.17	61.56	60.66	59.91	60.65	60.89
TiO ₂	0.37	0.41	0.45	0.46	0.4	0.29	0.23	0.58	0.45	0.43	0.81	0.63	0.58	0.47
Al ₂ O ₃	19.86	19.35	19.64	19.27	19.65	20.31	19.77	20.32	19.8	19.48	18.42	19.47	18.81	19.55
Fe ₂ O ₃	2.62	2.53	2.86	3.06	3.35	1.67	4.39	4.49	2.42	2.6	3.45	3.14	3.47	3.08
MnO	0.11	0.13	0.13	0.12	0.14	0.1	0.11	0.15	0.13	0.13	0.14	0.14	0.15	0.13
MgO	0.13	0.19	0.16	0.17	0.14	0	0.02	0.47	0.24	0.26	0.44	0.48	0.33	0.23
CaO	0.68	1.18	0.95	0.97	0.94	0.58	0.46	0.88	1.33	0.91	1.71	1.64	1.46	1.05
Na ₂ O	8.67	7.41	8.26	7.74	7.56	8	7.69	8.54	8.4	7.45	7.06	7.59	7.08	7.80
K ₂ O	4.59	6.49	5.42	5.79	5.89	6.21	5.36	5.36	5.43	6.36	6.43	6.03	6.06	5.80
P ₂ O ₅	0.02	0.04	0.04	0.04	0.03	0.02	0.02	0.01	0.06	0.05	0.09	0.05	0.06	0.04
Total	98.77	98.78	99.22	99.01	98.54	98.67	100.01	100.09	98.43	99.23	99.21	99.08	98.65	99.05
CIPW NORM														
Or	27.13	38.35	32.03	34.22	34.81	36.7	31.68	31.68	32.09	37.59	38	35.64	35.81	34.29
Ab	57.36	44.67	51.21	50.34	47.47	46.91	55.84	45.38	47.06	46.9	44.32	43.2	47.37	48.31
An	1.72	0.37	0.51	0.74	2.29	1.17	2.15	1.28	0.29	0.93		1.25	1.65	1.10
Ne	8.67	9.77	10.12	8.21	8.94	11.26	5	14.56	13.01	8.74	7.93	11.39	6.79	9.57
Cor							0.53							
Aeg(Ac)											0.69			
Di	0.52	1.02	0.86	0.91	0.75			1.23	1.29	1.4	2.36	2.58	1.77	1.13
Wo		1.25	0.74	0.63	0.15	0.4			1.34	0.2	1.08	0.67	0.62	0.54
Il	0.24	0.28	0.28	0.26	0.3	0.21	0.24	0.32	0.28	0.28	0.3	0.3	0.32	0.28
Hem	2.62	2.53	2.86	3.06	3.35	1.67	4.39	4.49	2.42	2.6	3.21	3.14	3.47	3.06
Ap	0.05	0.09	0.09	0.09	0.07	0.05	0.05	0.02	0.14	0.12	0.21	0.12	0.14	0.10
NORMATIVE MINERALOGY														
D.I.	93.16	92.79	93.36	92.77	91.22	94.87	92.52	91.62	92.16	93.23	90.25	90.23	89.97	92.17
AN/AB+AN	0.03	0.01	0.01	0.01	0.05	0.02	0.04	0.03	0.01	0.02	0.00	0.03	0.03	0.02
S.I.	0.81	1.14	0.96	1.01	0.83	0.00	0.11	2.49	1.46	1.56	2.53	2.78	1.95	1.36
100Mg/Mg+Fe(Mol)														
Agpatic Index	0.97	0.99	0.99	0.99	0.96	0.98	0.93	0.98	1	0.98	1.01	0.98	0.97	0.98
TRACE ELEMENTS AND REE (ppm)														
Rb	118	160	161	150	111	147	121	149	115	143	105	151	154	137
Li	30	39	39	47	17	19	37	52	17	43	18	41	35	33
Sr	419	590	2393	497	1223	1086	854	1666	513	360	741	305	477	856
Ba	5	n.d.	n.d.	n.d.	n.d.	n.d.	n.d.	23	3	n.d.	n.d.	n.d.	n.d.	3
V	33	37	52	46	34	27	52	85	37	38	52	47	55	46
Cr	5	n.d.	2	n.d.	2	0	2	23	3	n.d.	2	n.d.	n.d.	3
Zn	98	81	113	117	68	61	108	163	46	104	75	98	105	95
Ga	36	28	29	28	30	27	29	33	27	26	19	n.d.	n.d.	24
Sc	3	7	4	5	3	3	8	6	n.d.	3	4	n.d.	n.d.	4
Y	21	18	11	19	7	8	7	12	11	15	19	17	20	14
Zr	796	636	725	494	520	165	278	852	183	353	318	511	543	490
Nb	126	94	76	87	36	51	47	88	70	102	142	138	123	91
Th	16	16	11	16	8	5	8	6	n.d.	4	3	9	14	9
La	39	60	39	51	21	26	30	30	50	46	69	66	71	46
Ce	57	78	35	81	21	30	33	35	68	66	105	104	110	63
Nd	14	15	n.d.	19	n.d.	5	3	5	13	12	22	27	28	12.56
Pr				8.15		7.55			7.21	7.12		8.31	9.11	
Sm				1.90		1.57			1.29	1.56		2.71	3.08	
Eu				0.87		0.69			0.77	0.65		0.92	0.97	
Gd				13.19		6.03			9.73	9.03		6.05	5.25	
Dy				3.03		2.18			2.17	2.37		2.54	2.94	
Er				2.46		1.07			1.54	2.03		1.80	2.13	
Yb				1.22		0.55			0.80	0.87		1.01	1.32	
Lu				0.19		0.08			0.15	0.15		0.18	0.14	

Table 7.7: Major and trace element analyses of the garnet bearing feldspathoidal syenite and alkali syenite.					
	Garnet bearing feldspathoidal syenite			Alkali Syenites	
	BD-3	BD-4	Average	K-1	
MAJOR ELEMENTS					
SiO ₂	55.87	56.09	55.98		61.35
TiO ₂	0.65	0.97	0.81		0.8
Al ₂ O ₃	21.43	19.57	20.5		18.04
Fe ₂ O ₃	4.5	5.05	4.775		3.77
MnO	0.19	0.18	0.185		0.15
MgO	0.39	0.63	0.51		0.38
CaO	3.32	3.23	3.275		1.81
Na ₂ O	8.17	7.87	8.02		5.1
K ₂ O	4.76	4.76	4.76		7.46
P ₂ O ₅	0.08	0.15	0.115		0.07
Total	99.96	98.5	98.93		98.93
CIPW NORM					
Or	28.13	28.13	28.13		44.09
Ab	35.87	39.57	37.72		43.16
An	7.74	4.02	5.88		4.3
Ne	18.02	14.64	16.33	Ti	1.09
Di	2.09	3.38	2.74		1.58
Wo	1.67	1.67	1.67	Ol	0.15
Il	0.41	0.39	0.40		0.32
Hem	4.5	5.05	4.78		3.77
Ap	0.19	0.35	0.27		0.16
NORMATIVE MINERALOGY					
D.I.	82.02	82.34			88.34
AN/AB+AN	0.18	0.09			0.09
S.I.	2.19	3.44	2.82		2.27
100Mg/Mg+Fe(Mol)					
Agpaitic Index	0.86	0.93			0.91
TRACE ELEMENTS AND REE (ppm)					
Rb	104	108	106		82
Li	21	23	22		17
Sr	4454	3032	3743		1081
Ba	4425	3109	3767		751
V	74	90	82		72
Cr	6	7	6		n.d
Zn	68	100	84		59
Ga	23	23	23		21
Sc	5	5	5		
Y	75	21	48		16
Zr	382	305	343		238
Nb	88	115	101		130
Th	1	12	7		2
La	167	87	127		81
Ce	167	116	142		127
Nd	22	21	22		34
Pr					14.92
Sm					3.38
Eu					1.63
Gd					17.03
Dy					4.00
Er					3.30
Yb					1.45
Lu					0.11

Table 7.8: Average composition of Feldspathoidal Syenites of the Koga complex.									
	Sodalite-				Garnet bearing	Foyaltic	Pulaskitic		
	Sodalite-rich	cancrinite-rich	Feldspathoidal		feldspathoidal	feldspathoidal	Feldspathoidal	feldspathoidal	Alkali
	foyaltes	foyaltes	foyaltes		syenites	syenites	syenites	syenites	syenites
			Agpaltic	Miaskitic		Phonilitic trend	Trachytic trend		
No. of sample	[5]	[3]	[6]	[5]	[2]	[6]	[12]	[13]	[1]
Major Elements (wt. %)									
SiO ₂	57.71	57.05	57.96	57.07	55.98	59.12	60.29	60.89	61.35
TiO ₂	0.16	0.15	0.21	0.18	0.81	0.17	0.51	0.47	0.8
Al ₂ O ₃	21.99	23.09	22.10	23.69	20.5	21.98	19.95	19.55	18.04
Fe ₂ O ₃	3.41	2.79	2.69	2.36	4.775	1.88	2.97	3.08	3.77
MnO	0.17	0.14	0.10	0.08	0.185	0.12	0.14	0.13	0.15
MgO	0.03	0.08	0.03	0.04	0.51	0.05	0.16	0.23	0.38
CaO	0.91	0.86	0.64	0.63	3.275	0.76	1.09	1.05	1.81
Na ₂ O	11.55	10.44	10.90	10.10	8.02	9.44	8.15	7.80	5.1
K ₂ O	3.19	5.25	5.30	5.28	4.76	6.20	6.15	5.80	7.46
P ₂ O ₅	0.01	0.02	0.01	0.02	0.115	0.03	0.04	0.04	0.07
Total	99.12	99.86	99.93	99.45	98.93	99.74	99.46	99.05	98.93
Trace Elements (ppm)									
Rb	188	124	100	118	106	156	151	137	82
Li	61	44	27	23	22	33	39	33	17
Sr	120	85	676	958	3743	151	351	856	1081
Ba	53	35	564	587	3767	68	153	3	751
V	30	22	30	30	82	18	42	46	72
Cr	2	1	9	7	6	5	4	3	u.d
Zn	125	83	101	69	84	63	102	95	59
Ga	29	39	37	34	23	35	29	24	21
Sc	1	2	3	3	5	2	4	4	n.d
Y	20	23	20	7	48	13	20	14	16
Zr	1052	295	1006	179	343	506	457	490	238
Nb	124	24	79	28	101	65	113	91	130
Th	15	6	19	5	7	12	14	9	2
La	32	27	30	19	127	60	56	46	81
Ce	52	37	42	22	142	66	85	63	127
ELEMENT RATIOS									
K/Rb	252.33	142.00	380.50	394.00	376	339.33	349.83	358.85	758
K/Ba	1287.00	1033.60	121.67	104.80	11	841.33	467.25	125.92	82.77
Rb/Sr	1.62	1.86	0.21	0.16	0.03	0.91	0.54	0.22	0.08

Table 7.9: Representative analyses of major and trace elements of Foyaites and Nepheline syenites from the typical alkaline provinces of the world.

	Foyaites					Nepheline syenites						
	1	2	3	4	5	6	7	8	9	10	11	12
No. of samples	[2]	[2]	[2]	[4]		[44]	[8]	[8]	[4]	[Ave]	[Ave]	[115]
Major Elements (Wt. %)												
SiO ₂	57.3	55.05	55.72	55.05	56.27	55.46	56.11	58.71	61.29	53.62	55.74	55
TiO ₂	0.35	0.4	0.48	0.44	0.09	0.75	0.4	0.75	0.68	1.12	0.85	0.6
Al ₂ O ₃	22.6	21.45	20.99	22.13	21.55	21.15	20.72	19.26	18	17.39	18.26	20.96
Fe ₂ O ₃	2.7	2.94	3.34	3.33	2.97	3.1	4.67	4.04	3.4	5.45	5.5	4.5
MnO	0.24	0.13	0.21	0.16	0.17	0.13	0.09	0.17	0.14	0.26	0.25	0.15
MgO	0.34	0.2	0.27	0.38	0.04	0.59	0.5	0.8	0.69	1.98	1.01	0.77
CaO	0.6	1	1.3	1.77	1.12	1.8	1.37	1.63	1.74	1.22	2.57	2.31
Na ₂ O	10.63	10.55	9.43	10.01	10.5	8.36	8.95	7.79	5.99	10.07	8.53	8.23
K ₂ O	5.32	5.45	5.92	5.24	6.24	6.45	5.82	5.71	6.23	5.86	4.82	5.58
P ₂ O ₅	0.04	0.05	0.06	0.45	0.07	0.1	0.22	0.23	0.21	0.2	0.42	0.13
TRACE ELEMENTS AND REE (ppm)												
Rb	176	11	220	233	280	182	115	118	174	230	94	
Li						32						
Sr		468	711	1036	65	717	120	253	571	610	881	
Ba	140	350	314	1143	57	534	310	1148	1334	630	1324	
V			16						20			
Cr				14			23					
Zn		29	127	202	92	73	80	81	75	210	107	
Pr												
Ga											21	
Sc	0.4				0.6						3	
Y		29	25		98	19		46	38	135	33	
Zr	530	680	963		519	561		489	326	3480	545	
Nb		143	355		117	186		129	217	695	145	
Th	102		34		26				19.5	35	15	
La	79				211						107	
Ce	138		215		444				182	860	167	
Nd	32				163							
Pr												
Sm	4.1				26.4							
Eu	0.68				2.2							
Dy												
Er												
Yb	1.9				8.7					10		
Lu	0.35				1.2							
ELEMENT RATIOS												
K/Rb	251	408	223	187	185	294	420	402	297	211	426	
K/Ba	315	129	157	38	909	100	156	41	39	77	30	
Rb/Sr		0.24	0.31	0.22	4.3	0.25	0.96	0.47	0.3	0.38	0.11	
Ba/Rb	0.8	3.2	1.4	4.9	0.2	2.9	2.7	9.7	7.7	1.03	14.1	
Ba/Sr		0.75	0.44	1.1	0.88	0.74	2.6	4.5	2.3		1.5	
1 = Nepheline - sodalite syenite, Mont Saint Hilaire Complex, South Quebec, Canada (Currie et al. 1986).												
2 = Nepheline - cancrinite syenite, Junguni, Chilwa, Malawi (Woolley and Jones, 1987).												
3 = Foyaites, Velasco Alkaline Province, Bolivia (Fletcher and Beddoe - Stephens, 1987).												
4 = Foidal syenites, Sarnu - Dandali, Rajasthan, India (Srivastava, 1989).												
5 = Foyaites, Motzfeldt Centre, South Greenland (Jones and Larsen, 1985).												
6 = Foyaites, Serra de Monchique, Portugal (Czygan, 1984).												
7 = Nepheline syenites, Kishangarh, Rajasthan, India (Srivastava, 1989).												
8 = Nepheline syenites, Mongoiowe, Chilwa, Malawi, (Woolley and Jones, 1987).												
9 = Pulaskites, Velasco Alkaline Province, Bolivia (Fletcher and Beddoe - Stephens, 1987).												
10 = Average, Lovozero Complex, USSR (Gerasimovsky, 1974 and Kogarko, 1987).												
11 = Average phonolite, Kenya rift Alkaline Province (Price et al. 1985).												
12 = Average nepheline syenite of the world (Le Maitre, 1976).												

Table 7.10. Selected compatible and incompatible trace element ratios for the Koga feldspathoidal syenite rocks.

Rock Type	Sample No.	Ti/V	Cr/Sc	Ti/Zr	Zr/Y	Ti/Nb	Ba/Nb	Zr/Nb	La/Nb	Y/Nb
Sodalite - cancrinite foyaite	MK- 1	39.20	0.44	3.4	28.9	29.1	1.2	8.5	0.80	0.30
	MK- 3	41.10		3.0	37.4	20.5	0.92	6.9	0.37	0.18
	SB-14	55.40	0.15	0.69	90.4	6.6	0.28	9.5	0.13	0.11
	SB-15	23.30	2.50	1.4	100.2	25.5	0.21	18.2	0.17	0.18
	SB-16	31.10		0.6	53.8	4.6	0.21	7.6	0.15	0.14
	K- 5					5.0			0.27	
	K- 6					29.0			0.45	
	K- 9					22.1			1.05	
Feldspathoidal foyaite	MK - 6	25.20	0.77	4.5	28.7	31.2	12.1	6.9	0.56	0.24
	MK-16	30.00	1.14	1.45	107.0	34.3	21.6	23.7	0.68	0.22
	SB - 5	58.90	7.5	4.4	62.5	32.7	14.6	7.5	0.29	0.12
	SB-11	46.70	2.9	18.0	10.0	60.0	32.1	3.3	0.67	0.33
	S - 4	36.00		0.15	106.4	3.1	0.86	20.4	0.34	0.19
	K - 2					5.5			0.36	
	SB - 1	39.5	0.91	13.8	12.9	42.6	12.9	3.1	0.55	0.24
	SB - 6	13.3	34.3	0.40	50.5	4.3	36.4	10.8	0.39	0.21
	SB-10	41.1		6.4	25.5	43.6	7.5	6.8	0.61	0.27
	S - 1	38.0	0.81	10.0	16.6	45.9	52.0	4.6	0.79	0.28
	S - 2	26.1	1.23	17.6	8.5	120.0	164.5	6.8	3.00	0.80
Foyaitic feldspathoidal syenites (Phonolitic - trend)	MK - 2	48.8	1.30	0.52	35.2	4.8	0.53	9.2	0.49	0.26
	MK-24	25.0	4.3	0.90	47.7	30.0	9.5	33.4	1.70	0.70
	MK-25	69.2	2.0	10.2	22.0	26.9	0.48	2.6	1.00	0.12
	S - 5	60.0	0.71	4.5	37.3	21.8	1.02	4.8	1.93	0.13
	S - 6	45.0	8.0	1.6	61.3	16.4	2.84	10.1	0.65	0.17
	K - 8					26.2	4.3		2.20	
Feldspathoidal syenites (Trachytic - trend)	MK - 4	114.4		4.9	20.6	23.9	1.3	4.8	0.69	0.24
	MK - 5	56.3	0.16	6.2	22.5	30.7	0.61	5.0	0.67	0.22
	MK-11	65.7	0.32	4.8	26.1	25.8	2.07	5.4	0.44	0.21
	MK-13	90.7		6.9	25.7	27.5	1.05	4.0	0.43	0.16
	MK-14	80.4		10.5	19.2	30.3	1.9	2.9	0.44	0.15
	MK-15	90.6	1.11	8.2	20.9	27.2	0.84	3.3	0.40	0.16
	MK-17	26.7		4.1	19.8	14.8	3.1	3.7	0.48	0.19
	MK-20	85.9		9.8	18.1	28.6	20.7	2.9	0.44	0.16
	MK-21	66.8	0.33	4.1	29.8	24.9	1.1	6.1	0.71	0.20
	MK-22	51.4		6.0	26.3	30.0	1.5	5.0	0.45	0.19
	S - 3	65.1	1.2	7.3	33.3	26.8	0.12	3.7	0.82	0.11
	BD - 1	74.6	10.26	14.8	15.5	30.3	0.46	2.0	0.41	0.13
Pulaskitic feldspathoidal syenites	MK - 8	69.4	1.72	2.8	37.2	17.6	2.9	6.3	0.31	0.17
	MK - 9	66.5		3.9	35.3	26.2	3.2	6.8	0.64	0.19
	MK-10	51.9	0.46	3.7	64.2	35.5	38.7	9.5	0.51	0.15
	MK-12	60.0		5.6	26.0	31.7	2.4	5.7	0.60	0.22
	MK-18	70.6	0.80	4.6	74.3	66.7	1.7	14.2	0.58	0.19
	MK-19	64.4	0.38	10.5	20.6	34.1	17.9	3.2	0.53	0.16
	SB - 2	26.5	0.26	5.0	38.6	29.4	3.4	5.9	0.64	0.15
	SB - 7	40.9	3.97	4.1	72.2	39.5	18.7	9.7	0.34	0.13
	SB - 9	73.0	1.36	14.8	16.6	38.6	10.9	2.6	0.54	0.16
	SB-12	67.9		7.3	23.5	25.3	2.1	3.5	0.40	0.15
	BD - 2	93.5	0.81	12.9	16.7	34.2	5.2	2.2	0.49	0.13
	K - 3					27.4			4.3	0.40
	K - 4					28.3			2.7	0.46
Garnet bearing felds. syenites	BD - 3	52.7	1.25	10.2	5.1	44.3	50.3	1.8	1.90	0.85
	BD - 4	64.7	1.56	19.1	14.5	50.6	27.0		0.76	0.18
Alkali syenite	K - 1			18.0	14.3	36.9	8.4		0.53	0.18

of SiO₂ contents (55 - 62 %). Most of the feldspathoidal syenite rocks are strongly peralkaline and are characterised by very high total alkali contents (Na₂O + K₂O) which range from 13 % to 18 %. This is reflected in their high normative nepheline values (8 % to 42 %). All these rocks also contain high modal nepheline. However, the feldspathoidal syenite from Sura, Bibi Dheri and Sahbaga are meta aluminous and are alkaline in character.

7.2.1 Total Alkali – Silica Diagram

Since the total alkalis are the major variable component in the composition of these rocks, it is appropriate to draw the alkali - silica diagram. Total alkalis against SiO₂ are plotted in Fig. 7.1 from the chemical analyses of the Koga feldspathoidal syenite complex. All the rock types of the Koga complex area fall within the well defined compositional range of the alkaline province of Gardar, SW Greenland (Upton, 1974) and the alkaline complexes of India (Ratnakar and Leelanandam, 1989, Leelanandam et al. 1989). The feldspathoidal syenites are relatively slightly enriched in alkalis as compared to the similar compositions of foyaites and foyaitic nepheline syenites from the known complexes of India – Rajasthan, (Srivastava, 1989) Gujrat (Sethna, 1989) and Andhra Pradesh (Leelanadam, 1989).

A spectrum of rock suites has been recognised in the Koga feldspathoidal syenite complex which clearly show systematic low temperature divergence away from the trachytic compositions both towards undersaturated and oversaturated cotectics of the petrogeny's residua system. The foyaites and foyaitic feldspathoidal syenites plot along the undersaturated agpaitic and phonoiitic trend departing to the left side away from the more trachytic compositions due to sodium enrichment. On the other hand feldspathoidal syenites, garnet bearing syenites and alkali syenite plot towards the oversaturated residua system representing pulaskite – alkali granite trend (Mateen, personal communication, 1993). The distribution of the Koga feldspathoidal rocks and their field associations

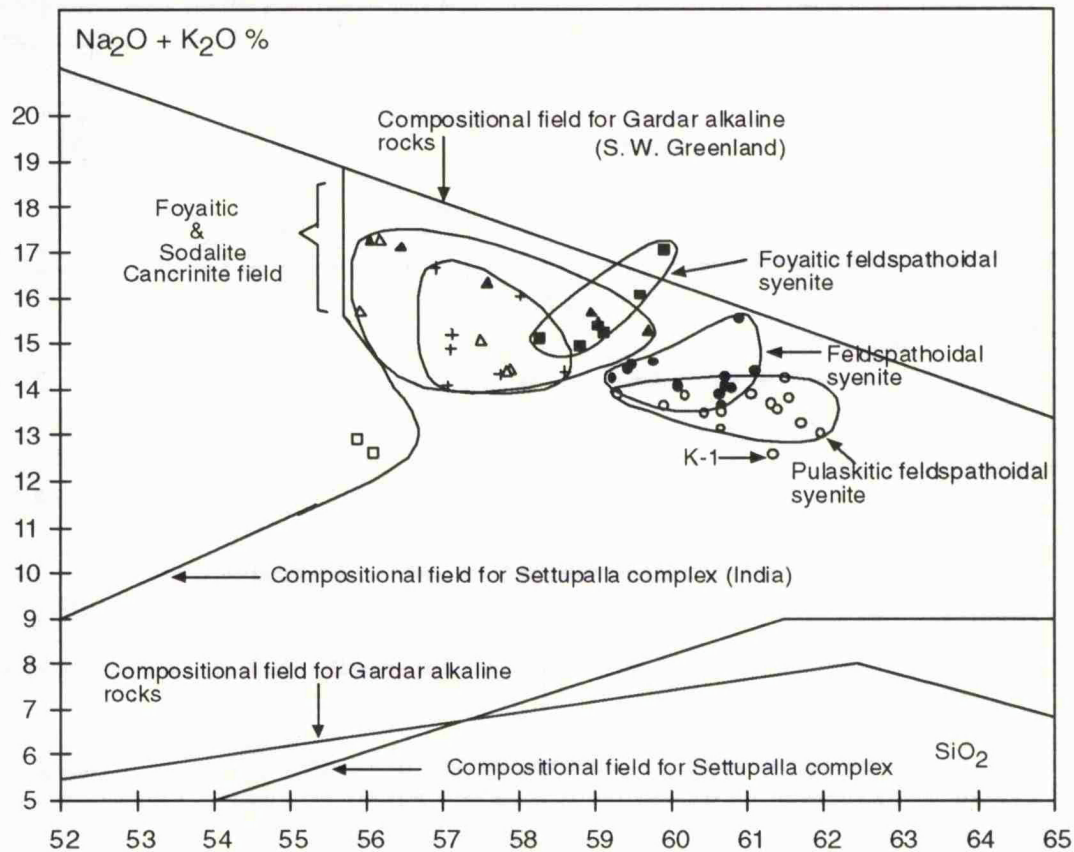


Fig. 7.1 Total alkali - silica diagram for the Koga feldspathoidal syenite rocks.

indicate that there is close similarity among the rock suites of Koga, Chilwa alkaline province and peralkaline rocks of Rajasthan, India. Four types of rock association with the Koga complex have been identified as follows,

- 1) Lamprophyres
- 2) Ijolite - carbonatite - fenites
- 3) Foyaitic feldspathoidal syenite - pulaskite - feldspathoidal syenites
- 4) Alkali syenites - quartz syenites - alkali granites

While there are lamprophyres within the area under investigation, none have been analysed. The ijolites, carbonatites and fenites lie outside the area (Mian, et al.1987).

7.2.2 Alkalinity

The Koga complex rocks are predominantly peralkaline agpaitic types, characterised by the excess of alkalis in relation to alumina. The feldspathoidal

syenite rocks from the complex have been grouped into two alkalic trends, agpaitic and miaskitic depending on higher and lower agpaitic index (taken as 0.98) as shown in Fig. 7.2. The majority of the rock analyses plot in the field of agpaitic syenites with agpaitic indices significantly higher than 1.0 (range from 0.98 to 1.12).

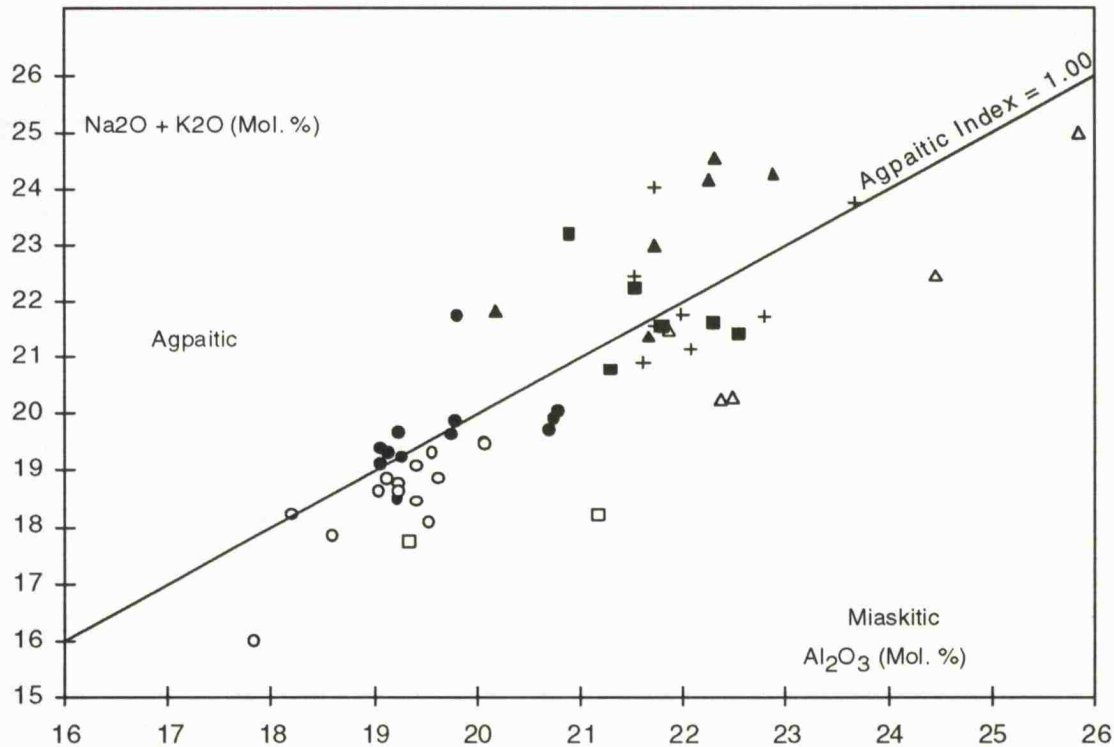


Fig. 7.2 Plot of total alkali against alumina in mol. proportions showing agpaitic - miaskitic symbols as in Table 7.1.

The rock suites of agpaitic trend consists of foyaites, sodalite rich feldspathoidal foyaites and foyaitic feldspathoidal syenites. These rocks occur as plugs, intrusions and pegmatite bodies in the area. The peralkaline agpaitic character is reflected by both normative and modal mineralogy, as indicated by the presence of acmite in the norm and distinct real mineral assemblage of sodalite, cancrinite, alkali pyroxenes, zircon and other accessory sodium bearing minerals.

The feldspathoidal syenites appear to be differentiated more towards the peralkaline composition with general increase in the degree of undersaturation. In fact, there is a marked increase in the degree of peralkalinity from Sura to Agarai, following westward trend up to Miani Kandao.

The dikes, pegmatites and minor intrusions from the Sahbaga, Bibi Dheri and Sura are typically miaskitic with agpaitic coefficient invariably less than 1, with a range of 0.86 to 0.97. The miaskitic nature of these rocks is also indicated by the modal composition of mafic and accessory minerals such as aegirine, biotite, garnet, zircon and titanite.

The feldspathoidal syenite rocks show high $\text{Na}_2\text{O} / \text{K}_2\text{O}$ ratio, with marked Na_2O domination over K_2O (Fig. 7.3), with the exception of a syenitic dike occurring west of Koga village (sample K-1, where $\text{K}_2\text{O} > \text{Na}_2\text{O}$). The $\text{Na}_2\text{O} / \text{K}_2\text{O}$ ratio trend vary considerably and mostly fall between 1 and 2. Nevertheless, the sodalite rich feldspathoidal foyaitic syenites show extreme enrichment of Na_2O over K_2O and the $\text{Na}_2\text{O} / \text{K}_2\text{O}$ ratios become as high as 6. The strong increase in Na_2O follows a negative trend from pulaskite to foyaite which involves a decrease in alkali and increase of aluminium (Upton, 1974, and Fletcher and Beddeo-Stephens, 1987). The extreme high alkalis compositions give rise to accumulation of nepheline and / or sodalite cancrinite due to the fractionating alkali feldspar and nepheline reacting with sodium and CO_2 bearing fluids.

Alkali syenite having higher concentrations of K_2O over Na_2O (sample K-1) but with similar level of silica (61.35%) to pulaskite-nordmarkite field may be the plausible representative of parent magma composition differentiating to pulaskite and nordmarkite which occur in the Koga complex (these rock units have been reported by Siddiqui et al. (1968). The $\text{Na}_2\text{O} / \text{K}_2\text{O}$ ratios fluctuate between wide ranges in the undersaturated alkaline rocks (0.7 to 6.0 in the study area). However, during the progressive differentiation of alkaline magmas beyond the trachytic stage, the $\text{Na}_2\text{O} / \text{K}_2\text{O}$ ratios tend to converge towards unity and felsic end members will have more or less equal distribution of Na_2O and K_2O , following the normal trends of oversaturated continental alkaline rock associations (McBriney, 1984).

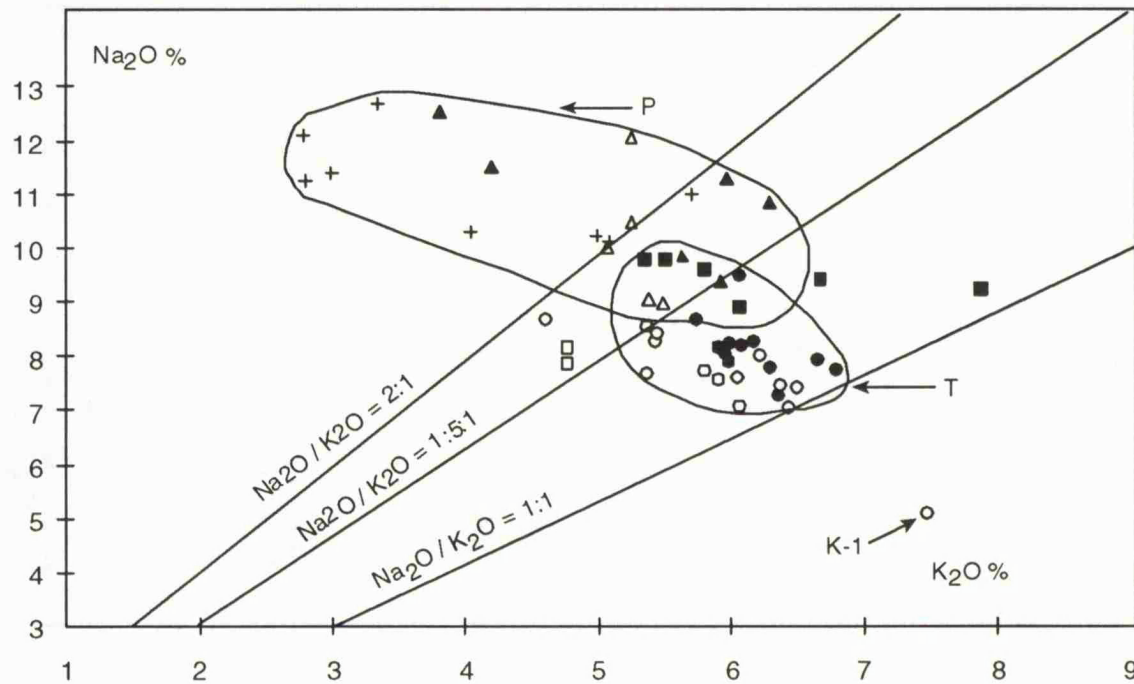


Fig. 7.3 Plot of Na₂O against K₂O showing both Na - enrichment in foyaites suites and relative abundance of K₂O, P-Phonolitic trend, T-Trachytic trend, symbols as in Table 7.1.

An outstanding feature of the chemistry of foyaites and foyaitic feldspathoidal syenites is that, they contain considerably higher Na₂O than any of the feldspathoidal syenite rocks of the area. The variation of Na₂O contents and agpaite indices within foyaites follow a linear relationship (Fig. 7.4). However, the foyaitic feldspathoidal syenites dikes and pegmatites show different trend. The Na₂O contents almost remain constant while agpaite indices increase up to 1.12, (Fig. 7.4). These feldspathoidal rock units show both trachytic and phonolitic trends and the K₂O contents increase relative to Na₂O. On the other hand, the main plugs and intrusions of the feldspathoidal syenites, pulaskitic feldspathoidal syenite and dikes of garnet bearing feldspathoidal syenite follow a linear decrease of both Na₂O contents and agpaite index. Whereas, the alkali syenite sample (K-1) has the lowest Na₂O contents and show typical miaskitic character with K₂O > Na₂O but it is off the diagram (on the left side of the diagram).

The large variations of alkali contents and the compositional modifications of major and trace elements may occur during or prior to the crystallisation and

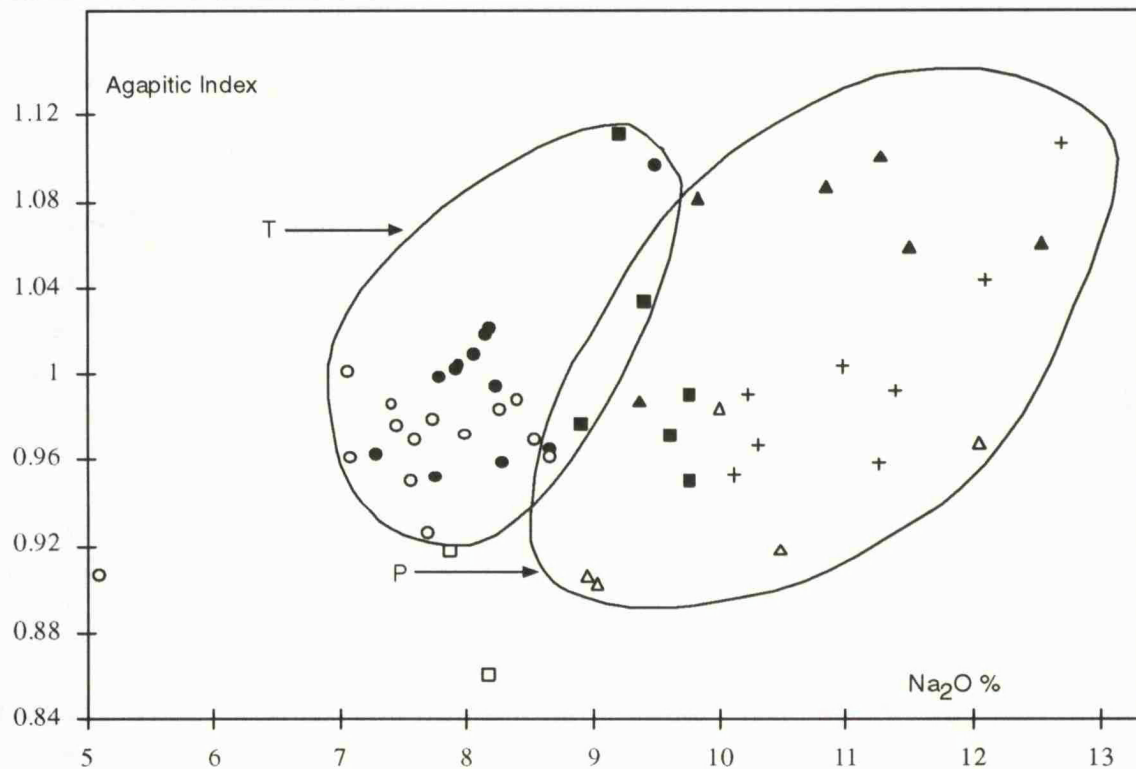


Fig. 7.4 Plot of agpaitic index versus Na_2O % showing phonolitic and trachytic trends.

solidification of feldspathoidal syenites and other alkali rocks (Noble, 1970, Baker and Henage, 1977 and Griffith and Gibson, 1980). In the cooling alkaline magma there is an insufficient Al_2O_3 available to react with all the alkalis to form feldspars. The large variations in Na_2O and K_2O contents of the analysed rock suites may be interpreted in terms of progressive crystallisation of alkali feldspar from an initially trachytic magma or ijolitic magma resulting in the increase of degree of undersaturation as well as peralkalinity. In addition, the feldspathoidal syenites of the Koga complex have undergone varying degrees of both Na and K metasomatism since these rocks are genetically associated with ijolite and carbonatites in the area. The Koga feldspathoidal syenite appears to be differentiated towards more agpaitic composition with a general increase in the degree of undersaturation.

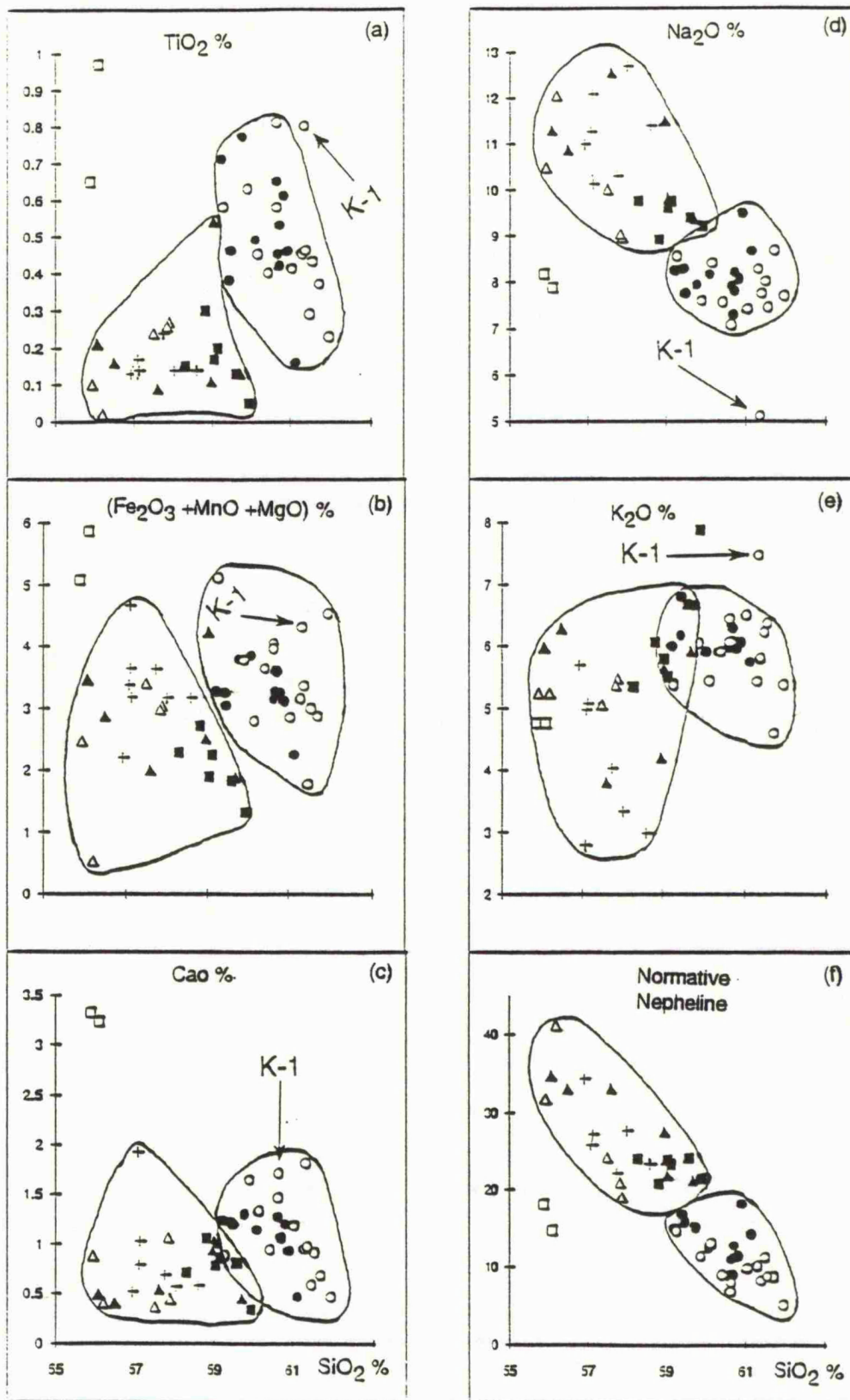


Fig. 7.5 Harker diagrams of major oxides variation against SiO_2 for the Koga complex rocks.

7.2.3 Geochemical Variation in Major Oxides

The geochemical variations of major elements are illustrated in terms of Harker variation diagrams of major oxides versus SiO_2 as shown in Fig. 7.5. These variation diagrams have limited use due to the small range of SiO_2 . Nevertheless, when the rocks of Koga complex are taken as a whole, interesting geochemical trends can be pointed out. The distribution pattern of each oxide may show possible lines of liquid descent and magmatic differentiation.

7.2.3.1 SiO_2

SiO_2 concentration ranges from 55 to 62 % with two distinct groups and displays trends of degree of silica undersaturation (Fig. 7.5f). The foyaites and foyaitic feldspathoidal syenites are restricted to SiO_2 from 56 - 60 % with progressive differentiation due to the crystallisation of nepheline with increasing degree of undersaturation depending on the availability of alkalis. This relationship of SiO_2 with high contents of alkalis and Al_2O_3 is a typical character of foyaites and feldspathoidal syenites. These rocks also display normal ijolitic (phonolitic) trend of increase in silica with differentiation.

The feldspathoidal syenites and pulaskitic feldspathoidal syenites, on the other hand, constitute a separate group which comprise intrusive bodies, plug and dikes in the area. These rock units have SiO_2 range from 59 % to 62 % and follow the normal trachytic trend of increasing silica while alkalis tend to decrease and Al_2O_3 contents remain more or less constant. These rock units tend to follow pulaskitic - nordmarkitic trend heading towards oversaturation of silica. However, all the Koga feldspathoidal syenite rock units remain strongly undersaturated in SiO_2 throughout the sequence of crystallisation because the magma must have been in the undersaturation side of the petrogeny's residua system during the time of emplacement.

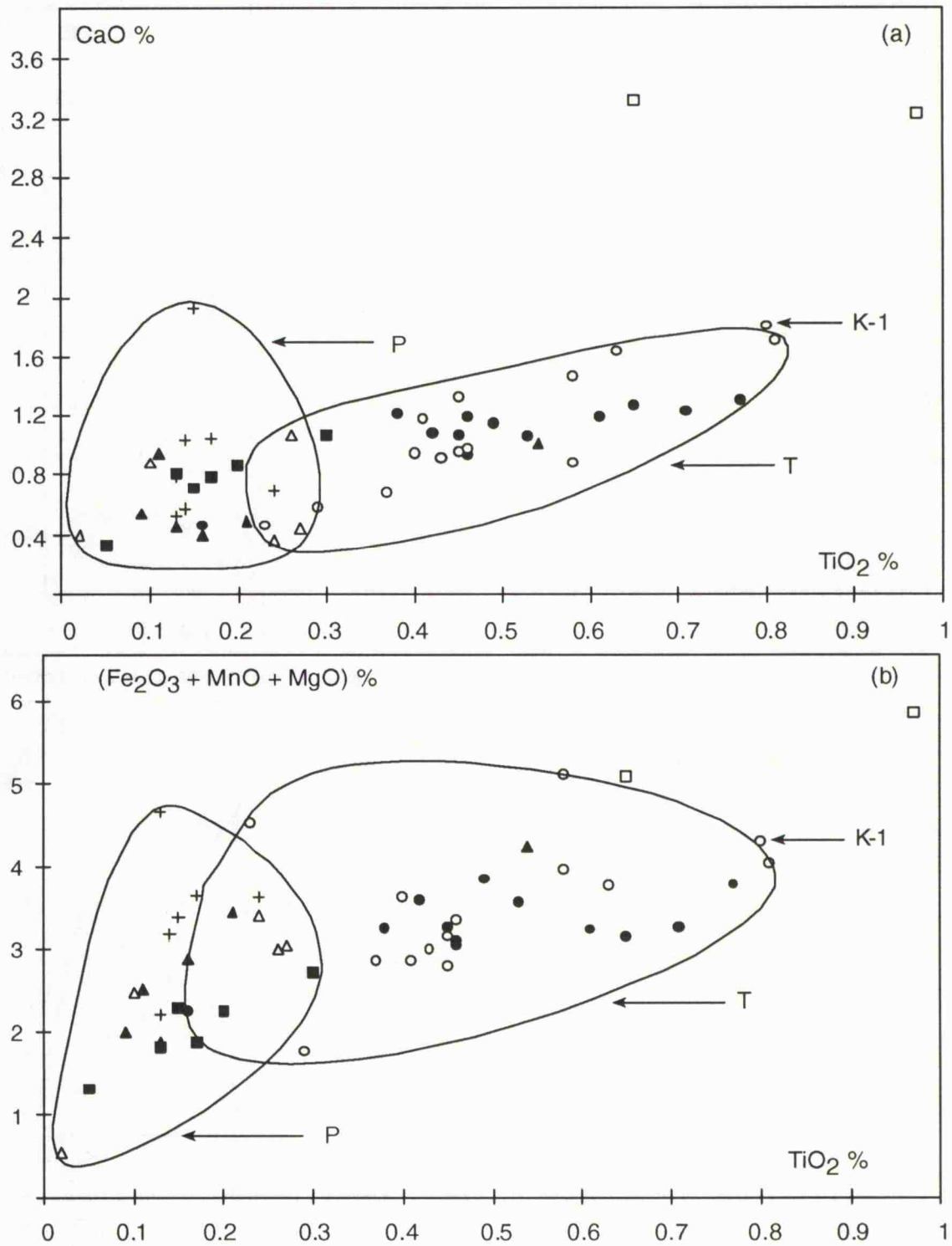


Fig. 7.6 CaO and (Fe₂O₃ + MnO + MgO) variation diagrams for the Koga complex rocks showing distinct TiO₂ depletion in foyaites.

7.2.3.2 TiO₂

TiO₂ contents of the feldspathoidal syenite complex vary and partly depend upon the types of the rock units. The foyaites, foyaitic feldspathoidal syenites and pulaskitic feldspathoidal syenite have low concentrations. On the other hand, the TiO₂ contents are relatively high in feldspathoidal syenite, garnet bearing feldspathoidal syenite and alkali syenite. Titanium forms its own minerals such as titanite (sphene) and / or may replace Fe and Mg in pyroxenes and biotite. The positive correlation of TiO₂ with CaO and with Fe₂O₃ + MnO + MgO is clearly shown in Fig. 7.6. This may be due to onset of differentiation sphene.

7.2.3.3 (Fe₂O₃ + MnO + MgO) and CaO

The variation patterns of (Fe₂O₃ + MnO + MgO) and CaO with SiO₂ are shown in Figs. 7.5b and 7.5c. All the feldspathoidal syenites of Koga are depleted in iron, manganese, magnesium and calcium (Fe₂O₃ = 0.53 % to 5.05 %, MnO = 0.01 % to 0.22 %, MgO = 0 to 0.63 % and CaO = 0.33 % to 3.32 %). There is a relative depletion of MgO, total iron and CaO in pulaskitic feldspathoidal syenite. The foyaites and foyaitic feldspathoidal syenites are extremely depleted in Fe₂O₃, MgO and CaO contents. On the other hand, garnet bearing feldspathoidal syenite and feldspathoidal syenite are relatively enriched in these oxides. Nevertheless, all the feldspathoidal syenites as a whole show systematic decrease of MgO, total iron and CaO contents as the differentiation index increases except in the garnet bearing feldspathoidal syenite. The reason for high values of CaO and lower values of Na₂O is not due to the substitution of Na₂O by CaO. These rocks have high values of both CaO and Fe₂O₃. These are distinct dikes which are rich in garnet (melanite), biotite and contain some aegirine. The deficiency of Na₂O is due to the higher colour index of these rocks. Other rocks of similar silica contents have lower colour index and higher contents of feldpathoids and feldspar.

The observed variations display an affinity for an igneous trend rather than metasomatic activity. Such trends are likely to have been caused by early

differentiation of ferromagnesian minerals and calcic plagioclase and characterise the magmatic lineage of these rocks. One of the plausible parental source could be the differentiating alkali basaltic or trachytic magma that might be responsible for the derivation of feldspathoidal syenites which relatively enriched in TiO_2 , Fe_2O_3 and CaO compared to the foyaites.

7.2.3.4 Na_2O and K_2O

Na_2O and K_2O contents of the feldspathoidal syenites are considerably higher compared to the average igneous rocks of syenitic and trachytic compositions. All the rock units of the Koga complex have $\text{Na}_2\text{O} > \text{K}_2\text{O}$ except alkali syenite, in which $\text{K}_2\text{O} > \text{Na}_2\text{O}$ (Na_2O ranges from 7 % to 12.8 % and K_2O , from 2.8 % to 7.8 %). The higher Na_2O and K_2O contents may be inherent to syenitic magma. Na_2O shows a negative correlation with SiO_2 . Both increasing and decreasing trends of Na_2O are observed in the feldspathoidal rocks of the complex which reflect the foyaitic - pulaskitic as well as trachytic trends. On the other hand, K_2O shows no systematic relationship with SiO_2 and D.I (Figs. 7.5a and 7.5e). Potassium behaves as an incompatible element and the variation of K_2O contents depends on the type of feldspathoidal syenite association.

7.2.4 Average Chemical Composition of the Koga Feldspathoidal Rocks

The average chemical compositions of various feldspathoidal rock units of the study area have been tabulated (Table 7.8), together with the published average analyses of foyaites and related nepheline syenite rocks from the typical alkaline provinces of the world (Table 7.9) for the geochemical comparison. The foyaites and foyaitic feldspathoidal syenites of the Koga complex exhibit general similarity in major and trace elements geochemistry with other alkaline provinces. The average contents of TiO_2 , MgO , CaO and P_2O_5 are slightly lower, while Na_2O and Al_2O_3 are relatively higher. The trace elements such as Sr, Ba, Y, REE and Nb are lower, especially in foyaites and foyaitic feldspathoidal syenites when

compared with the average abundance of the equivalent rock units from the known occurrences of the world. In general, the geochemical variations in the rocks under investigation, show the characteristic trend of alkali and alumina enrichment and strong depletion of Ti, Fe, Mg and Ca which is well comparable with the rift related under saturated alkaline complexes of the world.

7.3 Trace Element Geochemistry

The trace element geochemistry of the Koga feldspathoidal syenite is very variable. The compositional variations of the syenitic suites is influenced by a number of factors including melting of a compositionally heterogeneous mantle source as well as the order of crystallisation of parent magma coupled with variable degree of assimilation - fractional crystallisation producing most differentiated products of alkaline intrusive rocks. In addition, the trace element distributions might have been affected by the geodynamic setting through rifting and under thrusting of the NW continental margin of the Indo - Pakistan plate. The systematic trace element trends for the Koga feldspathoidal rocks are somewhat difficult to recognise. Nevertheless, the interpretation of trace element data as finger prints can be used to constrain the processes of partial melting and fractional crystallisation of alkaline magma in the region. The discussion will be focused on the geochemical comparison of rock units and significance of relationship between incompatible large ion lithophile (LILE), high strength field elements (HSFE) and rare earth elements (REE) concentration for the source regions and tectonic setting of feldspathoidal syenites.

7.3.1 Large Ion Lithophile Elements (K, Rb, Sr and Ba)

The distribution of K, Rb, Sr and Ba in the Koga feldspathoidal syenite complex show large variations in relative abundance and range from 78 - 223 ppm Rb, 64 - 4454 ppm Sr and 7 - 4425 ppm Ba, yielding wide spread elemental ratios

of K/Rb, K/Ba, Rb/Sr and Ba/Sr (Table 7.1). These lithophile elements generally behave as incompatible elements during partial melting of mantle material and consequently, are enriched during mantle metasomatism and magmatic differentiation (Eby, 1985 and Hawkesworth, 1987). The elemental ratios should remain relatively constant unless large proportions of crystallising phases are removed.

Ba and Sr show a strong geochemical coherence; (Fig. 7.8.b) the topologies of Fig. 7.7 (a) and (b) are very similar. However, Rb shows an increase behaviour compared with either Sr or Ba (Fig. 7.7.c); there is a negative correlation between Rb and Sr, Rb and Ba against Sr (Fig. 7.8), the Rb - Sr - Ba triangle plot (Fig. 7.9) and Rb, Sr and Ba versus K/Rb, K/Ba and Rb/Sr (Fig. 7.10) are also shown. It is quite clear from these diagrams that the Koga feldspathoidal syenites have two distinct geochemical trends in which Rb, Sr and Ba behaved as incompatible elements as well as strongly compatible lithophiles. The systematic enrichment and depletion of these elements has been genetically related with evolution of feldspathoidal syenites from the alkaline under-saturated magmas of the region.

The behaviour of Rb, Sr and Ba can be interpreted in terms of fractional crystallisation of rift related alkaline magmas into two stages: the early initial separation of olivine and pyroxene would concentrate Rb, Sr and Ba in the liquid phase and followed by increased crystallisation of more sodic plagioclase, alkali feldspar, nepheline and alkali pyroxenes. The later would rapidly deplete the concentrations of Ba, Sr, Mg and LREE in the residual liquid consequently yielding felsic under-saturated differentiates, the feldspathoidal syenites - syenites and alkali magmas (Griffith and Gibson, 1980, Miller and Mittlefehldt, 1984, Wolff and Storey, 1984, Woolley and Jones, 1987, Flohr and Ross, 1990 and Azambre et al. 1992).

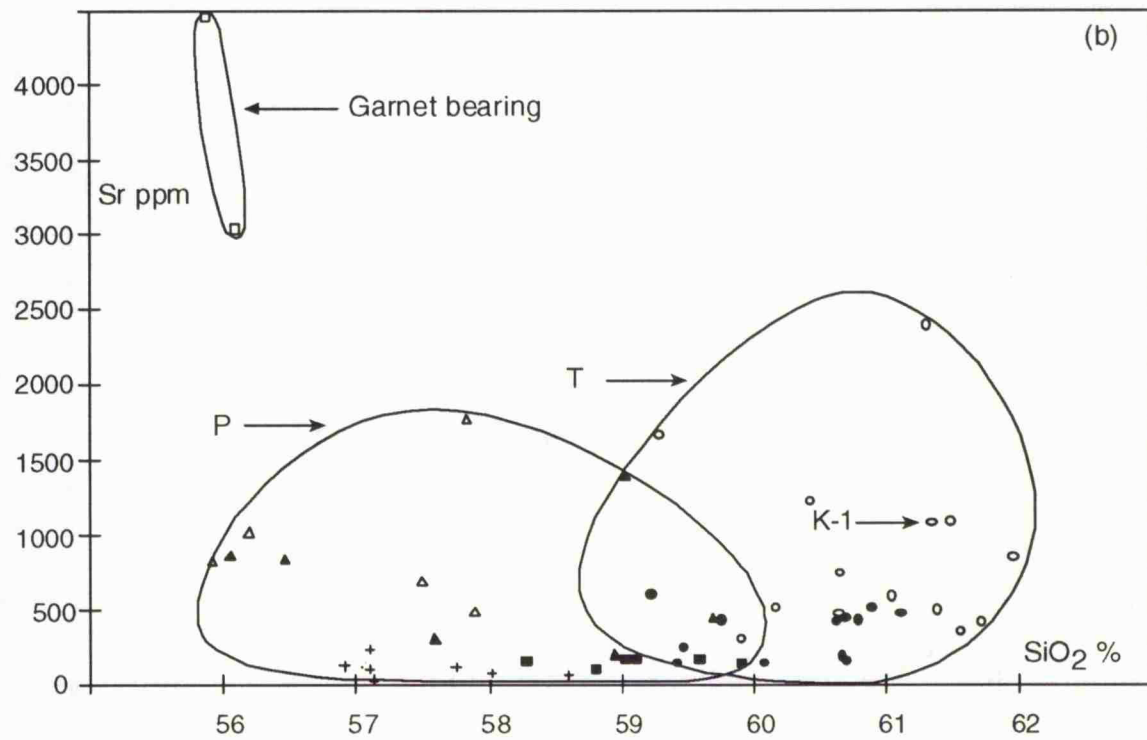
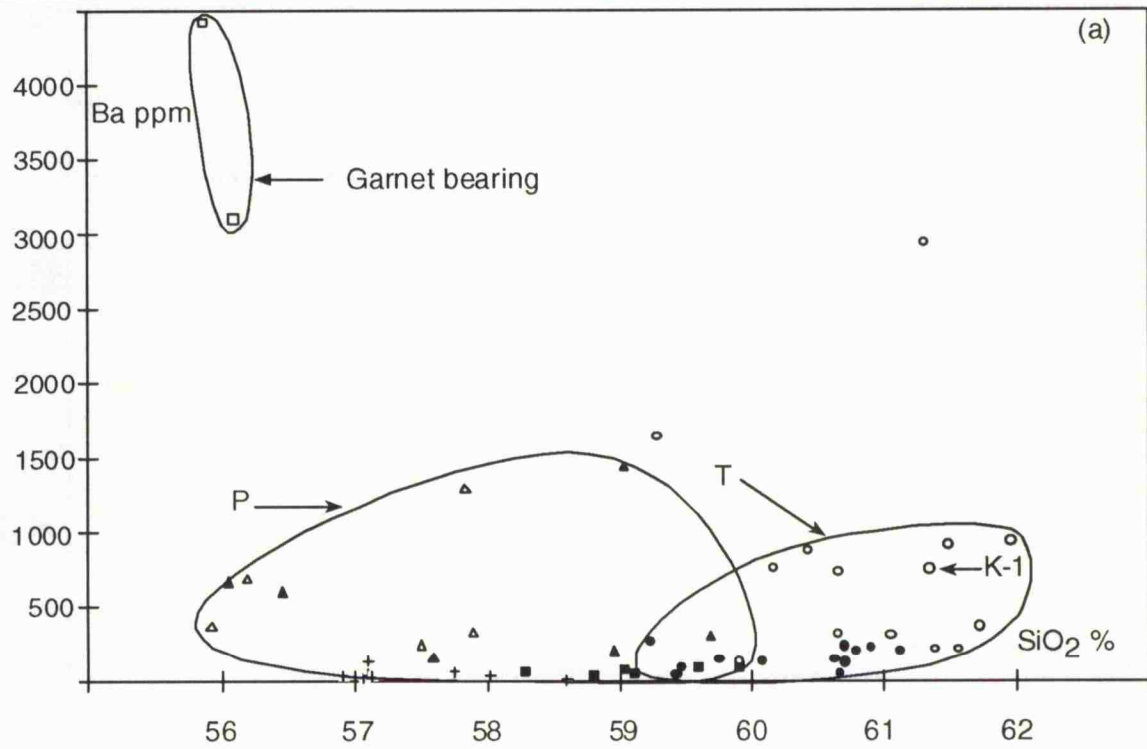


Fig. 7.7 Plots of variation of Ba, Sr, Rb contents and K/ Rb ratios against SiO₂ for the Koga feldspathoidal syenite rocks.

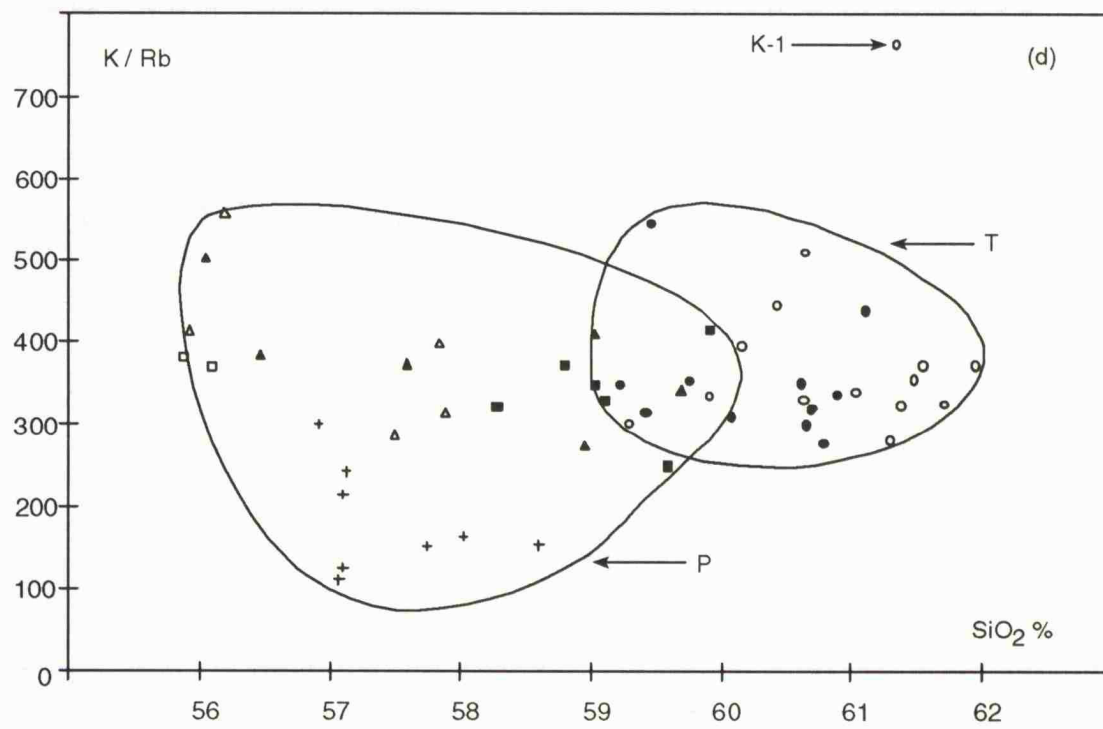
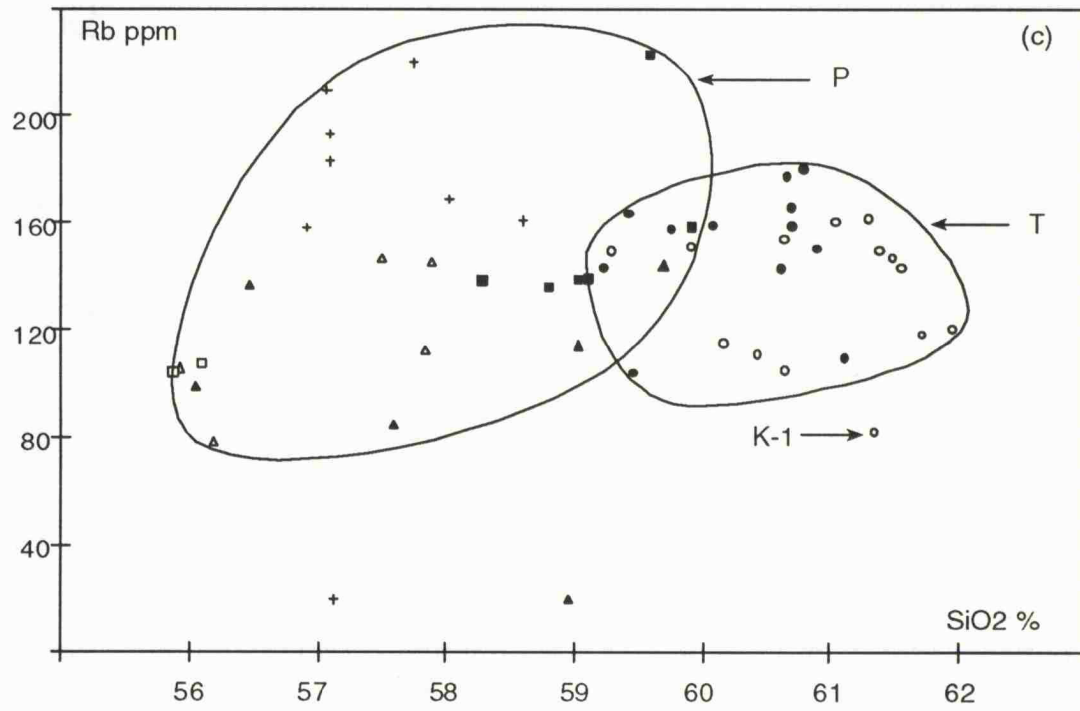


Fig. 7.7 Plots of variation of Rb and K/Rb ratios against SiO₂ for the Koga complex rocks.

The detailed relationship of Rb, Sr and Ba in the Koga complex rocks that may possibly be linked to the plausible parent magma is examined in detail.

7.3.1.1. Rb

The Rb concentrations are higher in sodalite rich foyaites and feldspathoidal syenites, displaying two distinct trends in opposite directions which is characteristic of undersaturated feldspathoidal rocks of alkaline complexes (Fig. 7.7c). Rb contents steadily increase with D.I. and increasing SiO_2 showing trends similar to

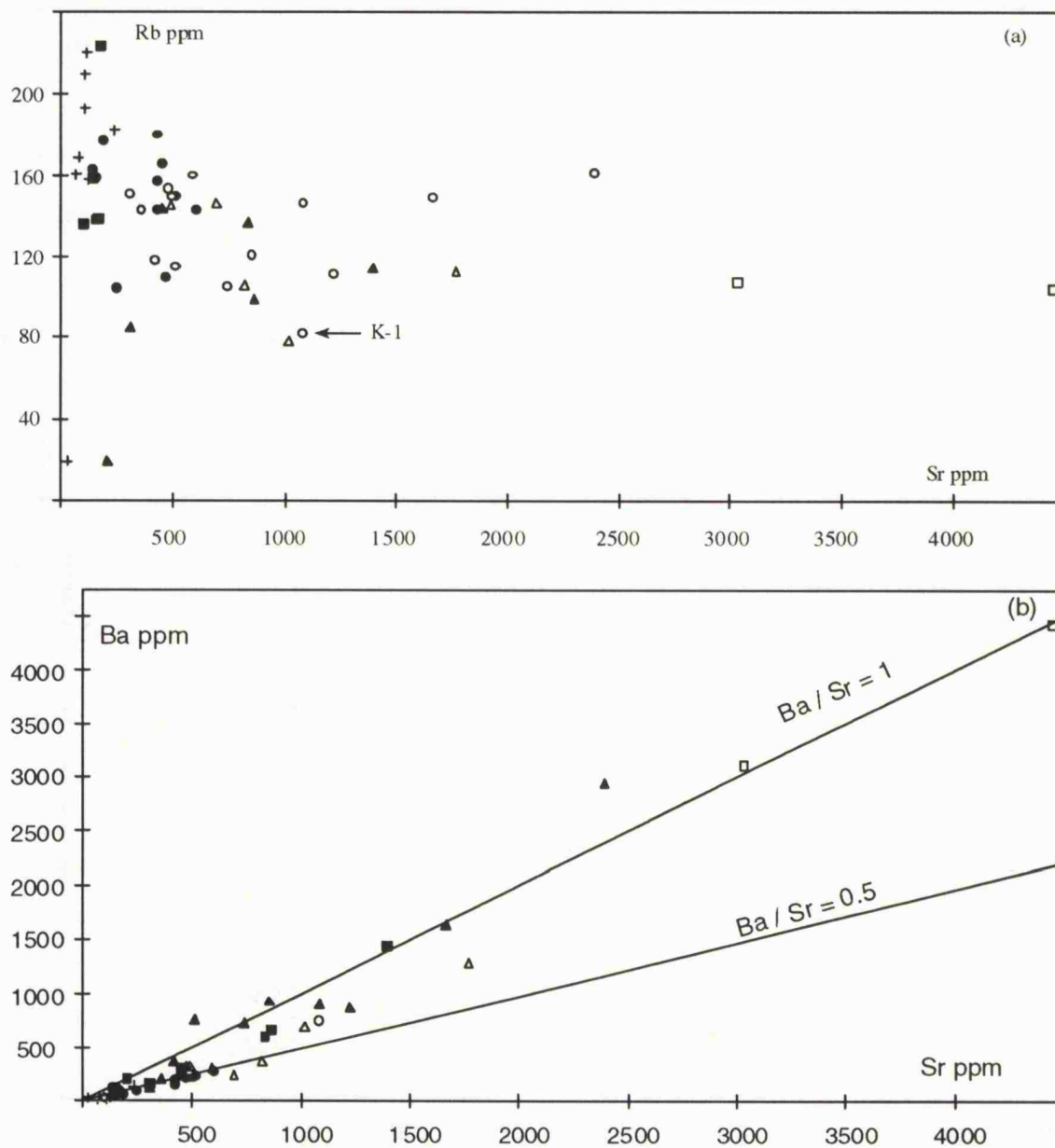


Fig. 7.8 Rb and Ba against Sr for the Koga complex rocks showing (a) enrichment of Rb in different groups and (b) linear correlation of Ba and Sr.

the normal trends of alkali basalt - trachyte - phonolite series. However, in case of foyaitic trend, increase of alkalis with decreasing SiO_2 content, Rb enrichment occurs with erratic increase from pulaskitic to foyaitic feldspathoidal syenites (Fig. 7.7c). The foyaites, pulaskitic garnet bearing feldspathoidal syenites and alkali syenite suites possess low concentration of Rb (average range 82 - 137 ppm).

7.3.1.2 Sr and Ba

The distribution of Sr and Ba exhibit some coherence and display well defined trends having relatively high Ba/Sr ratios ~ 1 and low Ba/Sr ~ 0.5 (Fig. 7.9).

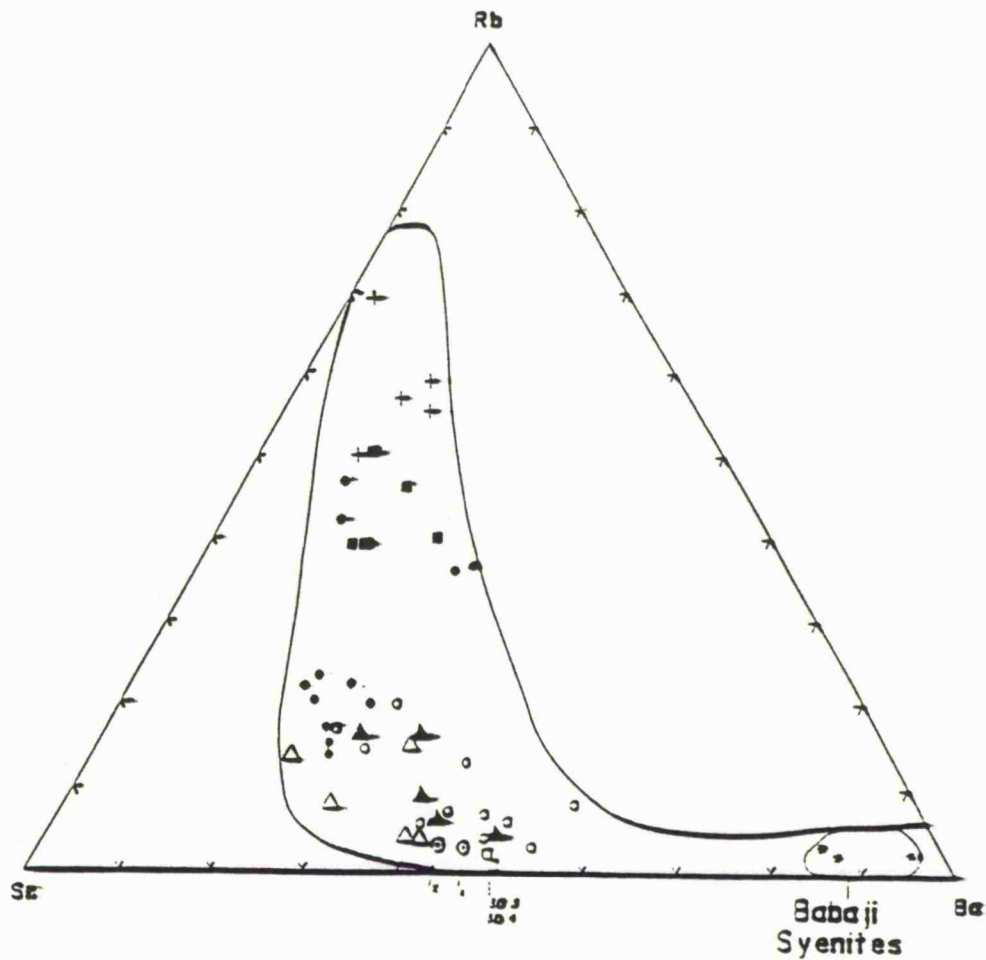


Fig. 7.9 Triangle plot of Rb - Sr - Ba relationship for the Koga complex rocks showing enrichment of Rb in foyaites and Ba in Babaji syenite.

The feldspathoidal foyaite - pulaskitic feldspathoidal syenites and garnet bearing feldspathoidal syenite possess high concentrations of Sr and Ba with Ba/Sr ratio around unity (0.9 - 1.05), following almost linear positive correlation between Ba and Sr. The highest concentration of Sr and Ba are recorded on the garnet bearing feldspathoidal syenite.

The sodalite rich foyaites and foyaitic feldspathoidal syenites have lowest Sr and Ba concentrations with decreasing Ba/Sr ratios (0.3 to 0.45). This decrease in the ratio is consistent with the increasing crystallisation of alkali feldspar. Ba gets depleted during late stages of crystallisation because it tends to favour K-feldspar than plagioclase (Siedner, 1965). Sr and Ba exhibit positive correlation with Ca due to the similar ionic radii. During the extensive igneous differentiation these elements behave compatibly and preferentially enter the sites of Ca and K in the silicate minerals particularly feldspar, partly nepheline, biotite and minor accessories.

7.3.1.3 K/Rb and K/Ba Ratios

K/Rb and K/Ba ratios are particularly significant in the petrogenetic interpretation of feldspathoidal syenites because their ratios are not significantly affected by any other mineral except K-feldspar or biotite. Rb versus K/Rb and Ba versus K/Ba plots are useful as there exist positive logarithmic relations between them (Fig. 7.10). More mafic rocks and mantle derived rocks through direct partial melting show higher K/Rb and low K/Ba ratios (Shaw, 1968, Taylor and Ahrens, 1959). On the other hand, the felsic and more silicic suites and crustal contaminated rocks have lower K/Rb and high K/Ba ratios. Sodalite cancrinite rich foyaites and some foyaitic feldspathoidal syenites exhibit lower K/Rb ratios and extremely high K/Ba ratios ($K/Rb = 141 - 330$ and $K/Ba = 711 - 1572$), whereas, the feldspathoidal foyaites, pulaskitic feldspathoidal syenites garnet bearing

feldspathoidal syenite and alkali syenite display increasing trend of K/Rb ratios (300 - 758) and very low K/Ba ratios (10 - 83). The Koga feldspathoidal rocks show somewhat higher varying K/Rb ratios in relation to the general main trend of igneous suites (average K/Rb ratios = 230, range = 150 - 300). The analysed rocks followed the general pattern showed by Heier and Adams, (1964) for the nepheline syenites. The higher K/Rb ratios in the feldspathoidal rocks compared to the average magmatic rocks is a typical feature of alkaline undersaturated rocks. Both K and Rb are enriched in the feldspathoidal syenites, potassium being relatively more concentrated during the crystallisation of the undersaturated magmas of trachytic syenitic compositions.

The K/Rb versus SiO₂ diagrams exhibit an interesting trend of average increase of K/Rb from foyaite to pulaskitic feldspathoidal syenite and alkali syenite (Fig. 7.7d). Similar behaviour is recorded for the Volasco alkaline rocks, Bolovia (Fletcher and Beddoe, 1987 and Stephens, 1987). This trend is mainly due to K-feldspar fractionation with some contribution of nepheline (Heier, 1966). The decreasing K/Rb ratios in sodalite rich foyaites are mainly due to the decrease of K-contents. The feldspathoidal foyaites have been derived from pulaskitic syenites and / or alkali syenites through the differentiation controlled by K-feldspar fractionation.

7.3.2 Compatible Transition Elements (V, Cr and Sc)

The abundances of first row transition trace elements in the analysed suites are markedly depleted (Sc = 0.4 - 7.8 ppm, V = 9 - 90 ppm and Cr = 1 - 41 ppm). The concentration of Ni and Co are below their detection limits (2.1 and 2.7 respectively). These elements are normally strongly compatible in mafic phases and show gradual decrease in concentration with increasing differentiation and SiO₂ contents, and corresponding decrease in major oxides of TiO₂, MgO, FeO,

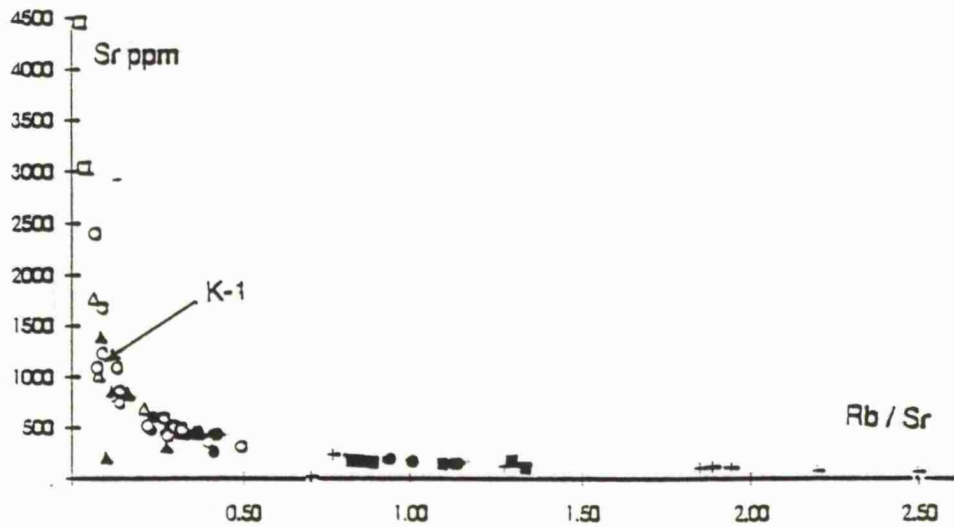
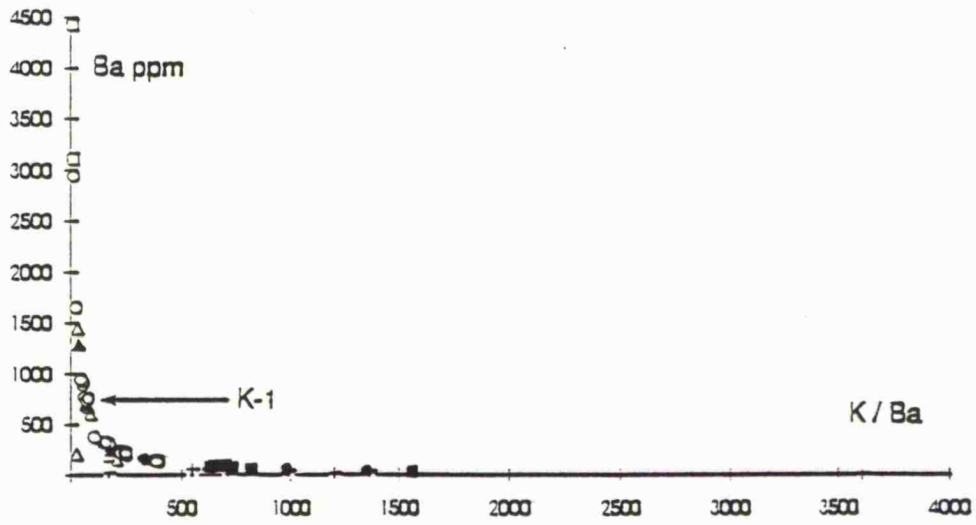
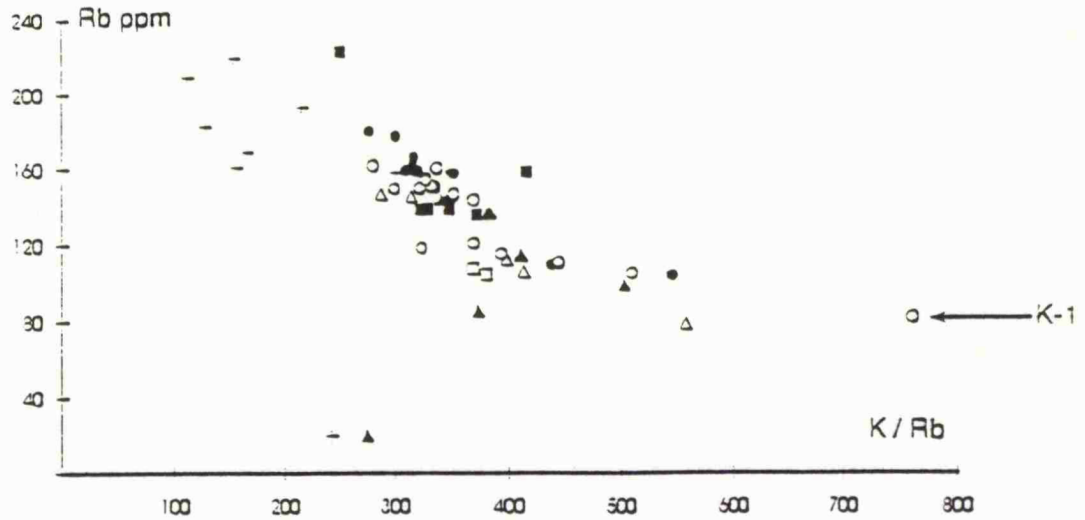


Fig. 7.10 Rb versus K/Rb, Ba versus K/Ba and Sr versus Rb/Sr for the Koga complex rocks, illustrating the logarithmic relationships and fractionation trend.

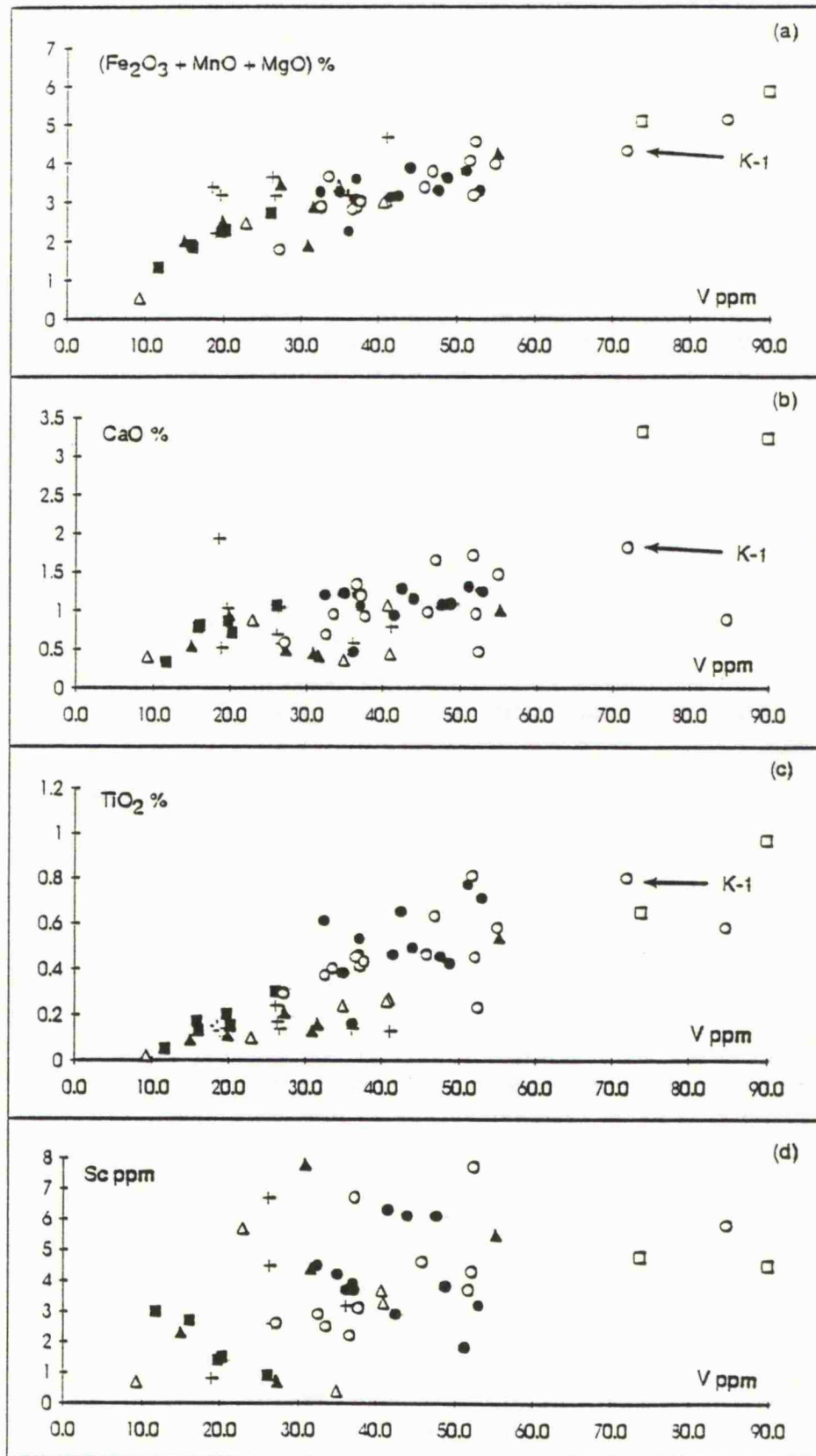


Fig. 7.11 Variation diagrams of $(Fe_2O_3 + MnO + MgO)$, CaO, TiO_2 and Sc against V.

CaO and P₂O₅. The sodium rich volcanic suites as well as nepheline syenite from the alkaline provinces are characterised by the similar geochemical trends (Miller and Mittlefehdt, 1984, Eby, 1985, Currie et al. 1986, Woolley and Jones, 1987, Flohr and Ross, 1990 and LeRoex et al. 1990). The low abundance of ferromagnesian trace elements strongly indicate that the feldspathoidal rocks have been derived from the less evolved magmas of trachytic composition.

In magmatic suites, Sc and Co preferentially enter the oxide phases (titanomagnetites) and pyroxenes. Ni is substituted mainly in olivine and Cr in pyroxenes. In alkaline series, V is largely accommodated in aegirine (Kempe and Deer, 1970 and Gomes et al. 1970). Several authors have proposed that the derivation of feldspathoidal syenites could be through the differentiation of mafic parental magmas by fractional crystallisation of olivine, pyroxene, plagioclase and magnetite. Such a fractionation will lead to depleted chemistry of ferromagnesian trace elements and strong enrichment of high field strength elements (HFSE).

The variation of Sc and major oxides contents are plotted against V concentration of the studied rocks to access the contribution of alkali pyroxene fractionation. V shows strong positive correlation especially with MgO + Fe₂O₃ and TiO₂. The foyaites show some deviation in these trends particularly in the plot of V versus CaO (Fig. 7.11b) in which CaO tends to decrease with increasing V contents which may be due to the fact that plagioclase was not involved.

The Cr/Sc versus Cr diagram is presented in Fig. 7.12 to examine the compositional trends of mineral fractionation. Most of the feldspathoidal rocks show a trend which may probably be similar to basaltic magmas derived from shallow - level differentiation through the precipitation of olivine, clinopyroxene, plagioclase and other minor phases (Engel et al. 1965, Blanchard et al. 1981, and Ujike, 1985). However, a few analysed foyaites and feldspathoidal syenites

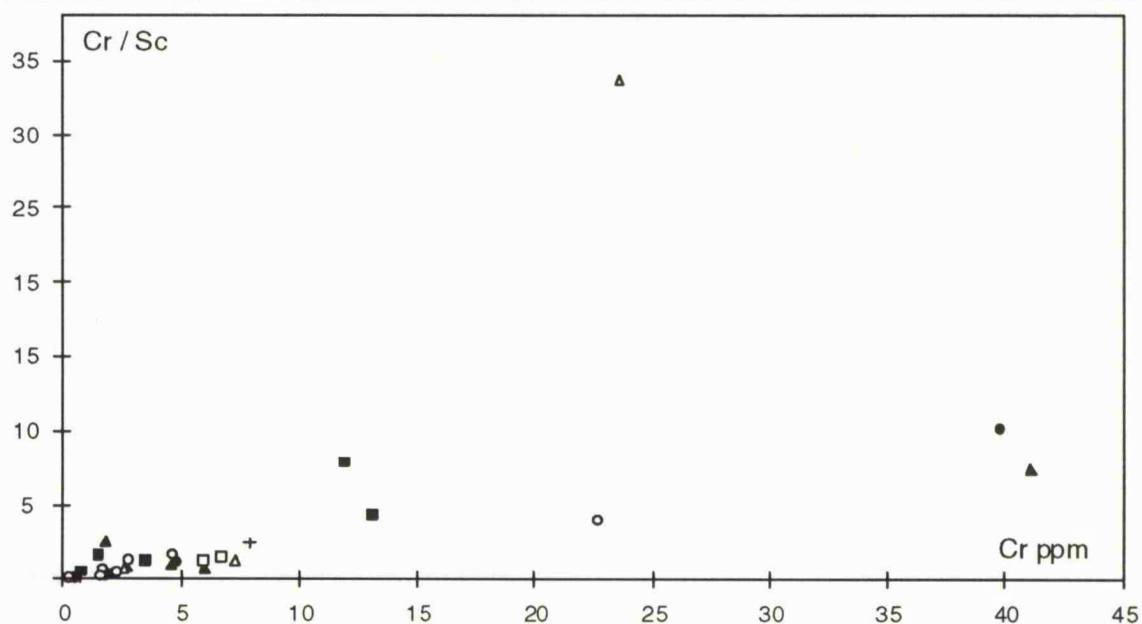


Fig. 7.12 Cr/Sc - Cr relations for the Koga complex rocks exhibiting compositional trends.

show large deviation from the main trend yielding higher Cr/Sc ratios (Fig. 7.12). This may be interpreted in terms of garnet fractionation and to some extent amphiboles in early stages of differentiation of primary mafic magma derived by partial melting. Among silicate minerals, garnet shows high partition coefficient for Sc and low values for Cr and separation of garnet phase will increase the Cr/Sc ratio in the melt (Ujike, 1985). This implied that at least some of the feldspathoidal rocks must have been derived from plausible trachytic magma that might be produced through the involvement of garnet/amphibole in the refractory residual phase.

7.3.3 High Field Strength Elements (Ti, Nb, Zr, Th, Y and LREE)

The abundances of Ti, Nb, Zr, Th, Y and LREE (La and Ce) in the feldspathoidal syenite rocks exhibit wide variations and has followed the general behaviour of strong enrichment towards undersaturated felsic suites. The relative element distributions are shown in the variation diagrams plotted against SiO₂ contents (Fig. 7.13). The concentrations in the analysed rock units range from 34 -

219 ppm Nb, 34 - 3617 ppm Zr, 1 - 37 ppm Th, 4 - 75 ppm Y, 5.5 - 167 ppm La and 8.5 - 167 ppm Ce.

Ranges for each rock suites are very similar. La and Ce show poor inverse general positive correlation with SiO₂. They show two distinct groups in all the plots Fig. 7.13 (a, b, c, d, e and f).

The high field strength elements (HFSE – with respect to charge / radius ratio) are considered to be highly immobile and insensitive to secondary processes and are not transported in the aqueous media (Wood, et al. 1979). On account of their large ionic size and oxidation state, they behave incompatibly with the result that they do not enter the major rock forming silicate mineral phases in the crystallising magmas except with limited substitutions in the early precipitating clinopyroxenes. These elements often show systematic behaviour in the differentiating magmatic series from mafic to felsic compositions (Sceal and Weaver, 1971, Weaver et al. 1972, Griffith and Gibson, 1980, Wolff and Storey, 1984, Le Roex, 1986, Le Roex et al. 1990 and Mahood and Stimac, 1990). They are also known to behave as residual elements and are characterised by high solubility in peralkaline silicate melt (Nicholls and Carmichael, 1969 and Baker and Henage, 1977). Numerous studies have shown that HFSE exhibit marked depletion in the rock suites from subduction related to island arcs and the strong enrichment in the alkaline rocks from the continental rift zones (Pearce and Cann, 1973, Carmichael et al. 1974, Floyd and Winchester, 1975, Arculus and Johnson, 1981, Briquieu et al. 1984, Ryerson and Watson, 1987, Azambre et al. 1992, Bradshaw, 1992 and Wallace and Carmichael, 1992). So the geochemical signatures of HFSE can be considered a diagnostic feature for the alkaline magmas and petrogenesis of the feldspathoidal syenite rocks of the study area. Ti, Nb and Zr are used as the index of variation for plotting the analytical data as shown in Figs. 7.14, 7.15, 7.16 and 7.17 respectively.

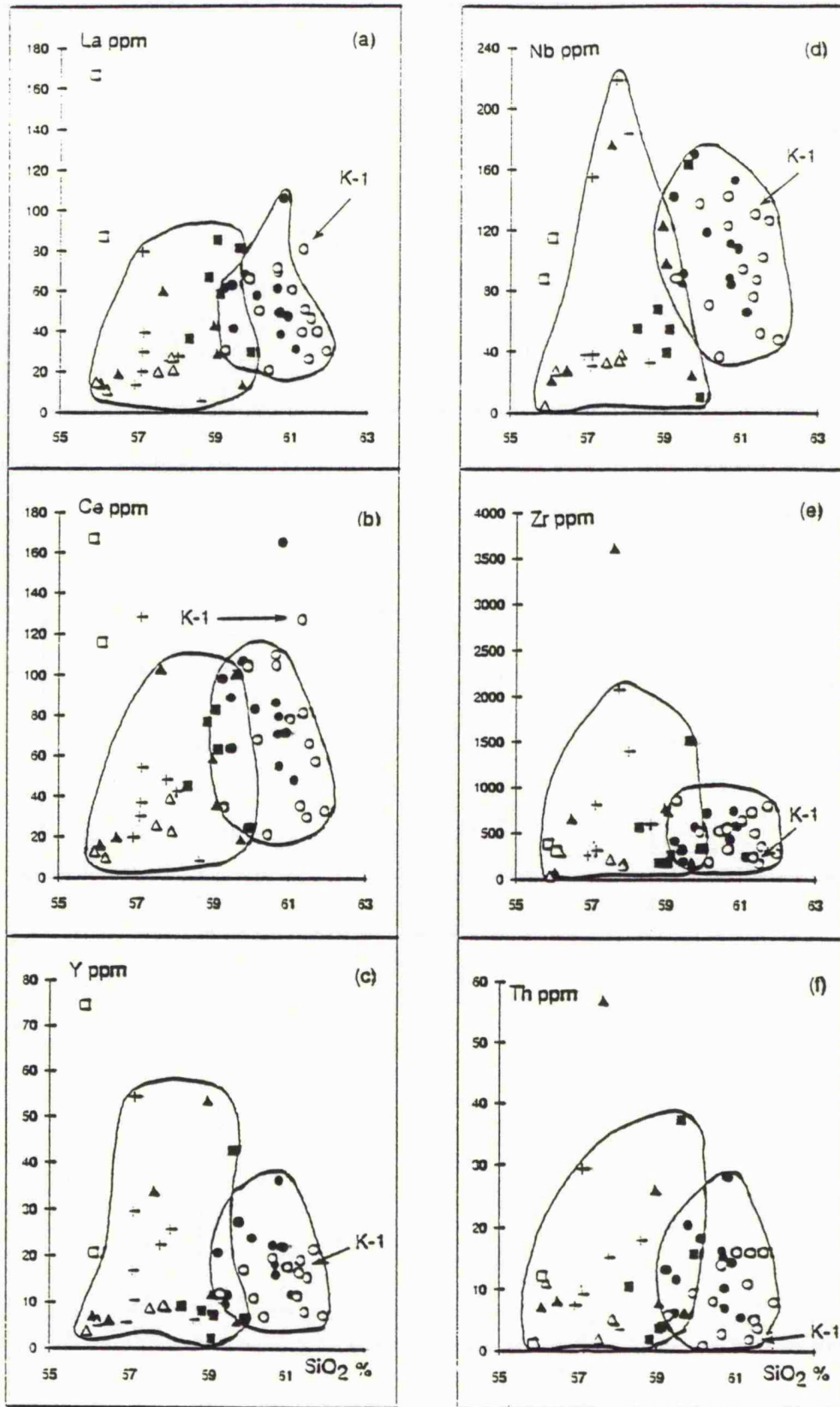


Fig. 7.13 Plots of variation trends of La, Ce, Y, Nb, Zr and Th against SiO₂ for the Koga complex rocks.

7.3.3.1. Ti

Fig. 7.14 illustrates the variation in abundances of Zr, Y, La and Sr against TiO_2 contents of the studied rocks. A positive correlation trend exists in the feldspathoidal rocks except some anomalous scatter points for the foyaites and foyaitic feldspathoidal syenites. Ti - Sr plot exhibits two distinct trends of positive correlation among foyaites, pulaskitic and garnet bearing feldspathoidal syenites as well as within feldspathoidal syenites. Similar positive linear relationship have been recorded in the nepheline syenite rocks from Magnet Cove, Arkansas (Flohr and Ross, 1990). TiO_2 and Y display similar correlation (Fig. 7.14). Thus Ti, Zr, La, Sr and Y all show compatible behaviour in the feldspathoidal rocks. These covariation trends of compatible (Ti and Y) and incompatible (HFSE) elements in the magmatic suites can be characterised for fractional crystallisation and partial melting to relate to the source rocks (Sun and Hanson, 1975 and Hanson, 1978).

7.3.3.2. Nb

The variation of LILE and HFSE are plotted against Nb contents as differentiation parameter for the rocks under investigation (Fig. 7.15 and 7.16). The observed ratios of Ba/Nb, Ti/Nb, La/Nb, Y/Nb and Zr/Nb are given in table 7.12. Nb shows scatter and general increase in concentration with silica (Fig. 7.13d) and displays a positive correlation with Ti, Y, La, Zr and Th with some deviation of scattered anomalous points for the samples of sodalite foyaites and feldspathoidal foyaites. Rb, Sr and Ba and to some extent Zr and Ti exhibit bimodal distribution patterns with respect to Nb contents. The feldspathoidal foyaites, pulaskitic feldspathoidal syenites and garnet bearing feldspathoidal syenite rocks yield high Sr/Nb and Ba/Nb ratios ($\text{Ba/Nb} = 7.5 - 52$). Sample S-2 shows abnormally high ratios of Ti/Nb, Ba/Nb and La/Nb. The feldspathoidal syenites have low ratios of Ba/Nb (0.46 - 6.1), Zr/Nb (2 - 6.1) and Y/Nb (0.11 - 0.24).

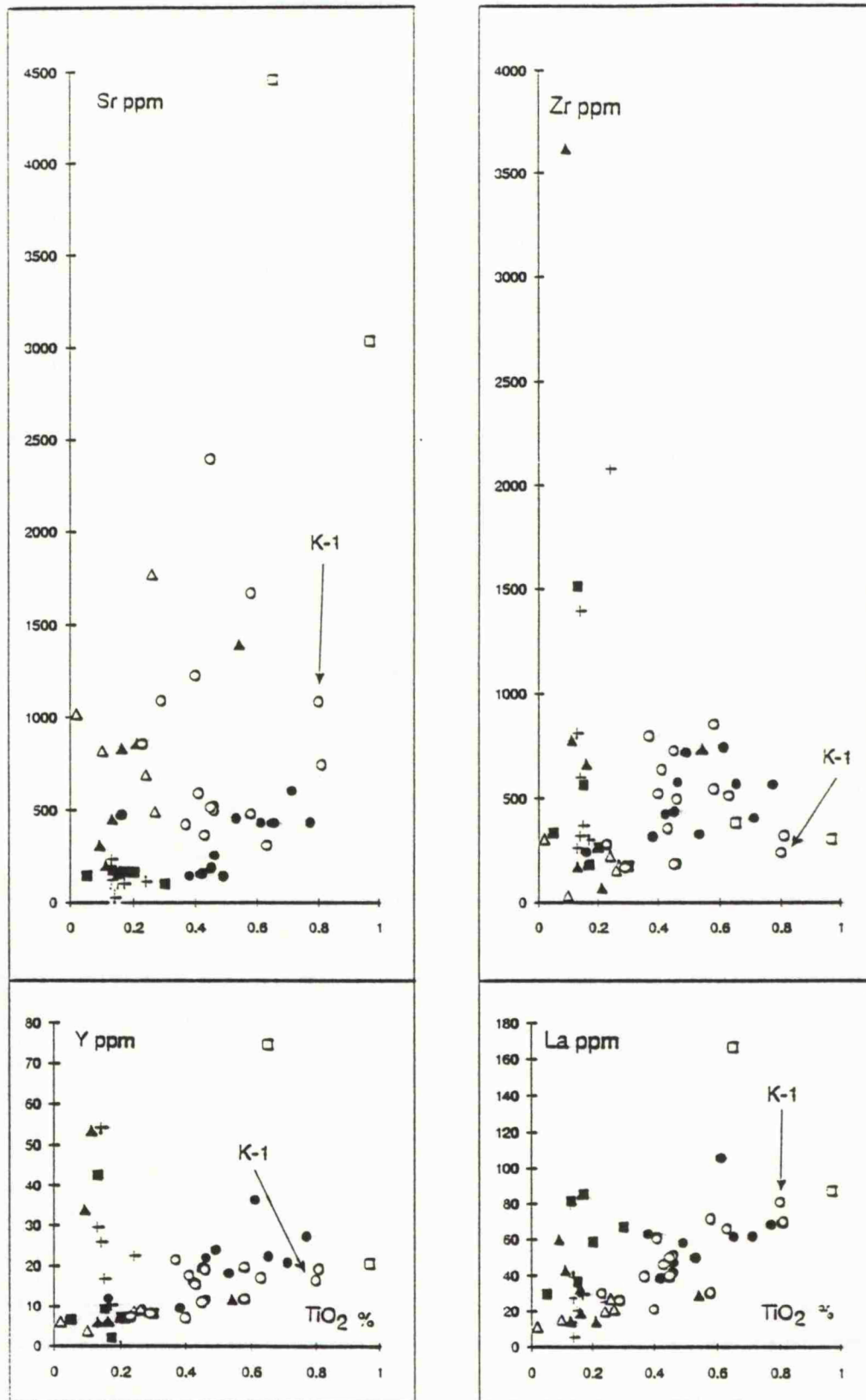


Fig. 7.14 Sr, Y, Zr and La variations against TiO_2 % of the Koga feldspathoidal syenite rocks.

which could be related to the source characteristics of Koga complex.

Numerous studies have shown that Nb concentrations increase systematically with differentiation in the alkali basalt - phonolite suites and particularly get enriched in the undersaturated feldspathoidal syenites in ring complexes along with Zr and REE (Sceal and Weaver, 1971, Gerasimovsky, 1974, Pearce and Norry, 1979, Le Roex, 1990 and many others). Nb does not form its own separate mineral in magmatic environment except some rare pyrochlore. In the feldspathoidal syenites, it is mainly fixed in Ti - Zr silicates, sphene, zircon and partly substituted in pyroxenes. Nb is transported in the residual fluids along with Zr and REE in the form of halogen complexes in the undersaturated alkaline rocks, particularly by the upward migration of chlorine in the differentiating mafic and trachytic magmas.

7.3.3.3. Zr

The patterns of Zr abundances within the analysed rock display large variation with increasing SiO₂ (Fig. 7.13e). Zr shows relative enrichment in sodalite rich foyaites and foyaitic feldspathoidal syenites, but the cancrinite rich foyaites and miaskitic foyaites have low Zr contents (34 - 300 ppm). The feldspathoidal syenites and pulaskitic feldspathoidal syenites are moderately enriched with Zr concentrations ranging from 240 ppm to 700 ppm (average Zr = 457 ppm and 484 ppm respectively). The overall abundances of Zr are relatively slightly lower when compared to agpaitic feldspathoidal syenites from other alkaline provinces.

Zr is a highly immobile trace element from mafic to intermediate igneous rocks and has been used as a geochemical discriminator to identify the type and tectonic setting of igneous suites (Pearce and Cann, 1973, Floyd and Winchester, 1975). Many studies have recorded that Zr contents are not significantly affected

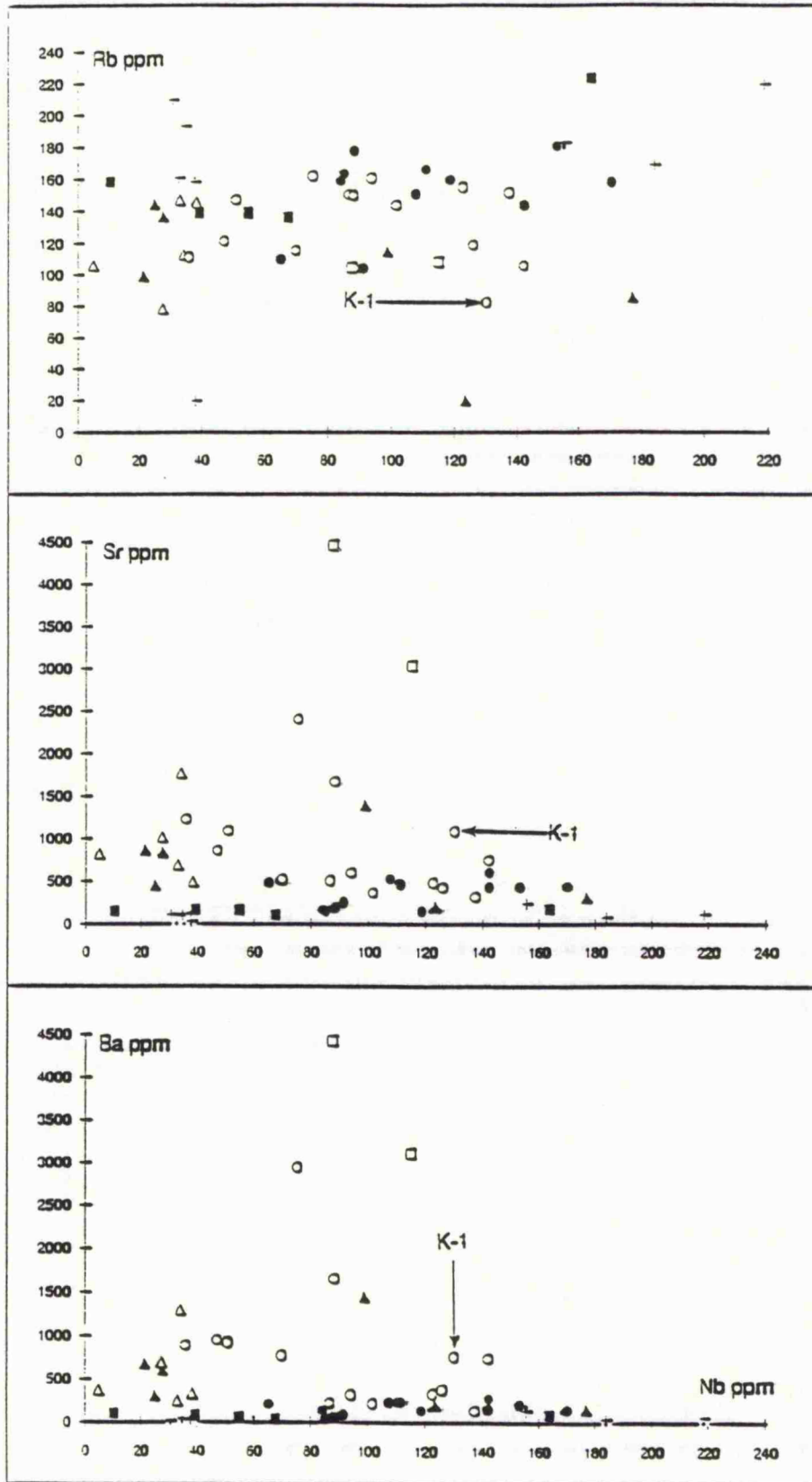


Fig. 7.15 Rb, Sr and Ba variations against Nb contents of the Koga feldspathoidal syenite rocks.

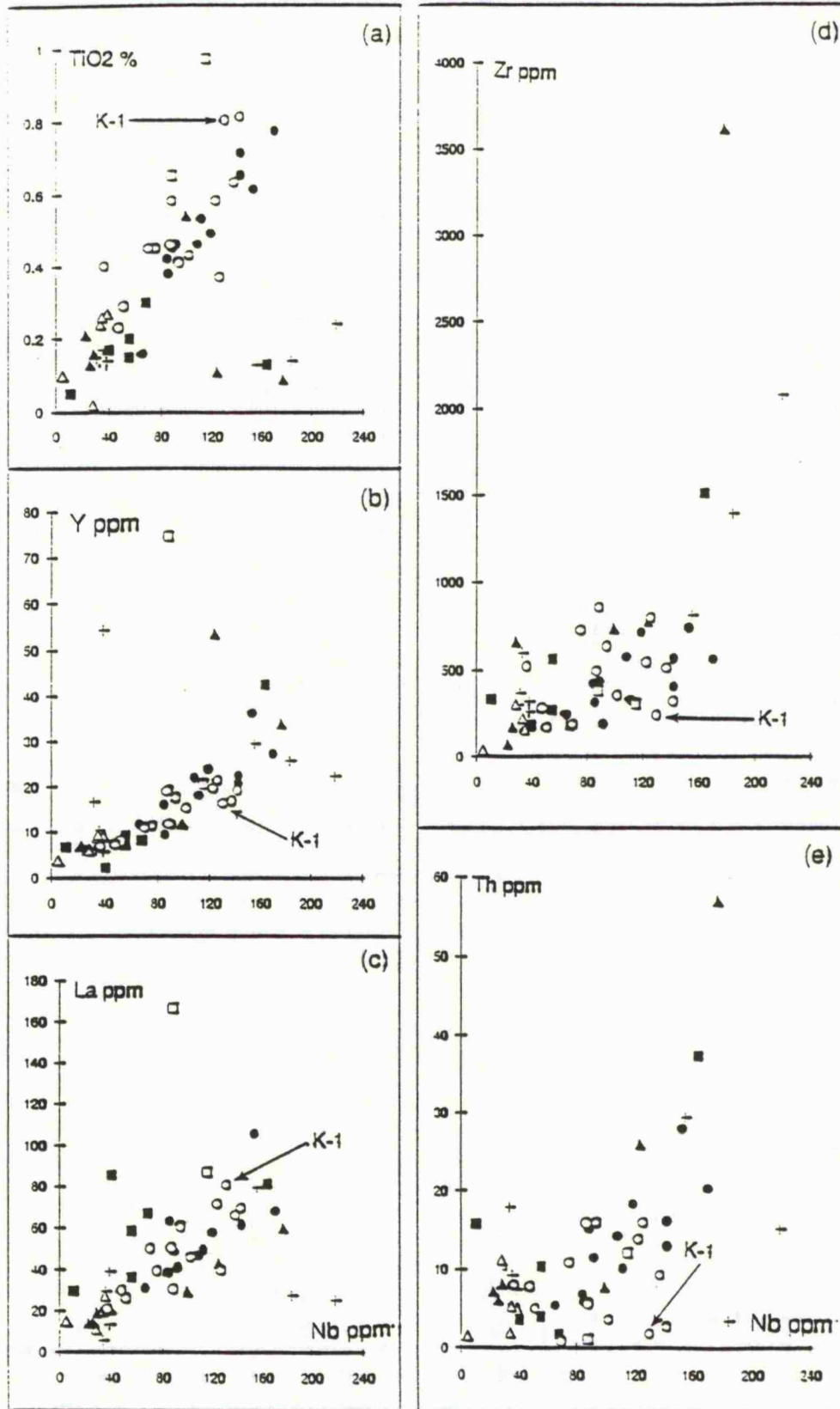


Fig. 7.16 Variation trends of TiO₂, Y, La, Zr and Th against Nb contents of the Koga complex rocks.

significantly affected by fractional crystallisation of major silicate phases from peralkaline silicic magmas (Sceal and Weaver, 1971, Baker and Henage, 1977, Griffiths and Gibson, 1980 and Le Roex, 1990).

Zr has a positive correlation with Y and it shows a bimodal distribution with La and Y Fig. 7.17 (a & b).

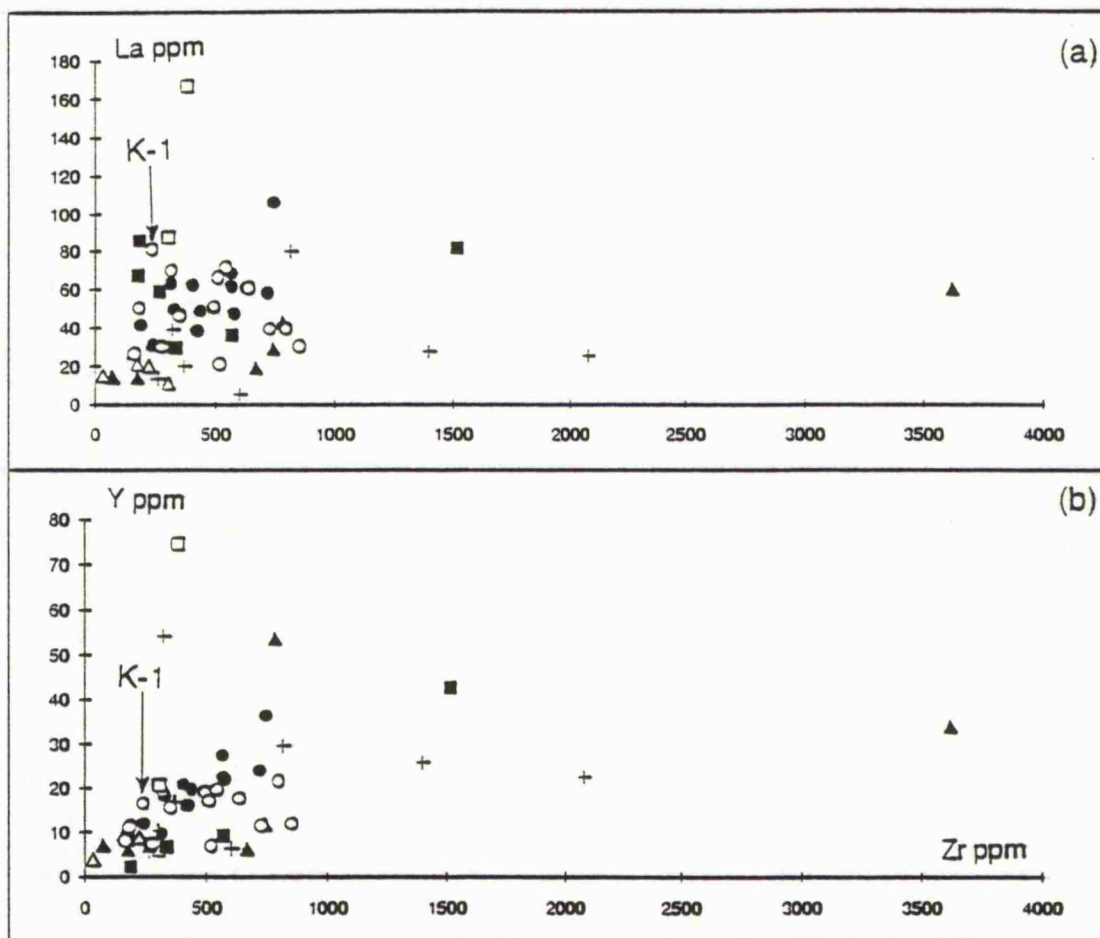


Fig. 7.17 Plots of La and Y against Zr for the Koga feldspathoidal syenite rocks.

Several authors have investigated the geochemistry of Zr in volcanic rocks and tried to relate the distribution of Zr (along with other HFSE) in the igneous source rocks. They have observed that in the non-peralkaline systems Zr is mostly removed by zircon crystallisation. They suggested that the zircon fractionation is

controlled by temperature, SiO₂ contents and alkalinity of melt tend to concentrate in the residual silicate liquids until zircon saturation is achieved (Watson, 1979, Watson and Harrison, 1983, Hinton and Upton, 1991, Keppler, 1991, and Rubin et al. 1993). Zr forms complexes with alkali metals in the presence of halogens and volatiles that do not allow zircon to fractionate until silica contents approach 68 wt %. The agpaitic nepheline syenite - phonolite may exhibit increasing Zr and decreasing SiO₂ with differentiation (Hall, 1978). The Koga feldspathoidal syenites have shown similar geochemical behaviour of Zr and other HFSE showing variable ratios in compatible trace elements (Table 7.12).

7.3.4 Rare Earth Elements (REE)

The rare earth elements (REE) as a geochemical coherent group are particularly important in the petrogenetic interpretation of feldspathoidal syenite rock suites. The variations in the shape of the REE patterns within the rock units may be directly related to their mineral - melt partitioning trends in minerals involved in partial melting or fractional crystallisation of alkaline magmas. The REE whole rock data for the rock samples are given in Table 7.2 - 7.7. The distribution range of the total REE contents and their relative fractionation ratios are presented in Table 7.11. The REE data are normalised using the standard chondrite abundances of Nakamura, (1974) and the normalised REE are plotted for each rock unit in Figs. 7.18 -7.20.

The total REE abundances vary from 35 to 309 ppm and all the feldspathoidal suites are strongly enriched in the light REE (LREE) relative to the heavy REE (HREE) with respect to chondrite abundances. The relative element fractionation ratios show large variation (range from LREE/HREE = 4.5 to 44.5, La/Yb = 20.7 to 159.7, (La/Yb)_n = 9.1 to 53.3 and (La/Sm)_n = 13.9 to 106.8).

Table 7.11. Rare earth element contents and their fractionation ratios in the Koga feldspathoidal syenite rocks.

Rock Type	Sample No.	LREE La-Eu	HREE Gd-Lu	Total REE	LREE/HREE	La/Yb	Ce/Yb	(La/Sm) _n	(La/Yb) _n
Sodalite - cancrinite foyaïtes	MK- 1	72.5	5.0	78	14.5	64.4	71.5	13.1	43.1
	SB-14	69.2	13.0	82	5.3	20.7	21.2	21.0	13.9
	K - 5	149.0	13.0	162	11.5	33.8	58.5	9.1	22.6
	K - 6	43.6	7.3	51	6.0	21.8	31.5	9.9	14.6
	K - 9	86.5	4.7	91	19.2	69.3	87.3	17.1	46.4
Feldspathoidal foyaïtes	MK- 6	42.6	9.2	52	4.6	30.5	41.1	21.6	20.4
	K- 2	127.1	9.4	137	13.5	39.8	54.3	12.5	26.6
	SB- 1	54.5	8.0	63	6.8	64.2	70.9	33.6	43.0
	SB- 6	30.9	3.7	35	8.4	54.4	50.5	13.4	36.4
	S- 1	89.0	8.0	97	11.1	42.3	61.4	13.1	28.3
Foyaitic feldspathoidal syenites	MK-24	42.2	4.0	46	10.6	52.5	58.2	15.5	35.1
	S - 5	221.0	5.0	226	44.2	159.3	132.3	46.7	106.5
	K - 8	178.3	5.8	184	30.0	159.7	142.2	55.3	106.8
Feldspathoidal syenites	MK - 5	180.0	18.6	199	9.7	57.2	80.0	16.7	38.2
	MK-21	236.0	31.4	267	7.5	50.8	64.8	25.9	34.0
	S - 3	187.0	7.0	194	26.7	78.4	96.0	17.9	52.4
	BD - 1	120.2	9.0	129	13.3	46.4	72.8	10.5	31.0
Pulaskitic feldspathoidal syenites	MK-12	151.0	20.1	171	7.5	42.7	54.9	16.8	28.6
	MK-19	90.0	9.9	100	9.1	50.0	71.8	10.8	33.4
	SB - 9	123.3	14.4	138	8.6	47.0	72.7	18.0	31.4
	SB-12	123.4	14.4	138	8.6	47.0	65.0	16.2	31.4
	K - 3	180.0	11.5	192	15.6	54.4	88.2	12.4	36.4
	K - 4	191.0	11.7	203	16.3	43.2	71.3	11.4	28.9
Alkali syenite	K - 1	283.0	26.0	309	10.9	47.2	100.9	12.5	31.5

The chondritic normalised REE pattern of the rocks show either no Eu anomaly, or a very slight negative anomaly in few samples (S-3 and S-5). Nevertheless, most of the foyaïtes and pulaskitic feldspathoidal syenites of miaskitic trend show pronounced negative Ce anomaly in their patterns (especially sample numbers SB-6, S-1 and MK-19). In the REE patterns, the size of Eu and Ce anomalies whether positive or negative can be defined in numerical terms as ratios Eu/Eu^* and Ce/Ce^* where Eu^* Ce^* are the interpolated values of Eu and Ce delineated from the two adjacent REE assuming no Eu and Ce anomalies in the patterns (Eu^* evaluated between Sm and Gd and Ce^* between La and Pr).

The occurrence of small negative Eu - anomaly in some feldspathoidal syenite samples reflect fractional crystallisation of plagioclase from the silicate melt. The anomalous behaviour of Eu is due to the fact that ionic radii of Eu^{2+} is

much larger than Eu^{3+} , so that Eu^{2+} in reducing condition can preferentially enter the feldspar along with Sr^{2+} and will produce a negative anomaly in REE pattern of the rock. In the case of the Koga feldspathoidal syenite suites, almost all the REE patterns show no Eu - anomaly, indicating that the silicate system has been crystallised under high oxygen fugacity (Philpotts, 1970 and Drake et al. 1975).

The presence of negative Ce - anomaly in foyaites and pulaskitic feldspathoidal syenite is very interesting. Ce can occur as Ce^{4+} under oxidizing condition in hydrous environment and may preferentially leach out from the rock during hydrothermal alteration (Otonello et al. 1979). Ce^{4+} can behave very similarly to Th^{4+} in silicate melts. The charge balance on substitution Ce^{4+} within the coherent REE group ($\text{REE}^{3+} \rightarrow \text{Ce}^{4+}$) becomes somewhat difficult in silicate phases in magma and during the mantle metasomatism. Ce may be transported in the form of fluoro - carbonate, similar to the geochemical behaviour of Th and U. Thus, under the reducing environment Ce selective rare earth minerals may crystallise in pegmatites of alkaline rocks and carbonatites (Clark, 1984).

Another important feature in the HREE patterns of the feldspathoidal syenite rocks is the distinct strong Gd and Er positive anomaly occurring together as shown in Figs. 7.18 b, 7.19 a and 7.20 a (in samples MK-6, MK-12, MK-24 and SB-1). HREE patterns are relatively flat in shape. Such a distinct whole rock HREE pattern for alkaline rocks perhaps have not been reported in literature. This is quite puzzling and not definitely explicable at this stage. A possible interpretation could be that gadolinium type or erbium type REE bearing mineral phases might have formed due to the volatile fluids and halogen gaseous phases in the magma. Alternatively, it has been recorded that distribution coefficients showed progressive increase from Ce to Er (0.35 to 43) in garnet from Japanese dacites (Schnetzlar and Philpotts, 1970). The garnets from eclogites have been analysed that showed heavier REE concentrations (White et al. 1972). Therefore, the observed positive

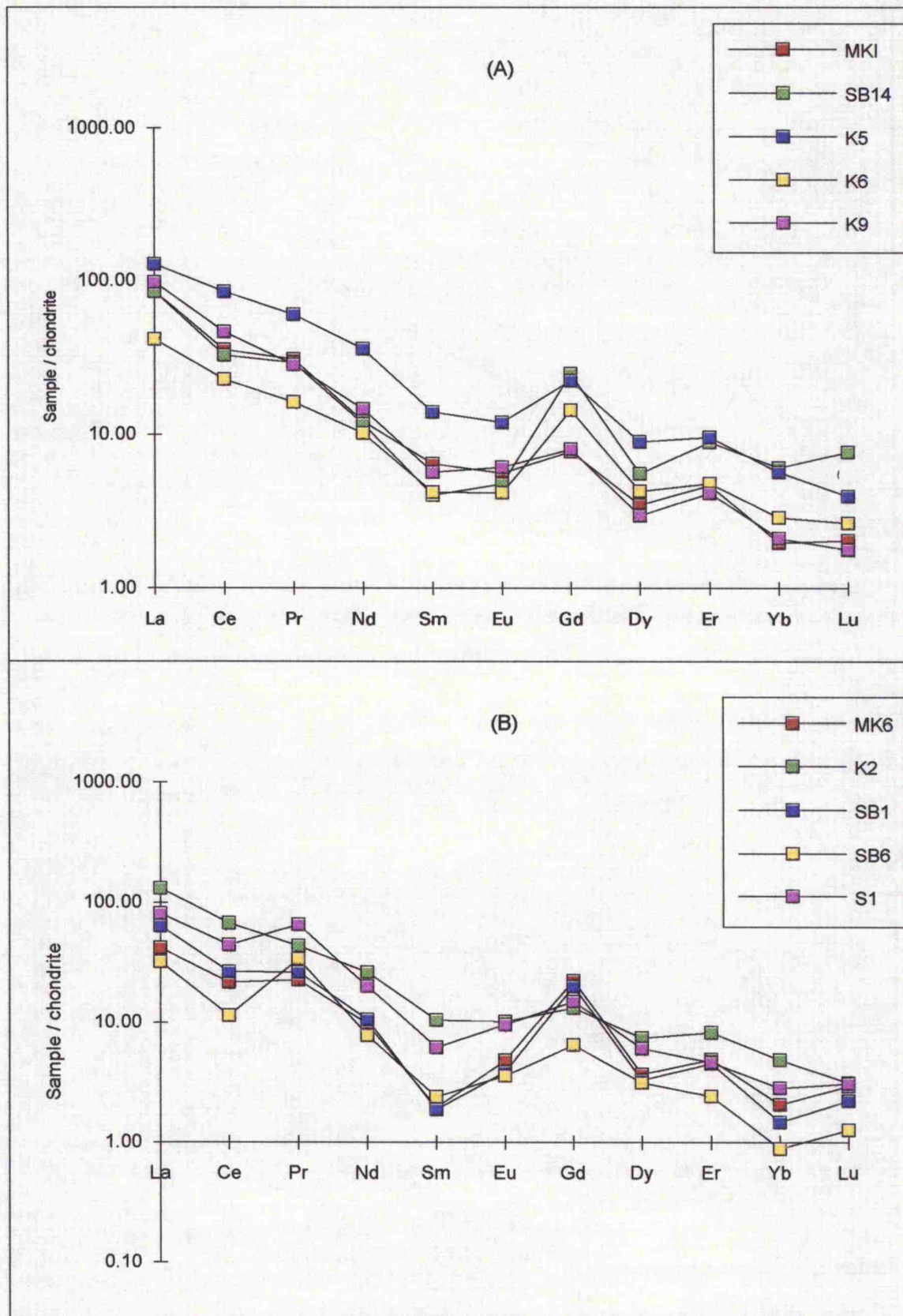


Fig. 7. 18 (A) Rare earth elements pattern of sodalite - cancrinite rich foyaites.
 (B) Feldspathoidal foyaites, agpaitic and miaskitic.

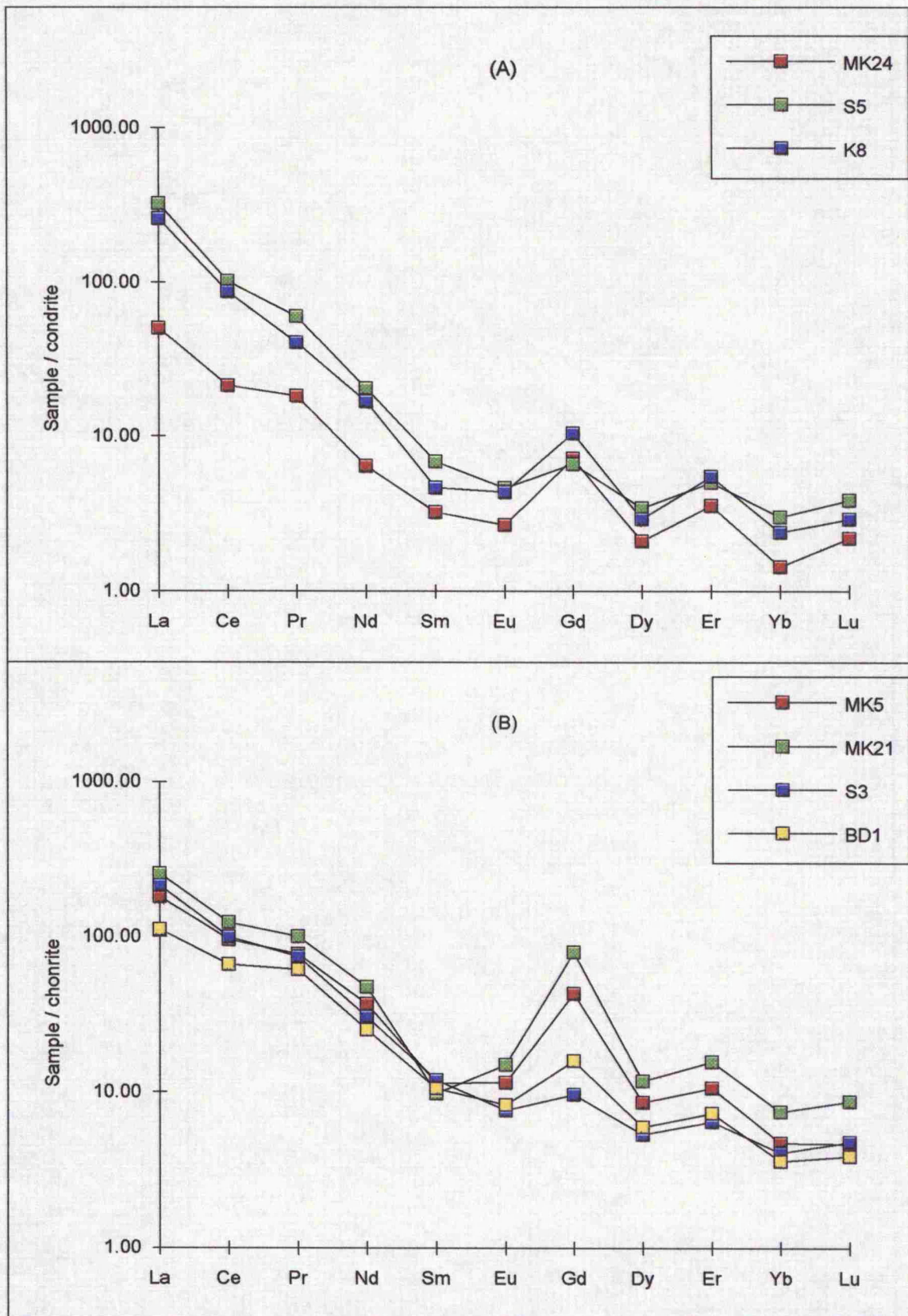


Fig. 7.19 (A) Rare earth elements pattern of foyaitic feldspathoidal syenite.
 (B) Feldspathoidal syenite.

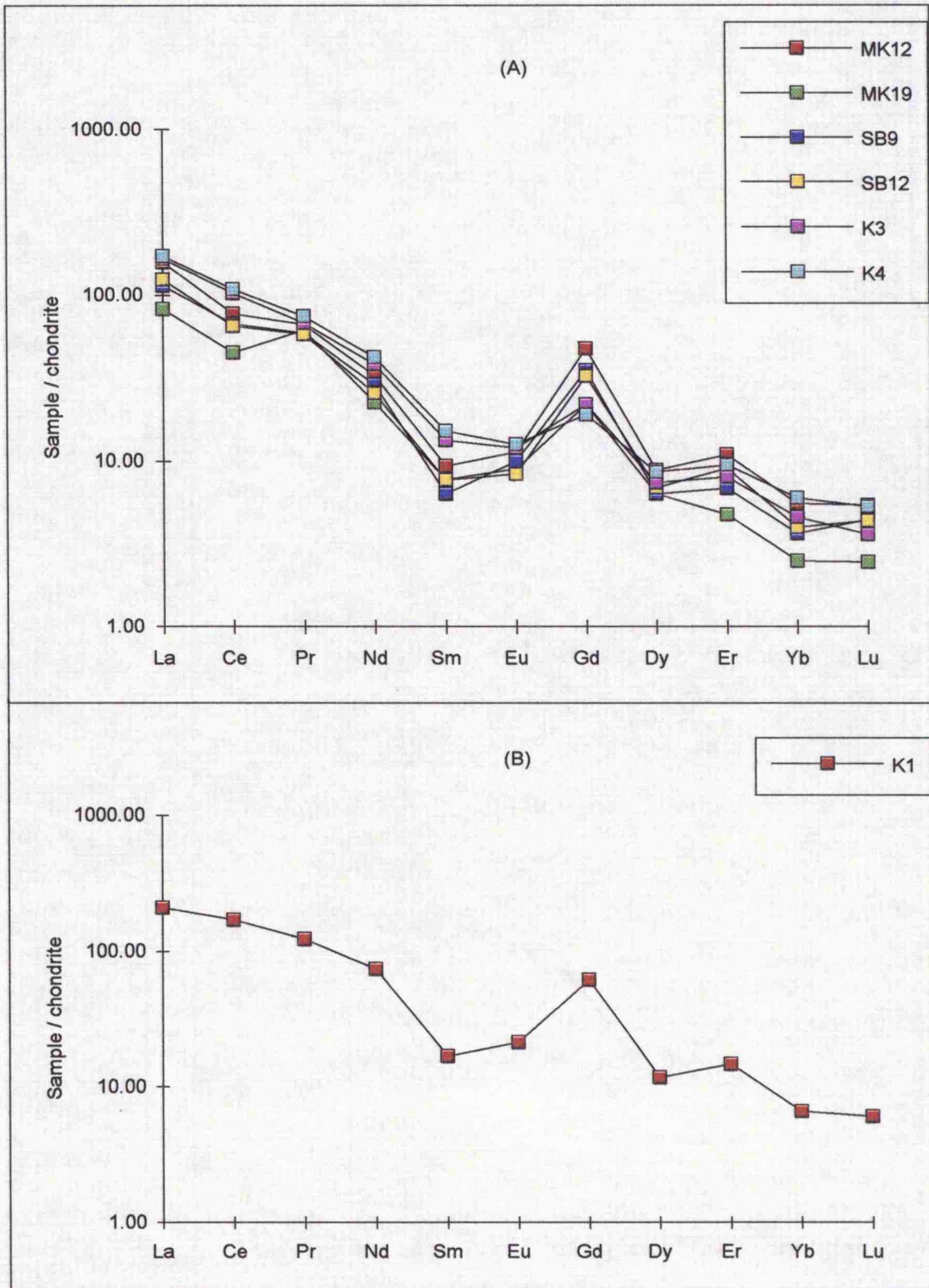


Fig. 7.20 (A) Rare earth elements pattern of pulaskitic feldspathoidal syenite.
 (B) Alkali syenite.

Gd and Er anomalies in the Koga feldspathoidal syenite rocks could be due to the presence of garnets (melanite) that might be enriched in HREE. It can be seen from Fig. 7.18 - 7.20 that the analytical procedure appears to give results for Ce, Gd and Er which are in reasonable agreement with the possible value for W-1 and Sy-2. Hence it would appear that anomalies are real. However, in other investigations Gd is often ignored because it has a positive anomaly. This problem requires further investigation.

Thus, among all the Koga feldspathoidal suites, the REE patterns of foyaites and some pulaskitic feldspathoidal syenite are the most distinct and complicated, showing steep LREE enrichment and relatively flatter HREE kinked patterns. Among them, five samples (SB-1, SB-6, MK-6, MK-24 and K-6) have overall lowest REE levels (35 - 63 ppm) with distinct Ce, Gd and Er anomalies (Figs. 7.18a, b and 7.19a).

The feldspathoidal syenites, garnet bearing feldspathoidal syenite and alkali syenite possess overall relatively high REE levels (162 - 309 ppm), displaying normal steep REE distribution patterns having strong LREE enrichment. Among these rock units three samples (S-3, S-5 and K-8) possess higher REE concentration showing very distinctly steep LREE enrichment pattern with relatively flatter kinked HREE slope having positive Gd and Er anomalies.

The observed REE distributions in the feldspathoidal rocks have strongly supported the fact that the REE abundances and shape of the REE patterns must have been controlled by garnet biotite and pyroxene fractionation in the alkaline magma. Several authors have shown that the progressive increase in the relative abundance of garnet in the rocks would correspondingly increase the REE concentrations (Schnetzler and Philopotts, 1970) and melanite garnet tend to generate flatter HREE patterns due to high mineral / melt partition coefficients for

the HREE in the alkaline rocks (Mitchell and Brunfelt, 1975, Flohr and Ross, 1989, 1990). The lack of Eu anomalies and high LREE concentration can only be generated by the partial melting of peridotites in the mantle. The strong fractionation of the LREE over the HREE (Fig. 7.19b) may be due to the presence of garnet as a residual phase during the partial melting (Kay and Gast, 1973).

*Chapter Eight***WEATHERING**

The road from Afghan camp No. 2 (approximately one Km west of Koga village) to Miani Kandao passes through a number of outcrops of fresh feldspathoidal syenite. These outcrops are surrounded by a brownish and more weathered rock. At other places rather rounded pieces / boulders of fresh rock are trapped in or perched upon what appears to be soil or weathered rock. In the past workers have tended to be confused by these relationships and have considered and mapped the fresh outcrop as separate bodies and the fresh pieces as boulders in a boulder bed.

8.1 Mineralogy

The following minerals are present in the weathered rocks;

Albite, microcline, nepheline, aegirine, sphene, magnetite, pyrite and clay minerals. Some of the minerals like pyrophanite and red brown material, which may be siderite were recognised by the EMPA.

The XRD trace is given in Fig. 8.1 which shows the minerals present in the weathered rocks.

8.2 Field Observations

A careful examination of the relationship of the fresh rock and its surroundings shows;

- i) Although the contact between the fresh rock and the surrounding matrix is sharp at many places, it is also found transitional at other places.
- ii) Whenever the surrounding rock is preserved it is also seen to comprise of feldspathoidal syenite.
- iii) The rounded "boulders" and fresh outcrop patches are generally surrounded by concentric shells of progressively altered rock.

iv) At places the boulders are seen to have joint boundaries with each other and the joints are seen to be progressively widening.

These observations prove that the feldspathoidal syenite body has undergone deep penetration chemical weathering and the so-called bodies of fresh rock or boulders (Fig. 8.2a) of fresh rock are nothing but relicts which have remained intact. The weathering penetrated along joints attacking the joint blocks more on the corners than on sides. The principal active weathering process is hydrolysis acting mainly through the kaolinization of feldspar and removal of KOH so formed through carbonation and solution. Physical weathering must have proceeded concurrently. As the rock was softened, diurnal temperature changes manifested themselves in terms of mass and granular exfoliation leading to the formation of concentric shells of progressively weathered rock and gradually disintegrating it into a powder (Fig. 8.2b). In fact at places all stages of transition from solid rock to powder can be seen (Fig. 8.3a).

Obviously the deep weathering of feldspathoidal syenite was accomplished sometime in the past when the slopes were gentler and the weathering front in main descended from above. The weathering front did not move down everywhere at the same rate. The gentler slopes and lower areas have undergone deeper weathering than the steeper slopes and higher areas. As at the present time the slopes are fairly steep, the main weathering must have occurred sometimes earlier perhaps in Late Quaternary when the slopes were gentler, the erosional process more sluggish and climate more humid and warmer. It led to the development over the outcrop of a deeply weathered rock cover of saprolite extending down with variable depth. The period of deeper weathering may have coincided with that during which the valleys were filled with alluvium to make the present day wide valley floors. That alluvial fill is now in the process of being dissected. Concurrently on the mountain slopes the saprolitic cover is being removed and fresher rock is being exhumed.

At lower level close to the alluvial fill of the valleys two beautiful sections of this deeply weathered cover are preserved in the form of *grus*. One section is exposed on the roadside just south of Koga village (G. R. 53183820) and other at the back of Sura village near a tomb and the Nai Roshni School (G R. 56383760).

The Sura section represents one of the best examples of the deep chemical weathering reported from anywhere in Pakistan. The vertical cut shows a depth of at least 4.5 to 6 m of kaolinized and deeply weathered rock (Fig. 8.3b). Allowing for erosion above and continuation of weathering in the part now covered with alluvial fill, deep chemical weathering may have affected a vertical thickness of 6 meters or more.

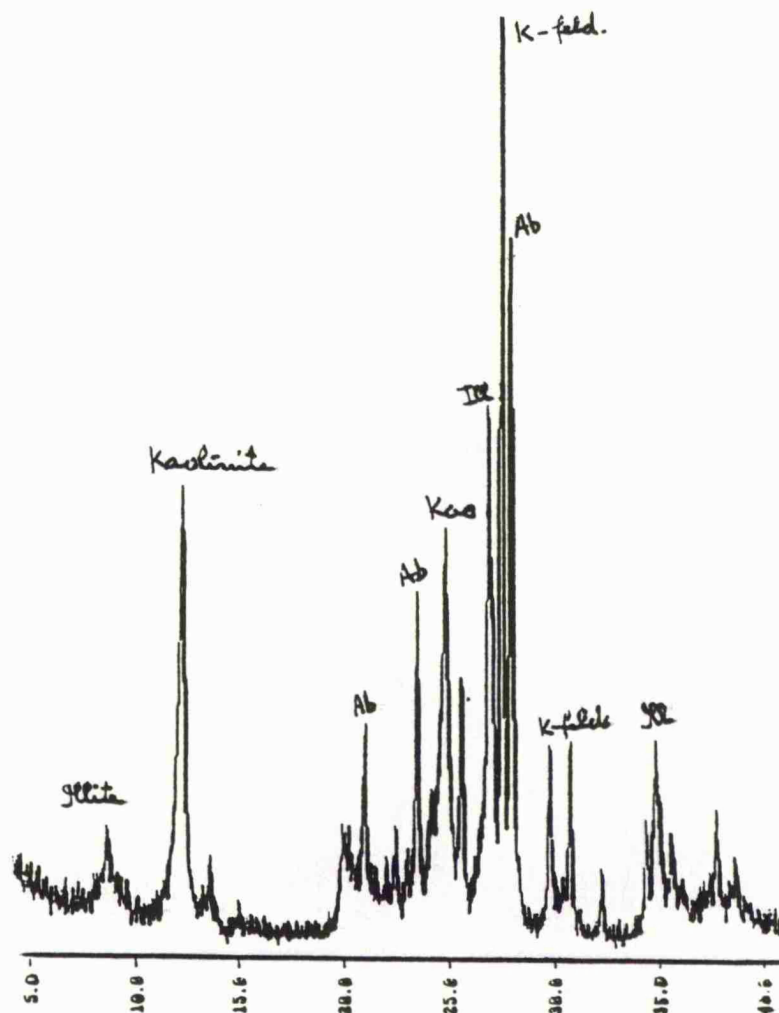


Fig. 8.1 XRD trace of the weathered rock showing presence of different minerals.

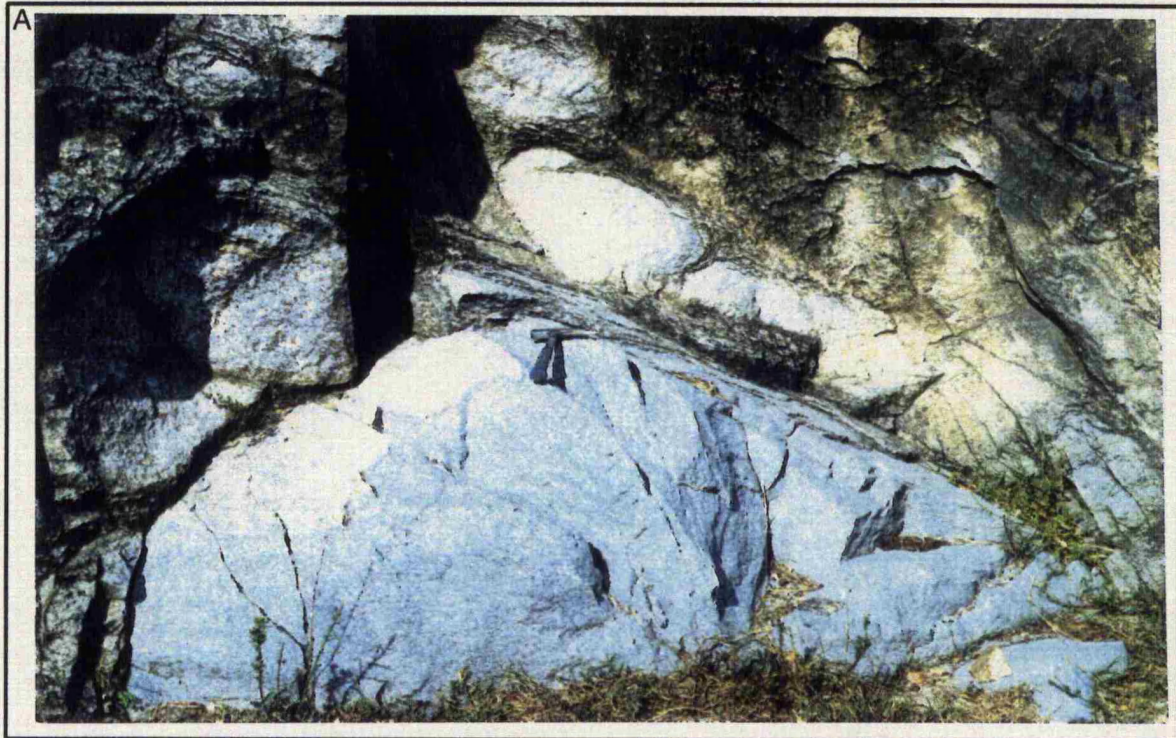


Fig. 8.2: (A) Photograph of fresh rock boulders showing relict which remained in contact (location as G. R. 53603491):(B) Photograph showing progressive weathering (location as sample Sb-4).



Fig. 8.3: (A) Photograph showing the complete transition of solid rock to powder (location as sample BW-6); (B) Photograph of deeply weathered rock showing the kaolinization of the rock (location as sample S-1).

	SiO ₂
SB-2	61.96
SB-3	64.38
SB-4	61.47
K-1	61.35
BW-6	60.47
S-1	57.84
BW-7	59.5

	Al ₂ O ₃
SB-2	19.77
SB-3	17.76
SB-4	21.19
K-1	18.04
BW-6	20.45
S-1	22.75
BW-7	26.85

	Na ₂ O
SB-2	7.69
SB-3	6.55
SB-4	6.41
K-1	5.1
BW-6	6.43
S-1	9.04
BW-7	1.85

	K ₂ O
SB-2	5.36
SB-3	6.52
SB-4	5.61
K-1	7.46
BW-6	4.47
S-1	5.37
BW-7	8.99

	T. Al
SB-2	13.05
SB-3	13.07
SB-4	12.02
K-1	12.56
BW-6	10.9
S-1	14.41
BW-7	10.84

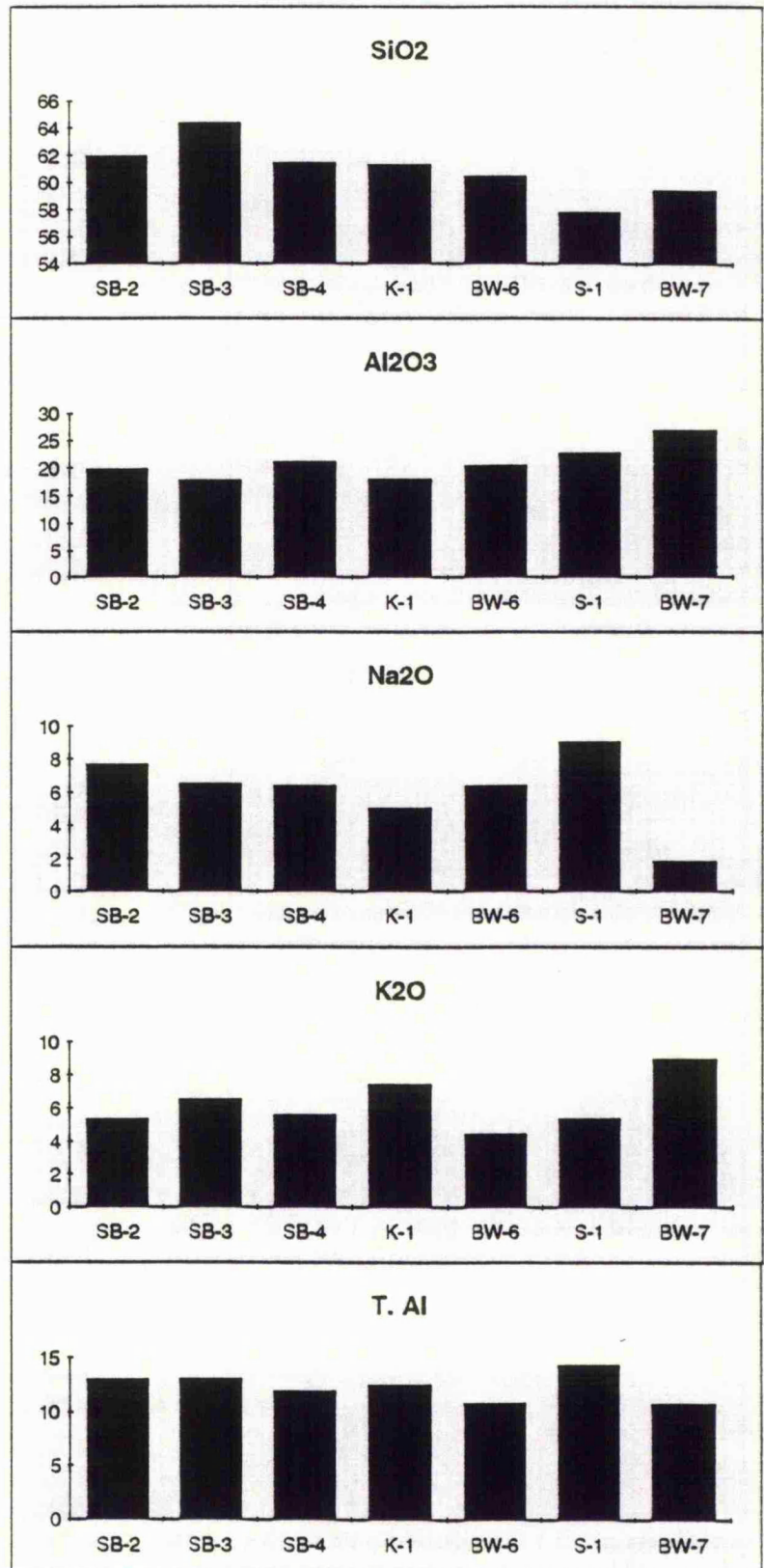
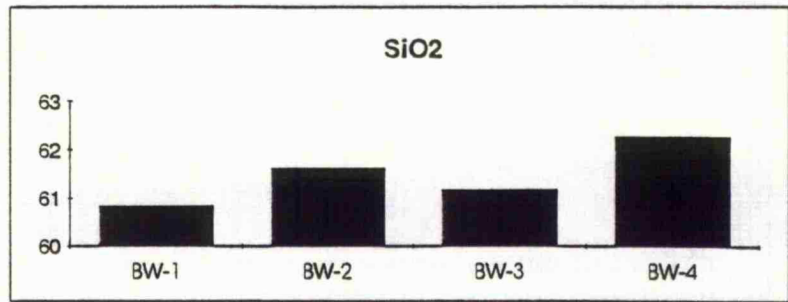
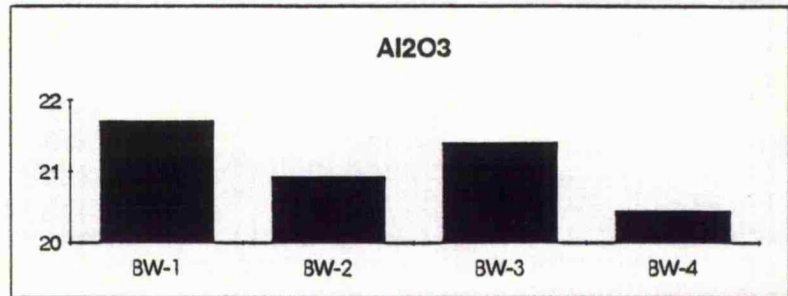


Fig.8.4 The comparison of SiO₂, Al₂O₃, Na₂O, K₂O, and Total Alkalies in the fresh rock (SB-2, K-1 and S-1) with different phases of weathered rock samples (SB-3, SB-4 and BW-6).

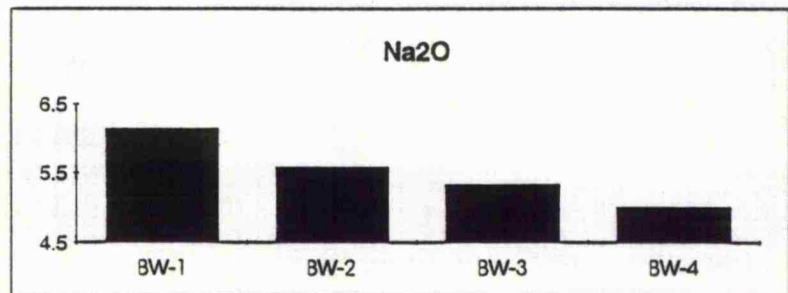
	SiO ₂
BW-1	60.84
BW-2	61.61
BW-3	61.17
BW-4	62.27



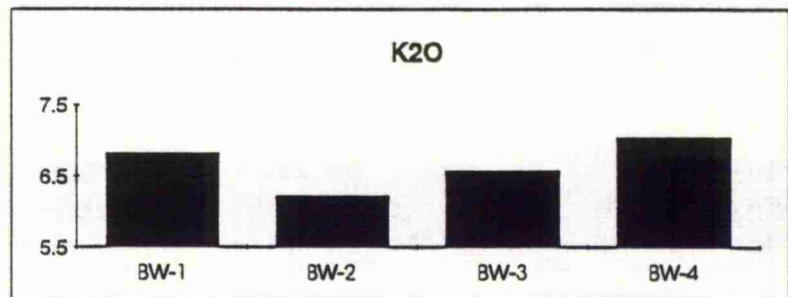
	Al ₂ O ₃
BW-1	21.71
BW-2	20.93
BW-3	21.41
BW-4	20.45



	Na ₂ O
BW-1	6.14
BW-2	5.58
BW-3	5.33
BW-4	5.01



	K ₂ O
BW-1	6.82
BW-2	6.22
BW-3	6.57
BW-4	7.04



	T. Al
BW-1	12.96
BW-2	11.8
BW-3	11.9
BW-4	12.05

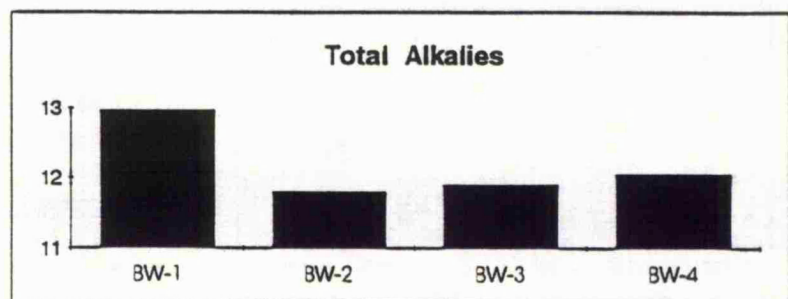


Fig.8.5 The comparison of SiO₂, Al₂O₃, Na₂O, K₂O, and Total Alkalies in the fresh rock (BW-1) with the different phases (BW-2 to BW-4) of weathering in a column from lower to upper portion.

Below the upper 0.6 m or so of rock that has been reduced to soil chemical weathering has attacked the individual constituents of the rock altering them and kaolinizing them but the gross texture of the rock is preserved as a ghost structure. Abundant kaolinized leucocratic pegmatite veins are seen criss- crossing the rock face. In contrast the rock itself is converted into a brown soft mass with white specks of kaolinized feldspar.

8.3 Comparison of Chemical Compositions

The comparison of the chemical composition between the adjoining rock S-1 (56383760) and weathered rock material BW-7 shows an increase in K_2O and significant decrease in Na_2O contents shown in Table 8.1, Fig. 8.4. The SiO_2 , Al_2O_3 and Fe_2O_3 all decrease.

Table 8.1 Chemical composition of the fresh rock samples (SB-2, BW-1, K-1 and S-1) and the weathered rock samples (SB-3, SB-4, BW-2,3,4,5,6 and BW-7).

	SiO ₂	TiO ₂	Al ₂ O ₃	Fe ₂ O ₃	MnO	MgO	CaO	Na ₂ O	K ₂ O	P ₂ O ₅	Total
SB-2	61.96	0.23	19.77	4.39	0.11	0.02	0.46	7.69	5.36	0.02	100.01
SB-3	64.38	0.33	17.76	2.85	0.12	0.19	0.36	6.55	6.52	0.04	99.77
SB-4	61.47	0.61	21.19	3.70	0.10	0	0.03	6.41	5.61	0.02	100.13
BW-1	60.50	0.54	19.37	3.36	0.13	0.20	1.34	7.32	6.96	0.05	99.63
BW-2	60.84	0.53	21.71	3.42	0.18	0.18	0.28	6.14	6.82	0.03	99.69
BW-3	61.61	0.55	20.93	3.30	0.12	0.32	0.95	5.58	6.22	0.05	99.24
BW-4	61.17	0.54	21.41	3.44	0.12	0.24	0.84	5.33	6.57	0.03	99.64
BW-5	62.27	0.39	20.45	3.43	0.12	0.17	0.33	5.01	7.04	0.03	99.39
K-1	61.35	0.80	18.04	3.77	0.15	0.38	1.81	5.10	7.46	0.07	98.93
BW-6	60.47	0.88	20.45	4.06	0.16	0.72	1.81	6.43	4.47	0.19	99.64
S-1	57.84	0.26	22.75	2.74	0.09	0.16	1.07	9.04	5.37	0.03	99.35
BW-7	59.50	0.28	26.85	1.67	0.07	0	0.15	1.85	8.99	0.03	99.39

The sample K-1 is not the actual representative fresh rock sample for BW-6, (G.R. 53003520) but taken from the more or less same rock unit.

Some 3 metres deep similar profile of deeply weathered feldspathoidal syenite is seen just south of Koga village on the roadside. Here the degree of alteration is slightly less than that met with in the Sura section. Apart from the relatively recent chemical weathering, feldspathoidal syenite also shows the effects of hydrothermal alteration. At such places the rock has developed a

reddish stain and secondary mica has developed. The hydrothermal alteration, however, is a minor phenomenon compared to chemical weathering.

The third comparison between SB-2 (fresh rock G.R. 53053612), SB-3 and SB-4 (weathered rocks G.R. 53303590 and 53703596 respectively Fig. 8.4), which shows an increase in K_2O , SiO_2 and decrease in Na_2O , Al_2O_3 and Fe_2O_3 but it is not as significant as in the case of BW-7.

The fourth example is in a column starting from a fresh rock below to the upper most weathered rock as follows:

- | | |
|------|--|
| BW-1 | Fresh rock (G. R. 53003520) |
| BW-2 | Weathered rock just above the fresh rock (6 inches above). |
| BW-3 | Weathered rock (20 inches from BW-1). |
| BW-4 | Weathered rock (36 inches from BW-1). |
| BW-5 | The top most weathered rock. |

The comparison of these samples is given in Fig. 8.5 and the other rocks in 10.1.

It is interesting to note that the total alkalis do not decrease below 10.84 which is pretty high but the iron is leached out.

The phenomenon of chemical weathering has an important bearing on reserve calculation. The reserves have been calculated on the basis of fresh rock exposure so far. Fresh rock, however, must continue below the variable depth of weathered rock everywhere, enlarging the reserves.

*Chapter Nine***PETROGENESIS**

Although the petrogenesis of the Koga feldspathoidal syenite complex is not under the aims of the present study nevertheless, a considerable body of new petrographic, mineralogical and geochemical data has been accumulated in this project. This provides some insight into the genesis of the Koga feldspathoidal syenite complex.

There are at least two distinct periods of magmatic / volcanic activity in the alkaline province. One is Permo - Carboniferous in age and is related to the break up of Gondwana land through Intra continental rifting.

The second activity is Tertiary in age. This is related to bending of Indian Plate during subduction. This bending caused tension and rifting. Unfortunately no absolute ages of the alkaline bodies have been determined. The published ages are mostly "RESET" ages.

Tectonically the alkaline province falls in the following Himalayan subdivisions.

(a) Tarbela, Koga, Ulla, Babaji, Ambela and Loe Shilman falls in the Lesser Himalaya South of MCT.

(b) Sillai Patti and Jambil fall in the Higher Himalaya North of the MCT.

It may therefore concluded that alkaline province is not restricted to the Lesser Himalaya alone.

9.1 The Alkaline Igneous Province of Northwest Pakistan

The Tertiary alkaline igneous rocks complexes occur as scattered bodies in a semi circle around northern and western parts of Peshawar plain. The complexes so distributed are comprised of Loe Shilman carbonatites, Shewa alkali

porphyries, Babaji soda granites and syenites and Koga nepheline syenite and associated carbonatites (Ashraf and Chaudhry, 1977), along with basic intrusions. These rocks are emplaced along E - W trending fault zones in the Early Palaeozoic metasediments forming a long belt which extends from Afghanistan through Khyber, Mohmand Agency, Malakand Agency, Malakand Lower Swat and Tarbela area. The distribution of alkaline and carbonatite complexes is given in Fig. 3.1.

The Koga nepheline syenite is not an isolated and independent local derivative, but it is a part of the alkaline province starting from Loe Shilman to Chamla (Ashraf and Chaudhry, 1977).

9.2 Regional Setting

The geology of NW Himalaya can be described under three main geological domains as follows;

- a) Indo-Pakistan plate
- b) Kohistan magmatic island arc sequence and
- c) Eurasian plate (Tahirkheli, 1979).

Two major suture zones separating these domains are the Main Mantle Thrust (MMT) and the Main Karakoram Thrust (MKT). The MMT marks the boundary along which the Indo-Pakistan plate has been subducted under the Kohistan island arc. The MKT marks the boundary along which Gawachi Back arc basin was closed and Kohistan arc was brought against Asian mass (but there is a melange zone in between, which varies from 500 M to 10 Km in width). The collision of the Indo-Pakistan plate with the Eurasian mass and subsequent under thrusting have developed deep imprints of stresses in Peshawar basin. It is likely that the tensional forces in the basin behind the zone of compression might be responsible for producing the rifting.

Major faults tectonics have been described in Peshawar basin and adjoining areas (Tahirkheli, 1979). The alkaline and carbonatite magmatism are suggested

to be related to the collision extensional tectonics in areas to the Indo-Pakistan plate.

9.3 Origin of the Alkaline Rocks and Carbonatite Complexes: Tectonic Constraints

Alkaline rocks are commonly associated with rifting (Sorensen, 1974, Smith et al. 1977, Bailey, 1978, and Taylor et al. 1980).

There is a correlation between alkaline magmatism and changes in the direction of plate movements creating reactivation of lithospheric shear zones and rifting within plates from the plate tectonic view point. The associated oblique sets of transcurrent faults originally under compression would open and propagate as tensional faults. This would allow fracturing through the continental lithosphere causing pressure release, channelling of volatiles, partial melting and generation of magma from the asthenosphere. The classic example of African rift related interplate alkaline magmatism is from Niger - Nigerian alkaline complexes (Bowden et al. 1987)

The overall plate tectonic approach suggests that it is within plate stress fields and fault reactivation which controls the sites of alkaline magmatism in the continental lithosphere. Based on this model the episodic partly mobile thermal anomaly in the mantle is relegated from a plume to a passive hotspot.

The Kohistan sequence interpreted as continental margin or island arc being sandwiched in the Himalayan continent - continent collision provides suitable explanation for the origin of the alkaline igneous province in Pakistan. Kempe and Jan, (1980), suggested that rifting in Peshawar basin was due to relief tension followed by the release of compressional thrusting triggered by collision of Indo - Pakistan and Eurasian plates.

Rifting is also evident in the Narbada River valley in case of domed Amba Dongar carbonatite and related syenites, ijolite and phonolites, in Gujrat

(Sukheswala and Udas, 1964), and may also occur in other Indian alkaline intrusions.

Similar interpretations have been advocated by some authors for the origin of ijolite from the Koga area (Le Bas et al. 1987), Carbonatites from the Silai Patti Butt et al. (1989), and Panjal tholeiitic basalts in Azad Kashmir (Butt et al. 1985). Butt et al. (1985) were of the opinion that Panjal basaltic volcanics of Permo - Carboniferous age from Azad Kashmir could be related to rifting of the Indian continent and considered to be integral continuation of Panjal traps in Jammu - Kashmir, Raj Mahal traps of West Bengal and Bihar and Sylhet traps of Bangladesh originated with rifting of Gondwanaland, initially proposed by Crawford, (1974). The alkaline and carbonatite magmatism in Koga and Silai Patti may possibly belong to a tensional episode linked with the break up of Gondwanaland.

The dates given below suggest that the Koga feldspathoidal syenite complex was formed not > 50 Ma, which is quite after the Gondwanaland break-up.

Alkaline granites of Warsak, Shewa and Shahbaz Garhi, and Koga syenite complex contain pyroxenes as an essential constituent and the field relations show that such bodies are related to faults or rifts as well as areas of cross-folds (Shams, 1980).

Taking into consideration of Warsak and Ambela areas as the two main centres of intrusion, two phases of activity may have been followed by the initial contact between the Indo-Pak subcontinental plate and the island arcs or continental margin at the southern edge of Eurasia, some 55 Ma ago, and the subsequent slowing down of the former plate's northward drift at about 53 Ma (Powell, 1979). Early activity took place 50 Ma (Koga syenite: N.J. Snelling, personal communication to S. F. A. Siddiqui, 1971) may have been followed by a later event at 41 Ma (riebeckite from the Warsak alkaline granite: Kempe, 1973).

9.4 Major Elements

The Koga feldspathoidal syenites of the project area constitute important rock units of the Koga undersaturated alkaline complex which is generally described as an integral part of the so-called Alkaline Igneous Province of Northwest Pakistan (AIPNP). Current geochemical investigations have indicated that at least three major rock associations occur with the Koga -Ambela alkaline complex (Mateen, personal communication 1993), namely; lamprophyre - carbonatite-fenites, ijolite - feldspathoidal syenites - syenites and syenites - quartz syenites - alkali granites. These three series generally form separate intrusions.

In order to visualise the petrogenetic evolution of the feldspathoidal syenite rocks it is necessary to consider overall aspects of nature of the mantle source, degree of partial melting of plausible magma and subsequent fractional crystallisation, and the extent of involvement of both lithospheric mantle and lower crust beneath the Koga - Ambela region.

The analysed feldspathoidal rocks exhibit a strong to moderate alkali enrichment and undersaturated character with slightly higher SiO_2 content than in other agpaitic and miaskitic syenite suites. They are strongly depleted in TiO_2 , MgO , CaO and P_2O_5 . The overall major element chemistry suggests that at least the feldspathoidal syenites, pulaskitic feldspathoidal syenites, garnet bearing feldspathoidal syenites and alkali syenite suites may have been primarily derived directly from a more mafic or trachytic magma. Some of the foyaites particularly sodalite / cancrinite rich foyaites are late stage differentiates emplaced as dikes and pegmatite bodies. The present analytical data (including unpublished results of the associated ijolites, Babaji syenites and alkali granites (Mateen, personal communication, 1993), strongly indicate that the feldspathoidal syenite suites are not formed from a single undersaturated magma series. In this respect the Koga undersaturated alkaline complex has similar genetic evolutionary history to typical rift related alkaline provinces of India and Africa.

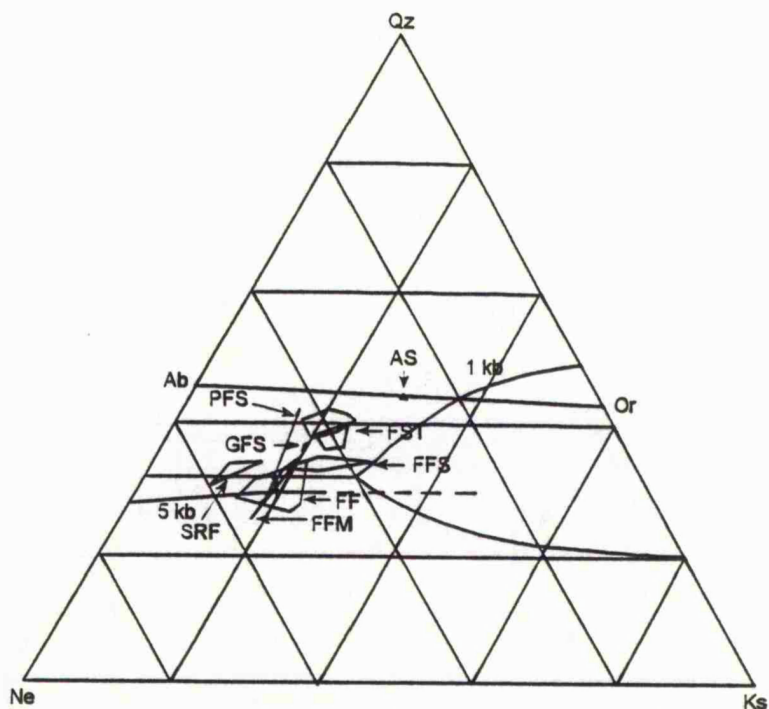


Fig. 9.1 Normative nepheline of different groups of the Koga complex rocks plotted on Ne - Qz - Ks, SRF=sodalite rich foyaites, FF and FFM=feldspathoidal foyaite apatitic and miaskitic, FFS=foyaitic feldspathoidal syenite, PFS=phonolitic feldspathoidal syenite, FST=feldspathoidal syenite trachytic, GFS=garnet feldspathoidal syenite and AS=alkali syenite.

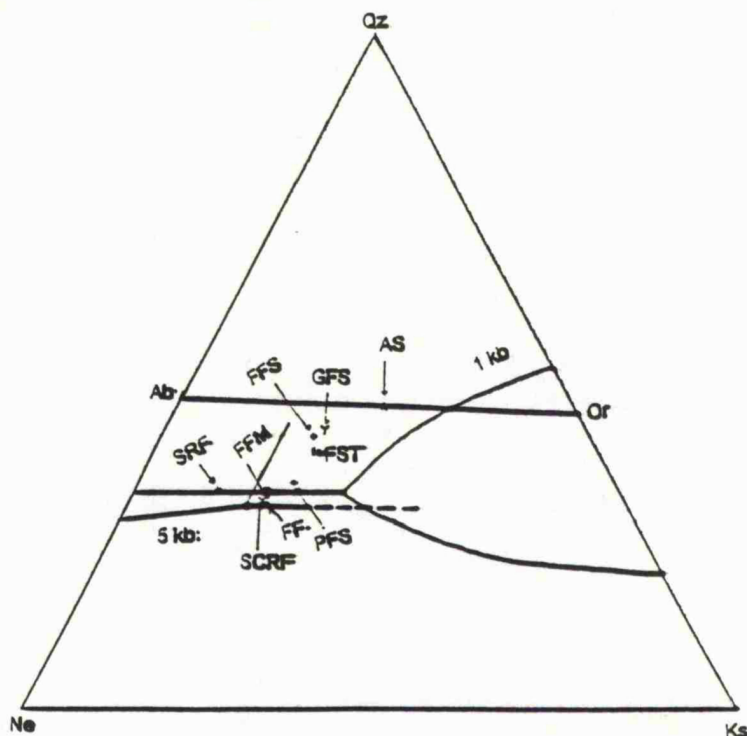


Fig. 9.2 Average normative nepheline of different groups of the Koga complex rocks plotted on Ne -Qz - Ks system, symbols as above and SCRF=sodalit-cancrinite rich foyaites.

The analyses of the rock samples of the different groups of the Koga feldspathoidal syenite complex are plotted with their averages in Fig. 9.1 and 9.2 respectively as CIPW normative wt. % in the nepheline - kalsilite - silica system after Hamilton and MacKenzie, (1965) at 1 Kb pressure, Taylor and MacKenzie, (1975) at 2 Kb pressure and Morse, (1970) at 5 Kb pressure.

All groups from the Koga complex plot at a pressure > 1 and < 5 Kb, except the sodalite rich foyaites. Hamilton and Mark, (1965) showed that rocks having 80 % or more normative nepheline, albite and orthoclase plot close to the 1 Kb nepheline - syenite minimum. The leucite field becomes contracted with increasing pressure.

The alkali syenite plots on the Ab - Or join, whereas, majority of the rock groups plot near the minima. The feldspathoidal foyaites are the most evolved rocks while the alkali syenite the least evolved, with the means of the foyaitic analyses plotting almost on the minima at 1 and 2 Kb P_{H_2O} . The final stage of crystallisation is represented by the cancrinite and sodalite rich foyaites. Although a trend from the ternary minima in the water saturated system from cancrinite to sodalite rich foyaites involves a rise in temperature, it may be that the high concentration of SO_3 , Cl and CO_2 alter the phase diagram, causing a shift of the minima towards the nepheline - quartz side of the diagram. A second possibility might involve the autometasomatism of foyaites by their own residual fluids.

It can be concluded from the petrography that the feldspathoidal syenite rocks of the Koga complex started as normal syenites with homogeneous feldspar and then exsolved and recrystallised. These feldspars may have formed at high temperature and then they attained a stable, low-temperature composition each containing little of the other in solid solution. Electron microprobe data also shows that the nephelines cluster tightly close to the nepheline - kalsilite line (Fig. 7.2), also indicates a low final equilibration temperature.

Chaudhry et al. (1981) outlined the differentiation sequence for the Koga complex, starting from Babaji soda granite. Through progressive evolution alkali enrichment resulted in the formation of Babaji nordmarkite, pulaskite and nepheline syenite. They argued the evolution of these rocks due to crystallisation differentiation and alkalis were distributed due to the concentration of volatiles. According to Chaudhry et al. (1981), soda granite and nepheline syenite were emplaced first, followed by the western body of pulaskite and nepheline syenite. At this stage pulaskitic pegmatites with either microcline only and or microcline albite - nepheline and pyroxene developed, and then the nepheline syenite. In this intrusion, nepheline syenite pegmatites consisting nepheline and microcline developed due to enrichment of alkalis.

Chaudhry et al. (1981), pleaded the process of alkali volatile enrichment after the formation of nepheline syenite proper which resulted in the generation of different dikes, rich in nepheline and pegmatites. These dikes and pegmatites followed the development of melanite and biotite bearing nepheline syenite of Koga, Bibi Dherai, Agarai and Sura. These dikes are aplitic which could be due to pressure quenching. This was followed by the formation of dikes near Agarai, Namdar, Ladi Patao and Miani Kandao. These were formed due to alkalis and volatile enrichment. These dikes are coarse grained to pegmatitic and the main intrusion forming activity came to an end. Finally after this, a rapid concentration of alkalis and volatiles formed the feldspathoid rich pegmatites - sodalite pegmatites with sodalite - nepheline - cancrinite - microcline - biotite and pyrite were formed, later on pegmatites with nepheline cancrinite - albite - biotite - calcite formed due to alkalis and F, H₂O, SO₃, CO₂ and S.

The above differentiation is possible but the mineralogy of the Koga feldspathoidal syenite do not totally confirm this. First of all the mafics i.e. pyroxenes and biotites (called pyroxenes by Chaudhry et al. 1981), were not formed in the Koga feldspathoidal syenite. The very nature of their occurrence as

aggregate and clots in thin sections reveals that they were carried from the source magma. Secondly the nepheline - cancrinite - albite - pyroxene - calcite pegmatites are not the last stage of formation but the pegmatites of sodalite - nepheline - cancrinite - microcline - biotite and pyrite (which could not be observed in the thin sections by the author), as described above.

It is therefore suggested that the sequence may be as follows:

Babaji soda granite → Babaji nordmarkite → alkali syenite → garnet bearing feldspathoidal syenite → pulaskitic feldspathoidal syenite → feldspathoidal syenite → foyaitic feldspathoidal syenite → feldspathoidal foyaites miaskitic → feldspathoidal foyaites agpaitic → sodalite - cancrinite rich foyaites and finally sodalite rich foyaites (see Fig. 9.2).

9.5 Trace Elements

The trace element geochemistry of the project rock units discussed here broadly demonstrates that at least three distinct primary magmas of syenitic compositions have been involved in the generation of the feldspathoidal rocks of the Koga complex. The units exhibiting distinct trace element signatures may be grouped accordingly as follow:

1. Alkali syenite – alkali granites (high potassic trend, $K > Na$). Alkali syenites are characterised by high concentration of Sr, Ba, Nb and high K/Rb ratios.
2. Feldspathoidal foyaites – pulaskitic feldspathoidal syenite – garnet bearing feldspathoidal syenites (Trachytic – miaskitic following the pulaskitic – foyaitic trend). These are characterised by low concentrations of Rb, Cr, Sc, Y, Nb, Zr, Th and LREE and high Sr and Ba and relatively high ratios of K/Rb, Ba/Sr, Cr/Sc, Zr/Y and Ba/Nb.
3. Foyaites – Foyaitic feldspathoidal syenites – feldspathoidal syenites (Phonolitic – agpaitic following ijolitic – nepheline syenite trend with sodium enrichment towards sodalite / cancrinite rich foyaites differentiates). The rock units

are characterised by relative high contents of Rb, Zn, Y, Nb, Zr, Th and LREE and strong depletion of Sr and Ba with relatively low Ba/Nb and Y/Nb.

9.6 Rare Earth Elements

The distinct variable trace element abundances and very interesting complex REE distribution patterns (strong LREE enrichment without Eu anomaly, significantly marked negative Ce anomaly and kinked HREE pattern with distinct positive Gd and Er anomalies) strongly indicate the complex magmatic evolutionary history of the Koga feldspathoidal syenite rocks.

The dual behaviour of LILE and HFSE (incompatible as well as compatible trend) within the analysed suite suggest both partial melting and fractional crystallisation processes were involved in the magmatic evolutionary trends leading to the variable trace element geochemistry. The REE patterns, Zr - Y, Nb - Ba and Nb - Y characteristics and Cr/Sc - Cr are consistent with the partial melting of the mantle sources. Both the deep asthenospheric source and shallow lithospheric mantle may have been involved through the varying degrees of melting. The strongly undersaturated melts probably produced by a small degree of partial melting of the deepest source of garnet lherzolite facies in the asthenospheric mantle. The observed variations in the trace elements and REE patterns perhaps suggest the complex processes of assimilation and contamination during the production of trachytic magmas and subsequent differentiation and emplacement of feldspathoidal rocks.

The source enrichment of LREE could be due to mantle metasomatism as well as involvement of oceanic crust subduction during the underthrusting of the Indo-Pakistan plate. The Ce and Eu negative anomalies in the REE patterns of feldspathoidal syenites strongly suggest this phenomenon. Alternatively, the REE characteristics in combination with Cr/Sc - Cr may be interpreted by the involvement of lower crust (granulite and eclogite facies) in the shallow level lithospheric mantle source melts (Neal and Taylor, 1989).

To proceed further with the investigation of the petrogenesis of the Koga complex require an investigation of Sr and Nd isotopes. This did not fall within the aims of the present study.

*Chapter Ten***MINERAL PROCESSING****Introduction**

Few raw materials can be used directly in industry without processing. In the case of nepheline syenite, it is very important that the material should be processed according to the requirements of the consumers. Nepheline syenite is processed to get rid of the deleterious minerals such as iron oxide, biotite, garnets, aegirine and amphiboles. Such processing has been done in the project by the crushing of the original material and processing it to get rid of the above minerals. The main object was to achieve the minimum percentage of iron contents in the form of Fe_2O_3 on laboratory scale by magnetic separator of relatively low intensity. The iron contents so achieved may not correspond to the stringent requirements for glass making but the present work aims to provide an indication of suitability for possible different uses in future.

Typical samples were taken from each of the lithological units to represent the whole Koga feldspathoidal syenite deposit. The choice was made in the field so that enough material could be collected for processing.

Raw material finer than 200 mesh is not desirable for glass making. So it is very important that the over crushing of the material should be avoided.

Two different procedures were adopted; firstly, from seven samples, weighing 15 Kg, 2 Kg of representative and identical samples were processed in Leicester and secondly, additional material was collected from the project area to provide large samples weighing up to 20 Kg, which were processed in Pakistan.

The grain sizes of the mafics were measured under the microscope before processing. These ranged from 0.01 mm to 10 mm.

10.1 Procedure Adopted in Leicester

10.1.1 Crushing

Seven samples, weighing 2 Kg were reduced to approximately 2 cm size by the fly press and passed through a jaw crusher to reduce the size to < 2 mm. They were sieved to give sizes ranging from 2 mm to 63 μ . The + 2 mm and + 1 mm material was passed through the roller crusher and sieved again. Then the material was subjected to the tungsten tema mill for 4 sec - after several attempts it was observed that 4 sec was the suitable time.

The material was washed through the sieves and each fraction was collected in different beakers and decanted. Some -63 μ material was also collected for analysis. Samples were dried over night in the oven at 105^o C. Each fraction was weighed to estimate the weight recovery (Table 10.1).

Table 10.1

Weight recovery of different fractions of samples after sieving and washing

Sample	K-2	K-3	K-4	K-5	K-6	K-8	K-9
Starting Wt. in grams	2068.50	1881.20	2031.40	1927.90	1975.40	2043.80	2236.60
2 mm	348.65	246.96	260.04	117.45	103.46	196.74	202.18
1 mm	368.50	355.64	500.79	511.13	393.80	445.31	397.25
500 μ	357.93	393.05	476.42	462.46	412.16	452.03	604.00
250 μ	226.94	231.31	261.82	248.98	272.64	240.53	327.80
125 μ	213.09	197.65	192.36	193.25	213.36	237.42	275.50
63 μ	349.89	271.55	164.92	207.48	374.49	300.95	238.60
Recovery in grams	1865.00	1696.16	1856.35	1740.75	1769.91	1872.98	2045.33

The chemical analyses of these samples are given in Table 10.2.

10.2 Procedure Adopted in Pakistan

In the second phase larger samples, weighing up to 30 Kg were reduced to approximately 3" size in the jaw crusher. This material was then passed through

the roller crusher twice and sieved through a 30 mesh BSS sieve. The + 30 mesh material was reduced in the disc crusher so that 100 % material passed through the 30 mesh sieve.

Table 10.2

Chemical analyses of different samples before processing

	SiO ₂	TiO ₂	Al ₂ O ₃	Fe ₂ O ₃	MnO	MgO	CaO	Na ₂ O	K ₂ O	P ₂ O ₅	Total
K-2	58.95	0.11	21.98	2.41	0.10	0.00	0.94	11.50	4.19	0.01	100.19
K-3	59.91	0.63	19.47	3.14	0.14	0.48	1.64	7.59	6.03	0.05	99.08
K-4	60.65	0.58	18.81	3.47	0.15	0.33	1.46	7.08	6.06	0.06	98.65
K-5	57.10	0.13	21.78	4.50	0.14	0.02	0.79	12.09	2.78	0.01	99.34
K-6	57.07	0.15	22.33	3.12	0.15	0.11	1.93	11.26	2.80	0.02	99.94
K-8	59.03	0.17	22.55	1.71	0.09	0.09	0.78	9.60	5.79	0.03	98.94
K-9	57.13	0.14	23.07	2.90	0.16	0.12	1.03	10.12	5.08	0.02	99.77

The chemical analyses of the material are given in Table 10.3.

Table 10.3

Chemical analyses different samples before processing

	SiO ₂	TiO ₂	Al ₂ O ₃	Fe ₂ O ₃	MnO	MgO	CaO	Na ₂ O	K ₂ O	P ₂ O ₅	Total
LP-1	61.03	0.57	20.01	2.07	0.12	0.10	10.45	7.81	6.70	0.20	100.06
LP-2	60.56	0.58	19.72	2.04	0.12	0.04	1.60	9.01	6.70	0.13	100.50
MK-1	59.83	0.13	21.52	2.37	0.14	0.01	0.80	8.89	6.59	0.05	100.53
S-1	56.49	0.16	22.69	3.24	0.14	0.15	2.03	8.99	5.95	0.28	100.12
S-6	56.01	0.17	21.49	3.73	0.14	0.10	2.02	10.38	5.96	0.27	100.27
SB-1	61.31	0.13	19.90	2.74	0.04	0.00	1.10	9.35	5.88	0.24	100.69

10.2.1 Sieving and Washing

The material was sieved on the vibrating sieve vibrator, through sieves ranging from + 100 mesh to + 200 mesh, and then material was washed and decanted. Maximum care was taken to avoid any loss except for the very fine

powder or the dust (slime), weight of the material given in Table 10.5. All fractions were dried over night in the oven at 105°C, and re weighed to estimate the percent recovery, given in Table 10.4.

Table 10.4

% recovery of different samples after sieving and washing

Mesh BSS	LP-1	% Rec	LP-2	% Rec	MK-1	% Rec	S-1	% Rec	S-6	% Rec	SB-1	% Rec
- 30 + 100	1975	94.95	2040	95.15	1554	60.28	1480	89.7	2010	95.7	870	86.48
- 100 + 170	303	73	540	81.82	400	87.15	470	67.14	288	70.59	126	74.12
- 170 + 200	81	47.93	60	43.17	160	64.52	156	55.71	120	75	90	77.59

10.3 Sizing Analysis

In view of the industrial size requirements each sample was divided into the following fractions; the first one was achieved in Leicester, while the second one in Pakistan.

- 1) 2 mm BSS
- 2) 1 mm BSS
- 3) 500 μ BSS
- 4) 250 μ BSS
- 5) 125 μ BSS
- 6) 63 μ BSS

Table 10.5

Starting weight of different samples before processing

	LP-1	LP-2	MK-1	S-1	S-6	SB-1
Starting Wt in grams	3164	3753	5262	3580	3159	1676
- 30 +100 mesh	2080	2144	2578	1650	2096	1006
- 100 +170 mesh	415	660	459	700	408	170
- 170 +200 mesh	169	139	248	280	160	116
- 200 mesh	500	810	1977	950	495	384

The second size range was as below;

- | | | |
|----|-------------|----------|
| 1) | - 30 | mesh BSS |
| 2) | - 30 + 100 | mesh BSS |
| 3) | - 100 + 170 | mesh BSS |
| 4) | - 170 + 200 | mesh BSS |

10.4 Magnetic Separators

In addition to the highly magnetic minerals, a number of weakly magnetic mafics were required to be separated from the non-magnetics. Effective separation of such magnetic materials required field intensities beyond 20,000 gauss, so an exceptionally high intensity magnetic separator was needed. The one used in Leicester was of the following description:

Make	Davies magnetic Works.
Model	45V.
Origin	UK.
Type	Roller Disc.
Field Intensity Level	variable up to 14000 gauss at 5 Amps.

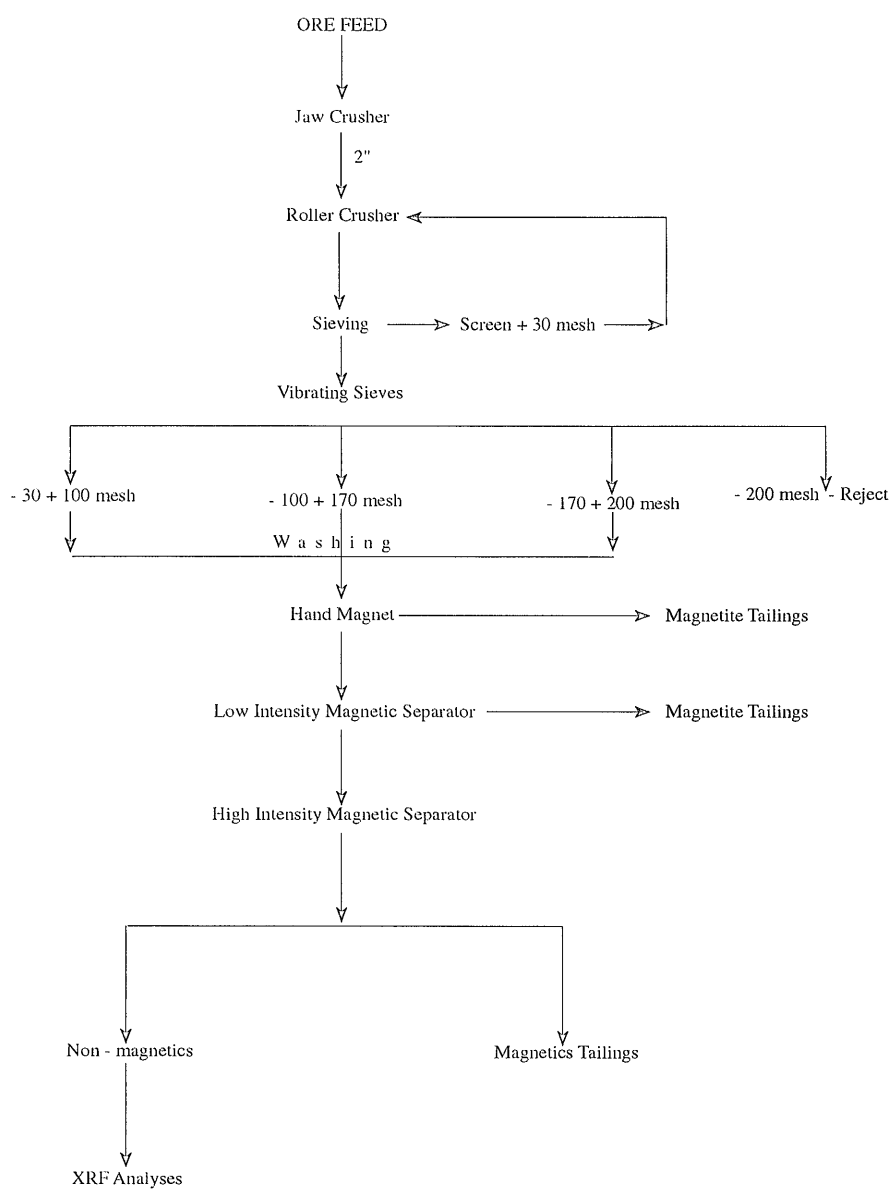
The feed speed is very slow if effective separation is to be achieved, rerunning is usually required.

The first separation used in Pakistan had the following description;

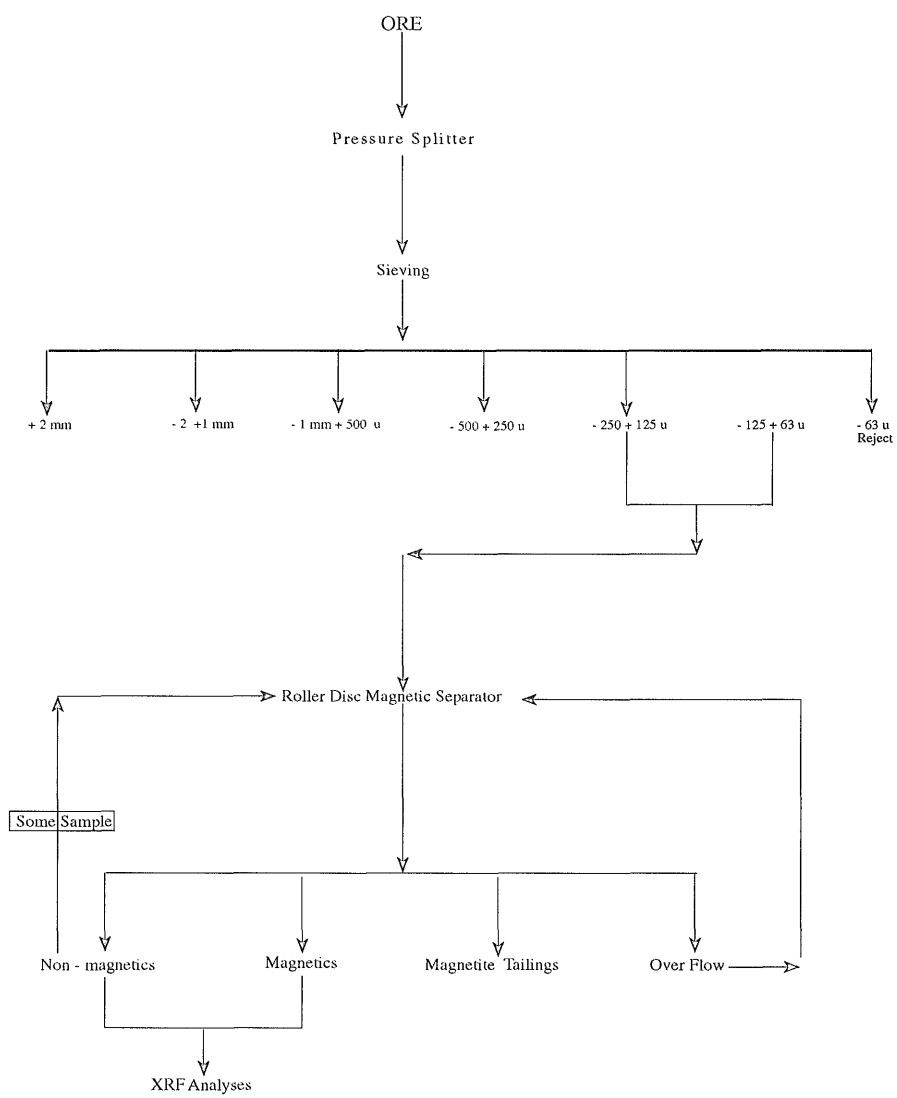
Make	General Electric Company.
Model	W1 Type 1 pH.
Origin	UK
Type	Induced.
Field Intensity Level	4.17 out put current 50 cycles at 5 amp.

Also used in Pakistan was a CARPCO high intensity Model.

Make	Hesearoh & Engineering Inc.
Origin	Florida U S A.



Flowsheet for the Magnetic Separation carried out in Pakistan



Flowsheet for the Magnetic Separation carried out in Leicester

10.5 Liberation Behaviour and Magnetic Separation Results

10.5.1 General

Crushed samples were observed by hand lens and in some cases under the stereoscopic microscope before and after the processing. Before passing through the magnetic separation, tramp iron was removed from the material using a horse shoe hand magnet.

At first only the following fractions were processed, using the Leicester equipment.

- 1 mm + 500 μ
- 500 + 250 μ
- 250 + 125 μ
- 125 + 63 μ

The percentage of non-magnetic and magnetic material thus recovered from magnetic separation of different size fractions is given in Table 10.6.

Table 10.6

% recovery of non-magnetics and magnetics of samples at different size fractions.

63 μ	K-2	K-3	K-4	K-5	K-6	K-8	K-9
% Rec. Non-magnetics	88.37	81.54	78.62	83.65	92.47	85.69	82.34
% Rec. Magnetics	7.88	18.46	21.26	16.21	6.30	13.32	17.66
125 μ							
% Rec. Non-magnetics	72.89	68.92	76.34	77.37	80.31	75.49	78.52
% Rec. Magnetics	23.96	31.02	23.56	21.93	17.90	22.56	20.26

The processed material, non-magnetics and magnetic fractions were analysed to estimate the success of magnetic separation. The results are given in Table 10.7 and 10.8 respectively. Some of the magnetic fractions have low total, nevertheless they give an idea of iron contents.

In the second phase, in Pakistan, the material was passed through the high intensity belt magnetic separator twice at 3 amperes. The results were not very

satisfactory as the magnetic disc could not be lowered closer than 2 cm from the belt. Further processing was done on the induced magnetic separator at an intensity of 2 amperes thrice which gave satisfactory results. The snag was that it took very long (approximately 45 to 50 minutes) to process even a small fraction of the material.

Table 10.7

Analyses of non-magnetic fraction.

Sample No.	K-2		K-3		K-4		K-5		K-6		K-8		K-9	
	63	125	63	125	63	125	63	125	63	125	63	125	63	125
SiO ₂	60.97	57.15	60.06	62.69	62.66	62.14	61.13	63.25	60.55	60.73	59.75	59.64	59.35	60.01
TiO ₂	0.02	0.01	0.33	0.08	0.04	0.08	0.26	0.06	0.05	0.03	0.18	0.09	0.03	0.01
Al ₂ O ₃	23.61	26.04	22.36	21.63	22.79	22.28	22.23	21.46	24.42	24.79	25.14	25.21	25.82	25.02
Fe ₂ O ₃	0.32	0.24	0.78	0.35	0.25	0.29	0.39	0.32	0.55	0.41	0.56	0.29	0.64	0.40
MnO	0.03	0.04	0.03	0.00	0.00	0.00	0.01	0.00	0.04	0.02	0.02	0.00	0.06	0.04
MgO	0.00	0.00	0.00	0.00	0.00	0.00	0.00	0.00	0.01	0.00	0.00	0.00	0.00	0.00
CaO	0.95	1.65	1.37	0.52	0.49	0.81	1.38	0.59	1.62	1.01	0.49	0.26	1.07	0.90
Na ₂ O	9.41	10.32	7.68	6.97	8.25	7.81	7.18	6.42	9.88	9.95	8.46	7.7	9.46	9.07
K ₂ O	3.4	3.97	5.46	6.21	5.4	5.80	6.22	7.07	1.93	2.14	5.38	6.77	3.90	4.32
P ₂ O ₅	0.03	0.03	0.08	0.04	0.04	0.08	0.09	0.02	0.02	0.02	0.04	0.02	0.02	0.02
Total	98.74	99.45	98.15	98.49	99.92	98.66	98.89	99.19	99.07	99.10	100.02	99.98	100.35	100.21

So only one fraction (-170, +200 mesh) of all the samples was processed. The purified material was analysed to see the iron contents, which are given in Table 10.9.

Size fractions > 63 μ , > 125 μ of K-2 and - 170 + 200 mesh of MK-1 samples were run for a second and third time. K-2 gave a very satisfactory results but MK-1 did not show any change in the third run as shown in Table 10.10 and Figs. 10.4, 10.5 and 10.6.

10.5.2 Grain-size and Mode of locking

10.5.2.1 Coarser Crystal Locking

Magnetite and amphiboles showed complex crystal inter growths in most of the samples. The liberation of these grains from nephelines and feldspars was observed to be poor in size fractions coarser than 30 mesh. It improved gradually for the smaller fractions. In fine textured samples, the liberation was however approximately 85 % to 90 % in sample S-1 and reduced down to 80% in MK-1.

Table 10.8

Analyses of magnetic fraction.

Sample No.	K-2		K-3		K-4		K-5		K-6		K-8		K-9	
	63	125	63	125	63	125	63	125	63	125	63	125	63	125
SiO ₂	54.38	59.41	40.81	46.19	40.01	46.52	41.50	45.52	43.92	46.36	49.53	53.63	37.81	43.46
TiO ₂	0.51	0.38	2.94	3.60	1.08	3.16	3.59	3.48	1.45	1.03	1.26	0.91	1.2	1.04
Al ₂ O ₃	17.45	18.10	12.77	15.80	18.76	13.85	13.07	14.34	15.31	16.23	12.83	15.99	19.65	19.80
Fe ₂ O ₃	10.54	7.40	23.27	9.58	25.11	15.15	22.59	22.75	25.23	23.72	17.96	12.37	23.96	20.07
MnO	0.50	0.38	1.20	0.47	1.74	0.69	1.22	0.58	1.91	1.33	1.01	0.68	1.70	1.42
MgO	0.24	0.17	1.38	0.56	0.64	1.33	1.89	0.93	1.16	0.70	1.21	0.82	0.67	0.73
CaO	0.34	0.34	2.13	3.18	2.33	5.14	2.94	2.29	0.83	0.80	5.13	3.22	2.08	1.17
Na ₂ O	4.17	4.55	3.82	5.74	1.75	4.47	2.95	4.52	4.92	6.15	4.41	6.44	2.33	3.51
K ₂ O	7.62	8.01	5.80	4.97	7.65	4.96	6.43	5.87	4.78	3.76	5.92	6.83	9.21	8.73
P ₂ O ₅	0.2	0.02	0.03	0.06	0.03	0.10	0.06	0.09	0.02	0.02	0.03	0.03	0.02	0.01
Total	95.77	98.75	94.15	90.15	99.10	95.37	97.46	100.3	99.52	100.1	99.29	100.9	98.64	99.93

10.5.2.2 Finer Crystal Locking

Fine crystals measuring from 0.05 to about 0.5 mm showed a severe problem for liberation. The worst minerals noted were magnetite and the amphiboles. Biotite crystals were usually well liberated due to their prominent

cleavage, even where the size of the crystals was less than 0.5 mm. It was observed that micas were mostly shattered off the non-magnetics during crushing.

Table 10.9

Analyses of non-magnetic material after processing on the belt magnetic separation.

	SiO ₂	TiO ₂	Al ₂ O ₃	Fe ₂ O ₃	MnO	MgO	CaO	Na ₂ O	K ₂ O	P ₂ O ₅	Total
LP-1	62.11	0.18	21.05	0.21	0.03	0.00	1.89	9.61	5.65	0.03	100.76
LP-2	60.83	0.18	21.75	0.22	0.02	0.00	2.06	8.87	5.94	0.25	100.12
MK-1	58.57	0.04	23.17	0.60	0.05	0.00	1.66	9.82	5.22	0.10	99.22
S-1	60.66	0.09	23.79	0.17	0.01	0.00	0.53	9.91	5.21	0.11	100.47
S-6	58.05	0.05	22.67	0.21	0.02	0.00	2.84	11.11	5.07	0.80	100.82
SB-1	62.32	0.02	20.79	0.14	0.01	0.00	1.58	10.58	4.49	0.33	100.26

Table 10.10

Analysis follows repeated runs on the magnetic belt separator.

	SiO ₂	TiO ₂	Al ₂ O ₃	Fe ₂ O ₃	MnO	MgO	CaO	Na ₂ O	K ₂ O	P ₂ O ₅	Total
63 μ											
K-2 1st. Run	60.97	0.02	23.61	0.32	0.03	0.00	0.95	9.41	3.40	0.03	98.74
K-2 2nd. Run	61.39	0.02	23.60	0.26	0.03	0.00	0.93	9.93	3.14	0.03	99.33
K-2 3rd. Run	61.81	0.02	21.65	0.13	0.09	0.00	0.99	11.24	3.03	0.02	98.98
125 μ											
K-2 1st. Run	57.15	0.01	26.04	0.24	0.04	0.00	1.65	10.32	3.97	0.03	99.65
K-2 2nd. Run	57.21	0.02	25.33	0.21	0.04	0.00	1.67	10.95	3.81	0.03	99.27
K-2 3rd. Run	57.18	0.02	23.46	0.12	0.08	0.00	1.75	12.27	3.60	0.01	98.49
-170 +200 mesh											
MK-1 1st Run	58.57	0.04	23.17	0.60	0.05	0.00	1.66	9.82	5.22	0.10	99.22
MK-1 2nd. Run	59.09	0.02	23.39	0.20	0.02	0.00	1.78	10.74	4.47	0.13	99.84
MK-1 3rd Run	58.64	0.02	23.36	0.20	0.03	0.00	1.76	12.39	4.47	0.12	100.99

However, in some samples magnetite locking with non-magnetics was found to be persistent in all +100 mesh samples. So the percentage weight of non-magnetic material was reduced drastically. On the other hand samples having a smaller percentage of magnetite but more amphiboles and biotites gave higher weight recoveries. Samples having feldspar and nepheline crystals measuring at least a few mm irrespective of the grain size of mafics normally gave much better liberation. On the other hand, fine textured samples containing higher percentage weight of mafics showed poor liberation in all + 100 mesh fractions.

10.6 Inclusions and Disseminations

In some samples crystals less than 0.02 mm were noted to be disseminated into coarser nepheline and feldspar crystals. Such textural varieties were found to be extremely undesirable. Because of the lesser percentage of mafic inclusions contained in larger non-magnetics, the grains invariably tend to go with larger clean non-magnetics. So it contributed to the higher percentage of Fe_2O_3 retained in the final non-magnetics. At lower vibration and higher magnet currents, non-magnetic crystals with magnetite inclusions were relatively easier to remove as compared to same size non-magnetic crystal containing fine inclusions of amphiboles and pyroxenes. On the whole it is concluded that mafic crystals or fine disseminations are a severe problem as far as liberation at + 100 mesh size range is concerned.

10.7 Results

The dry magnetic separation done on various sample fractions gave variable results. The comparison of original SiO_2 , Al_2O_3 , Fe_2O_3 , Na_2O , K_2O and total alkalis ($\text{Na}_2\text{O} + \text{K}_2\text{O}$) with the processed material is shown in the accompanying charts (Fig. 10.1 to Fig. 10.6).

The size fractions $> 63 \mu$, $> 125 \mu$ of K-2 and - 170 + 200 mesh of MK-1 samples were run through the magnetic separator three times to test the improvement of processing.

	SiO ₂ O	SiO ₂ P
K-2	58.95	60.97
K-3	59.91	60.06
K-4	60.65	62.66
K-5	57.1	61.13
K-6	57.07	60.55
K-8	59.03	59.75
K-9	57.13	59.35

	Al ₂ O ₃ O	Al ₂ O ₃ P
K-2	21.98	23.61
K-3	19.47	22.36
K-4	18.81	22.79
K-5	21.78	22.23
K-6	22.33	24.42
K-8	22.55	25.14
K-9	23.07	25.82

	Fe ₂ O ₃ O	Fe ₂ O ₃ P
K-2	2.41	0.32
K-3	3.14	0.78
K-4	3.47	0.25
K-5	4.5	0.39
K-6	3.12	0.55
K-8	1.71	0.56
K-9	2.9	0.64

	Na ₂ O O	Na ₂ O P
K-2	11.5	9.41
K-3	7.59	7.68
K-4	7.08	8.25
K-5	12.09	7.18
K-6	11.26	9.88
K-8	9.6	8.46
K-9	10.12	9.46

	K ₂ O O	K ₂ O P
K-2	4.19	3.4
K-3	6.03	5.46
K-4	6.06	5.4
K-5	2.78	6.22
K-6	2.8	1.93
K-8	5.79	5.38
K-9	5.08	3.9

	Na ₂ O+K ₂ O O	Na ₂ O+K ₂ O P
K-2	15.69	12.81
K-3	13.62	13.14
K-4	13.14	13.65
K-5	14.87	13.4
K-6	14.06	11.81
K-8	15.39	13.84
K-9	15.2	13.36

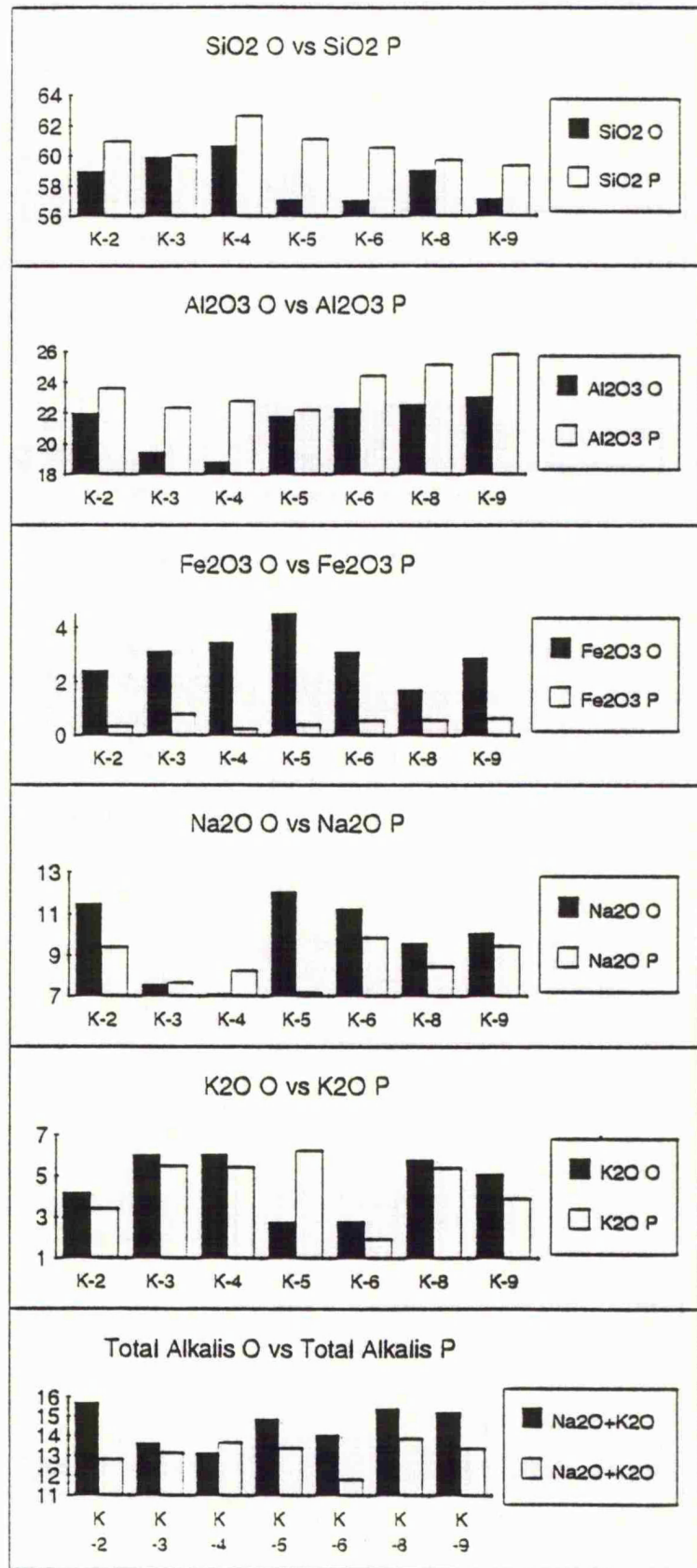


Fig. 10.1 The change in the original (O) contents of SiO₂, Al₂O₃, Fe₂O₃, Na₂O, K₂O and total alkalis are compared with the processed (P) ones in different samples of > 63 μ size fraction.

	SiO ₂ O	SiO ₂ P
K-2	58.95	57.15
K-3	59.91	62.69
K-4	60.65	62.14
K-5	57.1	63.25
K-6	57.07	60.73
K-8	59.03	59.64
K-9	57.13	60.01
	Al ₂ O ₃ O	Al ₂ O ₃ P
K-2	21.98	26.04
K-3	19.47	21.63
K-4	18.81	22.28
K-5	21.78	21.46
K-6	22.33	24.79
K-8	22.55	25.21
K-9	23.07	25.02
	Fe ₂ O ₃ O	Fe ₂ O ₃ P
K-2	2.41	0.24
K-3	3.14	0.35
K-4	3.47	0.29
K-5	4.5	0.32
K-6	3.12	0.41
K-8	1.71	0.29
K-9	2.9	0.4
	Na ₂ O O	Na ₂ O P
K-2	11.5	10.32
K-3	7.59	6.97
K-4	7.08	7.18
K-5	12.09	6.24
K-6	11.26	9.95
K-8	9.6	7.7
K-9	10.12	9.07
	K ₂ O O	K ₂ O P
K-2	4.19	3.97
K-3	6.03	6.21
K-4	6.06	5.8
K-5	2.78	7.07
K-6	2.8	2.14
K-8	5.79	6.77
K-9	5.08	4.32
	Na ₂ O+K ₂ O	Na ₂ O+K ₂ O
K-2	15.69	14.29
K-3	13.62	13.18
K-4	13.14	12.98
K-5	14.87	13.31
K-6	14.06	12.09
K-8	15.39	14.47
K-9	15.2	13.39

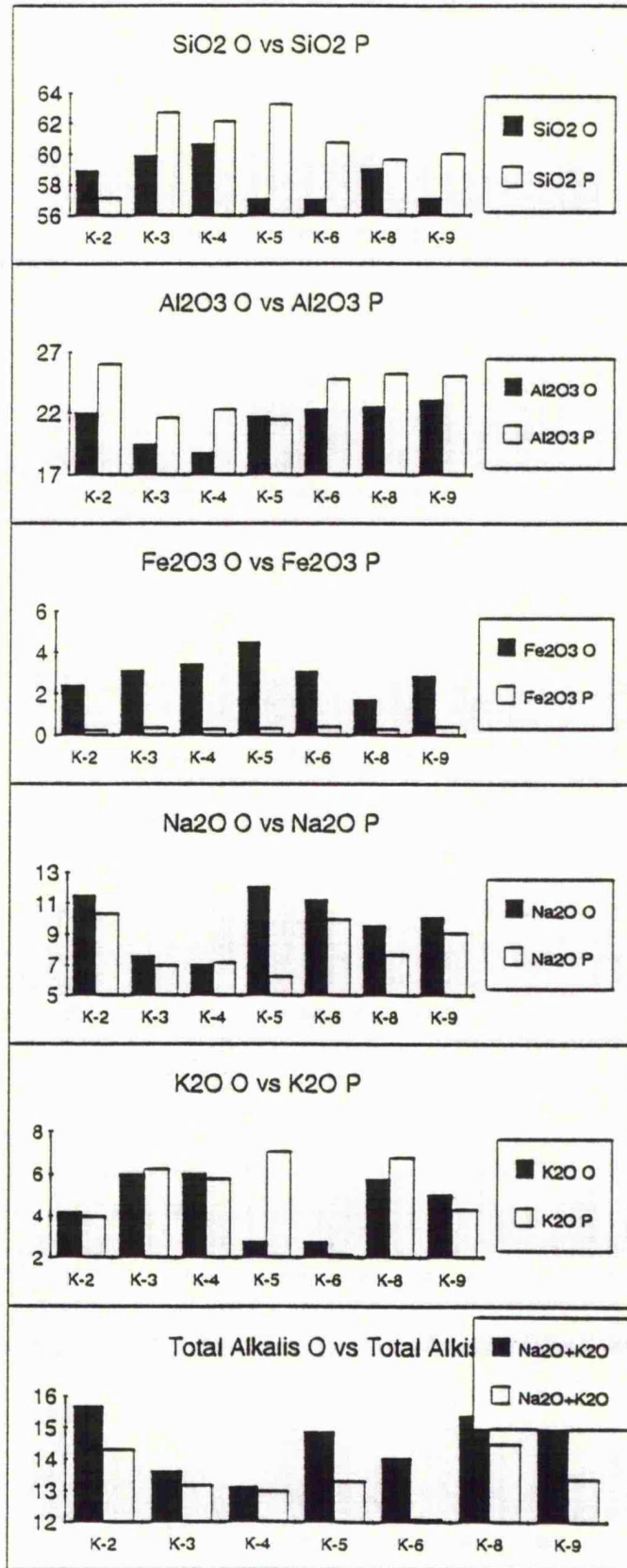


Fig. 10.2 The change in the original (O) contents of SiO₂, Al₂O₃, Fe₂O₃, Na₂O, K₂O and total alkalis are compared with the processed (P) ones in different samples of > 125 μ size fraction.

	SiO ₂ O	SiO ₂ P
LP1	61.03	62.11
LP2	60.56	60.83
MK1	59.83	58.57
SB1	61.31	62.32
SP1	56.49	60.66
SP6	56.01	58.05

	Al ₂ O ₃ O	Al ₂ O ₃ P
LP1	20.01	21.05
LP2	19.72	21.75
MK1	21.52	23.17
SB1	20.02	20.79
SP1	22.69	23.79
SP6	21.49	22.67

	Fe ₂ O ₃ O	Fe ₂ O ₃ P
LP1	2.07	0.21
LP2	2.04	0.22
MK1	2.37	0.6
SB1	2.97	0.14
SP1	3.24	0.17
SP6	3.73	0.21

	Na ₂ O O	Na ₂ O P
LP1	7.81	9.61
LP2	9.01	8.87
MK1	8.89	9.82
SB1	9.35	10.58
SP1	8.99	9.91
SP6	10.38	11.11

	K ₂ O O	K ₂ O P
LP1	6.7	5.65
LP2	6.7	5.94
MK1	6.59	5.22
SB1	5.88	4.49
SP1	5.95	5.21
SP6	5.96	5.07

	Na ₂ O+K ₂ O O	Na ₂ O+K ₂ O P
LP1	14.51	15.26
LP2	15.71	14.81
MK1	15.48	15.036
SB1	15.23	15.07
SP1	14.94	15.115
SP6	16.34	16.18

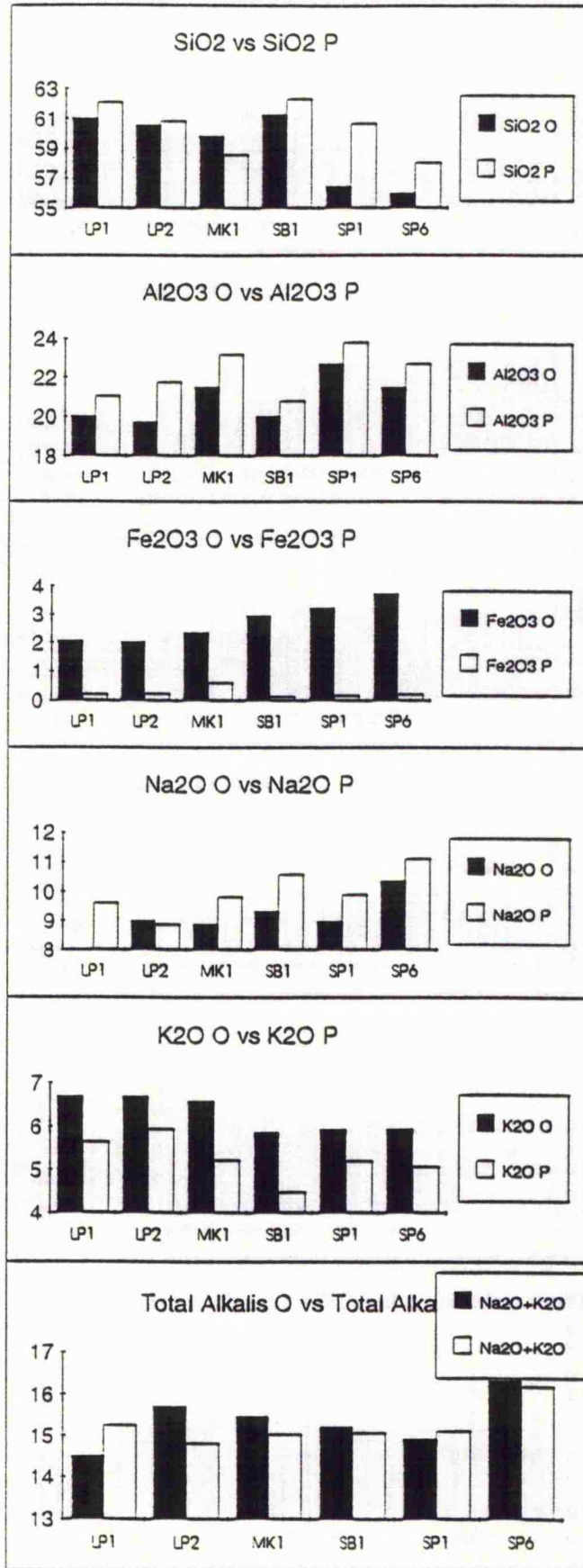


Fig. 10.3 The comparison of the original (O) contents of SiO₂, Al₂O₃, Fe₂O₃, Na₂O, K₂O and total alkalis are compared with the processed (P) ones in different samples of - 170 + 200 mesh size fraction.

K-2			
SiO ₂ O	SiO ₂ R1	SiO ₂ R2	SiO ₂ R3
58.95	60.97	61.39	61.81

K-2			
Al ₂ O ₃ O	Al ₂ O ₃ R1	Al ₂ O ₃ R2	Al ₂ O ₃ R3
21.98	23.61	23.6	21.65

K-2			
Fe ₂ O ₃ O	Fe ₂ O ₃ R1	Fe ₂ O ₃ R2	Fe ₂ O ₃ R3
2.41	0.32	0.26	0.13

K-2			
Na ₂ O O	Na ₂ O R1	Na ₂ O R2	Na ₂ O R3
11.5	9.41	9.93	11.24

K-2			
K ₂ O O	K ₂ O R1	K ₂ O R2	K ₂ O R3
4.19	3.4	3.14	3.03

K-2			
Tot. Al. O	Tot. Al. R1	Tot. Al. R2	Tot. Al. R3
15.69	12.81	13.07	14.27

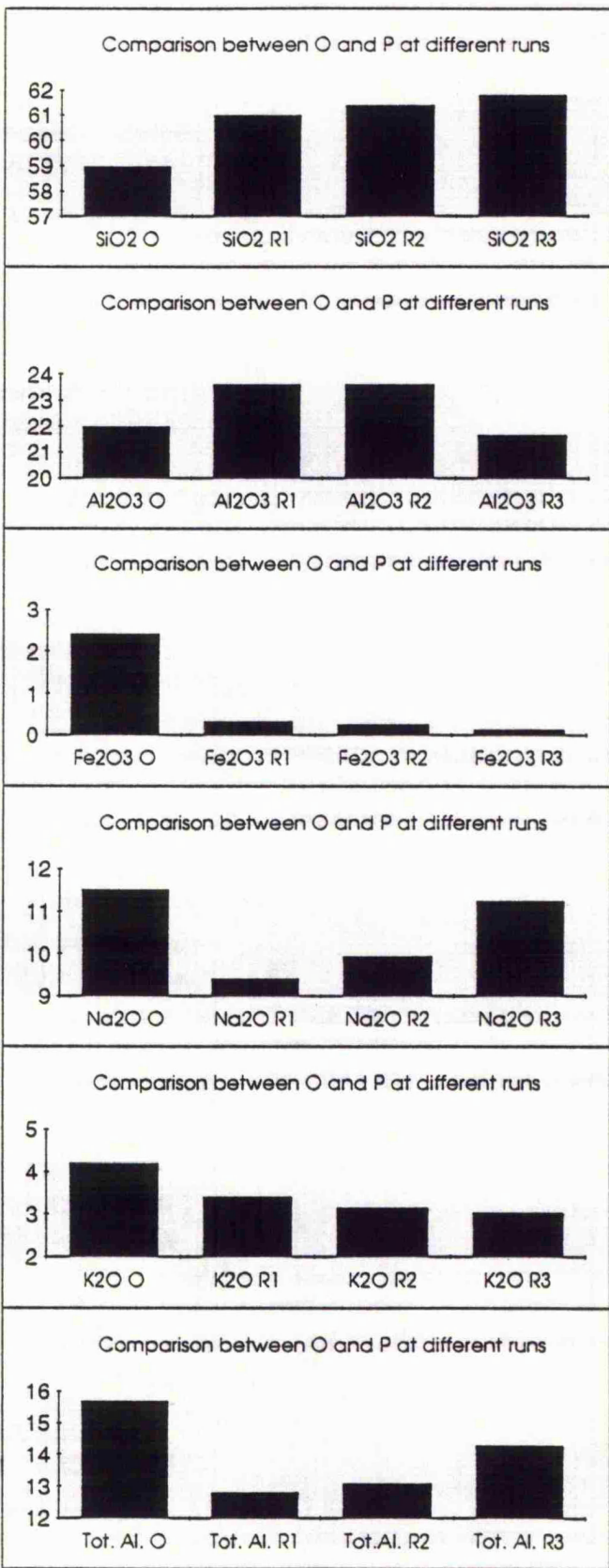


Fig. 10.4 The comparison of the original (O) contents of SiO₂, Al₂O₃, Fe₂O₃, Na₂O, K₂O and total alkalis (Tot. Al.) with the processed (P) ones in different samples of size fraction > 63 μ at different runs, 1st, 2nd and 3rd (R1, R2 and R3).

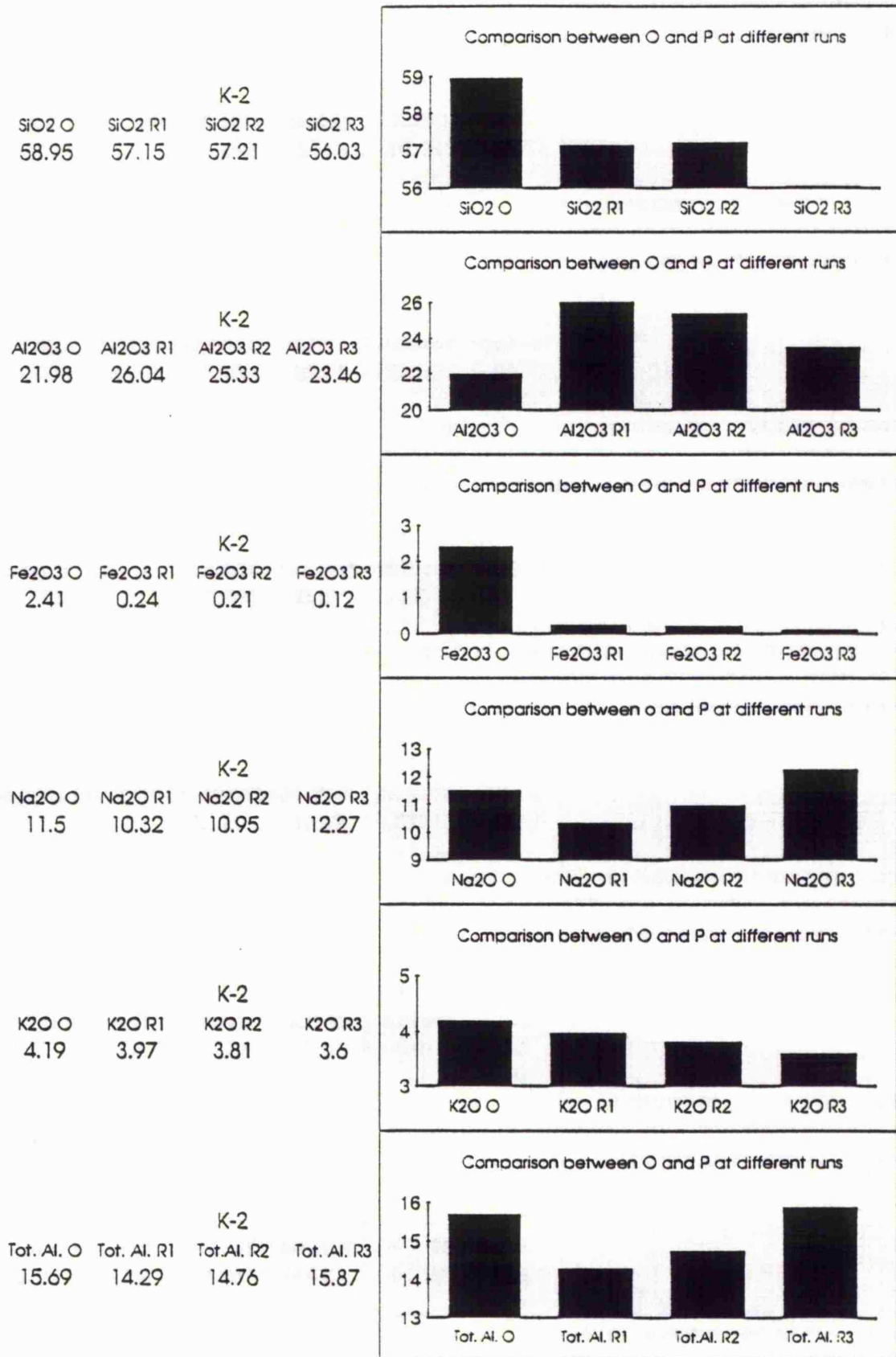
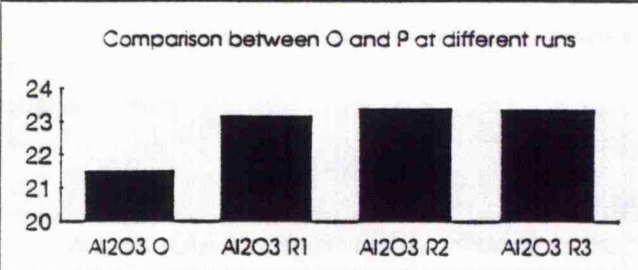


Fig. 10.5 The comparison of the original (O) contents of SiO₂, Al₂O₃, Fe₂O₃, Na₂O, K₂O and total alkalis (Tot. Al.) with the processed (P) ones in different samples of size fraction > 125 μ at different runs, 1st, 2nd and 3rd (R1, R2 and R3).

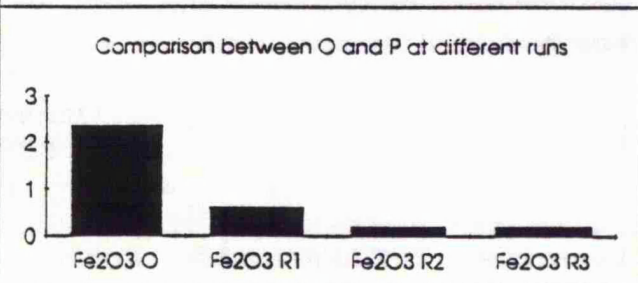
MK-1			
SiO ₂ O	SiO ₂ R1	SiO ₂ R2	SiO ₂ R3
59.83	58.57	59.09	58.64



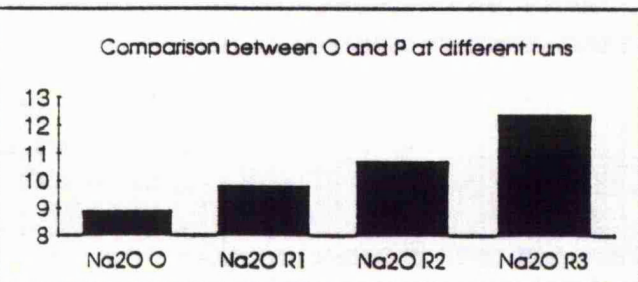
MK-1			
Al ₂ O ₃ O	Al ₂ O ₃ R1	Al ₂ O ₃ R2	Al ₂ O ₃ R3
21.52	23.17	23.39	23.36



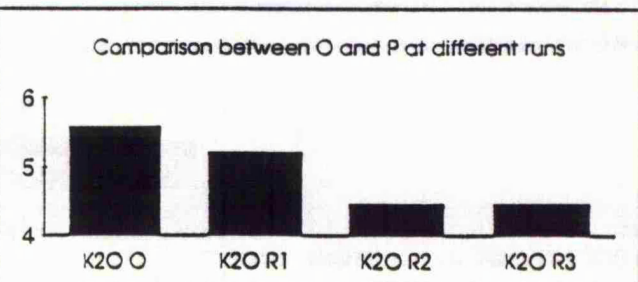
MK-1			
Fe ₂ O ₃ O	Fe ₂ O ₃ R1	Fe ₂ O ₃ R2	Fe ₂ O ₃ R3
2.37	0.6	0.2	0.2



MK-1			
Na ₂ O O	Na ₂ O R1	Na ₂ O R2	Na ₂ O R3
8.89	9.82	10.74	12.39



MK-1			
K ₂ O O	K ₂ O R1	K ₂ O R2	K ₂ O R3
5.59	5.22	4.47	4.47



MK-1			
Tot. Al. O	Tot. Al. R1	Tot. Al. R2	Tot. Al. R3
15.48	15.04	15.21	16.86

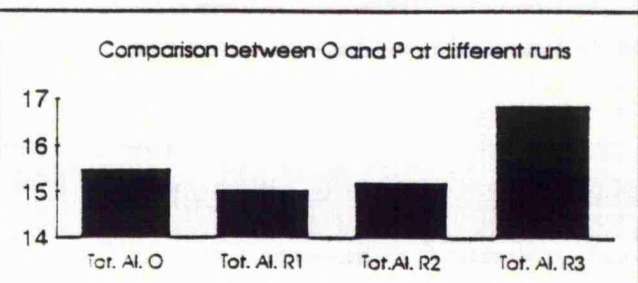


Fig. 10.6 The comparison of the original (O) contents of SiO₂, Al₂O₃, Fe₂O₃, Na₂O, K₂O and total alkalis (Tot. Al.) with the processed (P) ones in different samples of size fraction - 170 + 200 mesh at different runs, 1st, 2nd and 3rd (R1, R2 and R3).

In the 63 μ fraction, it was observed that there is a gradual increase in SiO_2 and an initial increase then decrease in Al_2O_3 . The Na_2O and total alkalis contents at first decreased and then increased gradually but remained lower than the original material. There were systematic decreases in Fe_2O_3 and K_2O . Fe_2O_3 was successfully reduced by 94.41 %.

In > 125 μ size fraction of sample K-2 SiO_2 , Fe_2O_3 and K_2O decreased gradually, except for Fe_2O_3 which decreased dramatically in the first run and overall there was 95 % removal. Na_2O and total alkalis decreased in the first run then became higher than the starting material. There was an increase in Al_2O_3 after the first run, then it decreased and remained higher than the original material.

In - 170 + 200 mesh size fraction of sample MK-1, there is an increase in Na_2O and Al_2O_3 and systematic decrease in Fe_2O_3 and K_2O with the successive runs but Fe_2O_3 remained stable in the third run. Total alkalis decreased at first and finally increased by 8.92 %, whereas SiO_2 did not show a consistent trend.

It was observed that the processing is more effective in 125 μ and - 170 + 200 mesh size fraction as compared to the > 63 μ fraction in all respects.

10.8 Comparison with Industrially Processed Material

Some of the world processed typical nepheline syenite analyses are given in Tables 10.11 and 10.12 along with one of the Norsk Neflin analysed in Leicester University.

The feldspathoidal syenite processed from the project area is similar in chemical composition to the one from Indusmin and IMC as both are rich in Na_2O . However, nepheline syenite from Norsk Neflin, North Cape has potash greater than soda. In Table 10.12 the figures quoted for Na_2O and K_2O in IMC is total alkalis.

It may be possible to reduce the iron contents to < 0.1 % from the Koga feldspathoidal rocks if processed on the high intensity magnetic separator which could not be accessed during this study.

Table 10.11 Nepheline Syenite - Typical Product Specification, Glass Grades.

Product Designation Typical Chemical Analysis	Indusmin		IMC		Norsk Neflin	Norsk Neflin
	330	333	Summit,	Ridge,	North Cape,	Analysed at
	%	%	%	%	%	Leicester
SiO ₂	59.90	60.00	60.20	60.10	55.90	56.02
TiO ₂	N.D	N.D	N.D	N.D	N.D	0.06
Al ₂ O ₃	23.50	23.40	23.50	23.40	24.20	26.89
Fe ₂ O ₃	0.08	0.35	0.07	0.50	0.10	0.23
MgO	0.10	0.10	Trace	Trace	Trace	BDL
CaO	0.60	0.70	0.30	0.30	1.30	1.21
Na ₂ O	10.20	9.90	10.60	10.50	7.90	6.51
K ₂ O	5.00	4.80	5.10	4.90	9.00	9.03
P ₂ O ₅	BDL	BDL	BDL	BDL	0.10	0.06
L.O.I	0.60	0.70	0.40	0.30	1.00	
Total	99.98	99.95	100.17	100.00	99.40	100.01

Norsk Neflin, North Cape, also contains 0.3 % BaO and 0.3 % SrO

Table 10.12 Nepheline Syenite - Typical Product Specification, Ceramic Grades.

Product Designation Typical Chemical Analyses	Indusmin			IMC			Norsk Neflin
	A-200	A-270	A-400	Crest	Peak	Apex	North Cape
	%	%	%	%	%	%	%
SiO ₂	60.70	60.70	60.70	60.20	60.20	60.20	56.00
Al ₂ O ₃	23.30	23.30	23.30	23.50	23.50	23.50	24.20
Fe ₂ O ₃	0.07	0.07	0.07	0.07	0.07	0.07	0.10
MgO	0.10	0.10	0.10	Trace	Trace	Trace	Trace
CaO	0.70	0.70	0.70	0.30	0.30	0.30	1.20
Na ₂ O	9.80	9.80	9.80	15.30	15.30	15.30	7.80
K ₂ O	4.60	4.60	4.60	15.30	15.30	15.30	9.10
L.O.I	0.70	0.70	0.70	0.40	0.40	0.40	1.00

*Chapter Eleven***CONCLUSIONS AND RECOMMENDATIONS**

The study of the Koga feldspathoidal syenite was aimed to assess rocks of the complex for commercial uses.

11.1 Geology

The Koga feldspathoidal syenite complex is a part of the Ambela alkaline complex. The various rock types found in the Koga feldspathoidal syenite complex are:

- Sodalite rich foyaites
- Sodalite-Cancrinite rich foyaites
- Feldspathoidal foyaites
- Foyaitic feldspathoidal syenites
- Garnet bearing feldspathoidal syenite
- Feldspathoidal syenites
- Pulaskitic feldspathoidal syenite
- Alkali syenite

11.2 Petrographic Composition

The above mentioned rocks contain the following minerals, which have been identified by optical, X-ray and electron microprobe. Each mineral species is remarkably constant in composition throughout the complex. The different rock types contain different proportions of some or all of these minerals.

- a). Nepheline
- b). Microcline
- c). Albite
- d). Sodalite
- e). Cancrinite
- f). Pyroxene (aegirine)

- g) Biotite
- h) Sphene
- i) Garnet (melanite)
- J) Iron ore(magnetite)
- k) Amphibole

The rocks are coarse to medium grained and hypidiomorphic. There is little inter growth of the mafic minerals with the feldspar / feldspathoids. The mafics occur generally as aggregated clots. They also occasionally occur in some rocks as discrete grains (Fig. 5.4a).

The rock types identified in Miani Kandao, Naranji Kandao and Sahbaga are sodalite - cancrinite rich foyaite, foyaitic feldspathoidal syenite feldspathoidal syenite and pulaskitic feldspathoidal syenite while at Bibi Dheri, Agarai and Sura are garnet bearing feldspathoidal syenite and foyaitic feldspathoidal syenite. The alkali syenite is located near Koga village.

11.3 Chemical Composition

The chemical analyses of fifty five representative samples of the Koga feldspathoidal syenite complex were carried out to judge the initial chemistry of the deposit and were aimed to;

- a) Judge the maximum and range of iron contents within the various rock units of the complex.
- b) Evaluate the industrially important percentage of alkalis.
- d) Evaluate CaO contents.

The chemical analyses showed the variation of iron contents (Fe_2O_3), total alkalis ($\text{Na}_2\text{O} + \text{K}_2\text{O}$) and CaO in different rock units. The average and the range of Fe_2O_3 , total alkalis ($\text{Na}_2\text{O} + \text{K}_2\text{O}$) and CaO are given in Table 11.1.

Table 11.1

Average and range of Fe₂O₃, total alkalis and CaO.

Rock Type	Average % Fe ₂ O ₃	Range	Average Alkalis	Range	Average CaO	Range
Sodalite rich foyaites	3.41	3.00 - 4.5	14.74	14.04 - 16.04	0.91	0.57 - 1.93
Sodalite-cancrinite rich foyaites	3.41	2.04 - 3.43	15.69	15.20 - 16.67	0.91	0.52 - 1.04
Feldspathoidal foyaites	2.52	0.53 - 3.94	15.79	14.43 - 17.29	0.63	0.36 - 1.07
Foyaitic feldspathoidal syenites	1.88	1.68 - 2.47	15.64	15.10 - 17.08	0.76	0.33 - 1.06
Garnet feldspathoidal syenites	4.77	4.50 - 5.05	12.78	12.63 - 12.93	3.27	3.23 - 3.32
Feldspathoidal syenites	2.97	2.12 - 3.46	14.30	13.64 - 15.54	1.09	0.46 - 1.27
Pulaskitic feldspathoidal syenites	3.08	1.67 - 3.47	13.61	13.14 - 14.21	1.05	0.46 - 1.71
Alkali syenite	3.77		12.56		1.81	

11.4 Petrogenetic Indications

The geochemical and mineralogical evidence suggests a magmatic progression from Babaji soda granite → Babaji nordmarkite → alkali syenite → garnet bearing feldspathoidal syenite → pulaskitic feldspathoidal syenite → feldspathoidal syenite → foyaitic feldspathoidal syenite → feldspathoidal foyaites, miaskitic → feldspathoidal foyaites, agpaitic → sodalite - cancrinite rich foyaites and finally sodalite rich foyaites. There are indications of both phonolitic and trachytic trends.

This complex forms the much part of the Alkaline Igneous Province of Northwest Pakistan which includes carbonatites, fenites in addition to the alkali syenite, lamprophyres, syenites and granodiorites.

11.5 Magnetic Separation

Magnetic separation was done to judge the success of removal of the ferromagnesian minerals from different rock units to meet the required

commercial specifications. The samples were chosen to cover the whole Koga complex rock units under investigations.

In general taking into consideration of the whole complex, it was observed that the processing was more effective on the $> 125 \mu$ and $- 170 + 200$ mesh size fractions in all respects.

A maximum of 95 % of the Fe_2O_3 was removed by magnetic separation, leading to finally iron contents as low as 0.12 %.

Feldspathoidal syenite is a hard rock and produces large amounts of fines during crushing and pulverising processes. So care was taken to produce minimum fines as far as possible.

11.6 Mineral Processing

Commercially the minimum iron contents required in the various types of glass sands in British Standards 2975: 1988 are given below;

	Maximum content
	per cent
	Fe_2O_3
Sand for fine grade optical glassware	0.013
Sand for tableware and lead crystal glasses	0.013
Sand for general colourless glassware, including containers	0.030
Sand for clear flat glass	0.030
Sand for coloured container glasses	0.250
Sand for insulating fibres	0.300

In whitewares, the maximum acceptable iron content in nepheline syenite is 0.1% expressed as Fe_2O_3 . To achieve this nepheline syenite is beneficiated to contain not more than 0.08% Fe_2O_3 . Nepheline syenite which contains 2 or 3% Fe_2O_3 can also be used, where whiteness of the fired products is not necessary, as in structural clay products.

It is obvious from the chemical analyses after the magnetic separation that some of the purified material can not be used in optical glassware and lead crystal glasses as judged by the commercial criteria listed above. Nevertheless,

the alkali contents of most of the rock units are satisfactory, except garnet bearing feldspathoidal syenite and alkali syenite as the alkali contents are lower than 13 %. Processed rock samples having Fe₂O₃ contents > 0.14 % and < 0.25 % can be used for coloured container glasses and also for sheet glasses which is required in hot countries like Pakistan where some times the temperature is as high as 50°C, to give a tint to protect from the sun.

It can also be used in the whiteware if more processing of the material is done with a high intensity magnetic separator which could not be accessed in this study.

11.7 Resources

Total resources have been calculated as 121.05 million metric tons (ECL Report 1979) for the whole Koga feldspathoidal syenite complex. The author is of the opinion that resources may not be so great but they are enough for the production of pure material for many years to come.

According to the World mineral statistics 1986 - 1990, there are three countries, Norway, Soviet Union and Canada, which produced 305,000, 1,650,000 and 533,000 tonnes of nepheline syenite in 1990. Pakistan could well aim to produce 10,000 tonnes annually which can be used in the appropriate industries.

11.8 Mining Proposal and Location for the Quarry

The feldspathoidal syenite is compact and hard rock and yields easily to blasting. The mining can be carried out at Agarai, Landi Patao and Miani Kandao. But author is of the opinion that for the starting point it can be operated at Landi Patao because it is on the road and will be very near to the processing plant.

10,000 tpa of pure material needs 15,000 tpa of raw material (as shown by the mineral process estimates) for 20 years = 300,000 tonnes.

Density 2.7, volume = 810,000 m³.

Allowances for problems in working the pit and overburden that are for 1 x 10⁶ m³.

From the contours of the area centred at G. R. 53253490, the pit dimensions should be $200 \times 150 \times 75 = 1,125,000 \text{ m}^3$

Overburden $33,000 \text{ m}^3$

Net volume $= 1,092,000 \text{ m}^3$

11.9 RECOMMENDATIONS

- 1) Present work indicates that the feldspathoidal syenite deposit can be processed to make acceptable commercial material.
- 2) It is recommended that before starting the extractive operations further processing involving a high intensity magnetic separator should be undertaken. The reserve for the portion of the deposit to be extracted should be defined through detailed site investigations, i.e. drilling, mapping and a full economic appraisal prepared. At an early stage a pilot plant should be established to define detailed plant requirements and product quality.
- 3) A possible place for a quarry to produce 15,000 tonnes of raw material to produce 10,000 tonnes of final product is Landi Patao centred at G. R. 53253490.

It is therefore concluded that the Afghan camp No. 2 (one Km west of Koga village) is the most suitable place for the installation of a processing unit, keeping in view the environmental conditions. It is only 60 Km from the main railhead and has sufficient supply of water and electricity, which can be supplied from 11 kVA line to Daggar, 9 Km from the proposed site.

- 4) Isotopic studies are recommended for the determination of absolute age and petrogenesis of the Koga feldspathoidal syenite complex.

Appendix 5.1: Samples Numbers and Grid References

A number of samples collected from the study area are given in Table A 5.1 along with the weathered samples.

Table A 5.1 Sample Numbers and Grid References

Sample No	Grid Reference	Sample No.	Grid Reference
MK-1	52803320	SB-1	53003600
MK-2	52753327	SB-2	53053612
MK-3	52703326	SB-3	53303590
MK-4	53103490	SB-4	53703596
MK-5	53003460	SB-5	53813580
MK-6	53903570	SB-6	53803581
MK-7	53903580	SB-7	53823580
MK-8	54103570	SB-9	53823583
MK-9	53903580	SB-10	53213550
MK-10	53803580	SB-11	53203551
MK-11	53803570	SB-12	53203550
MK-13	53503540	SB-13	52703435
MK-14	53303540	SB-14	53413561
MK-15	53193531	SB-15	53303571
MK-16	53003520	SB-16	53613550
MK-17	53153510	SB-17	53613551
MK-18	52953495	K-1	52813795
MK-19	52803460	K-2	53013598
MK-20	52573347	K-3	53813590
MK-21	52303340	K-4	54213589
MK-22	52213341	K-5	53233549
MK-24	55603758	K-6	52173349
MK-25	55703750	K-8	55913651
S-1	56383760	K-9	52813317
S-2	56383760	BD-1	54253820
S-3	56403770	BD-2	54153830
S-4	56403770	BD-3	54203828
S-5	56403744	BD-4	54283826
S-6	56403744	SP-1	56383762
LP-2	53203541	Bw-1	53003520
BW-2	53003520	BW-3	53003520
BW-4	53003520	BW-5	53003520
BW-6	53183820	BW-7	56383760

Appendix 6.1: Details of the Method used for Microprobe Analyses

The analyses were carried out by Jeol Superprobe JXA-8600 with an online computer for ZAF correction. Quantitative analyses were done using wavelength dispersive system using the following operating conditions: accessory voltage, 15 Kv; Probe current, 3×10^{-8} A (30 nA); 20 (2 x 10) seconds peak, 10 (2 x 5) seconds negative background and 10 (2 x 5) seconds positive background counting time. The diameter of the defocused beam was 10 μm .

All the silicate phase were analysed for common major and minor oxides i.e. SiO_2 , Al_2O_3 , total iron represented as FeO, MnO, MgO, CaO, Na_2O and K_2O along with Cr_2O_3 and NiO. In some feldspars BaO and SrO were also analysed.

The following standards were used for the microprobe analyses: Wollastonite (natural for Si and Ca); rutile (natural for Ti); Jadeite (natural for Al and Na); magnetite (natural for Fe); rhodonite (natural for Mn); MgO (synthetic for Mg); microcline (natural for K); Cr (synthetic for Cr).

The minimum detection limits are given in Table A6.1:

Table A6.1 Minimum detection limits (MDL) Wt. % (3 sigma)

Oxides	Orthoclase	Aegirine	Magnetite	Albite	Nepheline
	MDL	MDL	MDL	MDL	MDL
SiO_2	0.02	0.02	0.03	0.02	0.02
TiO_2	0.05	0.05	0.06	0.04	0.04
Al_2O_3	0.02	0.02	0.02	0.02	0.02
Cr_2O_3	0.04	0.04	0.06	0.04	0.05
FeO	0.05	0.05	0.05	0.04	0.04
MnO	0.04	0.05	0.06	0.05	0.05
MgO	0.02	0.02	0.02	0.02	0.02
CaO	0.03	0.03	0.03	0.03	0.02
Na_2O	0.02	0.02	0.02	0.02	0.02
K_2O	0.02	0.02	0.02	0.02	0.02
NiO	0.05	0.05	0.06	0.05	0.04

Oxides	Biotite MDL	amphibole MDL	Garnet MDL	Cancrinite MDL	Sodalite MDL
SiO ₂	0.03	0.02	0.03	0.02	0.02
TiO ₂	0.04	0.05	0.06	0.04	0.04
Al ₂ O ₃	0.02	0.02	0.02	0.02	0.02
Cr ₂ O ₃	0.05	0.04	0.06	0.04	0.04
FeO	0.05	0.05	0.06	0.05	0.05
MnO	0.05	0.05	0.06	0.05	0.05
MgO	0.02	0.02	0.02	0.02	0.02
CaO	0.03	0.03	0.03	0.02	0.02
Na ₂ O	0.02	0.02	0.02	0.02	0.02
K ₂ O	0.02	0.02	0.03	0.02	0.02
NiO	0.05	0.05	0.07	0.04	0.04

These values are calculated to 3 decimal places, rounded up to 2 decimal places.

MDL calculated as 3 standard deviations of background above background, converted to equivalent wt. % oxide.

Three different analysing crystals used in the microprobe for different channels are as follows:

Si	CH1	TAP
Ti	CH2	PET
Al	CH1	TAP
Cr	CH3	LiF
Fe	CH3	LiF
Mn	CH3	LiF
Mg	CH1	TAP
Ca	CH2	PET
Na	CH1	TAP
K	CH2	PET
Ni	CH3	LiF

PET Pentaerythritol
TAP Thallium acid phthalate
LiF Lithium fluoride.

Appendix 7.1: Geochemical Data Acquisition

This appendix refers to the sampling, analytical techniques used to obtain geochemical data during this project. Complete data sets are presented in the tables in the relevant sections.

Rock Powder Preparation

All analysed samples were cleaned, crushed and powdered in the following way. Weathered surfaces were removed by hammer, large samples were split using a hydraulic press before crushing to <1mm using a hardened steel fly-press.

Approximately 50g of sample was powdered in a Podmore agate tema for 15 minutes. This powder was stored in sealed plastic bags. A minimum volume of 1000x the maximum grain size of the original sample was crushed under the fly press.

X-Ray Fluorescence

Major Element Analysis

Approximately equal amount of each powdered sample was dried overnight at 110°C to remove H₂O. Loss on ignition (H₂O⁺) was calculated after the sample had been placed in a muffle furnace at 950°C for 90 minutes. Platinum crucibles were used to contain the sample in the furnace.

All major elements analysed were performed on a glass disc (fusion beads). To make the bead, 1.0 g of ignited sample, dried in the oven at 110°C overnight and cooled in the dessicator was thoroughly mixed with 5.0 g of flux - a eutectic mixture of lithium metaborate and lithium tetraborate (Johnson - Mathey Spectroflux JM100B - 1988 batch and Englehard XRF fusion flux, standard grade for 1989 batch) was used. Each day a 5.0 g sample of the flux was fused to determine its loss on ignition. This loss was added to each 5.0 g of flux used in bead manufacture.

The sample and the flux was ignited in 95 % Pt / 5 % Au crucible inside a vertical tube furnace at 1100°C for 15 minutes. During this time the crucible

was removed periodically from the furnace and swirled over a Bunsen burner to eliminate gas bubbles and ensure the homogeneity of the melt. After 15 minutes the melt was cast between aluminium discs, and left between the discs for 5 - 10 minutes to ensure annealing. The cast bead was left overnight between sidanyo bricks on a hot-plate at 250°C. After labelling the finished bead was stored in a polythene bag before analysis.

Analyses were performed on a Philips PW 1400 X-ray spectrometer (1988 batch) and ARL 8420+ spectrometer (1989 batch). Totals of 98.5 - 101 % were accepted. New discs were made and analysed where totals fell outside of this range. Fusion beads were analysed for the following elements (expressed as oxides) using a rhodium anode X-ray tube:

SiO₂, TiO₂, Al₂O₃, Fe₂O₃, MnO, MgO, CaO, Na₂O, K₂O and P₂O₅.

The standards, such as AC-E, BCR-1, BOB-1, GH, JA-1, JG-3, MRG-1, PCC-1, SO-2, UB-69 and W-1 were run alternately with each batch of samples to monitor and quantify the precision and accuracy of the machine.

Trace Element Analysis

Approximately 15 gm of powdered sample was placed in a glass beaker. A small amount (15 - 20 drops) of Mowiol solution (a solution of polyvinyl alcohol in a 1:5 mix of methanol and distilled, deionised H₂O) was added to bind the powder. A powdered pellet was pressed at 15 tons per square inch on a 50 ton ram, and allowing the pellet to dry overnight. The pellet was labelled with its unique number; each storage bag was labelled with this number and the original sample number.

Samples were run on a Phillips PW 1400/10 XRF fitted with either a kW rhodium anode tube (1988 batch) or a tungsten anode tube (1989 batch) for the following elements:

Nb, Zr, Y, Sr, Rb, Th, Ga, Zn and Ni

A tungsten anode tube was also used for:

V, Cr, La, Ce, and Nd.

The lower detection limits for the major as well as trace elements are given below in Table A7.1:

Table A7.1 Lower Detection Limits for Major and Trace elements on XRF (ppm).

ARLF Lower Limits of Detection - ARL 8420+ (Fusion Beads)										
Sample	SiO ₂	TiO ₂	Al ₂ O ₃	Fe ₂ O ₃	MnO	MgO	CaO	Na ₂ O	K ₂ O	P ₂ O ₅
GA	0.01	0.002	0.005	0.002	0.002	0.011	0.003	0.016	0.002	0.002
RHT Lower Limits of Detection - PW -1400										
	Th	Nb	Zr	Y	Sr	Rb	Ga	Zn	Ni	
DR-N	1.4	0.5	0.6	0.5	0.6	0.4	1.3	0.8	1.9	
W-1	1.5	0.5	0.6	0.5	0.7	0.4	1.4	0.9	2.1	
MRG-1	1.7	0.6	0.7	0.6	0.8	0.5	1.8	1.1	2.6	
GH	1.1	0.4	0.5	0.4	0.5	0.3	0.9	0.6	1.2	
GA	1.1	0.4	0.5	0.4	0.5	0.3	1.0	0.7	1.3	
AN-G	1.3	0.5	0.5	0.4	0.6	0.3	1.2	0.7	1.5	
TRANMET Lower Limits of Detection - ARL 8420+										
	Sc	V	Cr	Co	Cu	Ba	La	Ce	Nd	
MRG-1	4.2	4.0	3.5	2.7	1.4	6.0	3.5	6.0	3.4	
NIM-G	3.6	3.2	2.0	2.0	0.8	3.1	2.6	4.3	2.4	

Accuracy

Some fusion beads were made from different samples at different time intervals to check the precision of the analyses obtained (K-2, S-5, SB-7, S-1 and SP-1) along with one international standard SY-2, shown in Table A2.2 and their comparison in Fig. A 7.1 and Fig. A 7.2.

Where (O) represents the analyses carried out with all samples, (T) represents analyses obtained at different time intervals on different fusion beads and (S) shows the analysis of International Standard published in the literature.

Table A7.2 Chemical Analyses of Major Elements Obtained at Different Time Intervals.

Sample	SiO ₂	TiO ₂	Al ₂ O ₃	Fe ₂ O ₃	MnO	MgO	CaO	Na ₂ O	K ₂ O	P ₂ O ₅	Total
K-2 O	58.95	0.11	21.98	2.41	0.10	0.00	0.94	11.50	4.19	0.01	100.19
K-2 T	59.15	0.11	21.98	2.45	0.10	0.00	0.94	11.93	4.19	0.00	100.85
S-5 O	59.11	0.20	22.06	2.06	0.13	0.05	0.86	9.76	5.49	0.02	99.74
S-5 T	59.18	0.20	22.21	2.02	0.12	0.06	0.85	9.18	5.51	0.03	99.36
SB-7 O	59.29	0.58	20.32	4.49	0.15	0.47	0.88	8.54	5.36	0.01	100.09
SB-7 T	58.35	0.58	20.02	4.64	0.16	0.35	0.87	8.25	5.86	0.01	99.09
S-1 O	57.84	0.26	22.75	2.74	0.09	0.16	1.07	9.04	5.37	0.03	99.35
S-1 T	56.49	0.16	22.69	3.24	0.14	0.15	2.03	8.99	5.95	0.28	100.12
SP-1 O	60.03	0.09	23.49	0.18	0.01	0.00	0.54	9.79	5.08	0.11	99.32
SP-1 T	60.66	0.09	23.79	0.17	0.01	0.00	0.53	9.91	5.21	0.11	100.48
SY-2 S	60.05	0.14	12.04	6.38	0.32	2.69	7.96	4.31	4.44	0.43	98.76
SY-2 O	60.60	0.14	12.14	6.33	0.24	2.68	8.16	4.24	4.57	0.43	99.53
SY-2 T	59.75	0.14	11.97	6.29	0.23	2.67	8.09	4.23	5.54	0.43	98.34

Inductively Coupled Plasma Spectrometry

The powdered samples were analysed for rare earth elements with two standards and one blank with a batch of eight. This was carried out by the Inductively Coupled Plasma Spectrometry (ICP) method. The following procedure was adopted for preparing and analysing the samples:

0.5 gm of the powdered ignited samples were weighed into a labelled 100 ml PTFE beakers. Care was taken to avoid the spray of sample on the walls of the beakers and this was done by the use of anti - stat gun. The samples were damped with few drops of distilled de ionised (dd) H₂O. 15 ml of HF (40 %) and 4 ml of HClO₄ (60 %) added to each beaker and heated on the hot plate at 180°C until no liquid remained. This was followed by the addition of 4 ml HClO₄

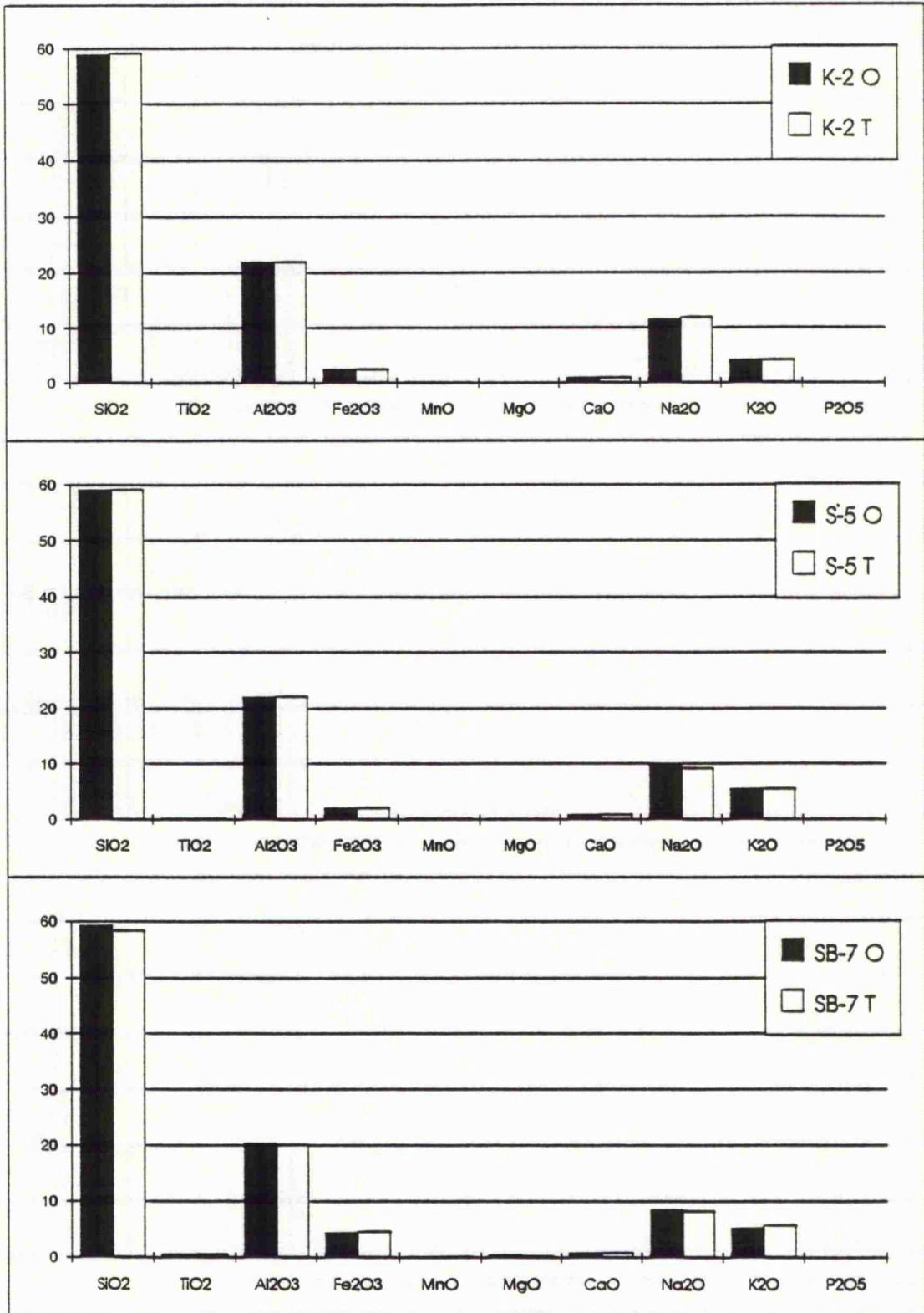


Fig. A 7.1 Comparison of different samples analysed at different time intervals, O = original sample analysed first time and T = sample analysed second time.

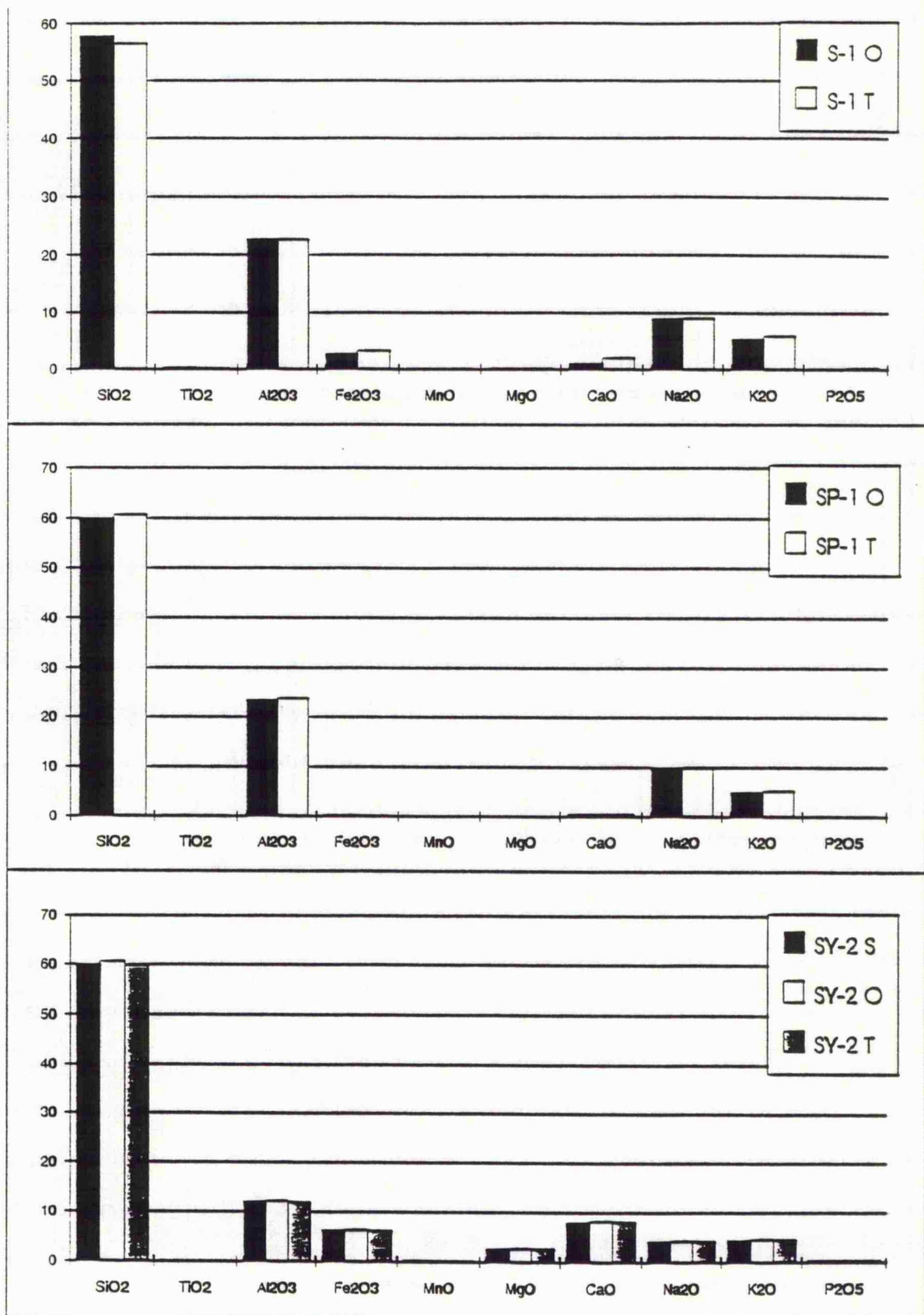


Fig. A 7.2 Comparison of different samples analysed at different time intervals. O = original sample analysed first time and T = sample analysed second time, SY = international Standard, S = published values

and a little dd H₂O and replaced the beakers on the hot plate until incipient dryness. These acids were added in a fume cupboard and all the safety regulations were observed. 25 % of HCl was added and warmed to dissolve the residue. The liquid sample was transferred to 100 ml Pyrex beaker, rinsing with dd H₂O a few times to remove all the sample and was made up to 50 ml with dd H₂O.

Samples was run through different columns with 450 ml of 1.7N HCl and collected in beakers after the addition of 600 ml of 4N HCl along with the blank and two standards. The samples were evaporated until 50 ml was left and then transferred to Pyrex beakers by rinsing the 800 ml beakers two three time. 2 ml of concentrated HNO₃ was added when 10 - 20 ml was left after evaporation. Finally evaporated to dryness and removed from the hot plate and left for cooling. Beakers were covered with cling film after cooling.

Samples were run through a Philip PV8050 spectrometer linked with a PV8490 source. The degree of precision and accuracy of the method was quantified by running one blank and two International Standards SY-2 and W-1, blank was used to correct the inter-element interference.

Powdered samples were also analysed for the Li contents. This was also done by the ICP. The digestion procedure is almost the same as for the REE determination except the samples were run through the columns.

Two International Standards SY-2 and W-1 analysed by the ICP are compared with the published values and their REE patterns are also shown in Fig. A 7.3 a and A 7.3 b.

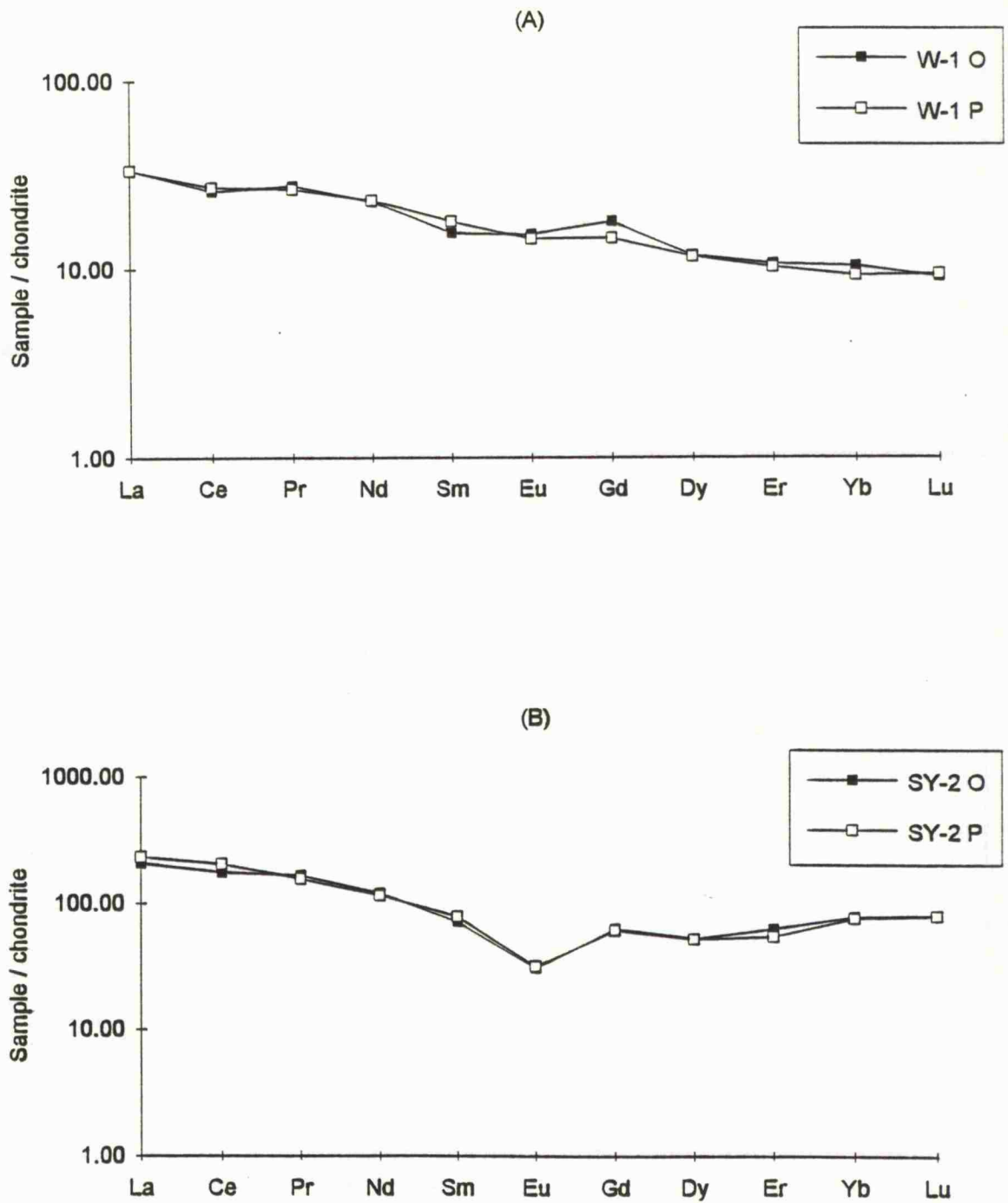


Fig. 7.3 REE patterns of (A) W-1 (O) analysed and W-1 (P) published values, (B) SY-2 (O) analysed and SY-2 (P) published values.

REFERENCES

- Ahmed, M., Ali, K. S. S., Khan, B., Shah, M. A., and Ullah, I.** (1969) The geology of the Warsak area, Peshawar, West Pakistan. *Geol. Bull. Pesh. Univ.* **4**, pp. 44 - 78.
- Ahmed, M. I.** (1951) Report on the Warsak hydro - electric project. Gov. of Pakistan.
- Ahmed, S., and Ahmed, Z.** (1974) Petrochemistry of the Ambela granites, southern Swat district, Pakistan. *Pakistan J. Sci.* **26**, pp. 63 - 69.
- Ahmed, R., and Ali, S. T.** (1977) Occurrence of phosphate in Loe Shilman carbonatite. *Geol. Surv. Pakistan Infom. Rel.* **101**, pp. 1 - 19.
- Allan, J. B., and Charsley, T. J.** (1968) Nepheline syenite and phonolite. *Nat. Env. Res. Coun. Inst. Geol. Sc. New York & London.*
- Anderson, T.** (1988) Evolution of peralkaline calcite carbonatite magma in the Fen complex, southeast Norway. *Lithos*, **22**, pp. 99 - 112.
- Anon.** (1968) Nepheline syenite 30 years rapid growth: Industrial Minerals Metal Bull. London. **7**, pp. 9 - 11.
- Anon.** (1971) Potash: A by-product of Soviet alumina from nepheline, process. Phosphorus and potassium. **53**, pp. 40 - 41.
- Appleyard, E. C.** (1974) Syn-orogenic igneous alkaliine rocks of eastern Ontario and northern Norway. *Lithos*, **7**, pp.15 - 21.
- Arculus, R. J., and Johnson, R. W.** (1981) Island arc magma source: a geochemical assessment of the role of slab - derived components and crustal contamination. *Geochem. J.* **15**, pp. 109 - 133.
- Ashraf, M., and Chaudhry, M. N.** (1976) The geochemistry and petrogenesis of albitites from Manshera and Batgram area, Hazara. *Geol. Bull. Punjab Univ.* **13**, pp. 65 - 84.
- Ashraf, M., and Chaudhry, M. N.** (1977) Note on the discovery of carbonatite from Maiakand. *Geol. Bull. Punjab Univ. No.14*, pp. 89 - 99.

References

- Azambre, B., Rossy, M., and Albarbrede, F.** (1992) Petrology of the alkaline magmatism from the Cretaceous North pyrenean Rift Zone (France and Spain). *Eur. J. Mineral.* **4**, pp.813 - 834.
- Bailey, D. K.**(1978) Continental rifting and mantle degassing. In *Petrology and Geochemistry of Continental Rifts*. Eds. Neumann and I. B. Ramberg, Riedel, Netherlands.
- Baker, B. H., and Henage, L., H.** (1977) Compositional changes during crystallization of some silicic lavas of the Kenya Rift Valley. *J. Volcanol. Geotherm. Res.* **2**, pp. 17 - 28.
- Balashov, Yu. A.** (1962) Evolution of rare earth composition and content in the intrusive phases of the Lovozero alkalic massif (Kola Peninsula). *Geochemistry*. pp. 233 - 247.
- Barham, D., Ou, B., Lim, I., and Lowe, J. C.** (1989) Nepheline syenite in whiteware slip. *J. Can. Ceram. Soc.* **58**, pp. 53 - 85.
- Benoit, P. H and Sclar, C. B.** (1991) Pyrophanite-Ilmenite solid solution in magnetite of the Beemerville nepheline syenite, Sussex county New Jersey. *Econ. Geol.* **86** (5) pp. 1115 - 1119.
- Berlin, R., and Henderson, C. M. B.** (1968) The distribution of Sr and Ba between the alkali feldspar, plagioclase and groundmass phases of porphyritic trachytes and phonolites. *Geochim. Cosmochim. Acta.* **33**, pp. 247 - 255.
- Bishop, A. C., and Woolley, A. R.** (1973) A basalt-trachyte-phonolite series from Ua Pu, Marquesas island, Pacific Ocean. *Contrib. Mineral. Petrol.* **39**, pp. 309 - 326.
- Blaxland, A. B and Upton, B. J.** (1978) Rare-earth distribution in the Tugtutoq Younger giant dyke complex: evidence bearing on alkaline magma genesis in south Greenland. *Lithos*, **11**, pp. 291 - 300.
- Blaxland, A. B., Breemen, O. V., and Steenfelt, A.** (1976) Age and origin of apgaitic magmatism at Ilimaussaq, south Greenland: Rb-Sr study. (

References

- Contribution to the mineralogy of Ilimaussaq, no. 41). *Lithos*, **9**, pp. 31 - 38.
- Bose, M. K.** (1970) Petrology of the intrusive alkalic suite of Karaput, Orissa. *J. Geol. Soc. India*. **11**, pp. 99 - 126.
- Bose, M. K., Ghosh, Roy, A. K., and Czygan, W.** (1982) K-Rb relations in the alkaline suites of Eastern Ghats Precambrian belt, India. *Lithos*, **15**, pp. 77 - 84.
- Bottinga, Y., and Weill, D. F.** (1972) The viscosity of magmatic silicate liquids: A model for calculation. *Am. J. Sci.* **272**, pp. 438 - 475.
- Bowden, P., Black, R., Martin, R. F., Ike, E. C., Kinnaird, J. A., and Batchelor, R. A.** (1987) In (Fitton, J. G. and Upton B. G. J. eds.) *Alkaline Igneous Rocks*, Geological Society Special Publication No.30, pp. 357 - 379.
- Bowden, P., and Whitley, J. E.** (1974) Rare-earth patterns in peralkaline and associated granites. *Lithos*. **7**, pp. 15 - 21.
- Bowen, P., and Whitley, J. E.** (1974) Rare-earth patterns in peralkaline and associated grains. *Lithos*, **7**, pp. 15 - 21.
- Bowen, N. L., and Ellestad, R. B.** (1936) Leucite and pseudoleucite. *Am. Mineral.* **21**, pp. 363 - 368.
- Bradshaw, T. K.** (1992) The adaptation of Pearce element ratio diagrams to complex high silica system. *Contrib. Mineral. Petrol.* **109**, pp. 450 - 458.
- Briqueu, L., Bougault, H., and Joron, J., L.** (1984) Qualification of Nb, Ta, Ti and V anomalies in magmas associated with subduction zones: petrogenetic implications. *Earth Planet. Sci. Lett.* **68**, pp. 297 - 308.
- Brown, W. L., and Ian Parsons.** (1981) Towards a more practical two-feldspar geothermometer. *Contrib. Mineral. Petrol.* **76**, pp. 369 - 377.
- Butler, J. R., and Smith, A. Z.** (1962) Zirconium, niobium and certain other trace elements in some alkali igneous rocks. *Geochim. Cosmochim. Acta.* **26**, pp. 945 - 953.

References

- Butler, J. R., Bowden, P., and Smith, A. Z.** (1961) K/Rb ratios in the evolution of younger granites of Northern Nigeria. *Geochim. Cosmochim. Acta.* **26**, pp. 89 - 100.
- Butt, K. A., Chaudhry, M. N., and Ashraf, M.** (1980) An interpretation of petroctectonic assemblage west of W. Himalayan syntaxis in Dir district and adjoining areas in northern Pakistan. *Geol. Bull. Univ. Peshawar (Spec. Issue).* **13**, pp. 79 - 86.
- Butt, K. A., Chaudhry, M. N., and Ashraf, M.** (1985) Evidence of an incipient Palaeozoic Ocean in Kashmir, Pakistan. *Kashmir J. Geol.* **31**, pp. 87 - 103.
- Butt, K. A., Arif, A. Z., Ahmed, J., Ahmed, A., and Qadir, A.** (1989) Chemistry and petrology of the Silai Patti carbonatite complex, North Pakistan. *Geol. Bull. Univ. Peshawar.* **22**, pp. 197 - 215.
- Carmichael, I. S., Turner, F. J., and Verhoogen, J.** (1974) *Igneous petrology* McGraw - Hill, New York.
- Chambers, A. D.** (1976) The petrology and mineralogy of the North Qoroq Centre, Igalliko Complex, South Greenland. Unpub. Ph. D. thesis, University of Durham.
- Chaudhry, M. N., Jafferri, S. A., and Saleemi, B. A.** (1974) Geology and petrology of Malakand granite and its environs. *Geol. Bull. Punjab Univ.* **10**, pp. 43 - 58.
- Chaudhry, M. N., Ashraf, M., and Hussain, S. S.** (1976) Geology and petrology of Malakand and a part Dir. *Geol. Bull. Punjab Univ.* **12**, pp 17 - 40
- Chaudhry, M. N., and Iqbal, M.** (1976) Geology and petrology of Malakand and a part of Dir (topo sheet 38 N / 14). *Geol. Bull. Punjab Univ.* **12**, pp. 14 - 40.
- Chaudhry, M. N., Ashraf, M., and Hussain, S. S.** (1981) Petrology of Koga nepheline syenite and pegmatite of Swat District. *Geol. Bull. Punjab Univ.* **16**, pp. 83 - 97.

- Chaudhry, M. N., and Shams, F. A.** (1983) Petrology of Shewa Porphyries of the Peshawar Plain Alkaline Igneous Province, NW Himalayas, Pakistan. In (F. A. Shamas, ed.) *Granites of Himalayas, Karakorum and Hindukush*. Inst. of Geol. Punj. Univ., Lahore Pakistan. pp. 171 - 182.
- Clague, D. A.** (1987) Hawaiian alkaline magmatism. In (Fitton, J. G. and Upton B. G. J. eds.) *Alkaline Igneous Rocks*, Geological Society Special Publication No.30, pp.227 - 252.
- Clark, M. A.** (1984) Mineralogy of the rare earth elements. In (Henderson, H. ed.) *Rare Earth Elements Geochemistry*. Developments in Geochemistry 2. Pp, 33 - 62.
- Coombs, D. S., and Wilkinson, J. F. G.** (1969) Lineages and fractionation trends in undersaturated volcanic rocks from East Otago Volcanic Province (New Zealand) and related rocks. *J. Petrol.* **10**, pp. 440 - 501.
- Corriveau, L., and Gorton, M. P.** (1992) Coexisting K-rich alkaline and shoshonitic magmatism of arc affinities in the Proterozoic: a reassessment of syenitic stocks in the southwestern Grenville Province. *Contrib. Mineral. Petrol.* **113**, pp. 262 - 279.
- Coulson, A. L.** (1936) A soda-granite suite in the North-West Frontier Province. *Proc. National Inst. Sci. India.* **2**, pp. 103 - 111.
- Crawford, A. R.** (1974) The Indus suture line, the Himalaya, Tibet and Gondwanaland. *Geol. Mag.* **111**, pp. 369 - 383.
- Cullers, L. R., and Medaris, L. G.** (1973) Experimental studies of the distribution of rare earths as trace elements among silicate minerals and liquids and water. *Geochim. Cosmochim. Acta.* **37**, pp. 1499 - 1512.
- Currie, K. L.** (1970) An hypothesis of the origin of alkaline rocks suggested by the tectonic setting of the Monteregian Hills. *Can. Mineral.* **10**, pp. 411 - 420.

References

- Currie, K. L., Eby, G. N., and Gittins, J.** (1986) The petrology of the Mont Saint Hilaire complex, southern Quebec: An alkaline gabbro - peralkaline syenite association. *Lithos.* **19**, pp. 65 - 81.
- Currie, K. L., Knutson, J., and Temby, P. A.** (1992) The Mud Tank carbonatite complex, Central Australia- an example of metasomatism at mid-crustal levels. *Contrib. Mineral. Petrol.* **109**, pp. 326 - 339.
- Czygan, W.** (1984) Petrography and geochemistry of foid syenites and related rocks of the Deccan trap area, India. *Indian mineral. Sukheswala Volume*, pp. 20 - 43.
- Deer, W. A., Howie, R. A., and Zussman, J.** (1982) An introduction to the rock-forming minerals. London: Longman.
- Deer, W. A., Howie, R. A., and Zussman, J.** (1992) An introduction to the rock-forming minerals. 2nd ed. London: Longman.
- Dietzel, A.** (1964) *Ber Dt. Keram. Ges.* 41.
- Drake, M. J., and Weil, D. F.** (1975) Partition of Sr, Ba, Ca, Y, Eu+2, Eu+3 and other REE between plagioclase feldspar and magmatic liquid: and experimental study. *Geochim. Cosmochim. Acta.* **39**, pp. 689 - 712.
- Dudas, F. O.** (1991) Geochemistry of igneous rocks from the Crazy Mountain, Montana, and tectonic model for the Mountain Alaklic Province. *J. Geoph. Earth.* **96**, B 8, pp. 13261 - 13277.
- Duke, N. A., and Edger, A. D.** (1977) Petrology of the Blue Mountain and Bigwood felsic alkaline complexes of the Greenville Province of Ontario. *Can. J. Earth. Sci.* **14**, pp. 515 - 538.
- Eby, G. N.** (1985) Age relation, chemistry and petrogenesis of mafic alkaline dikes from the Monteregian Hills and younger White Mountain igneous provinces. *Can. J. Earth Sci.* **22**, pp. 1103 - 1111.
- Eby, G. N.** (1987) The Monteregian Hills and White Mountain alkaline igneous province, eastern North America. In (Fitton, J. G. and Upton B. G.

References

- J. eds.) Alkaline Igneous Rocks, Geological Society Special Publication No. **30**, pp. 433 - 447.
- Edgar, A. D.** (1987) The genesis of alakiine magmas with emphasis on their source regions: inferences from experimental studies. In (Fitton, J. G. and Upton, B. J. eds.) Alkaline Igneous Rocks, Geological Society Special Publication No. **30**, pp. 29 - 52.
- Edgar, A. D., and Parker, L. M.** (1974) Comparison of melting relationships of some plutonic and volcanic peralkaline undersaturated rocks. *Lithos*, **7**, pp. 263 - 273.
- Ferguson, J.** (1970) The differentiation of agpaitic magmas: The Ilimaussaq intrusion, south Greenland. *Can. Mineral.* **10**, pp. 335 - 349.
- Ferguson, J.** (1973) The Pilanesberg alkaline Province, South Africa. *Trans. Geol. Soc. S. Africa.* **76**, pt. 3. pp. 249 - 270.
- Ferry, J. M.** (1978) Subsolidus phase relations in the nepheline-kalsilite system at 0.5, 2.0, and 5.0 kbar. *Am. Mineral.* **63**, pp. 1225 - 1240.
- Finch, A. A.** (1991) Conversion of nepheline to sodalite during subsolidus processes in alkaline rocks. *Min. Mag.* **55**, pp. 459 - 463.
- Fletcher, C. J. N., and Beddoe-Stephens, B.** (1987) The petrology, chemistry and crystallization history of the Velasco alkaline province, eastern Bolivia. In (Fitton, J. G. and Upton, B. G. J. eds.) Alkaline Igneous Rocks, Geological Society Special Publication No. **30**, pp. 403 - 413,
- Flohr, M. J. K., and Ross, M.** (1989) Alkaline igneous rocks of Magnet Cove, Arkansas: Metasomatized ijolite xenoliths from Diamond Jo quarry. *Am. Mineral.* **74**, pp. 113 - 131.
- Flohr, M. J. K., and Ross, M.** (1990) Alkaline igneous rocks of Magnet Cove, Arkansas; Mineralogy and geochemistry of syenites. *Lithos.* **26**, pp. 67 - 98.

References

- Floyd, P. A., and Winchester, J. A.** (1975) Magma type and tectonic setting discrimination using immobile elements. *Earth Planet. Sci. Lett.* **27**, pp. 211 - 218.
- Fodor, R. V., Frey, F. A., Bauer, G. R., and Clague, D. A.** (1992) Ages, rare-earth element enrichment and petrogenesis of tholeiitic and alkalic basalts from Kaboolawe, Island, Hawaii. *Contrib. Mineral. Petrol.* **110**, pp. 442 - 462.
- Freestone, I. C.** (1978) Liquid immiscibility in alkali-rich magmas. *Chemical Geol.* **23**, pp. 115 - 123.
- Galewicz, M., and Hejnar, W.** (1992) Benefits of nepheline syenite in technical glass melting. *J. Glass.* **2**, p 71.
- Gautier, I., Weis, D., Mennessier, J. P., Vidal, P., Giret, A., and Loubet, M.** (1990) Petrology and geochemistry of the Kerguelen Archipelago basalts (South Indian Ocean): evolution of the mantle sources from ridge to intraplate position. *Earth Planet. Sci. Lett.* **100**, pp. 59 - 76.
- Gerasimovsky, V. I.** (1974) Trace elements in selected groups of alkaline rocks. In H. Sorensen (Editor). *The alkaline rocks*. John Wiley, New York. pp. 402 - 412.
- Gittins, J.** (1961) Nephelinization in Haliburton - Bancroft district, Ontario, Canada. *J. Geol.* **69**, pp. 291 - 308.
- Gomes, C. de B., Moro, S. L., and Dutra, C. V.** (1970) Pyroxenes from the alkaline rocks of Itapirapura, Sao Paulo, Brazil. *Am. Mineral.* **55**, pp. 224 - 230.
- Gomes, C. D., Moro, S. L., and Dutra, C. V.** (1970) Pyroxenes from the alkaline rocks of Itapirapua, Soa Paulo, Brazil. *Am. Mineral.* **55**, pp. 224 - 230.
- Griffiths, P. S., and Gibson, I. L.** (1980) The geology and petrology of the Hannington trachyphonolite formation, Kenya Rift valley. *Lithos.* **13**, pp. 43 - 53.

References

- Gromet, P. L., and Silver, L. T.** (1983) Rare earth element distributions among minerals in a granodiorite and their petrogenetic implications. *Geochim. Cosmochim. Acta.* **47**, pp. 925 - 939.
- Hall, A.** (1987) *Igneous petrology*, Longman Sci. & Tech. Publishers, New York.
- Hamilton, D. L.** (1961) Nepheline as crystallization temperature indicators. *J. Geol.* **69**, pp. 321 - 329.
- Hamilton, D. L., and MacKenzie, W. S.** (1965) Phase-equilibrium studies in the system $\text{NaAlSi}_3\text{O}_8$ (nepheline) - KAlSi_3O_8 (kalsilite) - SiO_2 - H_2O . *Min. Mag.*, (Tilley Volume), **55**, pp. 214 - 231.
- Hanson, G. N.** (1978) Application of trace element to the petrogenesis of igneous rocks of granitic composition. *Earth. Planet. Sci. Lett.* **38**, pp. 26 - 43.
- Hawkesworth, C. J., Van calsteren. P., Rogers, N.W., and Menzies, M. A.** (1987) Enrichment processes and basalt volcanism. In M. A. Manzies & C. J. Hawkesworth (Editors) *Mantle metasomatism*. San Diego: Academic Press. pp. 365 - 388.
- Heier, K.S.** (1961) Layered Gabbro, hornblendite, carbonatite and nepheline syenite on Stjernoy, North Norway. *Norsk Geol. Tidsskr.* **41**, pp. 109 - 155.
- Heier, K.S.** (1964) Geochemistry of the nepheline syenite on Stjernoy, North Norway. *Norsk Geol. Tidsskr.* **44**, pp. 205 - 215.
- Heier, K.S.** (1965) Ageochemical comparison of the Blue Mountain (Ontario, Canada) and Stjernoy (Finnmark, North Norway) nepheline syenite. *Norsk Geol. Tidsskr.* **45**, pp. 41 - 52.
- Heier, K.S; and Taylor, S. R.** (1964) A note on the chemistry of alkaline rocks. *Norsk Geol. Tidsskr.* **44**, pp. 197 - 203.
- Heier, K. S.** (1966) Some cystallo-chemical relationships of nephelines and feldspars on Stjernoy, North Norway. *J. Petrol.* **7**, pp. 95 - 113.
- Heinrich, E. W.** (1946) Studies in the mica group. *J. Sci.* **244**, pp. 836 - 848.

References

- Heier, K. S., and Adams, J.** (1964) The geochemistry of the alkali metals. *Physics Chem. Earth*, **5**, pp. 253 - 381.
- Helmut, R.** (1990) What good flux? *J. CFI Ceram. Forum Intern.* **67**, pp. 95 - 96.
- Henderson, C. M. B.** (1980) The low-temperature inversion in sub-potassic nepheline. *Am. Mineral.* **65**, pp. 970 - 980.
- Henderson, C. M. B., and Gibb, F. G. F.** (1983) Felsic mineral crystallization trends in differentiating alkaliine basic magmas. *Contrib. Mineral. Petrol.* **84**, pp. 355 - 364.
- Henderson, P.** (1980) Rare earth element partition between sphene, apatite and other coexisting minerals of the Kangerdlugssuaq Intrusion, E. Greenland. *Contrib. Mineral. Petrol.* **72**, pp. 81 - 85.
- Hildreth, E. W.** (1981) Gradients in silicic magma chambers: implications for lithospheric magmatism. *J. Geophys. Res.* **86**, pp. 10153 - 10192.
- Hinton, R. W., and Upton, B. J.** (1991) The chemistry of zircon: Variations within and between large crystals from syenite and alkali basalt xenoliths. *Geochim. Cosmochim. Acta.* **55**, pp. 3287 - 3302.
- Huckenholz, H. G.** (1969) Synthesis and stability of Ti - andradite (schairer Vol.). *Am. J. Sci.* v. **267** - A. pp. 209 - 232.
- Irvine, T. N., and Baragar, W. R. A.** (1971) A guide to the classification of the common volcanic rocks. *Can. J. Earth Sci.* **8**, pp. 523 - 548.
- Irving, A. J., and Price, R. C.** (1981) Geochemistry and evolution of lherzolite-bearing phonolitic lavas from Nigeria, Australia, East Germany and New Zealand. *Geochim. Cosmochim. Acta.* **45**, pp. 1309 - 1320.
- Isztin, A. E., Downes, H., James, D. E., Upton, B. G. J., Dobosi, G., Ingram, G. A., Harmon, R. S., and Scharbert, H. G.** (1992) The petrogenesis of Pliocene alkaline volcanic rocks from the Pannonian Basin, Eastern Central Europe. *J. Petrol.* **34**, Pt.2. pp. 317 - 343.

References

- Jan, M. Q.** (1970) An alkaline Igneous Province in the North-West Frontier Province, West Pakistan. *Geol. Mag.* **107**, pp. 395 - 398.
- Jan, M. Q., Asif, M., and Tahirkheli, T.** (1981-a) The geology and petrography of the Tarbela "alkaline" complex. *Geol. Bull. Pesh. Univ.* **14**, pp. 1 - 28.
- Jan, M. Q., kamal, M., and Qureshi, A. A.** (1981-b) Petrology of the Loe-Shilamn carbonatite complex, Khyber Agency. *Geol. Bull. Pesh. Univ.* **14**, pp. 29 - 43.
- Jan, M. Q., and Kempe, D. R. C.** (1970) Recent researches in the geology of northwest West Pakistan. *Geol. Bull. Univ. Peshawar.* **5**, pp. 62 - 89.
- Jiraneck, J.** (1982) A rapid X-ray method of assessing the structural state of monoclinic K-feldspars. *Lithos.* **15**, pp. 85 - 87.
- Jones, A. P.** (1984) Mafic silicate from the nepheline syenites of the motzfeldt centre, South Greenland. *Min. Mag.* **48**, pp. 1 - 12.
- Jones, A. P., and Larsen, M. A.** (1985) Geochemistry & REE minerals of nepheline syenite from the Motzfeldt Centre, South Greenland. *Am. Mineral.* **70**, pp. 1087 - 1100.
- Kaplan, A. Yu.** (1961) The use of nepheline concentrates for the manufacture of bottles from dark green glass. *Glass ceram.* **17**, No. 5, pp. 239 - 241.
- Kapustin, Yu. L.** (1990) Koktygkhem nepheline syenite massif in Northeastern Tuva and its structural position. *Geolgiya i Geofizika.* **31**, No. 5. pp. 74 - 82.
- Kay, R. W., and Gast, P. W.** (1973) The rare earth content and origin of alkali-rich basalts. *J. Geol.* **81**, pp. 653 - 682.
- Kempe, D. R. C.** (1973) The petrology of the Warsak alkaline granites, Pakistan and their relationship to other alkaline rocks of the region. *Geol. Mag.* **110**, pp. 385 - 404.

References

- Kempe, D. R. C.** (1983) Alkaline granites, syenites and associated rocks of the Peshawar Plain Alkaline Igneous Province, NW Pakistan. In: (F. A. Shams ed). *Granites of Himalaya, Karakorum and Hindukush*. Inst. of Geol. Punj. Univ., Lahore, Pakistan. pp. 143 - 169.
- Kempe, D. R. C.** (1986) A note on the age of the Alkaline Rocks of the Peshawar Plain Alkaline Rocks of the Peshawar Plain Alkaline Igneous Province, N. W. Pakistan. *Geol. Bull. Pesh. Univ.* **19**, pp. 113 - 119.
- Kempe, D. R. C., and Deer, W. A.** (1976) The petrogenesis of the Kangerdlugssuaq alkaline intrusion, east Greenland. *Lithos*, **9**, pp. 111 - 124.
- Kempe, D. R. C., and Deer, W. A.** (1970) The rare earth elements and origin of alkali-rich basalts. *J. Geol.* **81**, pp. 653 - 682.
- Kempe, D. R. C., and Jan, M. Q.** (1970) An alkaline igneous province in the North-West Frontier Province, West Pakistan. *Geol. Mag.* **107**, pp. 395 - 398.
- Kempe, D. R. C., Jan, M. Q.** (1980) The Peshawar Plain Alkaline Province, NW Pakistan. *Geol. Bull. Pesh. Univ.* **13**, pp. 71 - 77.
- Keppler, H.** (1991) Influence on the solubility of high field strength elements in granitic melts. *EOS (Trans. Am. Geophys. Union)* **72**, pp. 532 - 533.
- Khan, I. H., Ahmed, S., Mohammad, W., Anwar, S., and Mahmood, F.** (1989) Utilization of nepheline syenite in industry. *Proceed. Nat. Sem. Prosp. and Probs. Min. based ind. in Pakistan*. pp. 82 - 89.
- Khan, M. I., and Hammad, M.** (1978) Petrology of Ulla granite, Gadoon area. Unpublished M. Sc. thesis, Univ. of Peshawar.
- Kingston, P. W., and Caley, W. F.** (1989) Nepheline syenite as a synthetic slag addition in secondary steelmaking. *J. Minerals Eng.* **2**, pp. 207 - 215.

References

- Kogarko, L. N.** (1987) Alkaline rocks of the eastern part of the Basaltic Shield (Kola Peninsula). In (Fitton, J. G. and Upton B. G. J. eds.) Alkaline Igneous Rocks, Geological Society Special Publication No.30, pp. 531 - 544.
- Kushiro, I., and Kuno, H.** (1963) Origin of primary basaltic magmas and classification of basaltic rocks. *J. Petrol.* 4, Pt. 1, pp. 75 - 89.
- Larsen, L. M.** (1976) Clinopyroxenes and coexisting mafic minerals from the Alkaline Ilimaussaq Intrusion, South Greenland. *J. Petrol.* 17, pp. 258 - 290.
- Larsen, L. M.** (1979) Distribution of REE and other trace elements between phenocrysts and peralkaline undersaturated magmas, exemplified by rocks from the Gardar igneous province, south Greenland. (Contribution to the mineralogy of ilimaussaq, no. 56). *Lithos*, 12, pp. 303 - 315.
- Larsen, L. M., and Sorensen, H.** (1987) The Ilimaussaq intrusion-progressive crystallization and formation of layering in an agpaitic magma. In (Fitton, J. G. and Upton, B. G. J. eds.) Alkaline Igneous Rocks, Geological Special Publication No. 30, pp. 473 - 488.
- Larsen, L. M., and Steenfelt, A.** (1974) Alkali loss and retention in an iron-rich peralkaline phonolite dyke from the Gardar province, south Greenland. (Contribution to the mineralogy of Ilimaussaq no.31). *Lithos*, 7, pp. 81 - 90.
- Le Bas, M. J., Le Maitre, R. W., Streckeisen, A., and Zaneittin, B.** (1986) A chemical classification of volcanic rocks based on the total alkali-silica diagram. *J. Petrol.* 27, pp. 745 - 750.
- Le Maitre, R. W.** (1976) The chemical variability of some common igneous rocks. *J. Petrol.* 17, pp. 589 - 637.
- Le Roex, A. P., Cliff, R. A., and Adair, B. J. I.** (1990) Tristan da Cunha, South Atlantic: geochemistry and petrogenesis of a basanite-phonolite lava series. *J. Petrol.* 31, pp. 779 - 812.

References

- Leake, B. E.** (1978) Nomenclature of amphiboles. *Min. Mag.* **42**, pp. 533 - 563.
- Leelanandam, C.** (1980) An alkaline province in Andhra Pradesh. *Curr. Sci.* **49**, pp. 550 - 551.
- Leelanandam, C.** (1981) Some observations on the alkaline province of Andhra Pradesh. *Curr. Sci.* **50**, pp. 799 - 802.
- Leelanandam, C.** (1989) The Prakasam Alkaline Province in Andhra Pradesh, India. *J. Geol. Soc. India*, **34**, pp. 25 - 45.
- Leelanandam, C., and Ratnakar, J.** (1983) The Purimetla alkaline pluton, Prakasam District, Andhra Pradesh. *Quart. J. Geol. Min. Met. Soc. India.* **55**, pp. 14 - 30.
- Leelanandam, C., and Reddy, K. K.** (1981) The Uppalapadu alkaline pluton, Prakasam, district, Andhra Pradesh. *J. Geol. Soc. India*, **22**, pp. 39 - 45.
- Lemarchand, F., Villemant, B., and Calas, G.** (1987) Trace element distribution coefficients in alkali series. *Geochim. Cosmochim. Acta.* **51**, pp. 1071 - 1081.
- LeRoex, A. P.** (1986) Geochemical correlation between southern African kimberlite and South Atlantic hotspots. *Nature*, **324**, pp. 243 - 245.
- LeRoex, A. P., Cliff, R. A., and Adair, B. J. I.** (1990) Tristan da Cunha, South Atlantic: Geochemistry and petrogenesis of a basanite-phonolite lava series. *J. Petrol.* **31**, pp. 779 - 812.
- Liegeois, J. P., Sanvage, J. F., and Black, R.** (1991) The Permo-Jurassic province of Tadhak, Mali: Geology, geochemistry and tectonic significance. *Lithos*, **27**, pp. 95 - 105.
- Madhavan, V., and Leelanandam, C.** (1988) Petrology of the Elchuru Alkaline Pluton, Prakasam District, Andhra Pradesh, India. *J. Geol. Soc. India.* **31**, pp. 515 - 537.
- Mahood, G. A., and Stimac, J. A.** (1990) Trace element partitioning in pantellerites and trachytes. *geochim. Cosmochim. Acta.* **54**, pp. 2257 - 2276.

References

- Maravic, H. V., Morteani, G., and Roethe, G.** (1989) The cancrinite/ carbonatite complex of Luesh, Kivu? NE- Zarire: Petrographic and geochemical studies and its economic significance. *J. African Earth Sci.* **9**, No. 2, pp. 341 - 155.
- Martin, N. R., Siddiqui, S. F. A., and King, B. H.** (1962) A geological reconnaissance of the region between the Lower Swat and Indus River of Pakistan. *Geol. Bull. Punjab Univ. Lahore.* **2**, pp. 1 - 14.
- McBriney, A. R.** (1984) *Igneous petrology.* San Francisco: Freeman, Cooper, 504 pp.
- McCarthy, T. S., and Groves, D. I.** (1979) The blue Tier batholith, northern Tasmania: a cumulate-like products of fractional crystallisation. *Contrib. Mineral. Petrol.* **71**, pp. 193 - 209.
- McLellan, G. W.** (1966) The expanding world of glass. *Discovery, London.* **27** (5) pp. 36 - 40.
- Mian, I., and Le Bas, M. J.** (1986) Sodic amphiboles in fenites from the Loe-Shilman carbonatite complex, NW Pakistan. *Min. Mag.* **50**, pp. 187 - 197.
- Mian, I., and Le Bas, M. J.** (1987) The biotite-phlogopite series in fenites from the Loe-Shilman carbonatite complex, NW Pakistan. *Min. Mag.* **51**, pp. 397 - 408.
- Miller, C. F., and Mittlefehdt, D. W.** (1984) Extreme fractionation in felsic magma chamber: a product of liquid state diffusion or fractional crystallisation? *Earth Planet. Sci. Lett.* **68**, pp. 151 - 158.
- Minnes, D. G., Lefond, S. J., and Blair, R.** (1983) Nepheline syenite. In (Lefond, S. J. ed.) *Industrial Minerals and Rocks*, 5th edition, Am. Inst. of Minn, Metal. and Petro. Engg. **2**, pp. 931 - 960.
- Mitchel, R. H., and Brunfeit, A. O.** (1975) Rare earth element geochemistry of the Fen alkaline complex, Norway. *Contrib. Mineral. Petrol.* **52**, pp. 247 - 259.

References

- Mitchell, R. H.** (1980) Pyroxenes of the Fen alkaline complex, Norway. *Am. Mineral.* **65**, pp. 45 - 54.
- Mitchell, R. H., and Platt, R. G.** (1978) Mafic mineralogy of ferroaugite syenite from the Coldwell complex. *Can. J. Petrol.* **19**, pp. 627 - 651.
- Mitchell, R. H., and Platt, R. G.** (1982) Mineralogy and petrology of nepheline syenites from the Coldwell alkaline complex, Ontario, Canada. *J. Petrol.* **23**, pp. 186 - 214.
- Miyashiro, A.** (1951) The ranges of chemical composition in nepheline and their petrogenetic significance. *Geochim. Cosmochim. Acta.* **1**, pp. 278 - 283.
- Mohsin, I. S.** (1989) Rock wool - An industry with future. *Proceed. Nat. Sem. Prosp. and Probs. Min. based ind. in Pakistan.* pp. 76 - 81.
- Mommsen, R. W.** (1984) Nepheline syenite and feldspar as functional filler / extender pigments. 8th Industrial Minerals, Intern. Cong. pp. 270 - 277.
- Morimoto, N.** (1988) Nomenclature of pyroxenes. *Am. Mineral.* **73**, pp. 1123 - 1133.
- Morogan, V.** (1989) Mass transfer and REE mobility during fenitization at Alno, Sweden. *Contrib. Mineral. Petrol.* **103**, pp. 25 - 34.
- Morozewicz, J.** (1928) Uber die chemische Zusammensetzung de gesteinsbildenden nephelines. *Fennia.* **22**, pp. 1 - 16.
- Morse, S. A.** (1970) Alkali feldspars with water at 5 Kb pressure. *J. Petrol.* **11**, pp. 221 - 253.
- Nag, S., Chakravorty, P. S., Smith, T. E., and Huang, C. H.** (1984) The petrology and geochemistry of intrusive alkaline rocks of Elchuru, Prakasam District, Andhra Pradesh, India. *Geol. J.* **19**, pp. 57 - 76.
- Nagasawa, H.** (1973) Rare-Earth distribution in alkali rocks from Oki-Dogo Island Japan. *Contrib. Mineral. Petrol.* **39**, pp. 301 - 308.

References

- Nakamura, N.** (1974) Determination of REE, Ba, Fe, Mg, Na and K in carbonaceous and ordinary chondrites. *geochim. Cosmochim. Acta.* **38**, pp. 757 - 775.
- Nash, W. P., and Wilkinson, J. F. G.** (1970) Shonkin Sag laccolith, Montana. 1. Mafic minerals and estimates of temperature, pressure, oxygen fugacity and silica activity. *Contrib. Mineral. Petrol.* **25**, pp. 241 - 269.
- Nelson, D. O., Nelson, K. L., Reeves, K. D., and Mattison, G. D.** (1987) Geochemistry of Tertiary alkaline rocks of the Eastern Trans-Peco Magmatic Province, Texas. *Contrib. Mineral. Petrol.* **97**, pp. 72 - 92.
- Nicholls, J., and Carmichael, I. S. E.** (1969) Peralkaline acid liquids: a petrological study. *Contrib. Mineral. Petrol.* **20**, pp. 268 - 294.
- Nicholls, J., and Carmichael, I. S. E.** (1969) Peralkaline acid liquids: a petrological study. *Contrib. Mineral. Petrol.* **20**, pp. 268 - 294.
- Noble, D.C.** (1970) Loss of sodium from crystallized comendite welded tuffs of the Miocene Grouse Canyon Member of the Belted Range Tuff, Nevada. *Geol. Soc. Am. Bull.* **81**, pp. 2677 - 2688.
- Nockolds, S. R.** (1947) The relation between chemical composition and paragenesis in biotite mica of igneous rocks. *Am. J. Sci.* **245**, pp. 401 - 420.
- Nystrom, J. O.** (1984) Rare earth element mobility in vesicular lava during low-grade metamorphism. *Contrib. Mineral. Petrol.* **88**, pp. 328 - 331.
- Ottoneo, G., Piccardo, G. B., and Ernst, W. G.** (1979) Petrogenesis of some Ligurian peridotites --11. Rare earth element chemistry. *Geochim. Cosmochim. Acta.* **43**, pp. 1273 - 1284.
- Panda, P. K., Patra, P. C., Patra, R. N., and Nanda, J. K.** (1993) Nepheline syenite from Rairakhol, Sambalpur District, Orissa. *J. Geol. Soc. India.* **41**, pp. 144 - 151.

- Parsons, I.** (1979) The Klokken gabbro-syenite complex, South Greenland: Cryptic variation and origin of inversely graded layering. *J. Petrol.* **20**, pp. 653 - 694.
- Pearce, J. A., and Cann, J. R.** (1973) Tectonic setting of basic volcanic rocks determined using trace element analyses. *Earth Planet. Sci. Lett.* **19**, pp. 290 - 300.
- Pearce, J. A., and Norry, M. J.** (1979) Petrogenetic implication of Ti, Zr, Y and Nb variations in volcanic rocks. *Contrib. Mineral. Petrol.* **69**, pp. 33 - 47.
- Peccerillo, A., and Wu, T. W.** (1992) Evolution of calc-alkaline magmas in Continental Arc Volcanoes: evidence from Alicudi, Aeolian Arc (Southern Tyrrhenian Sea, Italy). *J. Petrol.* **33**, Pt. 6. pp. 1295 - 1315.
- Philpotts, J. A.** (1970) Redox estimation from a calculation of Eu^{+2} and Eu^{+3} concentrations in natural phases. *Earth Planet. Sci. Lett.* **9**, pp. 257 - 268.
- Phoenix, R., and Nuffield, E. W.** (1949) Cancrinite, Ontario, Canada. *Am. Mineral.* **34**, pp. 452 - 455.
- Platt, R. G., Wall, F., William, C. T., and Woolley, A. R.** (1987) Zirconolite, chevkinite and other rare earth minerals from nepheline syenite of the Chilwa Alkaline Province, Malawi. *Min. Mag.* **51**, pp. 253 - 263.
- Platt, R. G., and Woolley, A. R.** (1986) The mafic mineralogy of the peralkaline syenites and granites of the Mulanje Complex, Malawi. *Min Mag.* **50**, pp. 85 - 99.
- Powell, M.** (1978) The crystallisation history of the Igdlertfigssalik nepheline syenite intrusion, Greenland. *Lithos.* **11**, pp. 99 - 120.
- Powell, M., and Powell, R.** (1977) A nepheline-alkali feldspar geothermometer. *Contrib. Mineral. Petrol.* **62**, pp. 193 - 204.
- Powell, M.** (1978) The crystallization history of the Igdlertfigssalik nepheline syenite, intrusion, Greenland. *Lithos.* **11**, pp. 99 - 120.

References

- Rae, D. A., and Chambers, A. D.** (1988) Metasomatism in the North Qoroq centre, South Greenland: cathodoluminescence and mineral chemistry of alkali feldspar. *Trans. R. Soc. Edinburgh.* **79**, pp. 1 - 12.
- Rafique, M., Chaudhry, M. N., and Ashraf, M.** (1987) Beneficiation and evaluation of a part of the nepheline syenite deposit of Swat as a raw material for glass manufacture. *Geol. Bull. Punj. Univ.* **22**, pp. 116 - 124.
- Ramberg, I. B.** (1972) Braided perthite in nepheline syenite pegmatite, Langesundsfjorden, Oslo Region (Norway). *Lithos.* **5**, pp. 281 - 306.
- Ratnakar, J., and Leelanandam, C.** (1986) A petrochemical study of the Purimetla alkaline pluton, Prakasam District, Andhra Pradesh, India. *J. Neues Jahrb. Mineral. ABH.* **156**, pp. 99 - 119.
- Ratnakar, J., and Leelanandam, C.** (1989) Petrology of the alkaline plutons from the eastern and southern Peninsular India. *Memoirs Geol. Soc. India.* **15**, pp. 145 - 176.
- Rayerson, F. J., and Watson, E. B.** (1987) Rutile saturation in magmas: implications for Ti-Nb-Ta depletion in island arc basalts. *Earth Planet. Sci. Lett.* **86**, pp. 225 - 239.
- Reddy, Y. Y., and Leelanandam, C.** (1986) Occurrence of nepheline syenites within the Pasupugallu gabbro-anorthosite pluton, Prakasam District, Andhra Pradesh. *Curr. Sci.* **55**, pp. 1190 - 1191.
- Rehman, S., and MacKenzie, W. S.** (1969) The crystallization of ternary feldspar: A study from natural rocks. *Am. J. Sci.* **267-A**, pp. 391 - 406.
- Rickwood, P. C.** (1989) Boundary lines within petrologic diagrams which use oxides of major and minor elements. *Lithos.* **22**, pp. 247 - 263.
- Rock, N. M. S.** (1976) Fenitization around the Monchique alkaline complex, Portugal. *Lithos.* **9**, pp. 263 - 279.

References

- Rock, N. M. S.** (1978) Petrology and petrogenesis of the Monchique Alkaline Complex, Southern Portugal. *J. Petrol.* **19**, Pt.2. pp. 171 - 214.
- Rock, N. M. S.** (1982) The Late Cretaceous alkaline igneous province in the Iberian peninsula, and its tectonic significance. *Lithos.* **15**, pp. 111 - 131.
- Roger, H., Mitchell., and Platt, R. G.** (1982) Mineralogy and petrology of nepheline syenite from the Coldwell Alkaline Complex, Ontario, Canada. *J. Petrol.* **23**, pp. 186 - 214.
- Rubin, J. N., Henry, C. D., and Price, J. G.** (1993) The mobility of zircon and other "immobile" elements during hydrothermal alteration. *Chemical Geology.* **110**, PP. 29 - 47.
- Rutler, M. J.** (1987) The nature of the lithosphere beneath the Sardinian Continental block: Mantle and deep crustal inclusions in mafic and alkaline lavas. *Lithos.* **20**, pp. 225 - 234.
- Sage, R. P.** (1987) Geology of carbonatite- alkalic rock complexes in Ontario. Nemegosenda Lake alkalic rock complex. District of Sudbury. Ont. Geol. Surv. Study, **34**, 132 pp.
- Sage, R. P.** (1988) Geology of carbonatite- alkalic rocks complexes in Ontario. Lackner Lake alkalic rock complex. District of Sudbury. Ont. Geol. Surv. Study, **32**, 141 pp.
- Sage, R. P.** (1988) Geology of carbonatite- alkalic rock complexes in Ontario. Sturgeon Narrows and Squaw Lake alkalic rock complexes. District of Thunder bay. Ont. Geol. Surv. Study, **49**, 117 pp.
- Sceal, J. S. C., and Weaver, S. D.** (1970) Trace element data bearing on the origin of salic rocks from the Quaternary volcano Paka, Gregory Rift, Kenya. *Earth Planet. Sci. Lett.* **12**, pp. 327 - 331.
- Schnetzler, C. C., and Philpotts, J. A.** (1970) Partition coefficients of rare earth elements between igneous matrix material and rock forming mineral phenocrysts. *Geochim. Cosmochim. Acta.* **43**, pp. 331 - 340.

References

- Sethna, S. F.** (1989) Petrology and geochemistry of the acid, intermediate and alkaline rocks associated with the Deccan basalts in Gujrat and Maharashtra. *Memoirs Geol. Soc. India.* **15**, pp. 47 - 61.
- Shafeeq, A., and Zulfiqar, A.** (1974) Petrochemistry of the Ambela granites, southern Swat District, Pakistan. *Pakistan J. Sci. Res. Lahore.*, **26**, pp. 63 - 69.
- Shams, F. A.** (1980) An anatectic liquid of granitic composition from Hazara Himalayas, Pakistan. *Ren. Atti Della Accad Naz dei Lincei.* **68**, pp. 207 - 215.
- Shaw, D. M.** (1968) A review of k-Rb fractionation trend by covariance analyse. *Geochim. Cosmochim. Acta.* **32**, pp. 573 - 601.
- Siddiqui, S. F. A.** (1965) Alkaline rocks of Swat, Chamlā. *Geol. Bull. Punjab Univ.* **5**, p 52.
- Siddiqui, S. F. A.** (1967) Note on the discovery of carbonatite rocks in the Chamlā area Swat State. *Geol. Bull. Punj. Univ.* **6**, pp. 85 - 88.
- Siddiqui, S. F. A., Chaudhry, M. N., and Shakoor, A.** (1968) Geology and petrology of the feldspathoidal syenite and associated rocks of the Koga area, Chamlā valley, Swat, West Pakistan. *Geol. Bull. Punjab Univ.* **7**, 1 - 30.
- Siedner, G.** (1965) Geochemical fetures of a strongly fractionated alkaline igneous suite. *Geochim. Cosmochim. Acta.* **29**, pp. 113 - 132.
- Singer, F., and Singer, S. S.** (1963) Industrial ceramics. In (Nepheline Syenite). London: Chapman and Hall Ltd.
- Smith, I. E. M., Chappel, B. W., Wall, G. K., and Freeman, R. S.** (1977) Peralkaline rhyolites associated with andesitic arc of the southwest Pacific. *Earth Planett. Sci. Lett.* **37**, pp. 230 - 236.
- Soerensen, H., and Larsen, L. M.** (1987) Layering in the Ilimaussaq alkaline intrusion, South Greenland. *J. Nato Asi. Ser. C.* **196**, pp. 1 - 28.

- Sorensen, H.** (1970) Internal structures and geological settings of the three agpaite intrusions- Khibina and Lovozero of the Kola Peninsula and Ilimaussaq, South Greenland. *Can. Mineral.* **10**, pp. 299 - 324.
- Sorensen, H. Ed.** (1974) *The Alkaline Rocks*. Wiley, London, xii + 622 pp.
- Speer, J. A.** (1984) Micas in igneous rocks. *Mineral. Soc. Am. Reviews in Mineralogy.* **13**, pp. 299 - 356.
- Srivastava, R. K.** (1989) Alkaline and peralkaline rocks of Rajasthan. *Memoirs Geol. Soc. India.* **15**, pp. 2 - 24.
- Stebbins, J. F., and Carmichael, I. S. E.** (1983) The high temperature liquid and glass heat contents and the heats of fusion of diopside, albite, sanidine and nepheline. *Am. Minerals.* **68**, pp. 717 - 730.
- Stephenson, D.** (1972) Alakalic clinopyroxenes from nepheline syenites of the South Qoroq Centre, South Greenland. *Lithos.* **5**, pp. 187 - 201.
- Stephenson, D.** (1974) Mn and Ca enriched olivines from nepheline syenites of the South Qoroq Centre, south Greenland. *Lithos.* **7**, pp. 35 - 41.
- Stephenson, D., and Upton, B. G. J.** (1982) Ferromagnesian silicates In a differentiated alkaline complex: Kungnat Fjeld, South Greenland. *Min. Mag.* **46**, pp. 283 - 300.
- Subbarao, K. V.** (1971) The Kunavaram Series- A group of alkaline rocks, Khammam District, Andhra Pradesh, India. *J. Petrol.* **12**, pt. 3, pp. 621 - 641.
- Sukheswala, R. N., and Udas, G. R.** (1964) Carbonatite of Amba Dongar, India - Some structural considerations. *Internat. Geol. Cong. Proc.* **22** Session, pp. 1 - 13.
- Sun, S. S., and Hanson, G. N.** (1975) Origin of Ross Island basanitoids and limitations upon the heterogeneity of mantle sources for alkali basalts and nephelinites. *contrib. Mineral. Petrol.* **52**, pp. 77 - 106.
- Taher, R. M.** (1989) A comparative petrochemical study of Gabal Abu Khruq and Gabal El Kahfa South Eastern Desert, Egypt. *Ann. Geol. Surv. Egypt.* **16**, pp. 111 - 117.

References

- Tahirkheli, R. A. K.** (1979) Geology of Kohistan and adjoining Eurasian and Indo-Pakistan continents, Pakistan. *Geol. Bull. Peshawar Univ. (Spec. Issue)*. **11**, pp. 1 - 30.
- Takla, M. A., and Griffin, W. L.** (1980) Cancrinite (microsommitite), metabasalt, St John's Island, Red Sea, Egypt. *Neues Jahrb. Min. Monat. Pp.* 345 - 352.
- Taylor, D., and MacKenzie, W. S.** (1975) A contribution to the pseudoleucite problem. *Contrib. Mineral. Petrol.* **49**, pp. 321 - 333.
- Taylor, G. H., and Wilson, R. C.** (1962) Particle size control of nepheline syenite for whitewares. *Bull. Am. Ceram. Soc.* **41**, pp. 12 - 13.
- Taylor, H. P., Frechen, J., and Degens, E. T.** (1967) Oxygen and carbon isotope studies of carbonatites from the Laacher See District, West Germany and the Alno District, Sweeden. *Geochim. et Cosmochim. Acta.* **31**, pp. 407 - 430.
- Taylor, R. P., Strong, D. F., and Kean, B. F.** (1980) The Topsails igneous complex: Silurian - Devonian peralkaline magmatism in western New foundland. *Can. J. Earth Sci.* **17**, pp. 425 - 439.
- Taylor, S. R., and Ahrens, L. H.** (1959) The significance of K/Rb ratios for the tektite origin. *Geochim. Cosmochim. Acta.* **15**, pp. 370 - 372.
- Taylor, S. R.** (1965) The application of trace element data to problems in petrology. *Physics Chem. Earth.* **6**, pp. 135 - 213.
- Taylor, G. H.** (1990) Nepheline syenite. *Ceram. Bull.* **69**, pp. 872 - 873.
- Thornton, C. P., and Tuttle, O. F.** (1960) Chemistry of igneous rocks: 1, differentiation index. *Am. J. Sci.* **252**, pp. 67 - 75.
- Tilley, C. E.** (1954) Nepheline-alkali feldspar parageneses. *Am. J. Sci.* **252**, pp. 65 - 75.
- Tilley, C. E.** (1957) Problems of alkali rock genesis. *Quart. J. Geol. Soc. London.* **113**, pp. 323 - 360.

References

- Tindle, A. G., and Pearce, J. A.** (1981) Petrogenetic modelling of in situ fractional crystallisation in the zoned Loch Doon pluton, Scotland. *Contrib. Mineral. Petrol.* **78**, pp. 196 - 207.
- Tullis, J., and Yund, R. A.** (1979) Calculation of coherent solvi for alkali feldspar, iron-free clinopyroxene, nepheline-kalsilite, and hematite-ilmenite. *Am. Mineral.* **64**, pp. 1063 - 1074.
- Tuttle, O. F., and Smith, J. V.** (1958) The nepheline-kalsilite system. II. Phase reactions. *Am. J. Sci.* **256**, pp. 571 - 589.
- Tyler, R. C., and King, B. C.** (1967) The pyroxenes of the alkaline igneous complexes of Eastern Uganda. *Min. Mag.* **36**, pp. 5 - 22.
- Ujike, O.** (1982) Microprobe mineralogy of plagioclase, clinopyroxene and amphibole as records of cooling rate in the Shirotori-Hiketa dike swarms, northeastern Shikoku, Japan. *Lithos.* **15**, pp. 281 - 293.
- Upton, B. G. J., Stephenson, D., and Martin, A. R.** (1985) The Tugtutq older giant dyke complex: mineralogy and geochemistry of an alkali gabbro - augite - foyaite association in the Garder Province of South Greenland. *Min. Mag.* **49**, pp. 623 - 642.
- Upton, B. G. J.** (1974) The alkaline province of South-West Greenland. In: H. Sorensen (editor). *The Alkaline Rocks*. John Wiley. New York. pp. 221 - 238.
- Vannucci, R., Shimizu, N., Piccardo, G. B., Ottolini, L., and Bottazzi, P.** (1993) Distribution of trace elements during breakdown of mantle garnet: an example from Zabargad. *Contrib. Mineral. Petrol.* **113**, pp. 437 - 449.
- Viladkar, S. G., and Avasia, R. K.** (1992) Pyroxenes from the alkaline rocks of the Chhota Udaipur Carbonatite-alkalic Province, Gujrat, India. *J. Geol. Soc. India.* **39**, pp. 313 - 319.
- Volkov, P. A.** (1932) New ideas on the use of nepheline in industry. *Dokl. Akad. Nauk SSSR, ser. A.* **7**, pp. 165 - 172. [In Russian.]

- Wallace, P., and Carmichael, S. E.** (1992) Alkaline and calc-alkaline lavas near Los Volcanes, Jalisco, Mexico: geochemical diversity and its significance in volcanic arcs. *Contrib. Mineral. Petrol.* **111**, pp. 423 - 439.
- Wallace, P., and Carmichael, S. E.** (1992) Alkali and calc-alkali lavas near Los Volcanes, Jalisco, Mexico: geochemical diversity and its significance in volcanic arcs. *Contrib. Mineral. Petrol.* **111**, pp. 423 - 439.
- Watkinson, D. H.** (1970) Experimental studies bearing on the origin of the alkalic rock - carbonatite complex and niobium mineralization at Oka, Quebec. *Can. Mineral.* **10**, pp. 350 - 361.
- Watson, E. B.** (1979) Zircon saturation in felsic liquids: Experimental results and applications to trace element geochemistry. *Contrib. Mineral. Petrol.* **70**, pp. 407 - 419.
- Watson, E. B., and Harrison, T. M.** (1983) Zircon saturation revisited: temperature and composition effects in a variety of crustal magma types. *Earth Planet. Sci. Lett.* **64**, pp. 295 - 304.
- Weaver, S. D., Seal, J. S. C., and Gibson, I. L.** (1972) Trace element data relevant to the origin of trachytic and pantelleritic lavas in the East African rift system. *Contrib. Mineral. Petrol.* **36**, pp. 181 - 194.
- Wendlandt, R. F., and Harrison, W. J.** (1979) Rare earth partitioning between immiscible carbonate and silicate liquids and CO₂ vapor: results and implications for the formation of light rare earth-enriched rocks. *Contrib. Mineral. Petrol.* **69**, pp. 409 - 419.
- White, A. J. R., Chappel, B. W., and Jakes, P.** (1972) Coexisting clinopyroxene, garnet and amphibole from an eclogite, Kakamui, New Zealand. *Contrib. Mineral. Petrol.* **34**, pp. 185 - 191.
- Wilkinson, J. F. G.** (1965) Some feldspar, nephelines and analcimes from the Square Top Intrusion, Nundle, N. S. W. *J. Petrol.* **6** Pt. 3. pp. 420 - 444.

References

- Wolf, J. A.** (1987) Crystallization of nepheline syenite in a subvolcanic system: Tenerife, Canary Island. *Lithos.* **20**, pp. 207 - 223.
- Wolff, J. A., and Storey, M.** (1984) Zoning in highly alkaline magma bodies. *Geolo. Mag.* **121**, pp. 563 - 575.
- Woolley, A. R.** (1987) Lithosphere metasomatism and the petrogenesis of the Chilwa Province of alkaline igneous rocks and carbonatites, Malawi. *J. African earth Sci.* **6**, No. 6. pp. 891 - 898.
- Woolley, A. R., and Jones, G. C.** (1987) The petrochemistry of the northern part of the Chilwa alkaline province, Malawi. In (Fitton, J.G. and Upton, B. G. J. eds.) *Alkaline Igneous Rocks*, Geological Society Publication No. **30**, pp. 335 - 355.
- Woolley, A. R., and Platt, R.G.** (1986) The mineralogy of nepheline syenite complexes from the northern part of the Chilwa Province, Malawi. *Min. Mag.* **50**, pp. 597 - 610.
- Woolley, A. R., and Platt, P. G.** (1988) The peralkaline nepheline syenites of the Junguni Intrusion, Chilwa Province, Malawi. *Min. Mag.* **52**, pp. 425 - 433.
- Wright, T. L.** (1968) X-ray and optical study of alkali feldspar: II. An X-ray method for determining the composition and structural state from measurement of 2θ values for three reflections. *Am. Mineral.* **53**, pp. 88 - 104.
- Yagi, K.** (1953) Petrochemical studies of the alkalic rocks of Morotu district, Sakhalin. *Bull. Geol. Soc. Am.* **64**, pp. 769 - 810.
- Yoder, H. S., and Tilley, C. E.** (1962) Origin of basalt magmas: An experimental study of natural and synthetic rock systems. *J. petrol.* **3**, pp. 342.
- Qian, Yu.** (1991) The exploitation and utilization of nepheline syenite produced in Yunnan (In Chinese). *Guisuanyan Tongbo*, **10** (3) pp. 31 - 38.